

SYNTHESIS OF FUNCTIONALIZED THIOPHENE BASED MATERIALS

by

Dushanthi Shamila Dissanayake

APPROVED BY SUPERVISORY COMMITTEE:

Dr. Michael C. Biewer, Chair

Dr. Mihaela C. Stefan

Dr. Jeremiah J. Gassensmith

Dr. Ronald A. Smaldone

Copyright 2017

Dushanthi Shamila Dissanayake

All Rights Reserved

This work is dedicated to my loving family

SYNTHESIS OF FUNCTIONALIZED THIOPHENE BASED MATERIALS

by

DUSHANTHI SHAMILA DISSANAYAKE, MPhil

DISSERTATION

Presented to the Faculty of

The University of Texas at Dallas

in Partial Fulfillment

of the Requirements

for the Degree of

DOCTOR OF PHILOSOPHY IN

CHEMISTRY

THE UNIVERSITY OF TEXAS AT DALLAS

December 2017

ACKNOWLEDGMENTS

Foremost, I would like to convey my sincere gratitude to my research supervisor, Dr. Michael C. Biewer, for his valuable guidance, encouragement, kindness and patience throughout the course of my research. His immense knowledge of organic chemistry, enthusiasm and work ethics always inspired me. I also would like to thank Dr. Mihaela C. Stefan for her valuable advice, continuous support and encouragement. I'm always motivated by her phenomenal passion and dedication towards science. Beside my advisors, I would like to thank the rest of my committee members Dr. Jeremiah Gassensmith and Dr. Ronald Smaldone for their advice, encouragement and support through my committee meetings.

I'm thankful to all the present and past members of the Biewer Lab for creating a pleasant working environment in the lab. I would like to offer my special thanks to Dr. Samodha S. Gunathilake and Dr. Peishen Huang for being my first mentors and very good friends. I extend my thanks to current group members Lakmal Gamage and Mahesh Udamulle Gedara for their support towards the end of my projects and Vasanthi Karmegam for being a good friend and a colleague in the lab. I also would like to thank my undergraduate students Tina Nguyen, Duyphuc Ngoc Ta (Phillip) and Rohit George for their help.

My sincere thanks goes to all the present and past Stefan lab members for being good friends and colleagues, specially Dr. Katherine Washington and Dr. Jia Du for being good friends and for all the help they have given to me in numerous ways. I always enjoyed all the good discussions we had on our research throughout our time together in the lab. I'm thankful to all the other past members of the group Dr. Hein Nguyen, Dr. Elizabeth Rainbolt, Dr. Taniya Pathiranage, Dr. Suchithra Senevirathne, Dr. Mahesh Bhatt, Dr. Ruvini Kularathne and Dr. Harsha Magurudeniya for their support throughout my research work. I extend my thanks to all the current members of the group Ruvanthi Kularathne, Chandima Bulumulla, Ruwan Gunawardhana, Yixin Ren, Crystal Niermann, Justin Miller, Muktadir Talukder, Erika Calubaquib, Pooneh Soltantabar and John Cue for their friendship and help.

I would like to offer my special thanks to our collaborators from The Pennsylvania State University, Dr. Enrique D. Gomez and his group members Dr. Youngmin Lee and Sang Ha Yoo for their kind support.

Furthermore, I extend my thanks to the Department of Chemistry staff, Dr. Gregory T. McCandless for Single crystal X-ray diffraction analysis and Dr. George McDonald, Betty Maldonado, Linda Heard, Kelli Lewis, Lydia Selvidge and Nancy Jacobsen from The Office of Research Compliance for being so helpful.

I would like to convey my thanks to Dr. Elizabeth Braun for being a very good friend outside the lab. I enjoyed all the talks we had on many areas of science whenever we were in the office. My sincere thanks go to all my UTD friends for their friendship and help.

Last but not least, I would like to thank my family, my father, my late mother, two sisters and my dear husband for their constant spiritual support, motivation, patience, assistance and standing by my side like a shadow throughout my whole life.

July 2017

SYNTHESIS OF FUNCTIONALIZED THIOPHENE BASED MATERIALS

Dushanthi Shamila Dissanayake, PhD
The University of Texas at Dallas, 2017

Supervising Professor: Dr. Michael C. Biewer

Functionalized thiophene based materials are promising candidates in many organic electronic applications such as organic field effect transistors, photovoltaic devices, organic light emitting diodes and sensors. Low temperature deposition and solution processing make these materials particularly interesting as their fabrication processes are much less complex than conventional silicon technology. Furthermore, the mechanical flexibility of organic materials makes them well-suited for plastic substrates in light weight and flexible products. Incorporation of different functional moieties can alter the optoelectronic properties of these materials. Attaching stimuli responsive compounds make these materials responsive towards the particular stimulus, and electron donating and withdrawing moieties can be used to tune the HOMO and LUMO energy levels. Spiroyrans are photochromic compounds which shows large structural variation upon absorption of light, and developing new synthetic methodologies to incorporate these units into thiophene based materials via a conjugated pathway is crucial in order to study the effect of photochromism on optoelectronic properties of a conjugated material. Functionalization of thiophene based materials with alkoxy substituents raise the HOMO level of the materials and thus lower the band gap. Application of alkoxy substituted polythiophene on organic electronic devices can demonstrate how charge transportation of the material is affected by the substituent.

Chapter 1 discusses the thiophene based conjugated materials and their electronic properties including band structure, conductivity and charge transport mechanism. The operation mechanism of organic field effect transistors and effect of functionalization of thiophene based materials with

photochromic spiropyrans and alkoxy groups with respect to organic electronic applications is discussed.

Chapter 2 demonstrates development of synthetic methodologies to incorporate photochromic spiropyran as a backbone unit into thiophene based polymers via a conjugated pathway.

Chapter 3 illustrates a new synthetic method to incorporate photochromic spiropyran substituents as pendent groups to thiophene repeat units through a conjugated pathway.

Chapter 4 discusses the synthesis of triethylene glycol monomethyl ether substituted polythiophene, optoelectronic properties and the charge carrier mobility with field-effect transistors and in Schottky diode. It also describes the applicability of doped polymer as an alternative to commercially available PEDOT: PSS.

TABLE OF CONTENTS

ACKNOWLEDGMENTS	v
ABSTRACT.....	vii
LIST OF FIGURES	xii
LIST OF TABLES	xx
LIST OF SCHEMES.....	xxi
CHAPTER 1 THIOPHENE BASED CONJUGATED MATERIALS.....	1
1.1 Abstract.....	1
1.2 Role of thiophene in materials chemistry	1
1.3 Energy bands and conductivity in conjugated materials.....	2
1.4 Charge transport in conjugated materials	3
1.5 Organic field-effect transistor (OFET) measurements	4
1.6 Photochromic spiropyrans in OFETs.....	6
1.7 Thiophene based spiropyran materials.....	8
1.8 Poly(3-alkoxythiophene)s.....	9
1.9 References.....	10
CHAPTER 2 ATTACHMENT OF SPIROPYRAN AS A BACKBONE UNIT INTO THIOPHENE BASED POLYMERS.....	15
2.1 Abstract.....	16
2.2 Introduction.....	16
2.3 Experimental	18
2.3.1 Materials.....	18
2.3.2 Analysis.....	18
2.3.3 Synthetic procedures	19
2.4 Results and Discussion	51
2.4.1 Photochromism of SPs with thiophene substituents in chromene moiety	51
2.4.2 Synthesizing ortho-hydroxy aromatic aldehydes with a thiophene unit	54
2.4.3 Benzene based photochromic SPs.....	55

2.4.4	Photochromism of the SP polymer	58
2.5	Conclusions and Future work	59
2.6	Acknowledgments.....	60
2.7	References.....	60
CHAPTER 3 ATTACHMENT OF SPIROPYRAN AS A PENDENT GROUP TO THIOPHENE BASED MATERIALS		63
3.1	Abstract.....	64
3.2	Introduction.....	64
3.3	Experimental.....	65
3.3.1	Materials.....	65
3.3.2	Analysis.....	65
3.3.3	Synthetic procedures	66
3.4	Results and Discussion	97
3.4.1	Thiophene substituted spiropyran (SP-T)	97
3.4.2	Monomrominated derivative (SP-T-Br).....	99
3.4.3	Systematic variation of thiophene substituents	99
3.4.4	UV-Vis kinetics.....	100
3.4.5	Dibrominated derivative of SP-T	106
3.4.6	Tribrominated derivative of SP-T	108
3.5	Conclusions.....	110
3.6	Acknowledgments.....	110
3.7	References.....	110
CHAPTER 4 TRIETHYLENE GLYCOL MONOMETHYL ETHER SUBSTITUTED POLYTHIOPHENE FOR ORGANIC ELECTRONIC APPLICATIONS		113
4.1	Abstract.....	114
4.2	Introduction.....	114
4.3	Experimental.....	115
4.3.1	Materials and methods	115
4.3.2	Analysis.....	115
4.3.3	Synthetic procedures	119
4.4	Results and Discussion	133

4.5	Conclusion	145
4.6	Acknowledgments.....	145
4.7	References.....	145
	APPENDIX.....	149
	BIOGRAPHICAL SKETCH	152
	CURRICULUM VITAE	

LIST OF FIGURES

Figure 1.1. Some of the important PTs and thiophene derivatives in organic electronics	1
Figure 1.2. Schematic diagram of band gap structure for semiconducting materials	2
Figure 1.3. (a) Polaron and bipolaron formation in polythiophene (b) schematic diagram of polaron and bipolaron states	4
Figure 1.4. Bottom-gate bottom-contact OFETs architecture	5
Figure 1.5. The field- effect phenomenon in OFETs under negative gate bias	6
Figure 1.6. Photochromism in (a) spiropyrans (b) diarylethenes (c) azobenzenes	7
Figure 1.7. Mechanism of photochemical isomerization of SP ²⁷	8
Figure 1.8. SP based thiophene materials	9
Figure 1.9. Recent reports on ethylene glycol mediated poly(alkoxythiophene)s.....	10
Figure 2.1. ¹ H-NMR spectrum of <i>tert</i> -butyl(2,5-dibromophenoxy)dimethylsilane	20
Figure 2.2. ¹³ C-NMR spectrum of <i>tert</i> -butyl(2,5-dibromophenoxy)dimethylsilane	21
Figure 2.3. ¹ H-NMR spectrum of <i>tert</i> -butyl(2,5-di(thiophene-2-yl)phenoxy)dimethylsilane and 2,5-di(thiophen-2-yl)phenol in downfield region.	23
Figure 2.4. ¹ H-NMR spectrum of <i>tert</i> -butyl(2,5-di(thiophene-2-yl)phenoxy)dimethylsilane and 2,5-di(thiophen-2-yl)phenol in upfield region.	23
Figure 2.5. ¹³ C-NMR spectrum of <i>tert</i> -butyl(2,5-di(thiophene-2-yl)phenoxy)dimethylsilane.....	24
Figure 2.6. ¹³ C-NMR spectrum of 2,5-di(thiophen-2-yl)phenol.....	24
Figure 2.7. ¹ H-NMR spectrum of 2-hydroxy-3,6-di(thiophen-2-yl)benzaldehyde.....	26
Figure 2.8. ¹³ C-NMR spectrum of 2-hydroxy-3,6-di(thiophen-2-yl)benzaldehyde	26
Figure 2.9. ¹ H-NMR spectrum of 1',3'3'-trimethyl-5,8-di(thiophen-2-yl)spiro[chromene-2,2'-indoline]	28

Figure 2.10. ¹³ C-NMR spectrum of 1',3'3'-trimethyl-5,8-di(thiophen-2-yl)spiro[chromene-2,2'-indoline]	28
Figure 2.11. Expanded ¹ H- ¹ H COSY spectrum of 1',3'3'-trimethyl-5,8-di(thiophen-2-yl)spiro[chromene-2,2'-indoline]	29
Figure 2.12. Expanded ¹ H- ¹ H NOESY spectrum of 1',3'3'-trimethyl-5,8-di(thiophen-2-yl)spiro[chromene-2,2'-indoline]	29
Figure 2.13. ¹ H-NMR spectrum of methyl 3-(2methoxy-2-oxoethylthio)propanoate.....	31
Figure 2.14. ¹³ C-NMR spectrum of methyl 3-(2methoxy-2-oxoethylthio)propanoate	32
Figure 2.15. ¹ H-NMR spectrum of methyl 4-oxotetrahydrothiophene-3-carboxylate	32
Figure 2.16. ¹³ C-NMR spectrum of methyl 4-oxotetrahydrothiophene-3-carboxylate	33
Figure 2.17. ¹ H-NMR spectrum of methyl 4-acetoxythiophene-3-carboxylate	34
Figure 2.18. ¹³ C-NMR spectrum of methyl 4-acetoxythiophene-3-carboxylate	35
Figure 2.19. ¹ H-NMR spectrum of methyl 4-hydroxythiophene-3-carboxylate.....	36
Figure 2.20. ¹³ C-NMR spectrum of methyl 4-hydroxythiophene-3-carboxylate	37
Figure 2.21. ¹ H-NMR spectrum of methyl 4-((<i>tert</i> -butyldimethylsilyl)oxy)thiophene-3-carboxylate	38
Figure 2.22. ¹³ C-NMR spectrum of methyl 4-((<i>tert</i> -butyldimethylsilyl)oxy)thiophene-3-carboxylate	39
Figure 2.23. ¹ H-NMR spectrum of (4-((<i>tert</i> -butyldimethylsilyl)oxo)thiophene-3-yl)methanol ...	40
Figure 2.24. ¹³ C-NMR spectrum of (4-((<i>tert</i> -butyldimethylsilyl)oxo)thiophene-3-yl)methanol ..	41
Figure 2.25. ¹ H-NMR spectrum of 4-((<i>tert</i> -butyldimethylsilyl)oxy)thiophene-3-carbaldehyde...	42
Figure 2.26. ¹ H-NMR spectrum of 5-bromo-4-((<i>tert</i> -butyldimethylsilyl)oxy)thiophene-3-carbaldehyde	43
Figure 2.27. ¹ H-NMR spectrum of 2,5-dibromo-4-((<i>tert</i> -butyldimethylsilyl)oxy)thiophene-3-carbaldehyde	44
Figure 2.28. ¹ H-NMR spectrum of 3,6-dibromo-2-hydroxybenzaldehyde.....	46

Figure 2.29. ¹³ C-NMR spectrum of 3,6-dibromo-2-hydroxybenzaldehyde	46
Figure 2.30. ¹ H-NMR spectrum of 5,8-dibromo-1', 3', 3'-trimethylspiro [chromene- 2,2'-indoline]	48
Figure 2.31. ¹³ C-NMR spectrum of 5,8-dibromo-1', 3', 3'-trimethylspiro [chromene-2,2'-indoline]	48
Figure 2.32. Expanded ¹ H- ¹ H COSY spectrum of 5,8-dibromo-1', 3', 3'-trimethylspiro[chromene-2,2'-indoline].....	49
Figure 2.33. Expanded ¹ H- ¹ H NOESY spectrum of 5,8-dibromo-1', 3', 3'-trimethylspiro [chromene-2,2'-indoline]	49
Figure 2.34. ¹ H-NMR spectrum of poly[1',3',3'-trimethylspiro(chromene-2,2'-indoline)-alt-(3,3'-dihexyl-2,2'-bithiophene).....	51
Figure 2.35. Optical absorbance of MC of thiophene substituted SP (a) in methanol (b) in toluene. All spectra are obtained upon irradiating 2×10 ⁻⁵ M solutions using a mercury arc lamp with a 334 nm line filter.....	53
Figure 2.36. Absorbance decay of MC peak in methanol at (a) 450 nm (b) 590 nm	53
Figure 2.37. Rough crystal structure of compound 15 (R1 = 0.10), the bond distances and angles are comparable to compound 1 of previously reported literature ²³ (a) Side view (b) Top view ...	56
Figure 2.38. UV-Vis spectra of polymer in toluene solution (black) and in thin film (red).....	58
Figure 2.39. (a) UV-Vis spectra of polymer in chloroform solution (black) and in thin film (red) (b) Optical absorbance of photomerocyanine the polymer in chloroform solution upon irradiating with mercury arc lamp with a 334 nm line filter.	59
Figure 3.1. ¹ H-NMR spectrum of 5-bromo-2,3,3-trimethyl-3H-indole.....	67
Figure 3.2. ¹³ C-NMR spectrum of 5-bromo-2,3,3-trimethyl-3H-indole.....	68
Figure 3.3. ¹ H-NMR spectrum of 1,2,3,3-tetramethyl-5-(thiophene-3-yl)-3H-indol-1-ium iodide.....	70
Figure 3.4. ¹³ C-NMR spectrum of 1,2,3,3-tetramethyl-5-(thiophene-3-yl)-3H-indol-1-ium iodide.....	70
Figure 3.5. Expanded ¹ H- ¹ H NOESY spectrum of 1,2,3,3-tetramethyl-5-(thiophene-3-yl)-3H-indol-1-ium iodide	71

Figure 3.6. Expanded ^1H - ^1H COSY spectrum of 1,2,3,3-tetramethyl-5-(thiophene-3-yl)-3H-indol-1-ium iodide	71
Figure 3.7. ^1H -NMR spectrum of 1',3'3'-trimethyl-6-nitro-5'-(thiophene-3-yl)spiro[chromene-2,2'-indoline]; peak assignment is based on 2D-NMR analysis.	73
Figure 3.8. ^{13}C -NMR spectrum of 1',3'3'-trimethyl-6-nitro-5'-(thiophene-3-yl)spiro[chromene-2,2'-indoline]	73
Figure 3.9. 2D-HSQC spectrum of 1',3'3'-trimethyl-6-nitro-5'-(thiophene-3-yl)spiro[chromene-2,2'-indoline]	74
Figure 3.10. Expanded 2D-HSQC spectrum of 1',3'3'-trimethyl-6-nitro-5'-(thiophene-3-yl)spiro[chromene-2,2'-indoline]	74
Figure 3.11. 2D-HMBC spectrum of 1',3'3'-trimethyl-6-nitro-5'-(thiophene-3-yl)spiro[chromene-2,2'-indoline]	75
Figure 3.12. Expanded ^1H - ^1H COSY spectrum of 1',3'3'-trimethyl-6-nitro-5'-(thiophene-3-yl)spiro[chromene-2,2'-indoline]	75
Figure 3.13. Expanded ^1H - ^1H NOESY spectrum of 1',3'3'-trimethyl-6-nitro-5'-(thiophene-3-yl)spiro[chromene-2,2'-indoline]	76
Figure 3.14. ^1H -NMR spectrum of 5'-(2-bromothiophen-3-yl)-1',3',3'-trimethyl-6-nitrospiro[chromene-2,2'-indoline] in comparison with 1',3'3'-trimethyl-6-nitro-5'-(thiophene-3-yl)spiro[chromene-2,2'-indoline] in downfield region	77
Figure 3.15. ^1H -NMR spectrum of 5'-(2-bromothiophen-3-yl)-1',3',3'-trimethyl-6-nitrospiro[chromene-2,2'-indoline] in comparison with 1',3'3'-trimethyl-6-nitro-5'-(thiophene-3-yl)spiro[chromene-2,2'-indoline] in upfield region	78
Figure 3.16. ^{13}C -NMR spectrum of 5'-(2-bromothiophen-3-yl)-1',3',3'-trimethyl-6-nitrospiro[chromene-2,2'-indoline]	78
Figure 3.17. Expanded ^1H - ^1H COSY spectrum of 5'-(2-bromothiophen-3-yl)-1',3',3'-trimethyl-6-nitrospiro[chromene-2,2'-indoline]	79
Figure 3.18. Expanded ^1H - ^1H NOESY spectrum of 5'-(2-bromothiophen-3-yl)-1',3',3'-trimethyl-6-nitrospiro[chromene-2,2'-indoline]	79
Figure 3.19. ^1H -NMR spectrum of 5'-([2,2'-bithiophene]-3-yl)-1',3',3'-trimethyl-6-nitrospiro[chromene-2,2'-indoline] in comparison with 5'-(2-bromothiophen-3-yl)-1',3',3'-trimethyl-6-nitrospiro[chromene-2,2'-indoline] in the downfield region	81

Figure 3.20. ¹ H-NMR spectrum of 5'-([2,2'-bithiophene]-3-yl)-1',3',3'-trimethyl-6-nitrospiro[chromene-2,2'-indoline] in comparison with 5'-(2-bromothiophen-3-yl)-1',3',3'-trimethyl-6-nitrospiro[chromene-2,2'-indoline] in the upfield region	81
Figure 3.21. ¹³ C-NMR spectrum of 5'-([2,2'-bithiophene]-3-yl)-1',3',3'-trimethyl-6-nitrospiro[chromene-2,2'-indoline]	82
Figure 3.22. Expanded ¹ H- ¹ H COSY spectrum of 5'-([2,2'-bithiophene]-3-yl)-1',3',3'-trimethyl-6-nitrospiro[chromene-2,2'-indoline]	82
Figure 3.23. Expanded ¹ H- ¹ H NOESY spectrum of 5'-([2,2'-bithiophene]-3-yl)-1',3',3'-trimethyl-6-nitrospiro[chromene-2,2'-indoline]	83
Figure 3.24. ¹ H-NMR spectrum of 5'-([2,2':5',2''-terthiophene]-3-yl)-1',3',3'-trimethyl-6-nitrospiro[chromene-2,2'-indoline] in comparison with 5'-(2-bromothiophen-3-yl)-1',3',3'-trimethyl-6-nitrospiro[chromene-2,2'-indoline] in the downfield region	84
Figure 3.25. ¹ H-NMR spectrum of 5'-([2,2':5',2''-terthiophene]-3-yl)-1',3',3'-trimethyl-6-nitrospiro[chromene-2,2'-indoline] in comparison with 5'-(2-bromothiophen-3-yl)-1',3',3'-trimethyl-6-nitrospiro[chromene-2,2'-indoline] in the upfield region	85
Figure 3.26. ¹³ C-NMR spectrum of 5'-([2,2':5',2''-terthiophene]-3-yl)-1',3',3'-trimethyl-6-nitrospiro[chromene-2,2'-indoline]	85
Figure 3.27. Expanded ¹ H- ¹ H COSY spectrum of 5'-([2,2':5',2''-terthiophene]-3-yl)-1',3',3'-trimethyl-6-nitrospiro[chromene-2,2'-indoline]	86
Figure 3.28. Expanded ¹ H- ¹ H NOESY spectrum of 5'-([2,2':5',2''-terthiophene]-3-yl)-1',3',3'-trimethyl-6-nitrospiro[chromene-2,2'-indoline]	86
Figure 3.29. ¹ H-NMR spectrum of 3,3'''-bis(1',3',3'-trimethyl-6-nitrospiro[chromene-2,2'-indolin]-5'-yl)-2,2':5',2'':5'',2'''-quaterthiophene	88
Figure 3.30. Expanded ¹ H- ¹ H COSY spectrum of 3,3'''-bis(1',3',3'-trimethyl-6-nitrospiro[chromene-2,2'-indolin]-5'-yl)-2,2':5',2'':5'',2'''-quaterthiophene	88
Figure 3.31. Expanded ¹ H- ¹ H NOESY spectrum of 3,3'''-bis(1',3',3'-trimethyl-6-nitrospiro[chromene-2,2'-indolin]-5'-yl)-2,2':5',2'':5'',2'''-quaterthiophene	89
Figure 3.32. ¹ H-NMR spectrum of [2,2'-bithiophene]-5-yltributylstannane	90
Figure 3.33. ¹³ C-NMR spectrum of [2,2'-bithiophene]-5-yltributylstannane	91
Figure 3.34. ¹ H-NMR spectrum of 5,5'-bis(trimethylstannyl)-2,2'-bithiophene	92

Figure 3.35. ^{13}C -NMR spectrum of 5,5'-bis(trimethylstannyl)-2,2'-bithiophene	92
Figure 3.36. ^1H -NMR spectrum of 5-bromo-1,2,3,3-tetramethyl-3H-indol-1-ium iodide	93
Figure 3.37. ^{13}C -NMR spectrum of 5-bromo-1,2,3,3-tetramethyl-3H-indol-1-ium iodide	94
Figure 3.38. ^1H -NMR spectrum of 5'-bromo-1',3',3'-trimethyl-6-nitrospiro[chromene-2,2'-indoline] in comparison with 1',3',3'-trimethyl-6-nitro-5'-(thiophene-3-yl)spiro[chromene-2,2'-indoline] in downfield region.....	95
Figure 3.39. ^1H -NMR spectrum of 5'-bromo-1',3',3'-trimethyl-6-nitrospiro[chromene-2,2'-indoline] in comparison with 1',3',3'-trimethyl-6-nitro-5'-(thiophene-3-yl)spiro[chromene-2,2'-indoline] in upfield region	96
Figure 3.40. ^{13}C -NMR spectrum of 5'-bromo-1',3',3'-trimethyl-6-nitrospiro[chromene-2,2'-indoline]	96
Figure 3.41. (a) Crystal structure and (b) partial unit cell representation of SP-T ($R[F2 > 2\sigma(F2)] = 0.050$).	98
Figure 3.42. Crystal structure of SP-T-Br indicating ratio between the two thiophene conformations in approximately 70:30 (the major conformation is indicated with solid bonds and the minor conformation is indicated with dashed bonds) ($R[F2 > 2\sigma(F2)] = 0.080$).	99
Figure 3.43. Isomerization of SP-T (a) Optical absorbance of photomerocyanine (MC) of SP-T (b) in methanol (c) in toluene. All spectra are obtained upon irradiating 1×10^{-5} M solutions using a mercury arc lamp with a 334 nm line filter.....	101
Figure 3.44. Maximum optical absorbance of photomerocyanine (a) in methanol (b) in toluene. All spectra are obtained upon irradiating 1×10^{-5} M solutions using a mercury arc lamp with a 334 nm line filter.....	101
Figure 3.45. Comparison of maximum optical absorbance of photomerocyanines in methanol and in toluene, all spectra are obtained upon irradiating 1×10^{-5} M solutions using a mercury arc lamp with a 334 nm line filter.....	103
Figure 3.46. Absorbance decay of photochromic peak in methanol.....	104
Figure 3.47. Absorbance decay of photochromic peak in toluene.....	105
Figure 3.48. ^1H -NMR analysis of the dibrominated compounds of SP-T in downfield region ..	108
Figure 3.49. (a) Crystal structure and (b) partial unit cell representation of tribrominated compound ($R[F2 > 2\sigma(F2)] = 0.065$).....	109

Figure 4.1. ^1H NMR spectrum of 3-hexylthiophene	120
Figure 4.2. ^{13}C NMR spectrum of 3-hexylthiophene.....	120
Figure 4.3. ^1H NMR spectrum of 2-bromo-3-hexylthiophene.....	121
Figure 4.4. ^{13}C NMR spectrum of 2-bromo-3-hexylthiophene.....	122
Figure 4.5. ^1H NMR spectrum of 3-(2-(2-(2-methoxyethoxy)ethoxy)ethoxy)thiophene	123
Figure 4.6. ^{13}C NMR spectrum of 3-(2-(2-(2-methoxyethoxy)ethoxy)ethoxy)thiophene	124
Figure 4.7. ^1H NMR spectrum of 2-bromo-3-(2-(2-(2-methoxyethoxy)ethoxy)ethoxy) thiophene.....	125
Figure 4.8. ^{13}C NMR spectrum of 2-bromo-3-(2-(2-(2-methoxyethoxy)ethoxy)ethoxy) thiophene.....	126
Figure 4.9. ^1H NMR spectrum of 3-hexyl-3'-(2-(2-(2-methoxyethoxy)ethoxy)ethoxy) bithiophene.....	127
Figure 4.10. ^{13}C NMR spectrum of 3-hexyl-3'-(2-(2-(2-methoxyethoxy)ethoxy)ethoxy) bithiophene.....	128
Figure 4.11. ^1H NMR spectrum of 2-bromo-3-hexyl-3'-(2-(2-(2-methoxyethoxy)ethoxy)ethoxy) bithiophene.....	129
Figure 4.12. ^{13}C NMR spectrum of 2-bromo-3-hexyl-3'-(2-(2-(2-methoxyethoxy)ethoxy)ethoxy) bithiophene.....	130
Figure 4.13. HSQC spectrum of 2-bromo-3-hexyl-3'-(2-(2-(2-methoxyethoxy)ethoxy)ethoxy) bithiophene.....	130
Figure 4.14. HMBC spectrum of 2-bromo-3-hexyl-3'-(2-(2-(2-methoxyethoxy)ethoxy)ethoxy) bithiophene.....	131
Figure 4.15. ^1H -NMR spectrum of poly[3-hexyl-3'-(2-(2-(2-methoxyethoxy)ethoxy)ethoxy) bithiophene]	132
Figure 4.16. Cyclic voltamogram of the polymer.....	134
Figure 4.17. UV-vis spectra of polymer in chloroform solution (black) and in thin film (red) (b) solution UV-Vis spectra of the polymer in THF and THF/water mixtures. (c) TEM images of the	

polymer drop-casted from (c) chloroform (d) THF/water (3:2) solvent mixture with 0.30 mg mL ⁻¹	136
Figure 4.18. DLS analysis of the polymer in chloroform	137
Figure 4.19. (a) GIWAXS data from a film of the polymer. (b) GIWAXS intensity vs scattering vector q. Both azimuthally-averaged data and in-plane line cuts are shown.....	138
Figure 4.20. (a) GIWAXS data in-plane and out of plane intensities (b) GISAXS data for the polymer	139
Figure 4.21. TGA thermogram of the polymer.....	140
Figure 4.22. DSC analysis of the polymer at 10 °C min ⁻¹	140
Figure 4.23. (a) Output curves of the polymer at different gate voltages (I _D Vs. V _D curves) (b) I _D Vs V _G (c) saturation mobility	142
Figure 4.24. Fitting lines of I-V ² curves for the calculation of charge mobility in pure polymer with the SCLC model in Schottky diodes.....	142
Figure 4.25. Transmittance of the polymer compared with that of PEDOT: PSS.....	144

LIST OF TABLES

Table 2.1. Half-lives of MC decay in methanol ^a	53
Table 3.1. Half-lives and rate of SP decay in various solvents ^a	106
Table 3.2. Photodegradation of SP in methanol ^a	106
Table 4.1. Molecular weights and optoelectronic properties of the polymer	134
Table 4.2. Conductivity of the polymer upon doping with iodine vapor and stability of doped films on air	143

LIST OF SCHEMES

Scheme 2.1. Synthesis of <i>tert</i> -butyl(2,5-dibromophenoxy)dimethylsilane	19
Scheme 2.2. Synthesis of <i>tert</i> -butyl(2,5-di(thiophene-2-yl)phenoxy)dimethylsilane	21
Scheme 2.3. Synthesis of 2,5-di(thiophen-2-yl)phenol	22
Scheme 2.4 Synthesis of 2-hydroxy-3,6-di(thiophen-2-yl)benzaldehyde	25
Scheme 2.5. Synthesis of 1',3'3'-trimethyl-5,8-di(thiophen-2-yl)spiro[chromene-2,2'-indoline]	27
Scheme 2.6. Synthesis of methyl 3-(2methoxy-2-oxoethylthio)propanoate	30
Scheme 2.7. Synthesis of methyl 4-oxotetrahydrothiophene-3-carboxylate	30
Scheme 2.8. Synthesis of methyl 4-acetoxythiophene-3-carboxylate (2).....	33
Scheme 2.9. Synthesis of methyl 4-hydroxythiophene-3-carboxylate	35
Scheme 2.10. Synthesis of methyl 4-((<i>tert</i> -butyldimethylsilyl)oxy)thiophene-3-carboxylate	37
Scheme 2.11. Synthesis of 4-((<i>tert</i> -butyldimethylsilyl)oxo)thiophene-3-yl)methanol	39
Scheme 2.12. Synthesis of 4-((<i>tert</i> -butyldimethylsilyl)oxy)thiophene-3-carbaldehyde.....	41
Scheme 2.13. Synthesis of 5-bromo-4-((<i>tert</i> -butyldimethylsilyl)oxy)thiophene-3-carbaldehyde	42
Scheme 2.14. Synthesis of 2,5-dibromo-4-((<i>tert</i> -butyldimethylsilyl)oxy)thiophene-3-carbaldehyde	43
Scheme 2.15. Synthesis of 3,6-dibromo-2-hydroxybenzaldehyde	45
Scheme 2.16. Synthesis of 5,8-dibromo-1', 3', 3'-trimethylspiro[chromene-2,2'-indoline].....	47
Scheme 2.17. Synthesis of poly[1',3',3'-trimethylspiro(chromene-2,2'-indoline)-alt-(3,3'-dihexyl-2,2'-bithiophene)].....	50
Scheme 2.18. Synthesis of thiophene substituted SP.....	52
Scheme 2.19. Synthesis of thiophene based aromatic diester.....	54

Scheme 2.20. Synthesis of the dibrominated silyl ether protected ortho-hydroxy aromatic aldehyde of thiophene	55
Scheme 2.21. Synthesis of benzene based photochromic SP	57
Scheme 2.22. SP Polymer synthesis	57
Scheme 2.23. A possible route to obtain dibrominated derivative of SP	60
Scheme 3.1. Synthesis of 5-bromo-2,3,3-trimethyl-3H-indole.....	66
Scheme 3.2. Synthesis of 1,2,3,3-tetramethyl-5-(thiophene-3-yl)-3H-indol-1-ium iodide	68
Scheme 3.3. Synthesis of 1',3',3'-trimethyl-6-nitro-5'-(thiophene-3-yl)spiro[chromene-2,2'-indoline]	72
Scheme 3.4. Synthesis of 5'-(2-bromothiophen-3-yl)-1',3',3'-trimethyl-6-nitrospiro[chromene-2,2'-indoline]	76
Scheme 3.5. Synthesis of 5'-([2,2'-bithiophene]-3-yl)-1',3',3'-trimethyl-6-nitrospiro[chromene-2,2'-indoline].....	80
Scheme 3.6. Synthesis of 5'-([2,2':5',2''-terthiophene]-3-yl)-1',3',3'-trimethyl-6-nitrospiro [chromene-2,2'-indoline]	83
Scheme 3.7. Synthesis of 3,3'''-bis(1',3',3'-trimethyl-6-nitrospiro[chromene-2,2'-indolin]-5'-yl)-2,2':5',2'':5'',2'''-quaterthiophene.....	87
Scheme 3.8. Synthesis of [2,2'-bithiophene]-5-yltributylstannane	89
Scheme 3.9. Synthesis of 5,5'-bis(trimethylstannyl)-2,2'-bithiophene	91
Scheme 3.10. Synthesis of 5-bromo-1,2,3,3-tetramethyl-3H-indol-1-ium iodide	93
Scheme 3.11. Synthesis of 5'-bromo-1',3',3'-trimethyl-6-nitrospiro[chromene-2,2'-indoline]	94
Scheme 3.12. Synthesis of SP-T	97
Scheme 3.13. Synthesis of SP-T-Br.....	99
Scheme 3.14. Synthesis of SP-T-T, SP-T-T-T and SP-T-T-T-T-SP	100
Scheme 3.15. Dibrominated derivatives of SP-T.....	107

Scheme 4.1. Synthesis of 3-hexylthiophene	119
Scheme 4.2. Synthesis of 2-bromo-3-hexylthiophene	121
Scheme 4.3. Synthesis of 3-(2-(2-(2-methoxyethoxy)ethoxy)ethoxy)thiophene	122
Scheme 4.4. Synthesis of 2-bromo-3-(2-(2-(2-methoxyethoxy)ethoxy)ethoxy)thiophene	124
Scheme 4.5. Synthesis of 3-hexyl-3'-(2-(2-(2-methoxyethoxy)ethoxy)ethoxy)bithiophene	126
Scheme 4.6. Synthesis of 2-bromo-3-hexyl-3'-(2-(2-(2-methoxyethoxy)ethoxy)ethoxy) bithiophene.....	128
Scheme 4.7. Synthesis of poly[3-hexyl-3'-(2-(2-(2-methoxyethoxy)ethoxy)ethoxy) bithiophene]	131

CHAPTER 1

THIOPHENE BASED CONJUGATED MATERIALS

1.1 Abstract

This chapter introduces thiophene based conjugated materials and their electronic properties including band structure, conductivity and charge transport mechanism. Organic field effect transistor applications in obtaining electrical parameters of these materials is also discussed. Further, the effect of functionalization of thiophene based materials with photochromic spiropyrans and alkoxy groups with respect to organic electronic applications is discussed.

1.2 Role of thiophene in materials chemistry

Functionalized derivatives of thiophenes or nitrogen heterocycles such as carbazoles, pyrroles and pyridines are compounds that show immense contribution for the development of materials chemistry targeting new technologies. These heterocycle based conjugated polymers are attractive due to the solution processability, light weight, good flexibility, easy fabrication, better charge transporting properties and hence, makes them ideal candidates to the new research world of plastic electronics.¹⁻³

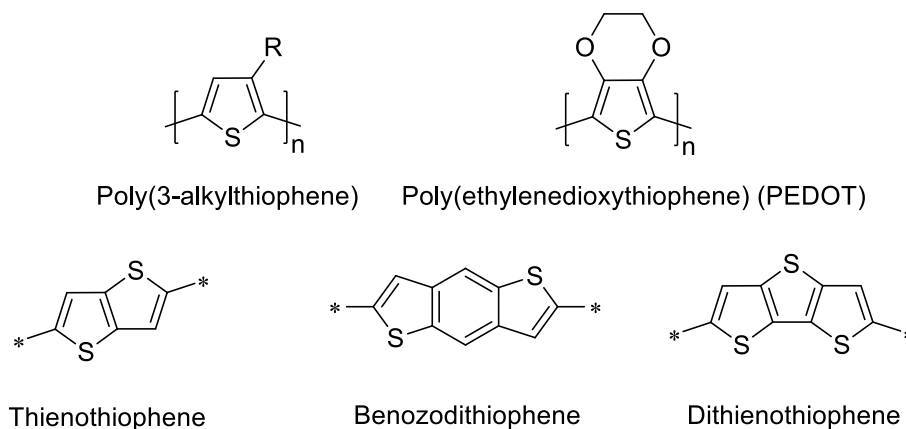


Figure 1.1. Some of the important PTs and thiophene derivatives in organic electronics

Elsenbaumer *et al.* reported the first solution processable and environmentally stable polythiophene (PT) in 1986.⁴ Since then, PTs evolved in many ways through functionalization.

Poly(alkylthiophene)s such as poly(3-hexylthiophene), abbreviated as P3HT and poly(alkoxythiophene)s such as poly(ethylenedioxythiophene), abbreviated as PEDOT are considered to be widely studied among PTs (figure 1.1).⁵⁻⁷ Other derivatives of thiophenes are also important in applications such as organic electronics and figure 1.1 illustrates some of the important PTs and thiophene derivatives.^{8,9}

1.3 Energy bands and conductivity in conjugated materials

The conjugation or the resonance interaction between the π -bonds results in delocalized π electron states. When the number of connected repeating units is very high, like in a long polymer chain, this phenomenon generates densely packed energy states.¹⁰ The highest occupied molecular π orbital is abbreviated as the HOMO and the lowest unoccupied molecular π orbital is abbreviated as the LUMO. Tuning the band gap between HOMO and LUMO is carried out through the functionalization of the conjugated systems. Electron donating substituents on monomer units raises the HOMO energy level while the electron withdrawing substituents lower the LUMO energy level. Furthermore, realization of donor-acceptor concept in conjugated systems facilitated the tuning of the energy levels into a new era.^{9,11} Schematic diagram of band gap structure for semiconducting materials is given in figure 1.2.

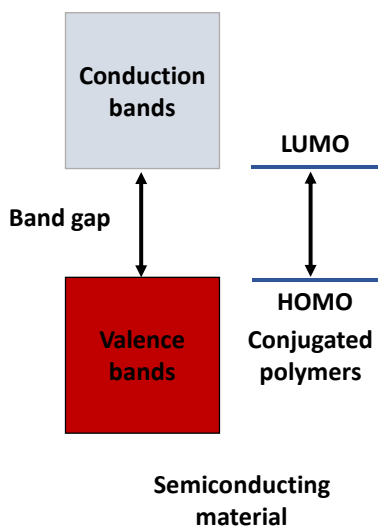


Figure 1.2. Schematic diagram of band gap structure for semiconducting materials

The polymers having conjugated double bonds are intrinsically conducting and in undoped state have a large bandgap of 3 – 6 eV between HOMO and LUMO and hence, show low conductivities of $10^{-7} - 10^{-11} \text{ S cm}^{-1}$. Doping reduces this band gap to 1 – 4 eV and elevation of electrons to the LUMO conduction band from the HOMO valance band show wide range of conductivity $10^{-5} - 10^3 \text{ S cm}^{-1}$ transforming a non-conducting or low conducting polymer to a semiconducting or even metallic conducting one.¹⁰

The doping in conjugated materials can be achieved through several methods, such as electrochemical doping (p-doping via electrochemical oxidation and n-doping via electrochemical reduction). The charge of the polymer gained through doping is balanced by counterion diffusion from the electrolyte into (or out of) the thin film during charging and discharging. This method leads to precise control of the doping level by the applied voltage.¹² Other doping methods include chemical doping (use of oxidation or reducing agents has a poor control over the doping level), radiation induced doping or photo-doping (material is locally oxidized and reduced by photo-absorption) and charge injection doping (electrons and holes injected from suitable metal contact directly into the π^* and π bands).^{10,13} Charge injection doping mechanism with respect to the organic field effect transistor applications will be discussed later in this chapter.

1.4 Charge transport in conjugated materials

In practice, charge transport in conjugated materials are dramatically affected by processing conditions, which can cause variation in morphology, microstructure, molecular packing and alignment of the material.¹⁴ Charge transport models developed for organic semiconductors have been developed to gain general properties of the charge transport mechanisms in conjugated materials. Charge carriers are radical cations (in oligomers) or polarons (the association of the charge with the induced deformation of the polymer chain, figure 1.3). Due to the weak *van der waals* interactions in conjugated polymers, charge transport is mainly due to the slow phonon assisted hopping mechanism. The key parameter for studying charge transport is the mobility μ .^{13,15}

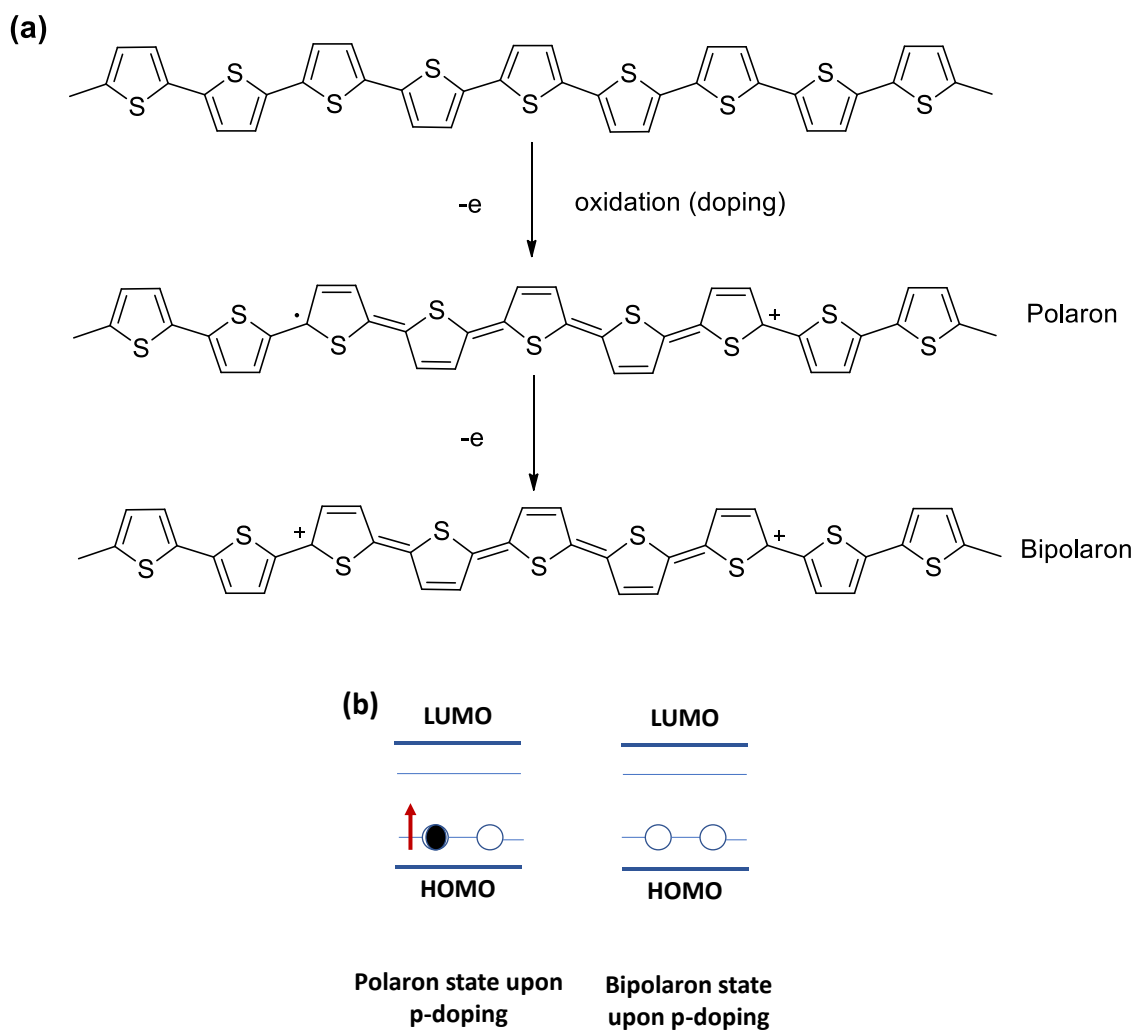


Figure 1.3. (a) Polaron and bipolaron formation in polythiophene (b) schematic diagram of polaron and bipolaron states

1.5 Organic field-effect transistor (OFET) measurements

Field-effect transistors allow charge injection doping in organic semiconducting materials and eventually the charge carrier mobility can be calculated.¹⁶ Charge carrier mobility measurements described in this thesis are based on bottom-gate bottom-contact architecture as shown in figure 1.4. OFETs are three-terminal devices, in which a voltage applied to the gate electrode controls the current flow between the source and the drain electrode under an imposed bias. V_G and V_D are the applied gate voltage and source-drain voltage respectively.

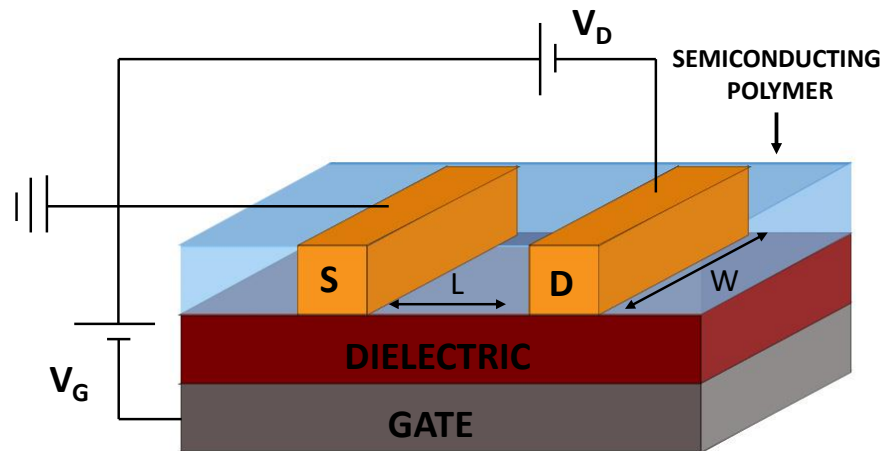


Figure 1.4. Bottom-gate bottom-contact OFETs architecture

In OFETs devices, gate/insulator assembly consists of a metal or doped semiconductor gate electrode coated with an insulating dielectric (typically thermally grown silicon dioxide or polymer insulators with 200-400 nm thickness). Metallic source and drain electrodes are often deposited via conventional photolithography. The organic thin-film is deposited on top of the devices through drop-casting or spin-casting.

The field-effect phenomenon of the devices is shown in figure 1.5. When a negative bias is applied to the gate electrode, HOMO and LUMO levels of the organic semiconducting material shifts up such that the HOMO becomes resonate with the Fermi level of the metal contact and electron spill out of the semiconducting material into the contacts, leaving positively charged holes in the semiconducting material. When a drain voltage is applied, these holes become the mobile charges and a drain source current (I_D) can be measured. Depending on the type of charge carriers (hole or electron), organic semiconductors are classified as p-type or n-type and the gate voltage bias is negative and positive respectively.¹⁷

Characterization of the OFETs can be performed in two ways, I_D - V_D or output curves (holding V_G constant while sweeping V_D) and I_D - V_G or transfer curves (holding the V_D constant while sweeping V_G). The threshold gate voltage (V_T) is the minimum gate voltage necessary to induce a current. I-V characteristics of a typical OFET in saturation is given by the equation 1.1.

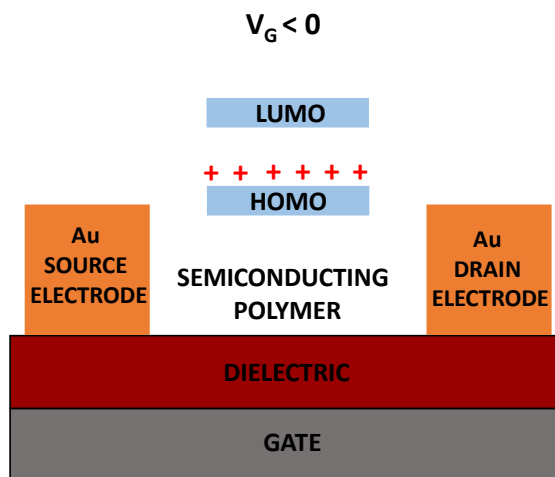


Figure 1.5. The field- effect phenomenon in OFETs under negative gate bias

$$I_{D,sat} = \frac{W}{2L} C \mu_{sat} (V_G - V_T)^2 \quad (1.1)$$

Where $I_{D,sat}$ - drain current in the saturation regime, W – channel width, L – channel length, C – capacitance of the insulating dielectric material per unit area, μ_{sat} – charge carrier mobility in saturation regime, V_G – gate voltage and V_T – threshold voltage. According to equation 1.1, device mobility can be calculated from the slope of the line drawn through the linear part of an $I_{D,sat}^{1/2}$ vs V_G plot and threshold voltage is given by the ratio of the intercept and slope. Another parameter which can be obtained by the OFETs is the on/off ratio (the ratio of the current in the ‘on’ and ‘off’ state), and is an indicative of the switching performance of OFETs.^{17,18}

1.6 Photochromic spiropyrans in OFETs

Photochromism is the ability of a molecule to undergo reversible structural changes upon absorption of light.¹⁹ Photochromic compounds attract considerable attention in organic electronics as light is an ideal and selective external trigger signal. Common photochromic systems studied in organic transistor applications are given in figure 1.6.²⁰⁻²² Spiropyrans (SPs) tend to absorb light in the range of 200-400 nm, which can produce the bond cleavage resulting in an open merocyanine form and the reversibility of this transformation is normally attained either thermally or photochemically (figure 1.6a).¹⁹ The mechanism of photochemical isomerization of SP is

shown in figure 1.7. In order to increase the thermal stability of the open merocyanine form, electron donating groups (R groups) are attached to the indoline moiety while electron withdrawing groups such as nitro groups are attached to the chromene moiety. Diarylethenes show ring closing and opening isomerization and are thermally irreversible, and resistant to photo fatigue but the isomerization is accompanied by a relatively small change in molecular conformation (figure 1.6b).²³ Azobenzenes, on the other hand, are structurally simple and readily accessed synthetically, but the *trans-cis* isomerization is quantitatively low (figure 1.6c).²⁴ Among different classes of photochromic materials, indoline SPs are notable for their high sensitivity (towards thermo, photo, acidic and ionic multi-responsive systems), resolving power, exhibiting photochromic properties in solution, in polymeric matrices and even in solid states, which are very convenient for their practical applications.²⁵⁻²⁷ Another unique feature of SPs is that the photoisomerization initiates a significant change in the electric dipole moment of SPs between closed and open forms (6.4 D for SP-closed and 13.9 D for MC-open) which is useful in macroscopic scale switchable molecular devices.^{28,29}

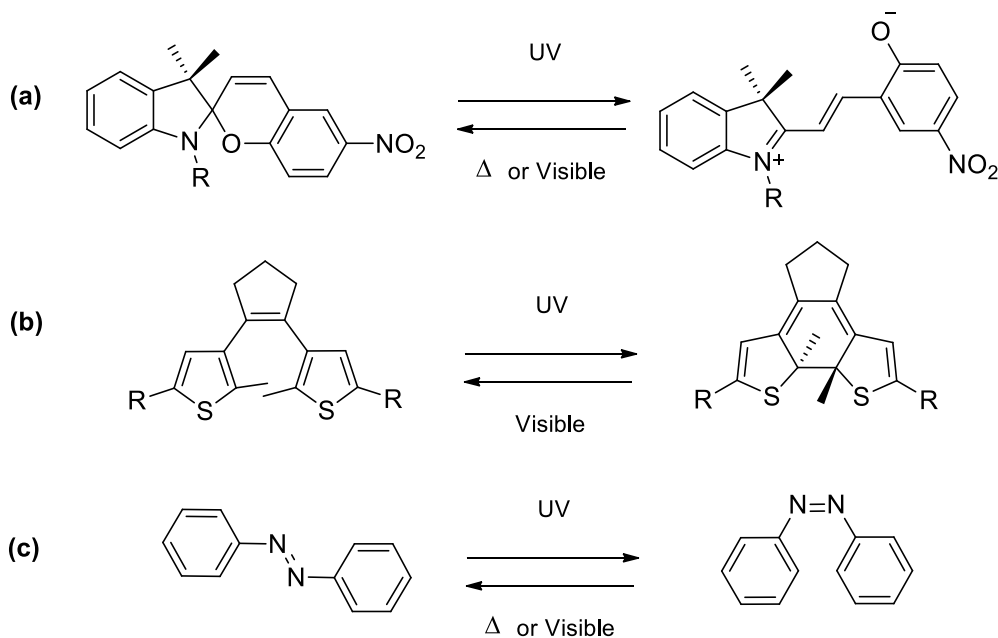


Figure 1.6. Photochromism in (a) spiropyrans (b) diarylethenes (c) azobenzenes

The growing interest of using these materials in organic electronic devices is evident by the number of recent reviews published in this field.²⁰⁻²² The studies reported so far on SP based OFETs are mainly based on blending approach of SP with organic semiconducting material in which phase separation is a major issue.^{28,30-32} SPs are notable among different classes of photochromic compounds due to their large structural and electronic transformation upon isomerization. In order to parlay these electronic differences associated with the two forms into materials based switch, the SP ultimately requires a covalent attachment through a conjugated pathway.

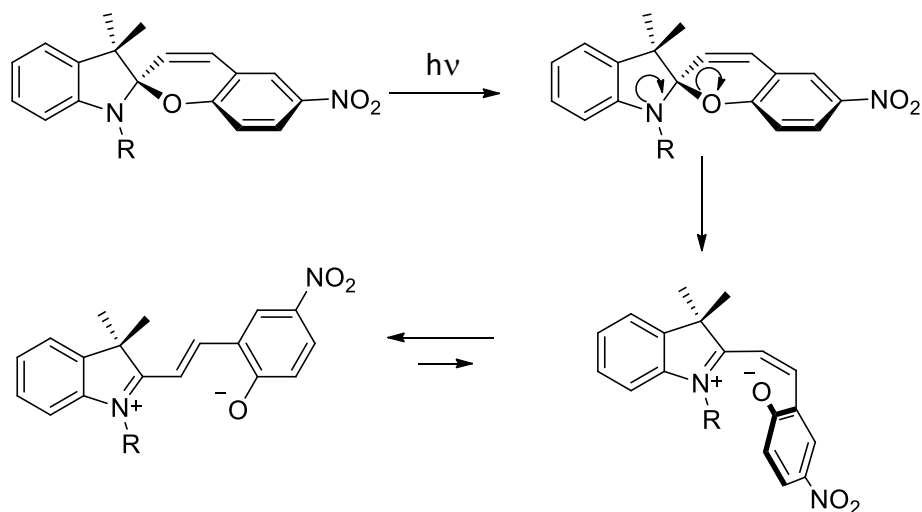


Figure 1.7. Mechanism of photochemical isomerization of SP²⁷

1.7 Thiophene based spiropyran materials

In the literature, very limited attempts have been made to incorporate thiophene into SPs. Attachment of thiophene into indoline nitrogen has been carried out via nucleophilic substitutions using (halogenoalkyl)thiophene as given in figure 1.8 (a and b). Longer alkyl chains showed better thermal stability of the open form.³³ Electrochemical polymerization has also been used to incorporate thiophene into SP based polymers (figure 1.8c);^{34,35} however, this method is not useful in obtaining photochromic polymers as oxidation of the SP at the indoline nitrogen below 0.8 V leads to isomers of oxidized MC, which limit the photochemical behavior of polymer films.³⁴ These attempts show the need of developing new synthetic methodologies to incorporate photochromic SP in to thiophene based materials via a conjugated pathway and such attempts are discussed in chapter 2 and 3.

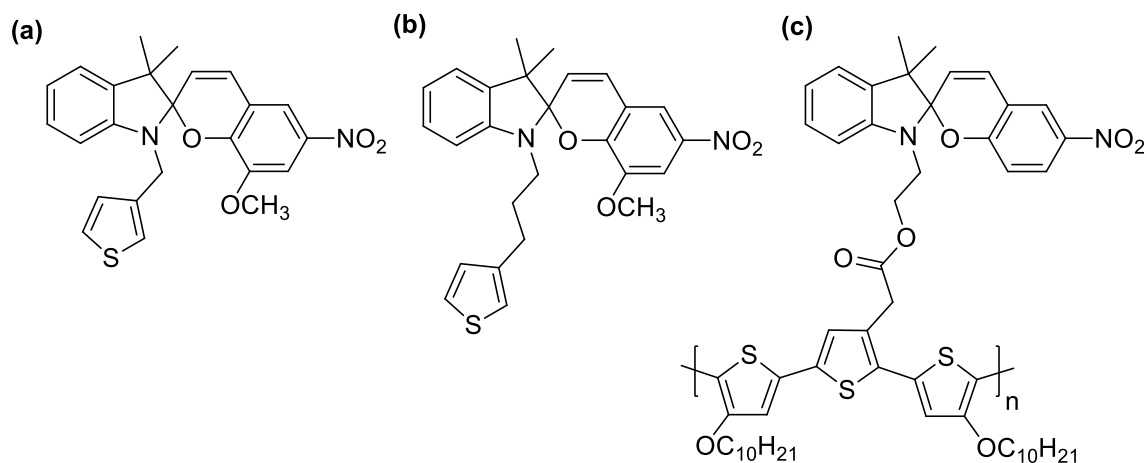


Figure 1.8. SP based thiophene materials

1.8 Poly(3-alkoxythiophene)s

Poly(alkylthiophene) based polymers are well established and widely studied in the field of OFETs.³⁶⁻³⁸ Poly(alkoxythiophene)s are another class of PTs with interesting properties and applications in organic electronics. Incorporation of alkoxy groups in polythiophenes led to polymers with very low oxidation potentials and low band gaps due to the electron donating nature of alkoxy groups. Furthermore, these polymers show highly stable conductivity over time.³⁹⁻⁴¹ PEDOT is one of the widely studied poly(alkoxythiophene)s which shows very high conductivity, stability in the oxidized state and ability to form almost transparent thin films (figure 1.1).⁷ poly(3,4- ethylenedioxythiophene): poly(styrenesulfonate) (PEDOT:PSS) is a commercially available conducting polymer used in organic photovoltaic applications and organic light emitting diode applications as a hole transporting layer.⁴²⁻⁴⁴

The acidity and hygroscopicity are major disadvantages associated with PEDOT:PSS which negatively impacted the stability of the devices;⁴⁵⁻⁴⁷ therefore, developing new materials with high conductivity, stability and processability are becoming important. Recently, ethylene glycol mediated poly(alkoxythiophene)s in organic electrochemical transistors targeting bioelectronic applications (figure 1.9a) and as materials of high conductivity, processability and thermal stability through solution doping (figure 1.9b) have been reported.^{48,49}

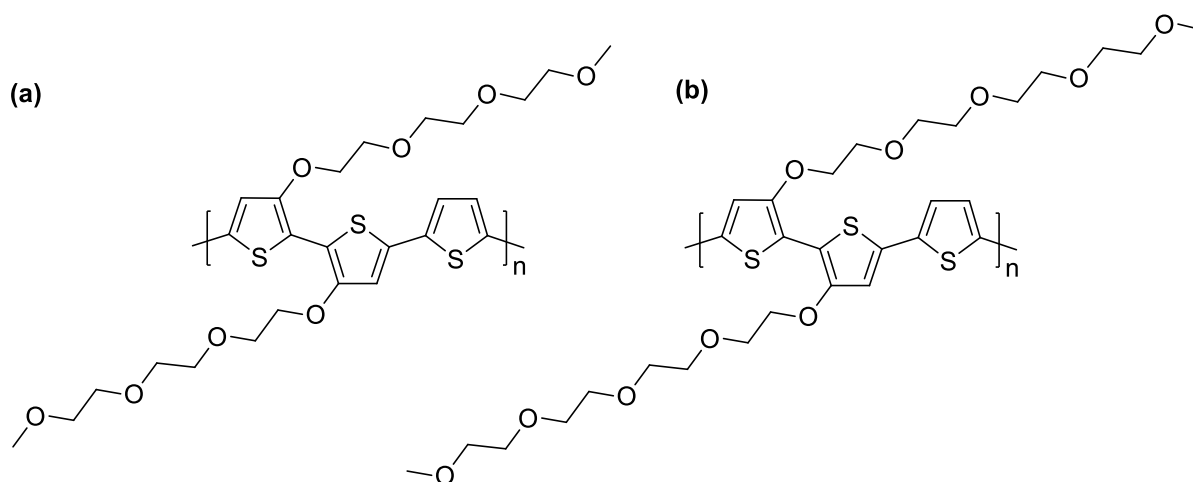


Figure 1.9. Recent reports on ethylene glycol mediated poly(alkoxythiophene)s

The application of ethylene glycol mediated poly(alkoxythiophene)s in organic field effect transistor applications will allow us to study the electrical properties of these materials and design new strategies to develop them further. Chapter 4 discuss the functionalization of polythiophene with triethylene glycol monomethyl ether targeting organic electronic applications.

1.9 References

1. Baeg, K.-J.; Caironi, M.; Noh, Y.-Y. Toward Printed Integrated Circuits based on Unipolar or Ambipolar Polymer Semiconductors. *Advanced Materials* **2013**, *25*, 4210-4244.
2. Forrest, S. R. The path to ubiquitous and low-cost organic electronic appliances on plastic. *Nature* **2004**, *428*, 911-918.
3. Arias, A. C.; MacKenzie, J. D.; McCulloch, I.; Rivnay, J.; Salleo, A. Materials and Applications for Large Area Electronics: Solution-Based Approaches. *Chemical Reviews* **2010**, *110*, 3-24.
4. Elsenbaumer, R. L.; Jen, K. Y.; Oboodi, R. Processible and environmentally stable conducting polymers. *Synthetic Metals* **1986**, *15*, 169-174.
5. McCullough, R. D. The Chemistry of Conducting Polythiophenes. *Advanced Materials* **1998**, *10*, 93-116.
6. Ewbank, P. C.; Stefan, M. C.; Sauvé, G.; McCullough, R. D.: Synthesis, Characterization and Properties of Regioregular Polythiophene-Based Materials. In *Handbook of Thiophene-Based Materials*; John Wiley & Sons, Ltd, 2009; pp 157-217.

7. Groenendaal, L.; Jonas, F.; Freitag, D.; Pielartzik, H.; Reynolds, J. R. Poly(3,4-ethylenedioxythiophene) and Its Derivatives: Past, Present, and Future. *Advanced Materials* **2000**, *12*, 481-494.
8. Bundgaard, E.; Helgesen, M.; Carlé, J. E.; Krebs, F. C.; Jørgensen, M. Advanced Functional Polymers for Increasing the Stability of Organic Photovoltaics. *Macromolecular Chemistry and Physics* **2013**, *214*, 1546-1558.
9. Cinar, M. E.; Ozturk, T. Thienothiophenes, Dithienothiophenes, and Thienoacenes: Syntheses, Oligomers, Polymers, and Properties. *Chemical Reviews* **2015**, *115*, 3036-3140.
10. Kar, P.: *Polymer Science and Plastics Engineering : Doping in Conjugated Polymers (1)*; Wiley-Scrivener: Somerset, US, 2013.
11. Swager, T. M. 50th Anniversary Perspective: Conducting/Semiconducting Conjugated Polymers. A Personal Perspective on the Past and the Future. *Macromolecules* **2017**.
12. Heinze, J.; Frontana-Uribe, B. A.; Ludwigs, S. Electrochemistry of Conducting Polymers—Persistent Models and New Concepts. *Chemical Reviews* **2010**, *110*, 4724-4771.
13. Petty, M. C.: Electrical Conductivity. In *Molecular Electronics*; John Wiley & Sons, Ltd, 2007; pp 65-128.
14. Dong, H.; Hu, W. Multilevel Investigation of Charge Transport in Conjugated Polymers. *Accounts of Chemical Research* **2016**, *49*, 2435-2443.
15. Horowitz, G.; Delannoy, P.: Charge Transport in Semiconducting Oligothiophenes. In *Handbook of Oligo- and Polythiophenes*; Wiley-VCH Verlag GmbH, 2007; pp 283-316.
16. Horowitz, G. Organic Field-Effect Transistors. *Advanced Materials* **1998**, *10*, 365-377.
17. Newman, C. R.; Frisbie, C. D.; da Silva Filho, D. A.; Brédas, J.-L.; Ewbank, P. C.; Mann, K. R. Introduction to Organic Thin Film Transistors and Design of n-Channel Organic Semiconductors. *Chemistry of Materials* **2004**, *16*, 4436-4451.
18. Reese, C.; Roberts, M.; Ling, M.-m.; Bao, Z. Organic thin film transistors. *Materials Today* **2004**, *7*, 20-27.
19. Bouas-Laurent, H.; Dürr, H.: Organic photochromism (IUPAC Technical Report). In *Pure and Applied Chemistry*, 2001; Vol. 73; pp 639.
20. Orgiu, E.; Samorì, P. 25th Anniversary Article: Organic Electronics Marries Photochromism: Generation of Multifunctional Interfaces, Materials, and Devices. *Advanced Materials* **2014**, *26*, 1827-1845.

21. Wakayama, Y.; Hayakawa, R.; Seo, H.-S. Recent progress in photoactive organic field-effect transistors. *Science and Technology of Advanced Materials* **2014**, *15*, 024202.
22. Fu, L.-N.; Leng, B.; Li, Y.-S.; Gao, X.-K. Photoresponsive organic field-effect transistors involving photochromic molecules. *Chinese Chemical Letters* **2016**, *27*, 1319-1329.
23. Irie, M. Diarylethenes for Memories and Switches. *Chemical Reviews* **2000**, *100*, 1685-1716.
24. Bandara, H. M. D.; Burdette, S. C. Photoisomerization in different classes of azobenzene. *Chemical Society Reviews* **2012**, *41*, 1809-1825.
25. Minkin, V. I. Photo-, Thermo-, Solvato-, and Electrochromic Spiroheterocyclic Compounds. *Chemical Reviews* **2004**, *104*, 2751-2776.
26. Ercole, F.; Davis, T. P.; Evans, R. A. Photo-responsive systems and biomaterials: photochromic polymers, light-triggered self-assembly, surface modification, fluorescence modulation and beyond. *Polymer Chemistry* **2010**, *1*, 37-54.
27. Klajn, R. Spiropyran-based dynamic materials. *Chemical Society Reviews* **2014**, *43*, 148-184.
28. Li, Y.; Zhang, H.; Qi, C.; Guo, X. Light-driven photochromism-induced reversible switching in P3HT-spiropyran hybrid transistors. *Journal of Materials Chemistry* **2012**, *22*, 4261-4265.
29. Toman, P.; Bartkowiak, W.; Nešpůrek, S.; Sworakowski, J.; Zaleśny, R. Quantum-chemical insight into the design of molecular optoelectrical switch. *Chemical Physics* **2005**, *316*, 267-278.
30. Ishiguro, Y.; Hayakawa, R.; Chikyow, T.; Wakayama, Y. Optical switching of carrier transport in polymeric transistors with photochromic spiropyran molecules. *Journal of Materials Chemistry C* **2013**, *1*, 3012-3016.
31. Ishiguro, Y.; Hayakawa, R.; Yasuda, T.; Chikyow, T.; Wakayama, Y. Unique Device Operations by Combining Optical-Memory Effect and Electrical-Gate Modulation in a Photochromism-Based Dual-Gate Transistor. *ACS Applied Materials & Interfaces* **2013**, *5*, 9726-9731.
32. Ishiguro, Y.; Hayakawa, R.; Chikyow, T.; Wakayama, Y. Optically Controllable Dual-Gate Organic Transistor Produced via Phase Separation between Polymer Semiconductor and Photochromic Spiropyran Molecules. *ACS Applied Materials & Interfaces* **2014**, *6*, 10415-10420.
33. Moustrou, C.; Samat, A.; Guglielmetti, R.; Dubest, R.; Garnier, F. Synthesis of Thiophene-Substituted Spiroyrans and Spirooxazines, Precursors of Photochromic Polymers. *Helvetica Chimica Acta* **1995**, *78*, 1887-1893.

34. Wagner, K.; Byrne, R.; Zanoni, M.; Gambhir, S.; Dennany, L.; Breukers, R.; Higgins, M.; Wagner, P.; Diamond, D.; Wallace, G. G.; Officer, D. L. A Multiswitchable Poly(terthiophene) Bearing a Spiropyran Functionality: Understanding Photo- and Electrochemical Control. *Journal of the American Chemical Society* **2011**, *133*, 5453-5462.
35. Wagner, K.; Zanoni, M.; Elliott, A. B. S.; Wagner, P.; Byrne, R.; Florea, L. E.; Diamond, D.; Gordon, K. C.; Wallace, G. G.; Officer, D. L. A merocyanine-based conductive polymer. *Journal of Materials Chemistry C* **2013**, *1*, 3913-3916.
36. Sirringhaus, H. 25th Anniversary Article: Organic Field-Effect Transistors: The Path Beyond Amorphous Silicon. *Advanced Materials* **2014**, *26*, 1319-1335.
37. Tsao, H. N.; Mullen, K. Improving polymer transistor performance via morphology control. *Chemical Society Reviews* **2010**, *39*, 2372-2386.
38. Sirringhaus, H. Device Physics of Solution-Processed Organic Field-Effect Transistors. *Advanced Materials* **2005**, *17*, 2411-2425.
39. Faid, K.; Cloutier, R.; Leclerc, M. Design of novel electroactive polybithiophene derivatives. *Macromolecules* **1993**, *26*, 2501-2507.
40. Chen, S. A.; Tsai, C. C. Structure/properties of conjugated conductive polymers. 2. 3-Ether-substituted polythiophenes and poly(4-methylthiophenes). *Macromolecules* **1993**, *26*, 2234-2239.
41. Sheina, E. E.; Khersonsky, S. M.; Jones, E. G.; McCullough, R. D. Highly Conductive, Regioregular Alkoxy-Functionalized Polythiophenes: A New Class of Stable, Low Band Gap Materials. *Chemistry of Materials* **2005**, *17*, 3317-3319.
42. Li, G.; Zhu, R.; Yang, Y. Polymer solar cells. *Nature Photonics* **2012**, *6*, 153-161.
43. Kim, Y. H.; Sachse, C.; Machala, M. L.; May, C.; Müller-Meskamp, L.; Leo, K. Highly Conductive PEDOT:PSS Electrode with Optimized Solvent and Thermal Post-Treatment for ITO-Free Organic Solar Cells. *Advanced Functional Materials* **2011**, *21*, 1076-1081.
44. Xu, R.-P.; Li, Y.-Q.; Tang, J.-X. Recent advances in flexible organic light-emitting diodes. *Journal of Materials Chemistry C* **2016**, *4*, 9116-9142.
45. Voroshazi, E.; Verreet, B.; Buri, A.; Müller, R.; Di Nuzzo, D.; Heremans, P. Influence of cathode oxidation via the hole extraction layer in polymer:fullerene solar cells. *Organic Electronics* **2011**, *12*, 736-744.
46. Jørgensen, M.; Norrman, K.; Krebs, F. C. Stability/degradation of polymer solar cells. *Solar Energy Materials and Solar Cells* **2008**, *92*, 686-714.

47. Norrman, K.; Gevorgyan, S. A.; Krebs, F. C. Water-Induced Degradation of Polymer Solar Cells Studied by H₂¹⁸O Labeling. *ACS Applied Materials & Interfaces* **2009**, *1*, 102-112.
48. Nielsen, C. B.; Giovannitti, A.; Sbircea, D.-T.; Bandiello, E.; Niazi, M. R.; Hanifi, D. A.; Sessolo, M.; Amassian, A.; Malliaras, G. G.; Rivnay, J.; McCulloch, I. Molecular Design of Semiconducting Polymers for High-Performance Organic Electrochemical Transistors. *Journal of the American Chemical Society* **2016**, *138*, 10252-10259.
49. Kroon, R.; Kiefer, D.; Stegerer, D.; Yu, L.; Sommer, M.; Müller, C. Polar Side Chains Enhance Processability, Electrical Conductivity, and Thermal Stability of a Molecularly p-Doped Polythiophene. *Advanced Materials* **2017**.

CHAPTER 2
ATTACHMENT OF SPIROPYRAN AS A BACKBONE UNIT INTO THIOPHENE
BASED POLYMERS

Authors - Dushanthi S. Dissanayake, Chinthaka M. Udamulle Gedara, Gregory T. McCandless,
Mihaela C. Stefan and Michael C. Biewer

Department of Chemistry and Biochemistry, BE26

The University of Texas at Dallas

800 West Campbell Road

Richardson, Texas 75080-3021

Dushanthi S. Dissanayake carried out the synthesis and characterization of the compounds and wrote the initial draft of this chapter. Chinthaka M. Udamulle Gedara reproduced the synthesis of 5,8-dibromo-1', 3', 3'-trimethylspiro[chromene-2,2'-indoline. Gregory T. McCandless performed the single crystal X-ray diffraction analysis. Professors Mihaela C. Stefan and Michael C. Biewer developed the initial idea for the project, aided in troubleshooting during the project, and edited chapter for publication.

2.1 Abstract

The incorporation of photochromic spiropyrans (SPs) in molecular electronic applications has attracted attention due to the large structural and electronic transformation upon isomerization. The challenge resides with the development of new synthetic methods to incorporate SP as a backbone unit into a polymer while preserving photochromism. In this chapter, a new synthetic method was demonstrated to incorporate thiophene substituents into chromene moiety of SPs. This compound showed photochromism in both polar (methanol) and non-polar (toluene) solvents indicating the possibility of preserving photochromism in SP when incorporated into thiophene based polymer through the chromene moiety. Further, we have shown a new route to synthesize dibrominated and *ortho*-hydroxy protected aromatic aldehyde of thiophene but, synthesis of all thiophene based photochromic polymers is unachievable through this compound due to the instability of *ortho*-hydroxy group. Moreover, a possible route to incorporate SP into thiophene based polymer was demonstrated.

2.2 Introduction

The photochromic SPs are notable in molecular electronic applications due to their large structural and electronic transformation upon isomerization.¹⁻⁴ The ring closed SP is colorless while the ring open merocyanine(MC) form is colored. Beside the color variation, the open and the closed form differ in properties such as electric dipole moment and π -conjugation.⁵⁻⁷ However, to make these structural features practically applicable, SP need to be covalently attached to a support.⁸ In organic electronics, any photochromic switching unit conjugated within a polymer backbone should lead to reversible conductivity and optoelectronic properties by modifying the available conjugated pathway. Therefore, it is important to develop methods to incorporate photochromic units covalently attached to the polymer backbone.

The incorporation of SP units into polymeric matrices can be carried out by polymerization of derivatized monomer units or copolymerization of these units with compatible monomer units, in which the SP can be introduced as a side chain or as a part of the main chain.^{9,10} Very limited number of attempts have been made to incorporate SP as a unit into the backbone. Ng and coworkers used Palladium catalyzed Sonogashira cross coupling reactions to incorporate

photochromic SP switch into the backbone of poly(p-phenylene ethynylene) and observed limited photochromic response as a result of relatively few of the photo switches undergoing the ring-opening within the polymer even in solution.¹¹ An alternating copolymer of SP and 9,9-dioctylfluorene via Suzuki polycondensation was reported by Komber and coworkers.¹² They optimized the reaction conditions to obtain high molecular weights and observed that only the para-brominated SPs were able to polymerize into high molecular weights. Polymerization of *ortho*-brominated SPs resulted in oligomers irrespective to the reaction conditions used and they speculate that the N-ethyl substituent in combination with the *ortho*-bromine substituent could provide a steric barrier to the catalyst. Utilizing SP as a mechanophore into the backbone of a polymer has been reported via step-growth polymerization of urethanes and radical polymerizations of SPs substituted with radically polymerizable units.^{13,14} Apart from that, electrochemical polymerization has also been used to synthesize MC-based conducting polymer.¹⁵ However, this method is not useful in obtaining photochromic polymers as oxidation of the SP at the indoline nitrogen below 0.8 V leads to isomers of oxidized MC, which limit the photochemical behavior of polymer films.¹⁶

All these literature reports show the need for developing new synthesis methods to incorporate SP as a backbone unit into polymers while preserving the photochromism. As polythiophenes are well-known and extensively studied conducting polymers, our ultimate goal is to incorporate SP as a backbone unit into a thiophene based polymer. We have recently reported a new synthetic method to incorporate indoline SP as a pendent group into a thiophene based material via a conjugated pathway.¹⁷ Here we report a new synthesis route to incorporate indoline SP as backbone unit into thiophene based polymers.

Indoline SP can be synthesized by the condensation of indolium salts with *ortho*-hydroxy aromatic aldehydes in the presence of a base (or methylene bases with *ortho*-hydroxy aromatic aldehydes).¹⁸ To incorporate SP as backbone unit we have modified the *ortho*-hydroxy aromatic aldehydes unit with thiophene substituents.

We have studied the photochromism of SP with thiophene substituents in chromene moiety. Further attempts have been made to study the possibility of synthesizing *ortho*-hydroxy aromatic aldehydes with thiophene unit targeting all thiophene based photochromic polymers. Finally, we

have come up with the possible strategy to incorporate SP as a backbone unit into thiophene based polymers.

2.3 Experimental

2.3.1 Materials

All commercial chemicals were purchased either from Sigma Aldrich Chemical Co. LLC. or from Fisher Scientific Co. LLC. and were used without further purification unless otherwise noted. All glassware and syringes were dried at 120 °C for at least 24 h before use and cooled in a desiccator. Tetrahydrofuran (THF) and toluene were dried over sodium/benzophenone ketyl and freshly distilled under nitrogen prior to use.

2.3.2 Analysis

NMR analysis: ^1H and ^{13}C NMR spectra and all 2D-NMR analysis were recorded at 25 °C using a Bruker AVANCE III 500 MHz NMR spectrometer, and were referenced to residual protio solvent (CHCl_3 : δ 7.26 ppm, Acetone: δ 2.05 ppm). The data are reported as follows: chemical shifts are reported in ppm on δ scale, multiplicity (s = singlet, d = doublet, t = triplet, q = quartet, m = multiplet).

GC-MS analysis: GC-MS analysis was performed on Hewlett-Packard Agilent 6890-5973 GC-MS workstation equipped with a Hewlett-Packard fused silica capillary GC column cross-linked with 5 % phenylmethylsiloxane. Helium was used as the carrier gas (1 mL min^{-1}). Sample analysis conditions: injector and detector temperature = 250 °C, initial temperature = 70 °C, temperature ramp = $10 \text{ }^\circ\text{C min}^{-1}$, final temperature = 280 °C.

Single crystal X-ray diffraction analysis: Single crystal X-ray diffraction analysis was performed using single crystals grown by slow evaporation method in ethanol, low temperature ($T = 90 \text{ K}$) single crystal X-ray diffraction datasets were with a Bruker Kappa D8 Quest diffractometer. This diffractometer has a microfocus Mo $K\alpha$ radiation source, liquid nitrogen

cryostream, and CMOS Photon 100 detector. After data collection, the datasets were integrated (Bruker SAINT) and scaled (Bruker SADABS, multi-scan absorption correction method).

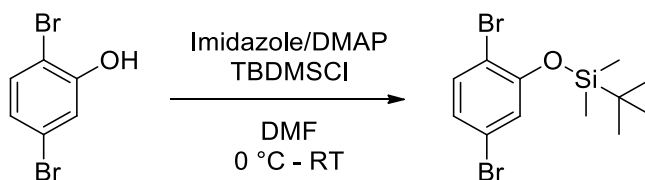
HR-MS analysis: HR-MS analysis was performed with Shimadzu LCMS IT-TOF instrument. Samples were re-suspended in CHCl₃, vortexed and injected (15 μL).

UV-Vis spectroscopic analysis: UV-Vis kinetics experiments were carried using an Agilent 8453 UV-Vis spectrometer coupled with a 500 W Oriel Hg arc lamp containing a 334 nm line filter. 1 cm cuvettes were used for the experiments. The solutions were freshly prepared prior to each experiment by stirring each compound overnight in the respective solvent.

Size Exclusion Chromatography (SEC) analysis: SEC analysis was performed on a Viscotek VE 3580 system equipped with ViscoGEL™ columns (GMHHR-M), connected to a refractive index detector/UV detector. GPC solvent/sample module (GPCmax) was used with HPLC grade THF eluent. The calibration was based on polystyrene standards. Sample analysis conditions: flow rate = 1.0 mL min⁻¹, injector volume = 100 μL, detector temperature = 30 °C and column temperature = 35 °C. Sample dissolved in THF was filtered through PTFE syringe (0.22 μm) filter prior to injection.

2.3.3 Synthetic procedures

Synthesis of tert-butyl(2,5-dibromophenoxy)dimethylsilane



Scheme 2.1. Synthesis of *tert*-butyl(2,5-dibromophenoxy)dimethylsilane

2,5-dibromophenol (1.0 g, 3.9 mmol), imidazole (0.66 g, 9.7 mmol), 4-Dimethylaminopyridine (24 mg, 0.19 mmol) and *tert*-butyldimethylsilyl chloride (2.1 g, 14 mmol) were kept in a 100 mL three-necked round bottomed flask under vacuum prior to the addition of dry N,N-dimethylformamide under nitrogen at 0 °C. The reaction mixture was allowed to stir at ambient temperature overnight, quenched with deionized water and extracted with ethyl acetate. The combined organic layers were washed with deionized water, dried over anhydrous MgSO₄ and evaporated under reduced pressure. The crude was purified by column chromatography using hexane as the eluting solvent. The pure compound was obtained as a clear oil (1.42 g, 3.9 mmol, 100%). ¹H-NMR (CDCl₃, 500 MHz; 7.36 (d, 1H, J=8.4), 7.00 (d, 1H, J=2.2), 6.95 (dd, 1H, J=8.4, J=2.2), 1.04 (s, 9H), 0.26 (s, 6H). ¹³C-NMR (CDCl₃, 500 MHz; 153.47, 134.18, 125.47, 123.41, 120.95, 114.41, 25.68, 18.36, -4.25). ¹H-NMR and ¹³C-NMR spectra are given in figure 2.1 and figure 2.2.

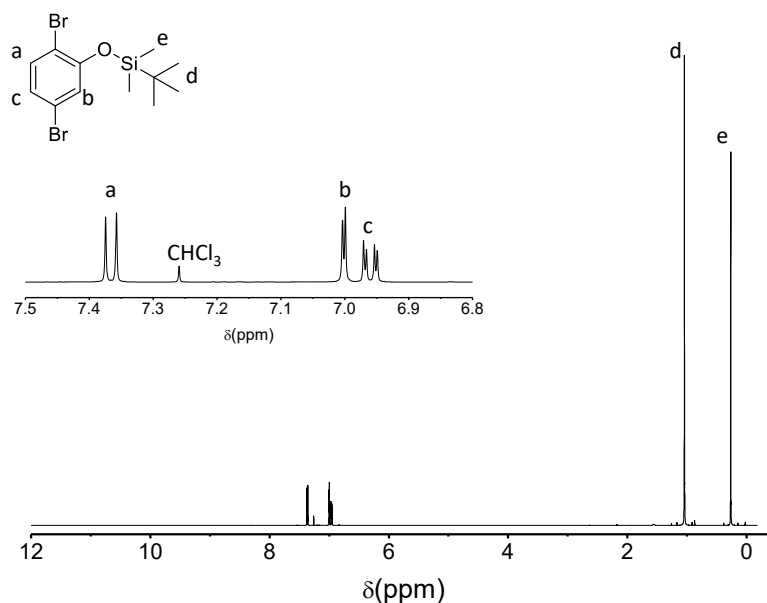


Figure 2.1. ¹H-NMR spectrum of *tert*-butyl(2,5-dibromophenoxy)dimethylsilane

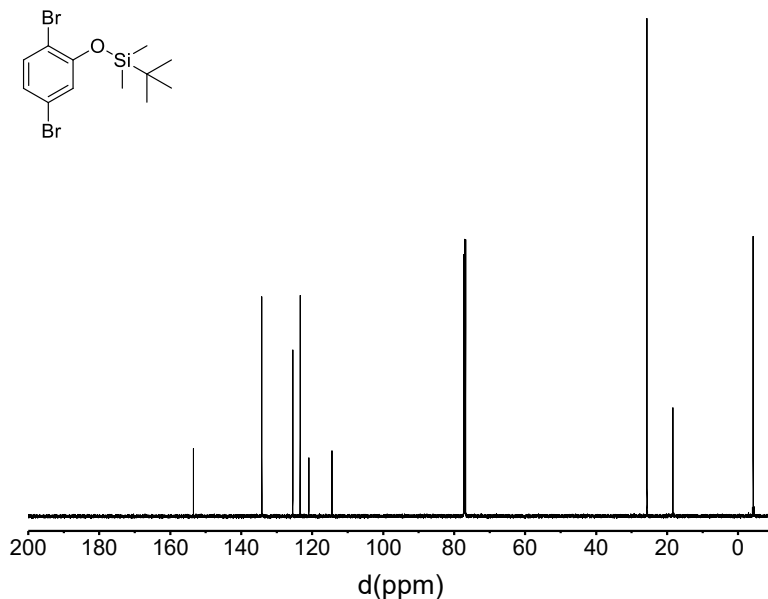
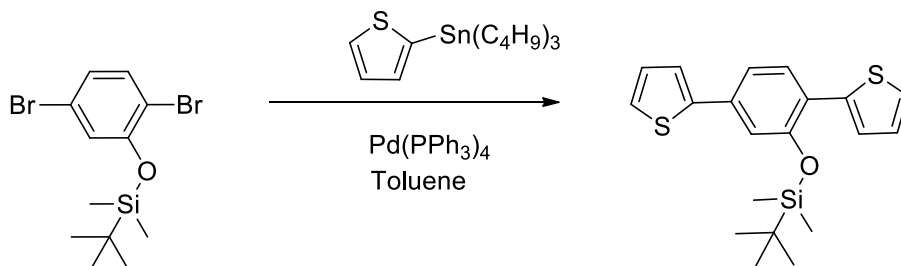


Figure 2.2. ^{13}C -NMR spectrum of *tert*-butyl(2,5-dibromophenoxy)dimethylsilane

Synthesis of *tert*-butyl(2,5-di(thiophene-2-yl)phenoxy)dimethylsilane

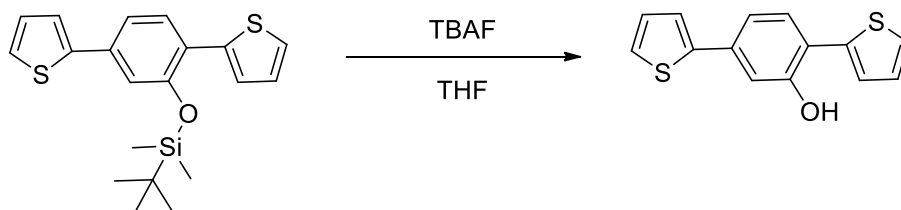


Scheme 2.2. Synthesis of *tert*-butyl(2,5-di(thiophene-2-yl)phenoxy)dimethylsilane

tert-butyl(2,5-dibromophenoxy)dimethylsilane (0.25 g, 0.68 mmol) was dissolved in dry toluene (10 mL) in a 100 mL three-necked round bottomed flask equipped with a reflux condenser and 2-(tributylstannyl) thiophene (0.50 mL, 1.5 mmol) was added to it under nitrogen and nitrogen was bubbled through this solution for 15 min prior to the addition of tetrakis(triphenylphosphine)-palladium(0) (80 mg, 0.068 mmol). The reaction mixture was allowed to reflux under nitrogen for 24 h, cooled to room temperature, quenched with deionized water (100 mL) and extracted with diethyl ether (100 mL \times 3). The combined organic layers were washed with deionized water (100

mL \times 3), dried over anhydrous MgSO_4 and evaporated under reduced pressure. The crude was purified through column chromatography using hexane as the eluting solvent to obtain the product as a white solid (0.18 g, 0.48 mmol, 70 %). $^1\text{H-NMR}$ (CDCl_3 , 500 MHz; 7.56 (d, 1H, $J=8.0$), 7.42 (dd, 1H, $J=3.5$, $J=1.0$), 7.32(dd, 1H, $J=5.0$, $J=1.0$), 7.30 (dd, 2H, $J=3.5$, $J=1.0$), 7.25 (dd, 1H, $J=8.5$, $J=2.0$), 7.21 (d, 1H, $J=2.0$), 7.09 (m, 2H), 0.10 (s, 9H), 0.25 (s, 6H). $^{13}\text{C-NMR}$ (CDCl_3 , 500 MHz; 152.46, 143.89, 139.67, 134.30, 129.89, 128.18, 126.83, 125.73, 125.30, 125.05, 124.93, 123.15, 119.09, 117.51, 26.12, 18.70, -3.75).

Synthesis of 2,5-di(thiophen-2-yl)phenol



Scheme 2.3. Synthesis of 2,5-di(thiophen-2-yl)phenol

tert-butyl(2,5-di(thiophene-2-yl)phenoxy) dimethylsilane (0.15 g, 0.40 mmol) was kept in a 100 mL three-necked round bottomed flask under vacuum for 15 minutes prior to the addition of freshly distilled tetrahydrofuran (10 mL) under nitrogen. Tetrabutylammonium fluoride (1.0 M in THF, 0.44 mL, 0.44 mmol) was added dropwise to this solution and reaction mixture was stirred at room temperature for 3 h, quenched with deionized water (100 mL) and extracted with ethyl acetate (100 mL \times 3). The combined organic layers were washed with deionized water (100 mL \times 3), dried over anhydrous MgSO_4 and evaporated under reduced pressure. The crude was purified through column chromatography using hexane as the eluting solvent to obtain the product as a yellow solid (0.098 g, 0.38 mmol, 95%). $^1\text{H-NMR}$ (CDCl_3 , 500 MHz; 7.43 (d, 1H, $J=8.5$), 7.41 (dd, 1H, $J=5.5$, $J=1.0$), 7.33(m, 2H), 7.30 (dd, 1H, $J=5.5$, $J=1.0$), 7.23 (m, 2H), 7.16 (dd, 1H, $J=5.0$, $J=3.5$), 7.09 dd, 1H, $J=5.5$, $J=3.5$), 5.58 (s, 1H). $^{13}\text{C-NMR}$ (CDCl_3 , 500 MHz; 152.63, 143.47, 138.49, 135.48, 130.39, 128.10, 127.92, 126.31, 125.94, 125.20, 123.52, 120.16, 118.62, 113.34). $^1\text{H-NMR}$ spectra of *tert*-butyl(2,5-di(thiophene-2-yl)phenoxy)dimethylsilane and 2,5-di(thiophen-2-yl)phenol are given in figure 2.3 and figure 2.4. $^{13}\text{C-NMR}$ spectra are given in figure 2.5 and figure 2.6.

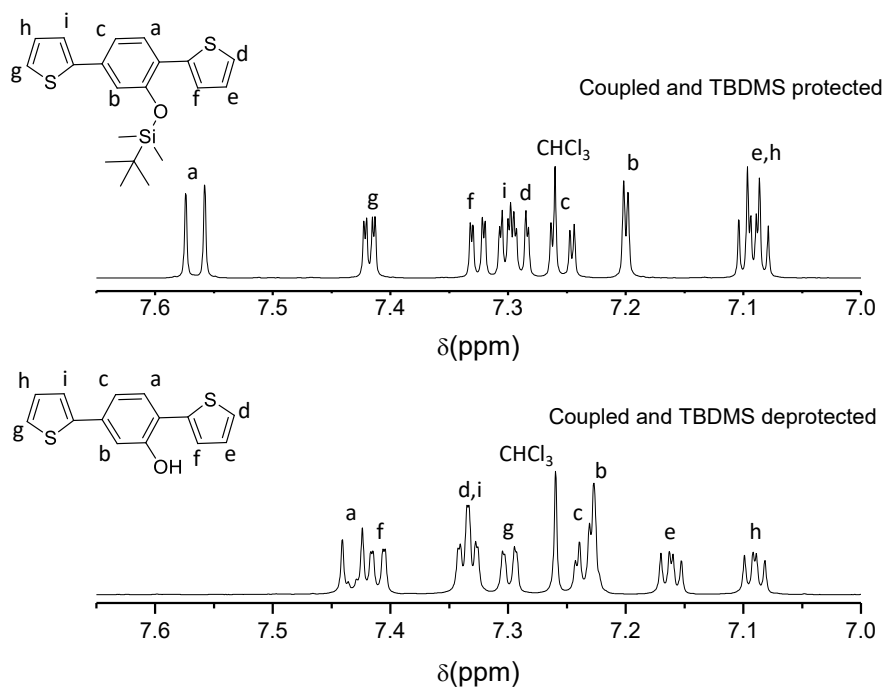


Figure 2.3. $^1\text{H-NMR}$ spectrum of *tert*-butyl(2,5-di(thiophene-2-yl)phenoxy)dimethylsilane and 2,5-di(thiophen-2-yl)phenol in downfield region.

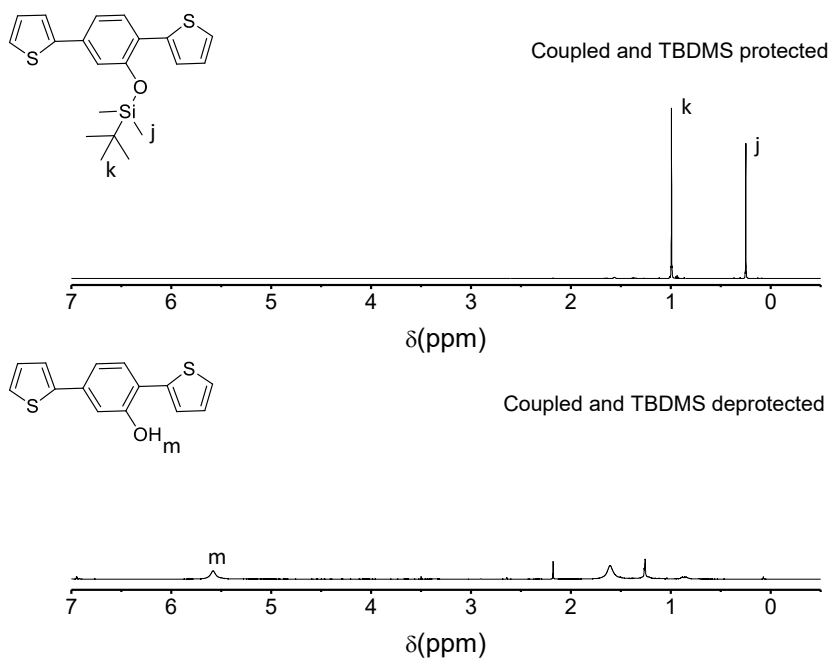


Figure 2.4. $^1\text{H-NMR}$ spectrum of *tert*-butyl(2,5-di(thiophene-2-yl)phenoxy)dimethylsilane and 2,5-di(thiophen-2-yl)phenol in upfield region.

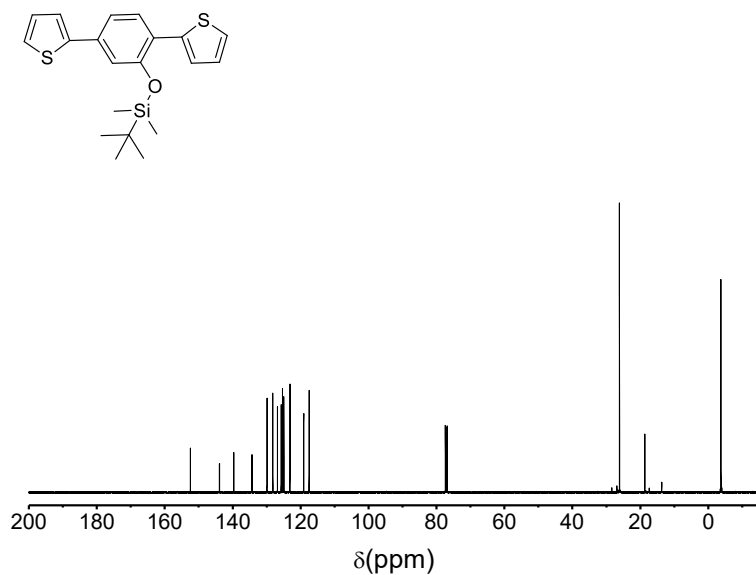


Figure 2.5. ¹³C-NMR spectrum of *tert*-butyl(2,5-di(thiophene-2-yl)phenoxy)dimethylsilane

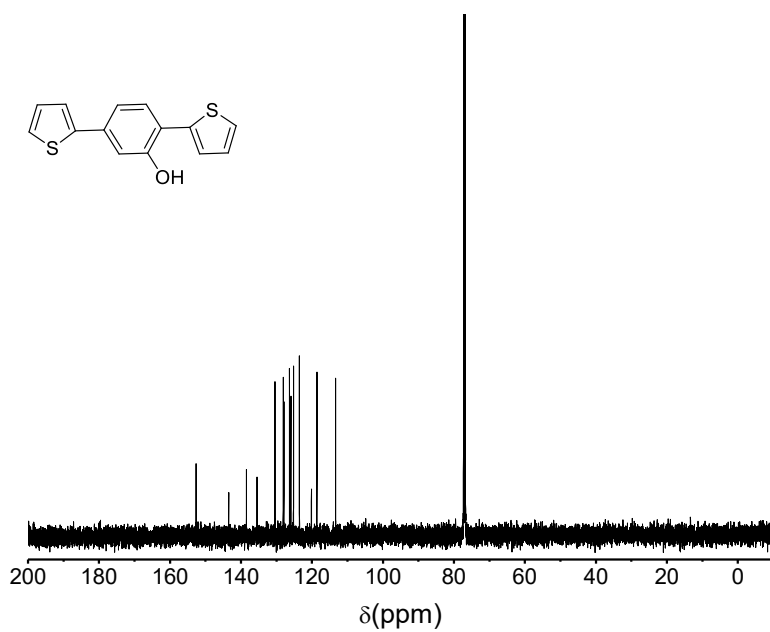
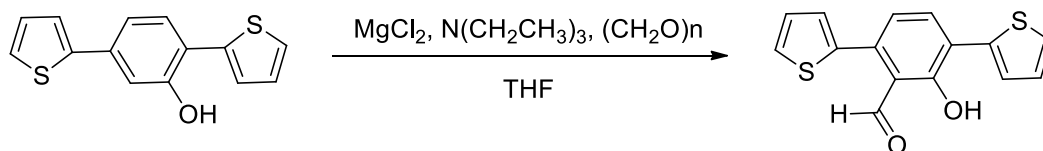


Figure 2.6. ¹³C-NMR spectrum of 2,5-di(thiophen-2-yl)phenol

Synthesis of 2-hydroxy-3,6-di(thiophen-2-yl)benzaldehyde



Scheme 2.4 Synthesis of 2-hydroxy-3,6-di(thiophen-2-yl)benzaldehyde

Anhydrous magnesium chloride beads (0.35 g, 3.7 mmol), and solid paraformaldehyde (0.22 g, 7.5 mmol) were kept under nitrogen in a dry 100 mL three-necked round bottomed flask equipped with a reflux condenser. Dry tetrahydrofuran (20 mL) was added by a syringe. Triethyl amine (0.53 mL, 3.7 mmol) was added dropwise by a syringe and the mixture was stirred for 10 minutes at room temperature. At this point, 2,5-di(thiophen-2-yl)phenol (0.19 mg, 0.75 mmol) was added dropwise by a syringe, resulting in a yellow color mixture. The reaction mixture was allowed to reflux under nitrogen for 6 h, cooled to room temperature, quenched with acidified deionized water (100 mL) and extracted with ethyl acetate (100 mL \times 3). The combined organic layers were washed with deionized water (100 mL \times 3), dried over anhydrous MgSO₄ and evaporated under reduced pressure. The crude was purified through column chromatography using ethyl acetate: hexane (1:9) as the eluting solvent to obtain the product as a yellow solid (0.12 g, 0.42 mmol, 57 %). ¹H-NMR (CDCl₃, 500 MHz; 12.91(s, 1H), 10.13(s, 1H), 7.88(d, 1H, J=8.0), 7.68(dd, 1H, J=4.0, J=1.5), 7.48(dd, 1H, J=5.5, J=1.5), 7.40(dd, 1H, J=5.0, J=1.0), 7.15(m, 2H), 7.11(dd, 1H, J=3.5, J=1.0), 7.07(d, 1H, J=8.0). ¹³C-NMR (Acetone d₆, 500 MHz; 197.46, 158.81, 138.32, 137.82, 137.04, 134.48, 130.25, 128.04, 127.99, 127.16, 126.46, 126.33, 122.63, 122.29, 118.22). ¹H-NMR and ¹³C-NMR spectra are given in figure 2.7 and figure 2.8.

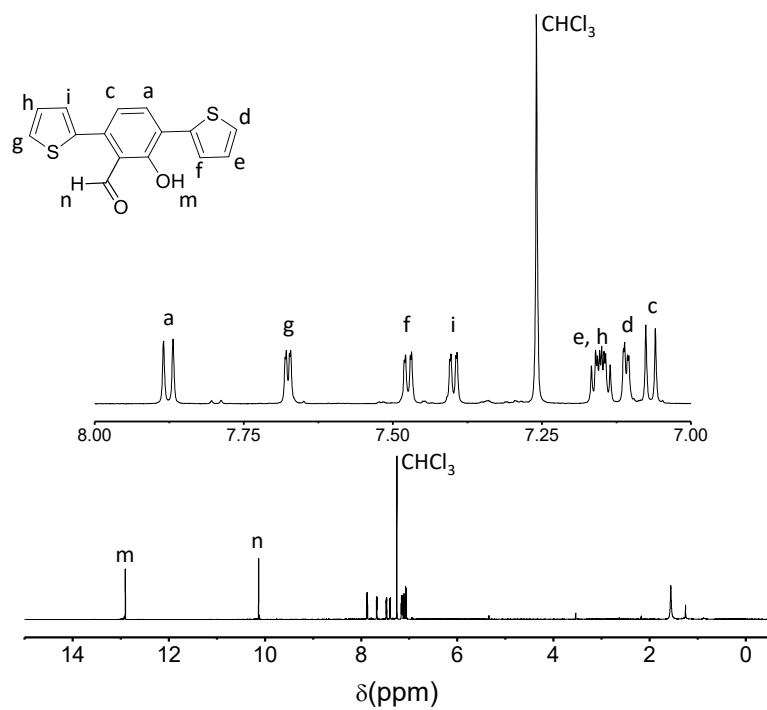


Figure 2.7. ¹H-NMR spectrum of 2-hydroxy-3,6-di(thiophen-2-yl)benzaldehyde

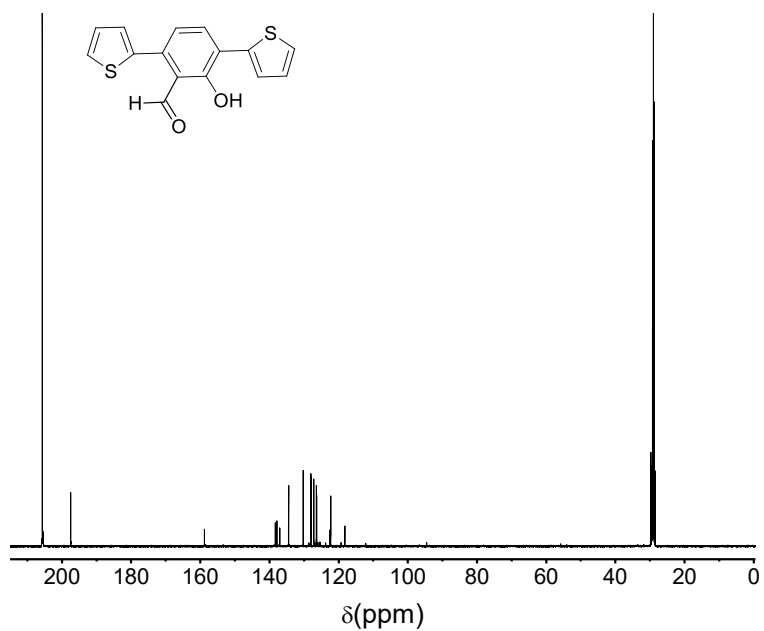
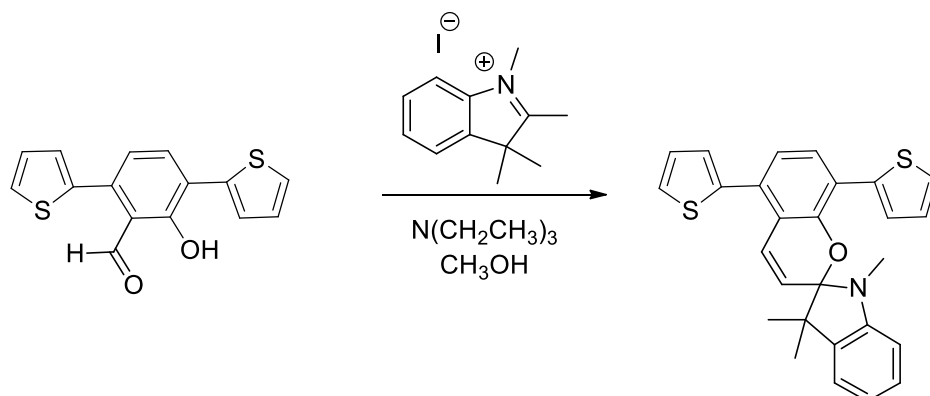


Figure 2.8. ¹³C-NMR spectrum of 2-hydroxy-3,6-di(thiophen-2-yl)benzaldehyde

Synthesis of 1',3',3'-trimethyl-5,8-di(thiophen-2-yl)spiro[chromene-2,2'-indoline]



Scheme 2.5. Synthesis of 1',3',3'-trimethyl-5,8-di(thiophen-2-yl)spiro[chromene-2,2'-indoline]

1,2,3,3-Tetramethyl-3H-indoleium iodide (40 mg, 0.13 mmol) and 2-hydroxy-3,6-di(thiophen-2-yl)benzaldehyde (37 mg, 0.13 mmol) was kept in a three-necked round bottomed flask equipped with a reflux condenser and kept under nitrogen for 10 min prior to the addition of methanol (10 mL). Three drops of triethylamine were added at room temperature and the reaction mixture was allowed to reflux gently for 2 h under nitrogen, allowed to cool to room temperature, quenched in deionized water and extracted with ethyl acetate (50 mL \times 3). The combined organic layer was washed with deionized water (50 mL \times 3), dried over magnesium sulfate and the solvent was evaporated under reduced pressure. The crude was purified by column chromatography using ethyl acetate:hexane (1:9) as the eluting solvent. The pure compound was obtained as brownish solid (29 mg, 0.066 mmol, 51 %). $^1\text{H-NMR}$ (CDCl_3 , 500 MHz; 7.59 (d, 1H, $J=8.5$), 7.40(d, 1H, $J=5.5$), 7.30(d, 1H, $J=10.5$), 7.26(d, 1H), 7.20(m, 1H), 7.15(m, 1H), 7.12(m, 2H), 7.06(d, 1H, $J=5.0$), 6.99(d, 1H, $J=8.0$), 6.86(m, 2H), 6.57(d, 1H, $J=7.5$), 5.84(d, 1H, $J=10.5$), 2.74(s, 3H), 1.33(s, 3H), 1.24(s, 3H)). $^{13}\text{C-NMR}$ (CDCl_3 , 500 MHz; 148.56, 140.96, 138.36, 136.86, 130.74, 127.88, 127.51, 127.40, 126.82, 126.42, 125.95, 125.67, 124.51, 122.29, 121.56, 120.50, 119.45, 119.42, 117.49, 107.32, 105.44, 51.66, 29.30, 25.56, 19.99). HRMS (ESI) m/z calcd for $\text{C}_{27}\text{H}_{23}\text{NOS}_2$ ($\text{M} + \text{H}$) $^+$ 442.1294, found 442.1288. $^1\text{H-NMR}$ and $^{13}\text{C-NMR}$ spectra are given in figure 2.9 and figure 2.10. 2D-NMR analysis is given in figure 2.11 and figure 2.12.

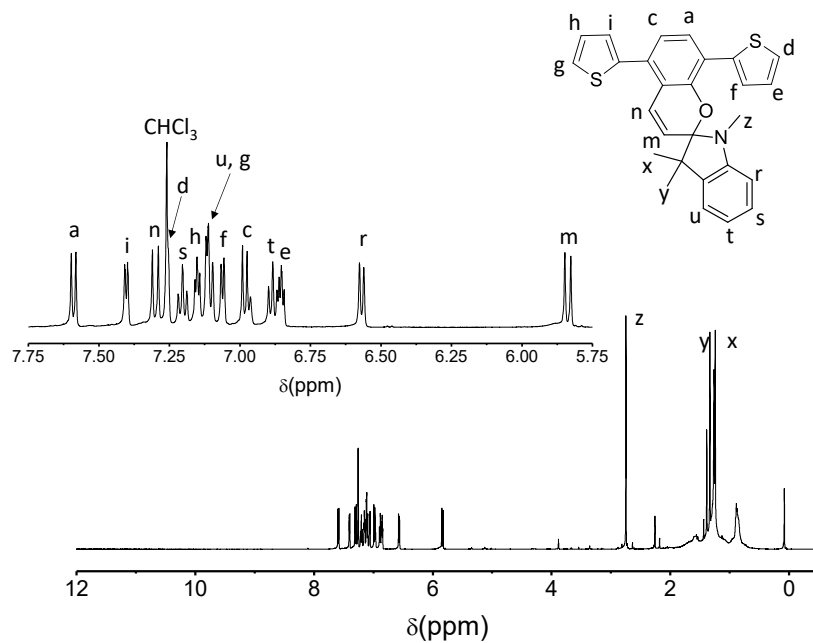


Figure 2.9. ^1H -NMR spectrum of 1',3'3'-trimethyl-5,8-di(thiophen-2-yl)spiro[chromene-2,2'-indoline]

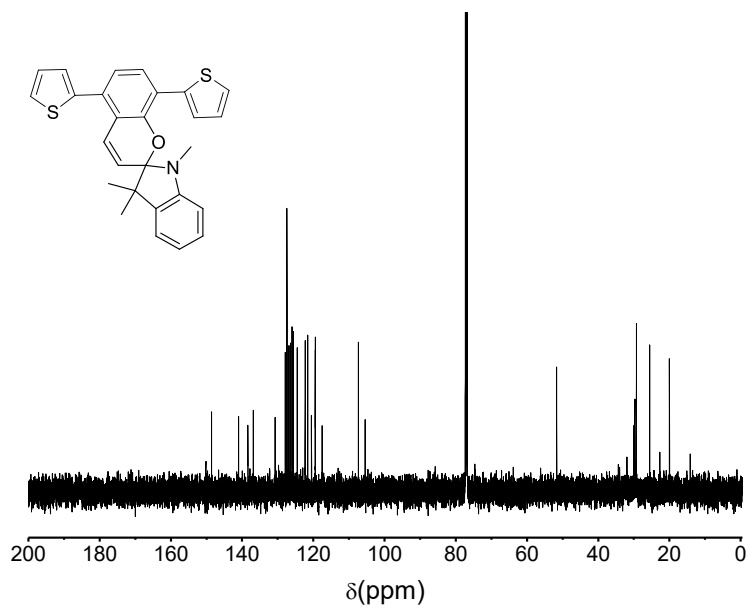


Figure 2.10. ^{13}C -NMR spectrum of 1',3'3'-trimethyl-5,8-di(thiophen-2-yl)spiro[chromene-2,2'-indoline]

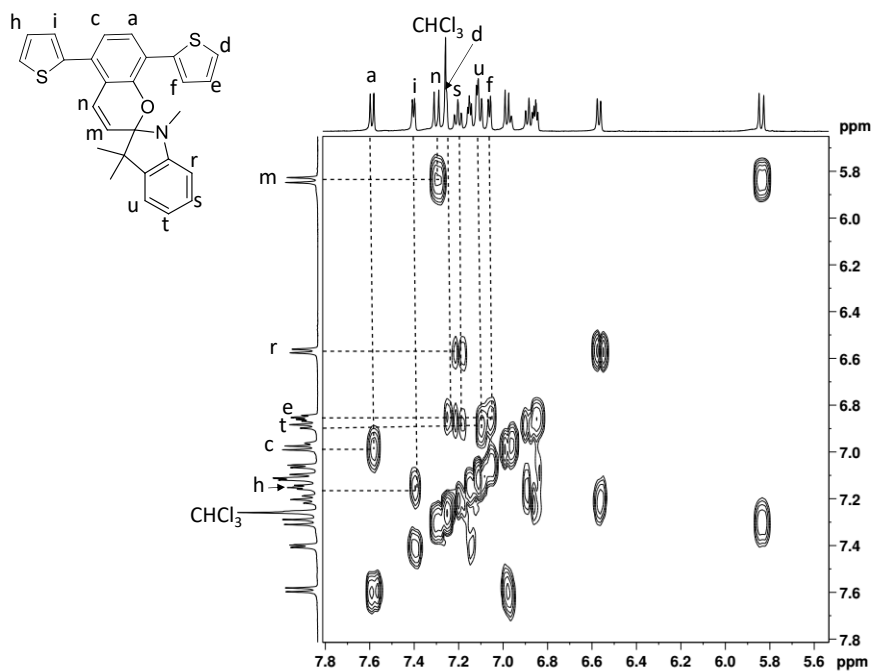


Figure 2.11. Expanded ^1H - ^1H COSY spectrum of 1',3',3'-trimethyl-5,8-di(thiophen-2-yl)spiro[chromene-2,2'-indoline]

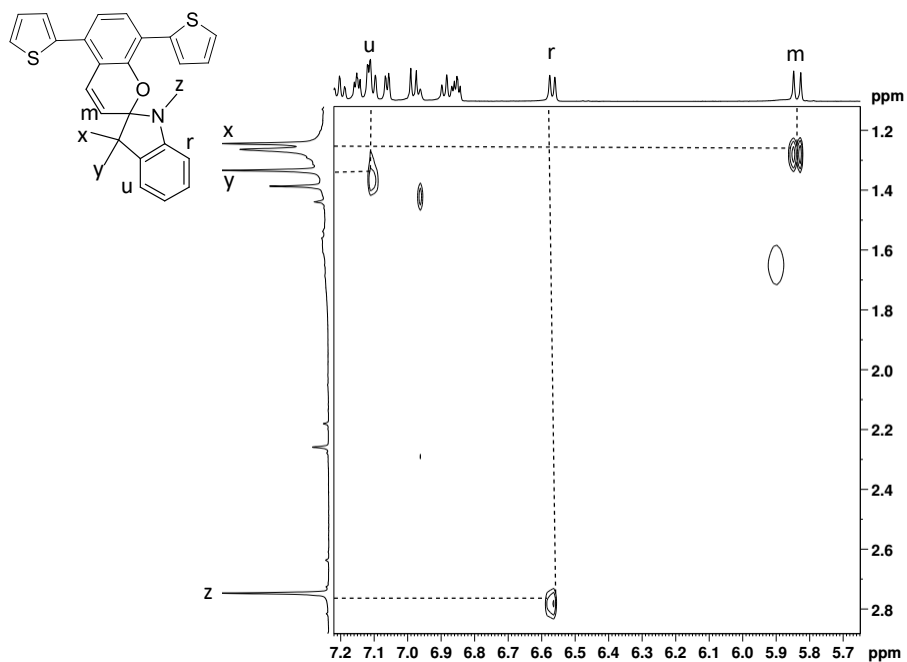
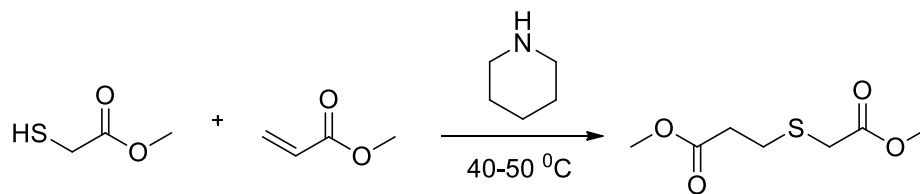


Figure 2.12. Expanded ^1H - ^1H NOESY spectrum of 1',3',3'-trimethyl-5,8-di(thiophen-2-yl)spiro[chromene-2,2'-indoline]

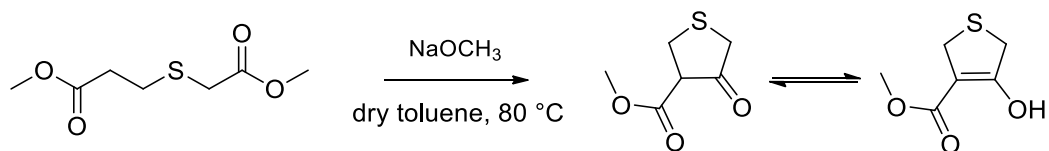
Synthesis of methyl 3-(2-methoxy-2-oxoethylthio)propanoate¹⁹



Scheme 2.6. Synthesis of methyl 3-(2-methoxy-2-oxoethylthio)propanoate

Methyl thioglycolate (27 g, 0.26 mol) was kept under N₂ in a three-necked round bottomed flask equipped with a reflux condenser for 10 min prior to the dropwise addition of piperidine (0.21 g, 0.0025 mol) while stirring the solution. Methyl acrylate (23 g, 0.26 mol) was added to the mixture during 45 min while maintaining the reaction mixture at 40-50 °C. During this period, another portion of piperidine (0.21 g, 0.0025 mol) was added. After the methyl acrylate had been added, the reaction mixture was warmed to 50 °C and maintained at that temperature for 15 min, cooled to room temperature, filtered, washed with deionized water (100 mL × 3) and dried over anhydrous Na₂SO₄ to obtain the product which was used for the next step without further purification (40 g, 0.21 mol, 81 %). ¹H-NMR (CDCl₃, 500 MHz; 3.70(s, 6H), 3.24(s, 2H), 2.89(t, 2H), 2.63(t, 2H)). ¹³C-NMR (CDCl₃, 500 MHz; 172.02, 170.68, 52.37, 51.77, 34.02, 33.37, 27.48). ¹H-NMR and ¹³C-NMR spectra are given in figure 2.13 and figure 2.14.

Synthesis of methyl 4-oxotetrahydrothiophene-3-carboxylate¹⁹



Scheme 2.7. Synthesis of methyl 4-oxotetrahydrothiophene-3-carboxylate

NaOCH₃ (6.4 g, 0.12 mol) was kept under N₂ in a three-necked round bottomed flask equipped with a reflux condenser for 1 h prior to the addition of dry toluene (200 mL). The mixture was

heated to 80 °C and methyl 3-(2methoxy-2-oxoethylthio)propanoate (9.2 g, 0.048 mol) was rapidly added. The resultant precipitate was dissolved as the reaction mixture was stirred and heated at 80 °C for 1h. An additional methyl 3-(2methoxy-2-oxoethylthio)propanoate (9.2 g, 0.048 mol) was added during 20 min at this point. The resultant massive precipitate was stirred and heated at 80 °C for 2h and then 15 min at boiling conditions under N₂. The mixture was allowed to cool, quenched with conc. HCl (12 mL) in ice water (50 mL). The toluene layer was separated and three ether extracts (100 ml x 3) of the aqueous layer were added to it. Resultant organic layer was dried over anhydrous MgSO₄, evaporated under reduced pressure and vacuum distilled to obtain the product (9.1 g, 0.057 mol, 59 %). ¹H-NMR (CDCl₃, 500 MHz; 10.95(s, 1H), 3.80(m, 7H)). ¹³C-NMR (CDCl₃, 500 MHz; 172.49, 169.62, 99.26, 51.69, 36.08, 31.45). ¹H-NMR and ¹³C-NMR spectra are given in figure 2.15 and figure 2.16.

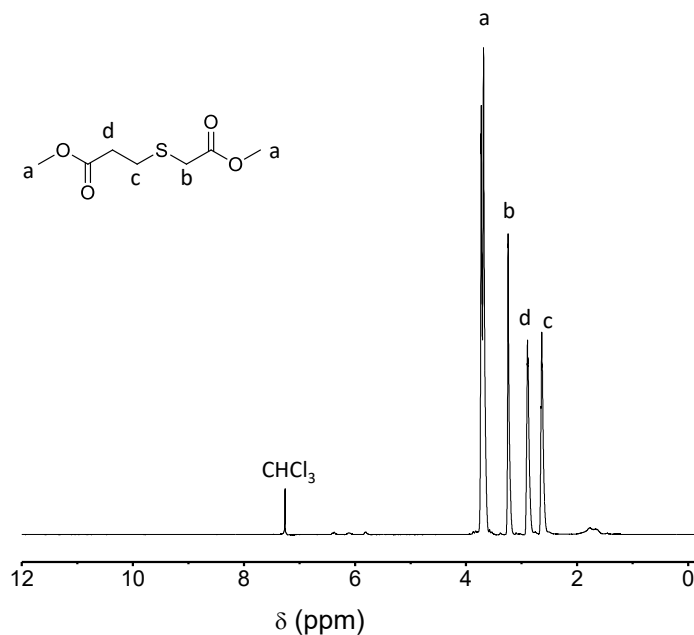


Figure 2.13. ¹H-NMR spectrum of methyl 3-(2methoxy-2-oxoethylthio)propanoate

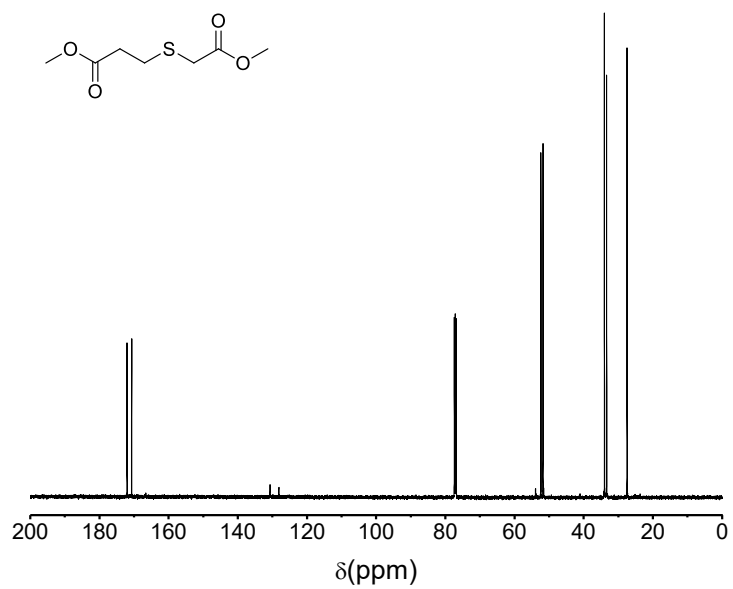


Figure 2.14. $^{13}\text{C-NMR}$ spectrum of methyl 3-(2-methoxy-2-oxoethylthio)propanoate

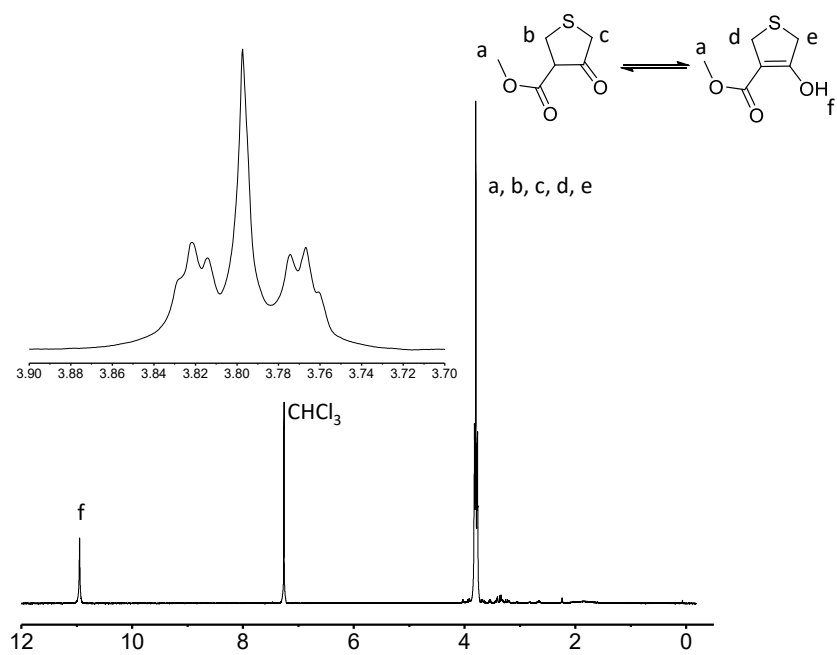


Figure 2.15. $^1\text{H-NMR}$ spectrum of methyl 4-oxotetrahydrothiophene-3-carboxylate

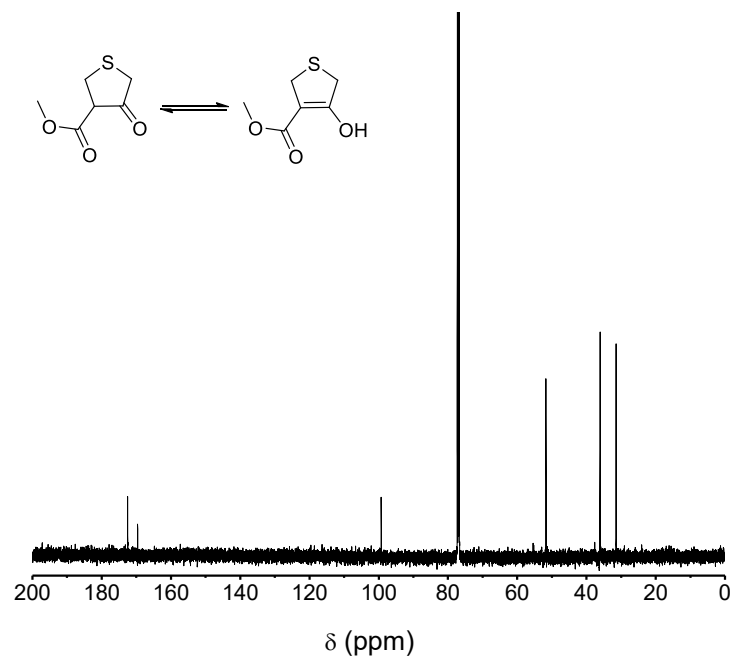
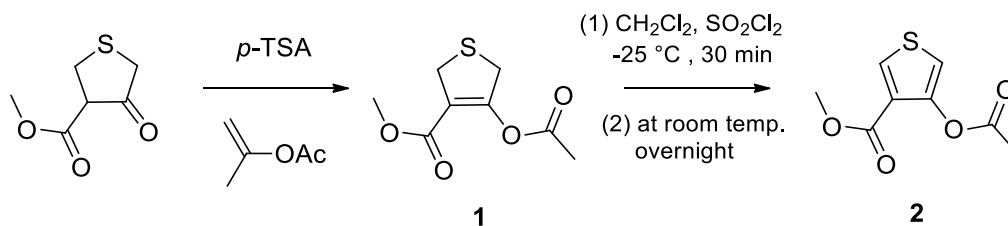


Figure 2.16. ^{13}C -NMR spectrum of methyl 4-oxotetrahydrothiophene-3-carboxylate

Synthesis of methyl 4-acetoxythiophene-3-carboxylate via methyl 4-acetoxy-2,5-dihydrothiophene-3-carboxylate



Scheme 2.8. Synthesis of methyl 4-acetoxythiophene-3-carboxylate (**2**)

Step 1

Synthesis of methyl 4-acetoxy-2,5-dihydrothiophene-3-carboxylate (1)

Methyl 4-oxotetrahydrothiophene-3-carboxylate (1.3 g, 0.0081 mol), *p*-TSA (0.0082 g, 0.000042 mol) and isopropenylacetate (10 mL) were mixed together in a three-necked round bottomed flask equipped with a reflux condenser and kept under reflux conditions overnight.

Step2

Synthesis of methyl 4-acetoxythiophene-3-carboxylate (2)

The above reaction mixture (**1**) was allowed to cool to the room temperature and CH_2Cl_2 (10 mL) was added. Resultant mixture was cooled to $-25\text{ }^\circ\text{C}$. Sulfuryl chloride (1.3 g, 0.8 mL, 0.0097 mol) was added dropwise over a period of 30 min while maintaining the temperature at $-25\text{ }^\circ\text{C}$. After the addition, the solution was stirred for an additional 30 min at $-25\text{ }^\circ\text{C}$ and allowed to stir at room temperature overnight. Additional solvent was removed through distillation and the crude was purified by column chromatography using ethyl acetate: hexane (1:9) as the eluting solvent. The pure compound was obtained as a white solid (1.2 g, 0.0060 mol, 75 %). $^1\text{H-NMR}$ (CDCl_3 , 500 MHz; 8.06(d, 1H, $J=3.7$), 6.97(d, 1H, $J=3.6$), 3.82(s, 3H), 2.32(s, 3H)). $^{13}\text{C-NMR}$ (CDCl_3 , 500 MHz; 169.37, 161.47, 146.52, 133.06, 124.90, 114.13, 51.76, 20.73). $^1\text{H-NMR}$ and $^{13}\text{C-NMR}$ spectra are given in figure 2.17 and figure 2.18.

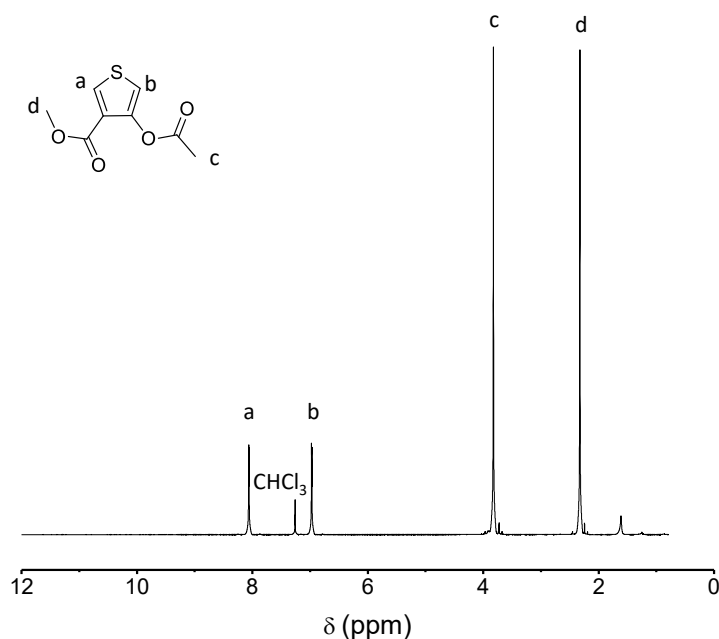


Figure 2.17. $^1\text{H-NMR}$ spectrum of methyl 4-acetoxythiophene-3-carboxylate

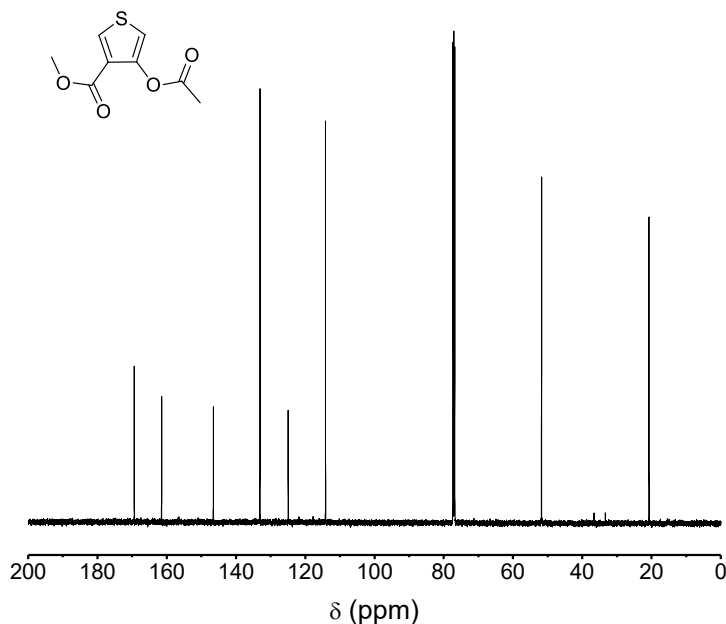
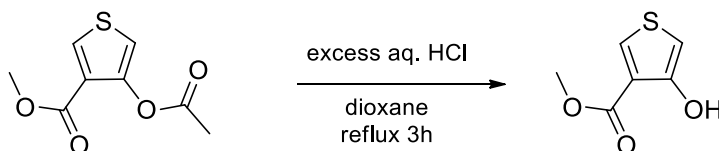


Figure 2.18. ^{13}C -NMR spectrum of methyl 4-acetoxythiophene-3-carboxylate

Synthesis of methyl 4-hydroxythiophene-3-carboxylate



Scheme 2.9. Synthesis of methyl 4-hydroxythiophene-3-carboxylate

Methyl 4-acetoxythiophene-3-carboxylate (0.25 g, 0.0012 mol) was dissolved in dioxane in a three-necked round bottomed flask equipped with a reflux condenser and 0.24 M HCl solution (10 mL) was added to the mixture dropwise at ambient temperature. After the addition was complete the reaction mixture was stirred and refluxed for 3 h. After each hour an aliquot of the reaction mixture was taken out, quenched with deionized water, extracted with ether and GC-MS analysis were carried out in order to monitor the consumption of starting materials. No starting materials were left over after 3h therefore reaction mixture was quenched with deionized water, extracted

with ether, dried over anhydrous MgSO_4 and evaporated under reduced pressure. Column chromatography was carried out using ethyl acetate: hexane (1:19) as the eluting solvent to purify the product. Collected fractions were evaporated under reduced pressure to obtain the white solid (0.11 g, 0.00072 mol, 57 %). $^1\text{H-NMR}$ (CDCl_3 , 500 MHz; 8.71(s, 1H), 7.89(d, 1H, $J=3.5$), 6.38(d, 1H, $J=3.5$), 3.92(s, 3H). $^{13}\text{C-NMR}$ (CDCl_3 , 270 MHz; 165.79, 155.66, 131.23, 119.35, 100.36, 52.12). $^1\text{H-NMR}$ and $^{13}\text{C-NMR}$ spectra are given in figure 2.19 and figure 2.20.

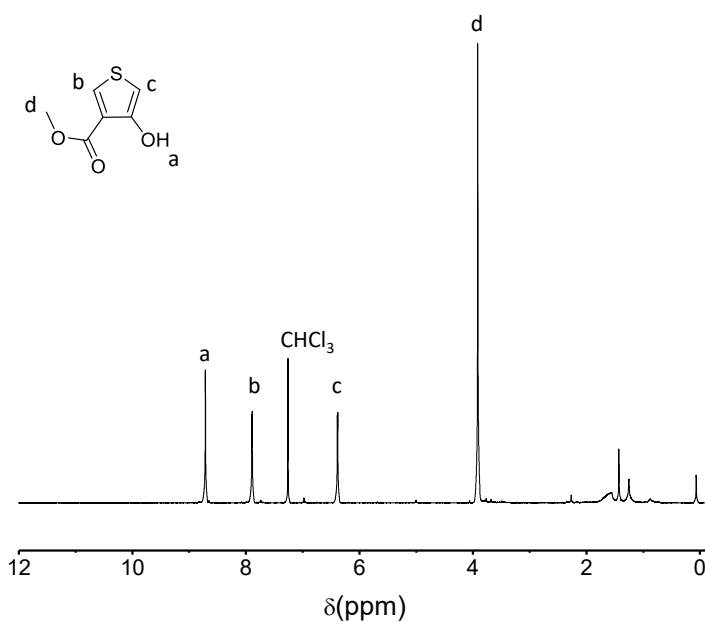


Figure 2.19. $^1\text{H-NMR}$ spectrum of methyl 4-hydroxythiophene-3-carboxylate

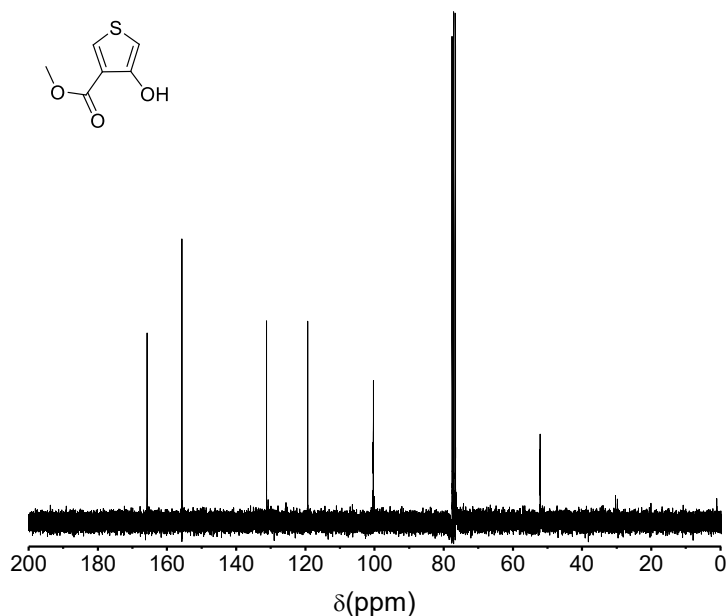
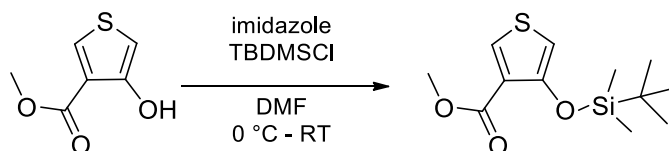


Figure 2.20. ^{13}C -NMR spectrum of methyl 4-hydroxythiophene-3-carboxylate

Synthesis of methyl 4-((tert-butyldimethylsilyl)oxy)thiophene-3-carboxylate



Scheme 2.10. Synthesis of methyl 4-((tert-butyldimethylsilyl)oxy)thiophene-3-carboxylate

Methyl 4-hydroxythiophene-3-carboxylate (0.43 g, 0.0027 mol) was dissolved in dry N,N-dimethylformamide under N_2 in a round bottomed flask and imidazole (0.516 g, 0.0076 mol) followed by *tert*-butyldimethylsilyl chloride (1.4 g, 0.0089 mol) were added at 0 °C. The reaction mixture was allowed to come to ambient temperature and an aliquot of the reaction mixture was taken out in 1 h, 1.5 h and 3 h intervals, quenched with deionized water, extracted with ether and TLC analysis were carried out in order to monitor the consumption of the starting materials. As no improvement in product formation was visualized after 1 h the reaction mixture was quenched

with deionized water and extracted with ether. The combined organic layers were washed with deionized water, dried over anhydrous MgSO_4 and evaporated under reduced pressure. Column chromatography was carried out with alumina using ethyl acetate: hexane (1:19) as the eluting solvent followed by with silica using ethyl acetate : hexane (1:49) as the eluting solvent to purify the product. Collected fractions were evaporated under reduced pressure to obtain the light yellow colored oil (0.62 g, 0.0023 mol, 84 %). $^1\text{H-NMR}$ (CDCl_3 , 500 MHz; 7.94(d, 1H, $J=3.7$), 6.33(d, 1H, $J=3.7$), 3.82(s, 3H), 1.01(s, 9H), 0.20(s, 6H)). $^{13}\text{C-NMR}$ (CDCl_3 , 500 MHz; 162.57, 152.12, 132.32, 125.67, 105.88, 51.36, 25.66, 18.22, -4.79). $^1\text{H-NMR}$ and $^{13}\text{C-NMR}$ spectra are given in figure 2.21 and figure 2.22.

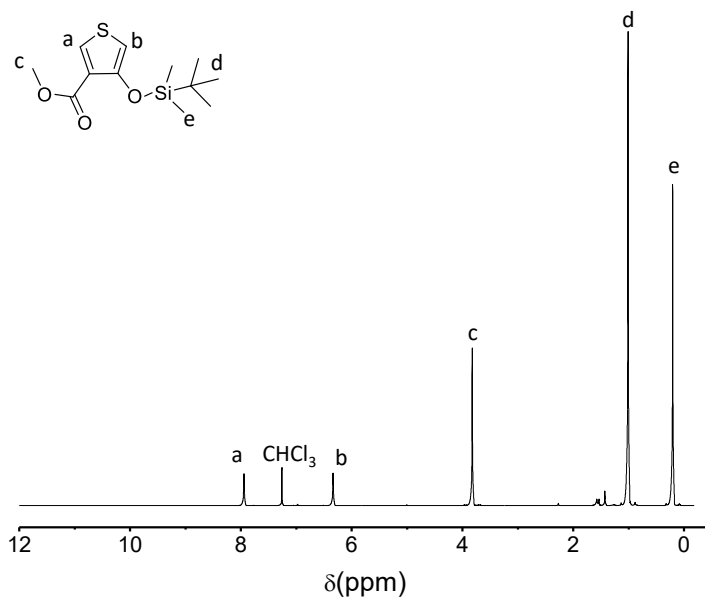


Figure 2.21. $^1\text{H-NMR}$ spectrum of methyl 4-((*tert*-butyldimethylsilyloxy)thiophene-3-carboxylate

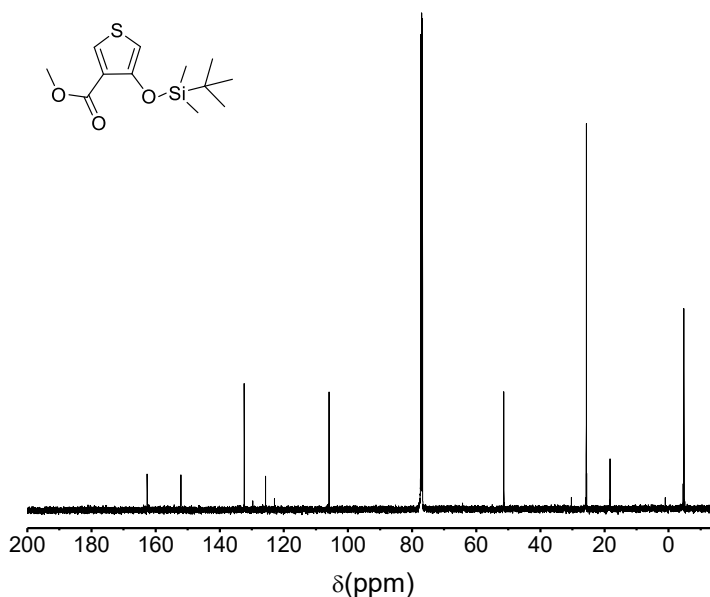
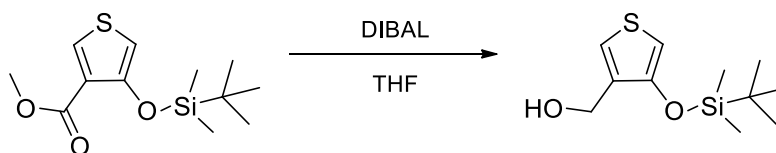


Figure 2.22. ^{13}C -NMR spectrum of methyl 4-((*tert*-butyldimethylsilyl)oxy)thiophene-3-carboxylate

Synthesis of (4-((*tert*-butyldimethylsilyl)oxy)thiophene-3-yl)methanol



Scheme 2.11. Synthesis of (4-((*tert*-butyldimethylsilyl)oxy)thiophene-3-yl)methanol

Methyl 4-((*tert*-butyl dimethyl silyl)oxy)thiophene-3-carboxylate (0.055 g, 0.00020 mol) was dissolved in dry THF in a round bottomed flask and the mixture was kept under N_2 for 15 min at $-84\text{ }^\circ\text{C}$ prior to the addition of diisobutylaluminum hydride (0.14 g, 0.00020 mol). The reaction mixture was stirred at $-84\text{ }^\circ\text{C}$ for 1h and an aliquot of the reaction mixture was taken out, quenched with saturated ammonium chloride solution, extracted with ether and GC-MS, TLC analysis were carried out in order to monitor the consumption of the starting materials. As more starting materials were left over even after 1h, the temperature of the reaction mixture was allowed to come to $0\text{ }^\circ\text{C}$

and GC-MS, TLC analysis were carried out $\approx -60\text{ }^\circ\text{C}$ and $\approx -20\text{ }^\circ\text{C}$. As the formation of the product did not show any improvement even at $\approx -20\text{ }^\circ\text{C}$, the reaction mixture was quenched with saturated ammonium chloride solution at $0\text{ }^\circ\text{C}$, extracted with ether, dried over anhydrous MgSO_4 and evaporated under reduced pressure. Column chromatography was carried out with alumina using ethyl acetate: hexane (1:19) as the eluting solvent to purify the product. Collected fractions were evaporated under reduced pressure to obtain the colorless oil (0.02 g, 0.000081 mol, 41 %). $^1\text{H-NMR}$ (CDCl_3 , 500 MHz; 7.09(d, 1H, $J=3.2$), 6.28(d, 1H, $J=3.2$), 4.56(s, 2H), 1.00(s, 9H), 0.25(s, 6H)). $^{13}\text{C-NMR}$ (CDCl_3 , 500 MHz; 150.71, 134.76, 121.01, 103.57, 59.01, 25.66, 18.08, -4.63) $^1\text{H-NMR}$ and $^{13}\text{C-NMR}$ spectra are given in figure 2.23 and figure 2.24.

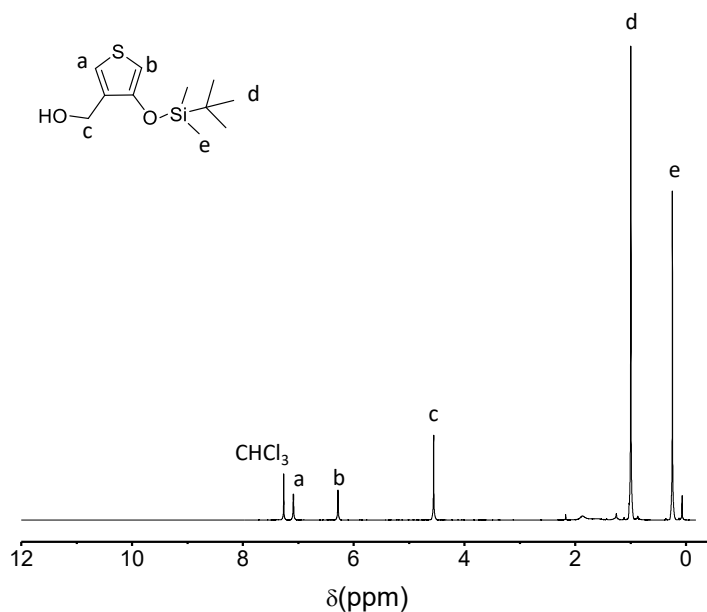


Figure 2.23. $^1\text{H-NMR}$ spectrum of (4-((*tert*-butyl)dimethylsilyloxy)thiophene-3-yl)methanol

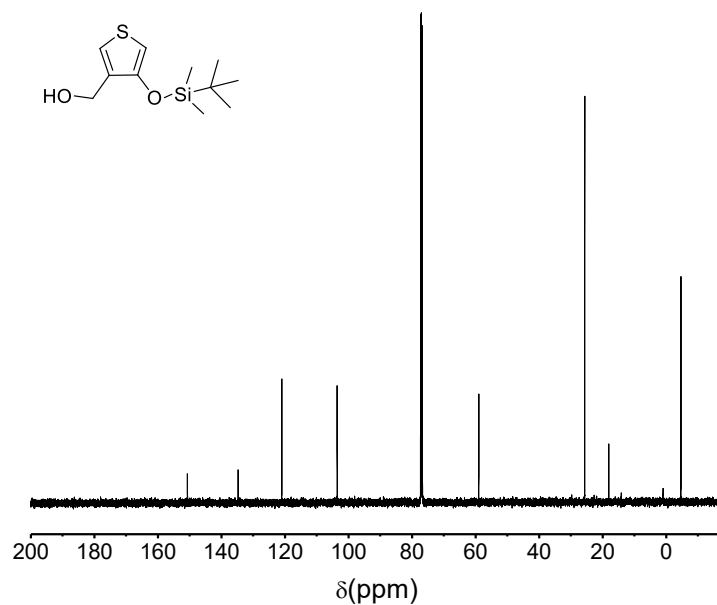
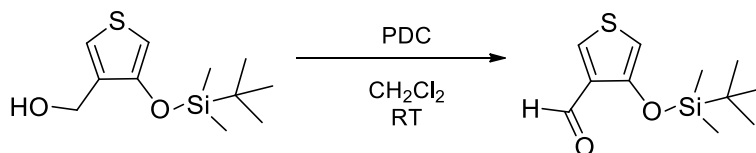


Figure 2.24. ^{13}C -NMR spectrum of 4-((*tert*-butyldimethylsilyl)oxy)thiophene-3-yl)methanol

Synthesis of 4-((*tert*-butyldimethylsilyl)oxy)thiophene-3-carbaldehyde



Scheme 2.12. Synthesis of 4-((*tert*-butyldimethylsilyl)oxy)thiophene-3-carbaldehyde

4-((*tert*-butyldimethylsilyl)oxy) thiophene-3-yl)methanol (0.14 g, 0.00057 mol) was dissolved in tetrahydrofuran (1 mL) in a round bottomed flask prior to the addition of pyridinium dichromate (0.24 g, 0.00063 mol) and dichloromethane (10 mL). The reaction mixture was allowed to stir at ambient temperature for 24 h, quenched with deionized water, extracted with ether. The combined organic layers were washed with deionized water, dried over anhydrous MgSO_4 and evaporated under reduced pressure. Column chromatography was carried out using ethyl acetate: hexane (1:19) to purify the product. Collected fractions were evaporated under reduced pressure to obtain the yellow colored oil (0.11 g, 0.00045 mol, 82 %). ^1H -NMR (CDCl_3 , 500 MHz; 9.88(s, 1H)

7.98(d, 1H, J=3.4), 6.34(d, 1H, J=3.4), 1.00(s, 9H), 0.26(s, 6H)). $^1\text{H-NMR}$ spectrum is given in figure 2.25.

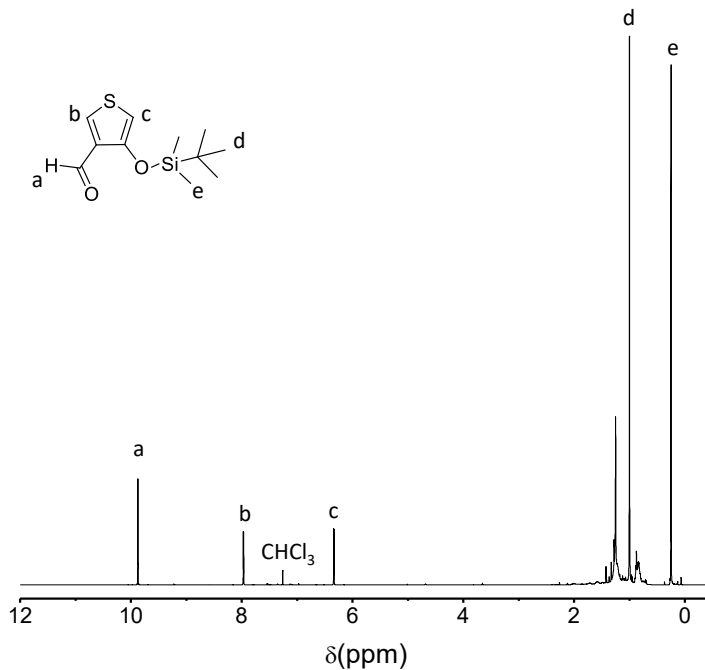
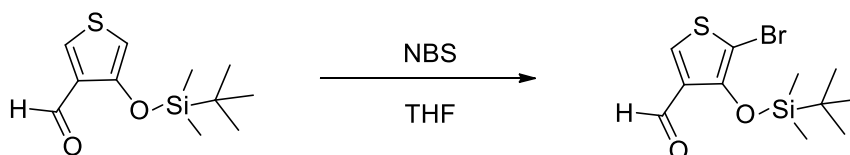


Figure 2.25. $^1\text{H-NMR}$ spectrum of 4-((*tert*-butyldimethylsilyl)oxy)thiophene-3-carbaldehyde

Synthesis of 5-bromo-4-((*tert*-butyldimethylsilyl)oxy)thiophene-3-carbaldehyde



Scheme 2.13. Synthesis of 5-bromo-4-((*tert*-butyldimethylsilyl)oxy)thiophene-3-carbaldehyde
 4-((*tert*-butyl dimethylsilyl)oxy)thiophene-3-carbaldehyde (40 mg, 0.16 mmol) was dissolved in tetrahydrofuran (5 mL) in a round bottomed flask prior to the addition of N-bromosuccinimide (66 mg, 0.37 mmol) at room temperature over a period of 10 min. An aliquot of the reaction mixture was taken out in 1 h, 3h and overnight intervals, quenched with deionized water, extracted with ether and TLC analysis were carried out in order to monitor the consumption of the starting materials. As no change in starting materials were observed even after overnight, reaction mixture was allowed to reflux gently for 3 h, quenched with deionized water and extracted with ether. The

combined organic layers were washed with deionized water, dried over anhydrous MgSO_4 and evaporated under reduced pressure. Column chromatography was carried out using ethyl acetate: hexane (1:49) to purify the product. Collected fractions were evaporated under reduced pressure to obtain the yellow colored oil (52 mg, 0.16 mmol, 99 %). $^1\text{H-NMR}$ (CDCl_3 , 500 MHz; 9.77(s, 1H) 7.98(s, 1H), 1.05(s, 9H), 0.26(s, 6H)). $^1\text{H-NMR}$ spectrum is given in figure 2.26.

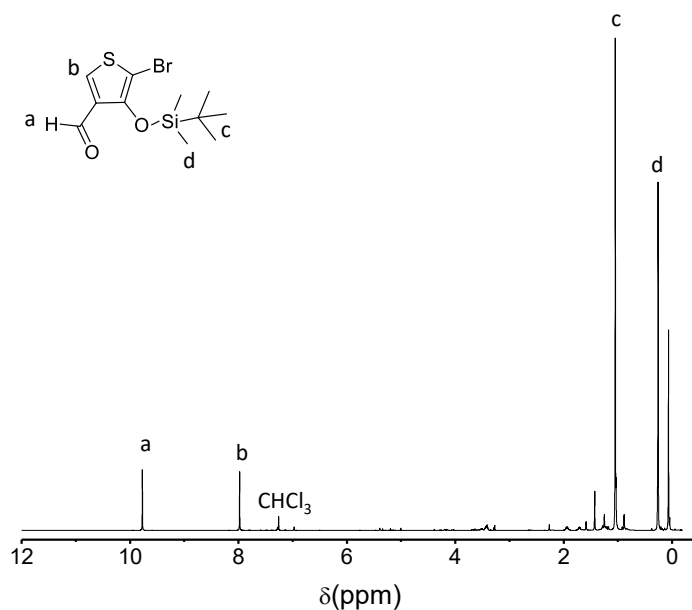
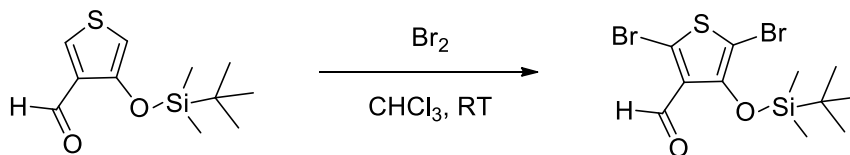


Figure 2.26. $^1\text{H-NMR}$ spectrum of 5-bromo-4-((*tert*-butyldimethylsilyl)oxy)thiophene-3-carbaldehyde

Synthesis of 2,5-dibromo-4-((*tert*-butyldimethylsilyl)oxy)thiophene-3-carbaldehyde



Scheme 2.14. Synthesis of 2,5-dibromo-4-((*tert*-butyldimethylsilyl)oxy)thiophene-3-carbaldehyde

4-((*tert*-butyl dimethylsilyl)oxy)thiophene-3-carbaldehyde (29 mg, 0.12 mmol) was dissolved in chloroform (20 mL) in a round bottomed flask prior to the addition of bromine (31 mg, 0.26 mmol) at room temperature. An aliquot of the reaction mixture was taken out in 3 h, 5 h, overnight and 24 h intervals, quenched with 4 M sodium hydroxide, extracted with ether and TLC analysis were carried out to monitor the consumption of the starting materials. As no starting materials were observed after 24 h, quenched with 4 M sodium hydroxide, extracted with ether, dried over anhydrous MgSO₄ and evaporated under reduced pressure. Column chromatography was carried out using ethyl acetate: hexane (1:99) to purify the product. Collected fractions were evaporated under reduced pressure to obtain the yellow colored oil (19 mg, 0.047 mmol, 39 %). ¹H-NMR (CDCl₃, 500 MHz; 9.81(s, 1H), 1.04(s, 9H), 0.25(s, 6H)). ¹H-NMR spectrum is given in figure 2.27.

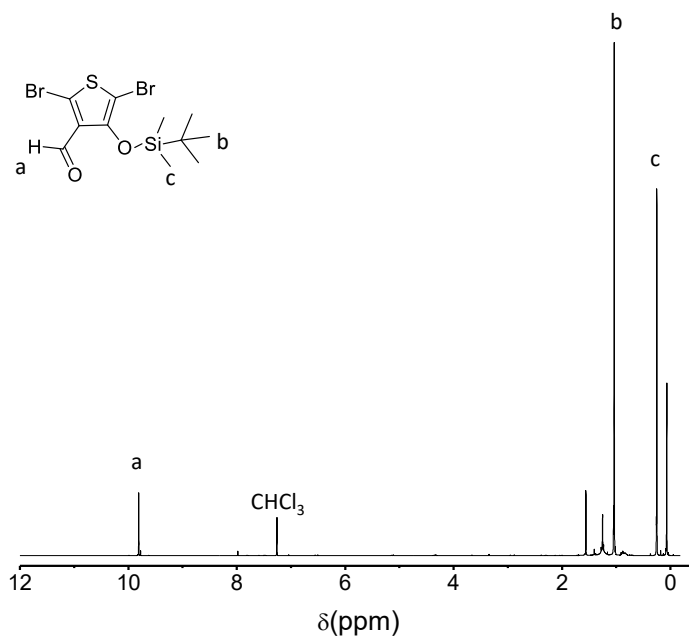
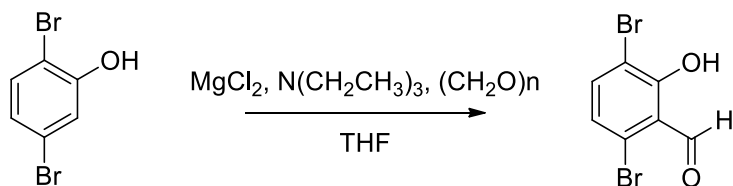


Figure 2.27. ¹H-NMR spectrum of 2,5-dibromo-4-((*tert*-butyl dimethylsilyl)oxy)thiophene-3-carbaldehyde

Synthesis of 3,6-dibromo-2-hydroxybenzaldehyde



Scheme 2.15. Synthesis of 3,6-dibromo-2-hydroxybenzaldehyde

Anhydrous magnesium chloride beads (3.8 g, 40 mmol), and solid paraformaldehyde (2.4 g, 79 mmol) were kept under nitrogen in a dry 250 mL three-necked round bottomed flask equipped with a reflux condenser. Dry tetrahydrofuran (100 mL) was added by a syringe. Triethylamine (5.6 mL, 40 mmol) was added dropwise by a syringe and the mixture was stirred for 10 minutes at room temperature. At this point, 2,5-dibromophenol (2.0 g, 7.8 mmol) was added dropwise by a syringe, resulting in a yellow color mixture. The reaction mixture was allowed to reflux under nitrogen for 12 h, cooled to room temperature, quenched with acidified deionized water (100 mL) and extracted with ethyl acetate (100 mL \times 3). The combined organic layers were washed with deionized water (100 mL \times 3), dried over anhydrous MgSO₄ and evaporated under reduced pressure. The crude was purified through column chromatography using ethyl acetate: hexane (1:19) as the eluting solvent followed by washing with cold hexane to obtain the product as a yellow solid (0.54 g, 1.9 mmol, ¹H-NMR (CDCl₃, 500 MHz; 12.64(s, 1H), 10.28(s, 1H), 7.60(d, 1H, J=8.5), 7.09(d, 1H, J=8.5)). ¹³C-NMR (CDCl₃, 500 MHz; 197.55, 160.45, 140.33, 126.56, 125.19, 118.24, 111.19). ¹H-NMR and ¹³C-NMR spectra are given in figure 2.28 and figure 2.29.

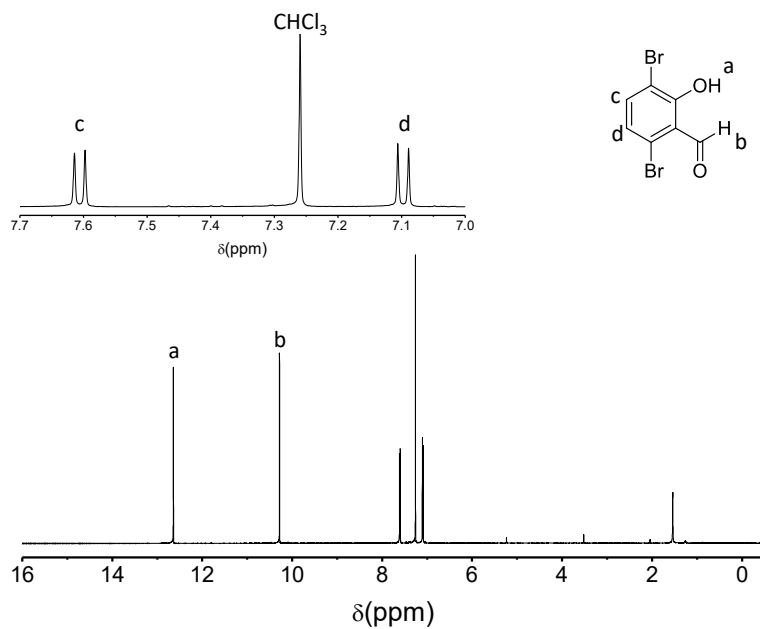


Figure 2.28. $^1\text{H-NMR}$ spectrum of 3,6-dibromo-2-hydroxybenzaldehyde

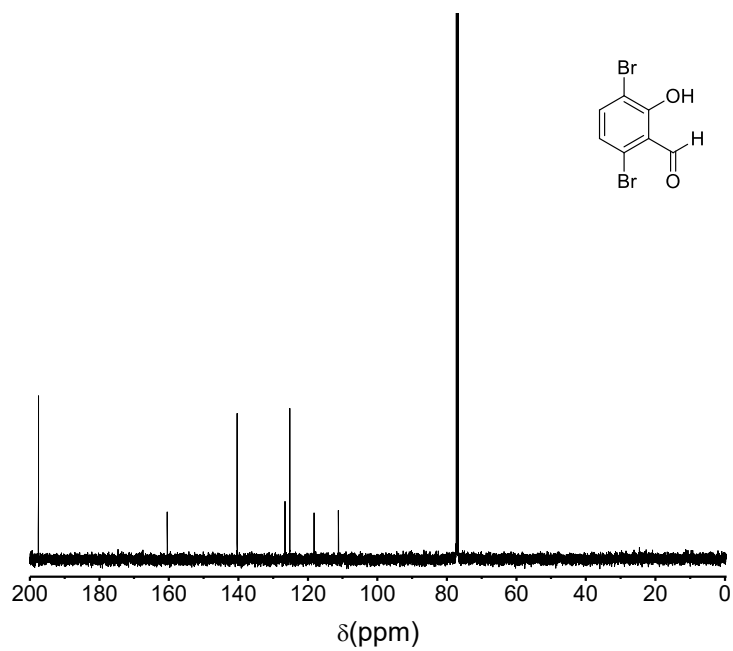
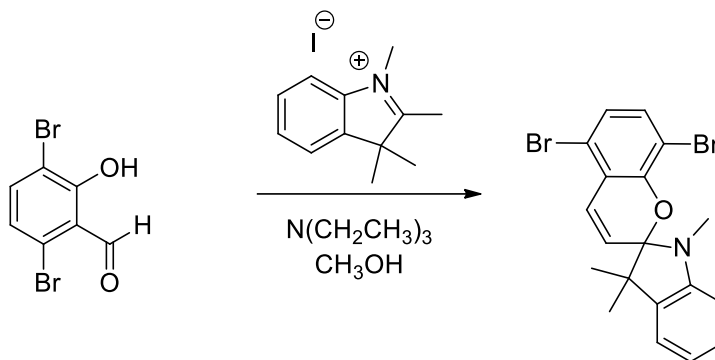


Figure 2.29. $^{13}\text{C-NMR}$ spectrum of 3,6-dibromo-2-hydroxybenzaldehyde

Synthesis of 5,8-dibromo-1', 3', 3'-trimethylspiro[chromene-2,2'-indoline]



Scheme 2.16. Synthesis of 5,8-dibromo-1', 3', 3'-trimethylspiro[chromene-2,2'-indoline]

1,2,3,3-Tetramethyl-3H-indoleium iodide (0.21 g, 0.69 mmol) and 3,6-dibromo-2-hydroxybenzaldehyde (0.19 g, 0.69 mmol) in methanol (20 mL) was kept in a 100 mL three-necked round bottomed flask equipped with a reflux condenser and kept under nitrogen for 10 min. Three drops of triethylamine were added at room temperature and the reaction mixture was allowed to reflux gently for 1 h under nitrogen, allowed to cool to room temperature, quenched in deionized water and extracted with ethyl acetate (100 mL \times 3). The combined organic layer was washed with deionized water (100 mL \times 3), dried over magnesium sulfate and the solvent was evaporated under reduced pressure. The crude was purified by column chromatography using ethyl acetate:hexane (1:19) as the eluting solvent. The pure compound was obtained as a white solid (0.13 g, 0.30 mmol, 43 %). $^1\text{H-NMR}$ (CDCl_3 , 500 MHz ;7.19(m, 3H), 7.08(d, 1H, $J=7.2$), 6.95(d, 1H, $J=8.5$), 6.87(m, 1H,), 6.54(d, 1H, $J=7.8$), 5.82(d, 1H, $J=10.5$), 2.72(s, 3H), 1.32(s, 3H), 1.20(s, 3H)) $^{13}\text{C-NMR}$ (CDCl_3 , 500 MHz; 151.72, 147.83, 136.32, 133.24, 127.98, 127.61, 124.65, 122.16, 121.42, 120.40, 119.77, 119.50, 108.71, 106.95, 105.99, 51.96, 28.95, 25.70, 20.31). $^1\text{H-NMR}$ and $^{13}\text{C-NMR}$ spectra are given in figure 2.30 and figure 2.31. 2D-NMR analysis is given in figure 2.32 and figure 2.33.

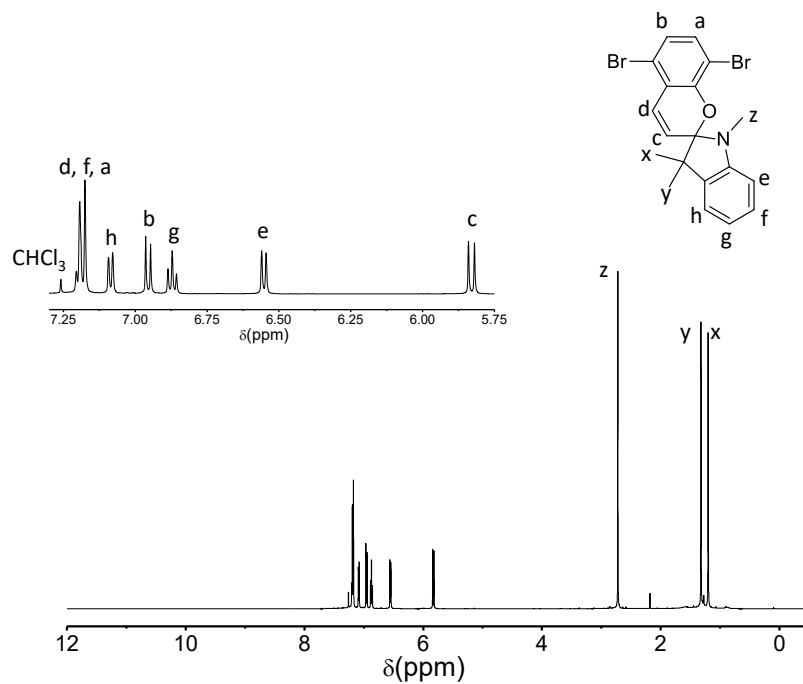


Figure 2.30. ¹H-NMR spectrum of 5,8-dibromo-1', 3', 3'-trimethylspiro[chromene-2,2'-indoline]

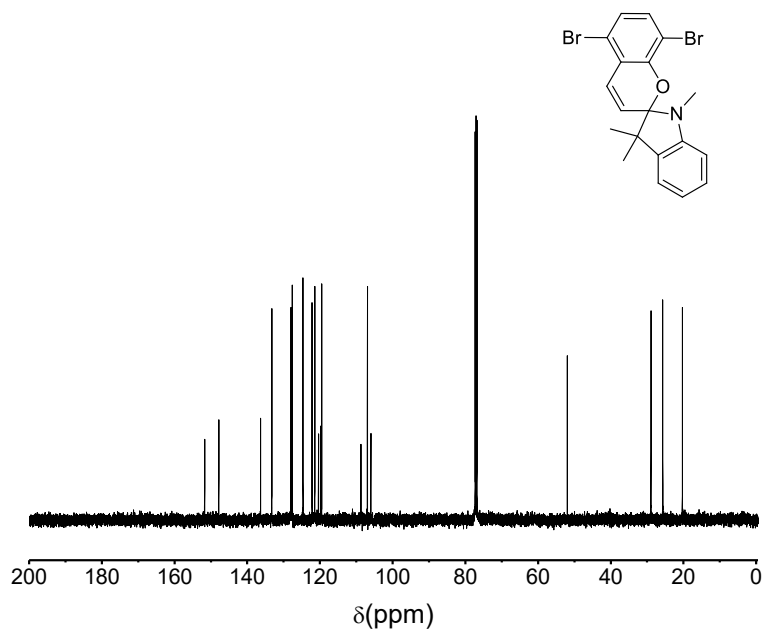


Figure 2.31. ¹³C-NMR spectrum of 5,8-dibromo-1', 3', 3'-trimethylspiro[chromene-2,2'-indoline]

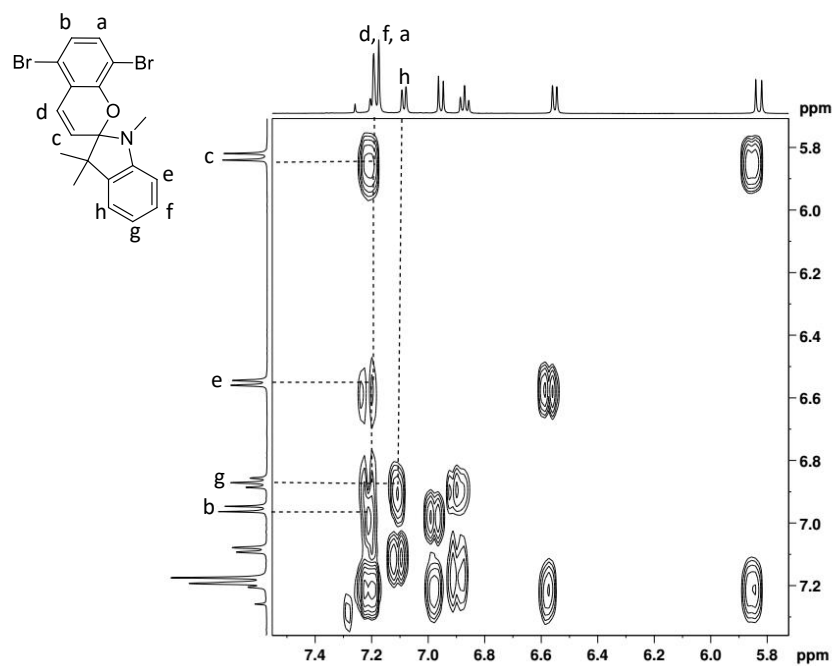


Figure 2.32. Expanded ^1H - ^1H COSY spectrum of 5,8-dibromo-1', 3', 3'-trimethylspiro[chromene-2,2'-indoline]

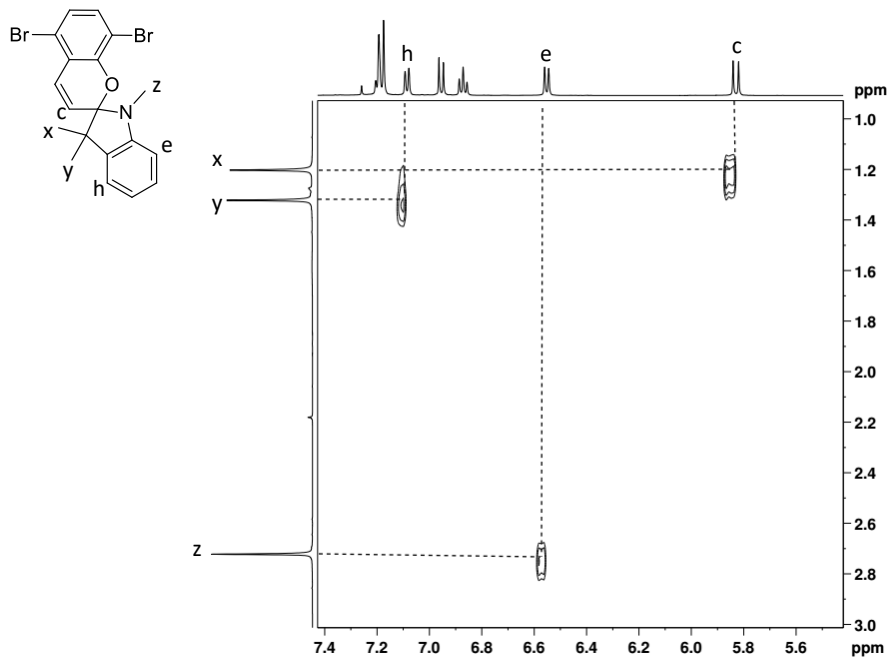
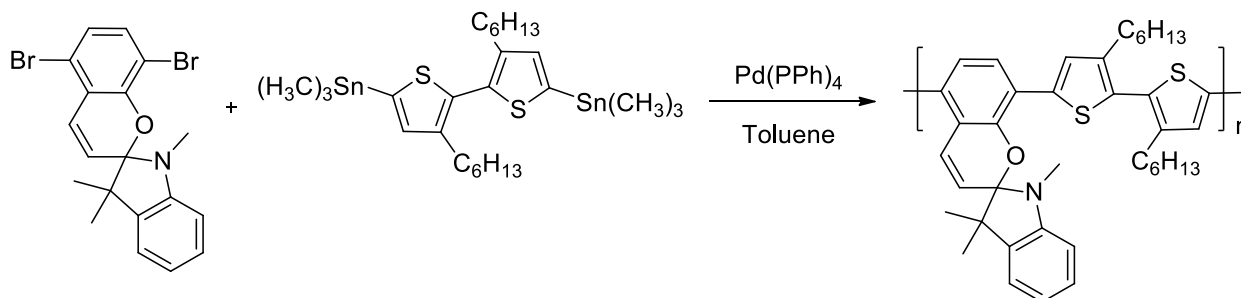


Figure 2.33. Expanded ^1H - ^1H NOESY spectrum of 5,8-dibromo-1', 3', 3'-trimethylspiro[chromene-2,2'-indoline]

Synthesis of poly[1',3',3'-trimethylspiro(chromene-2,2'-indoline)-alt-(3,3'-dihexyl-2,2'-bithiophene)]



Scheme 2.17. Synthesis of poly[1',3',3'-trimethylspiro(chromene-2,2'-indoline)-alt-(3,3'-dihexyl-2,2'-bithiophene)]

5,8-dibromo-1', 3', 3'-trimethylspiro[chromene-2,2'-indoline] (0.21 g, 0.48 mmol) was dissolved in dry toluene (3.6 mL) in a three-necked round bottomed flask equipped with a reflux condenser and (3,3'-dihexyl-[2,2'-bithiophene]- 5,5'-diyl)bis(trimethylstannane)) (0.32 g, 0.48 mmol) was added to it under nitrogen and nitrogen was bubbled through this solution for 15 min prior to the addition of tetrakis(triphenylphosphine)-palladium(0) (22 mg, 0.019 mmol). The reaction mixture was allowed to reflux under nitrogen for 48 h before precipitating the polymer in acidified methanol. The polymer was filtered and purified by soxhlet extraction with methanol, hexane and chloroform successively. The polymer was obtained from the chloroform fraction upon evaporation of the solvent as a yellow solid (65 mg, 22 %). $^1\text{H-NMR}$ (CDCl_3 , 500 MHz; 5.89 (br, 4H), 5.78 (d, 1H), 2.78 (br, 13H)) SEC: $M_n = 2730 \text{ g mol}^{-1}$, PDI = 2.37. $^1\text{H-NMR}$ spectrum is given in figure 2.34.

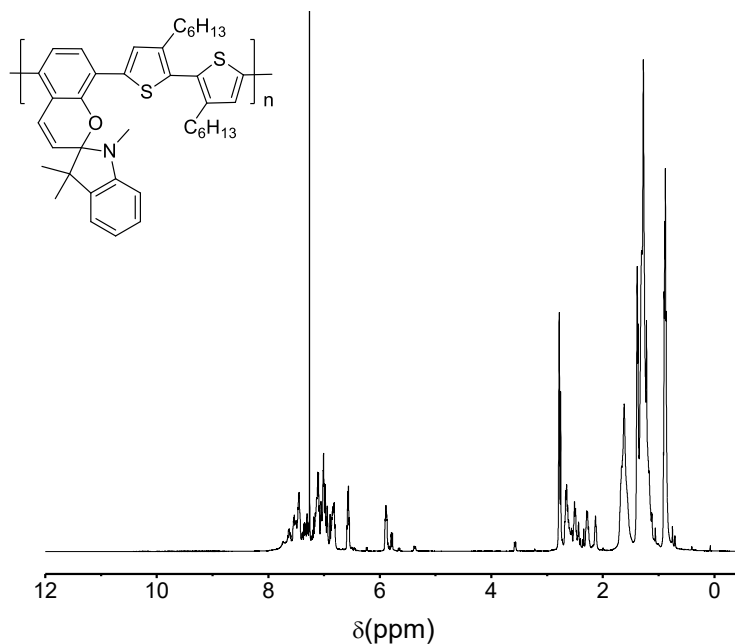


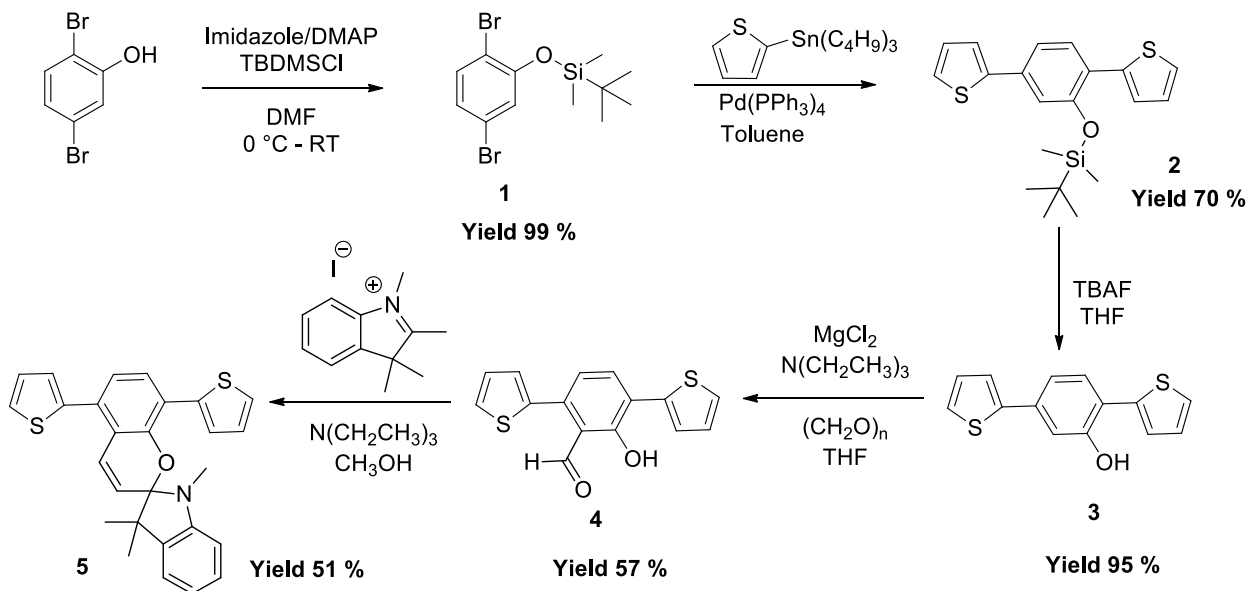
Figure 2.34. $^1\text{H-NMR}$ spectrum of poly[1',3',3'-trimethylspiro(chromene-2,2'-indoline)-*alt*-(3,3'-dihexyl-2,2'-bithiophene)]

2.4 Results and Discussion

2.4.1 Photochromism of SPs with thiophene substituents in chromene moiety

2,5-dibromophenol was used as the precursor compound to incorporate thiophene substituents with a SP along the conjugated backbone. As shown in scheme 2.18, hydroxyl group of 2,5-dibromophenol was protected as a silyl ether (compound **1**) prior the Stille coupling reaction with 2-(tributylstannyl) thiophene using tetrakis(triphenylphosphine)-palladium(0) as the catalyst (compound **2**). Tetrabutylammonium fluoride (TBAF) was used as the deprotecting reagent to yield compound **3**. Formylation of compound **3** under standard Duff reaction conditions was not attainable as compound **3** was not soluble in trifluoroacetic acid. Therefore, *ortho*-hydroxy aromatic aldehyde (compound **4**) was obtained with magnesium chloride, triethylamine and

paraformaldehyde.²⁰ Thiophene substituted SP (compound **5**) was then synthesized by reacting compound **4** with 1,2,3,3-Tetramethyl-3H-indoleium iodide in the presence of triethylamine.



Scheme 2.18. Synthesis of thiophene substituted SP

UV-Vis kinetic analysis of compound **5** was performed with 2×10^{-5} M solutions. The solutions were freshly prepared by stirring the compound overnight in the respective solvent. When the solution was photolyzed with a 500 W Oriel Hg arc lamp containing a 334 nm line filter, a maximum absorbance was noted at 450 nm and 590 nm in methanol (figure 2.35). This indicates that SP with thiophene substituents on chromene moiety could show photochromism. Even though compound **5** shows photochromism in polar methanol, the MC solution (open form) was colorless due to the absorbance of two complementary colors (at 450 nm and 590 nm). Photochromism in non-polar toluene can only be observed through continuous irradiation due to a very fast reverse reaction. Thermal decay measurements were performed in methanol during the photoexcitation of the colorless SP to MC and taking an absorbance reading of the λ_{max} of the MC as it decays every 15 s over 90 s (figure 2.36). MC showed a first order decay and table 2.1 summarizes the half-lives of the peaks at 450 nm and 590 nm. The decay rates in methanol is relatively fast ($t_{1/2} \approx 70$ s) due to the electron donating nature of thiophene units which does not stabilize the open MC form as it does with nitro substituents in the chromene moiety.¹⁷

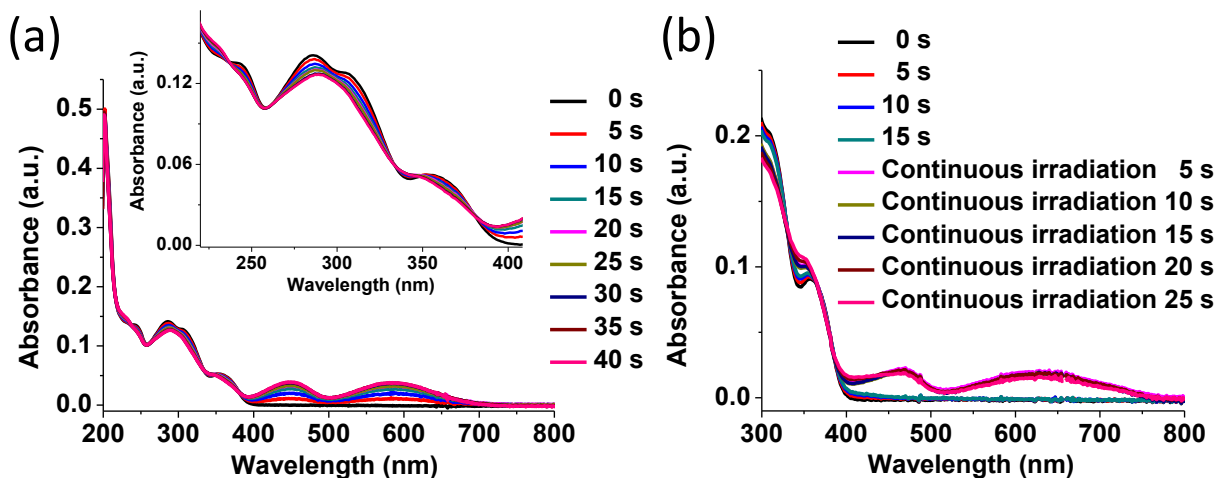


Figure 2.35. Optical absorbance of MC of thiophene substituted SP (a) in methanol (b) in toluene. All spectra are obtained upon irradiating 2×10^{-5} M solutions using a mercury arc lamp with a 334 nm line filter.

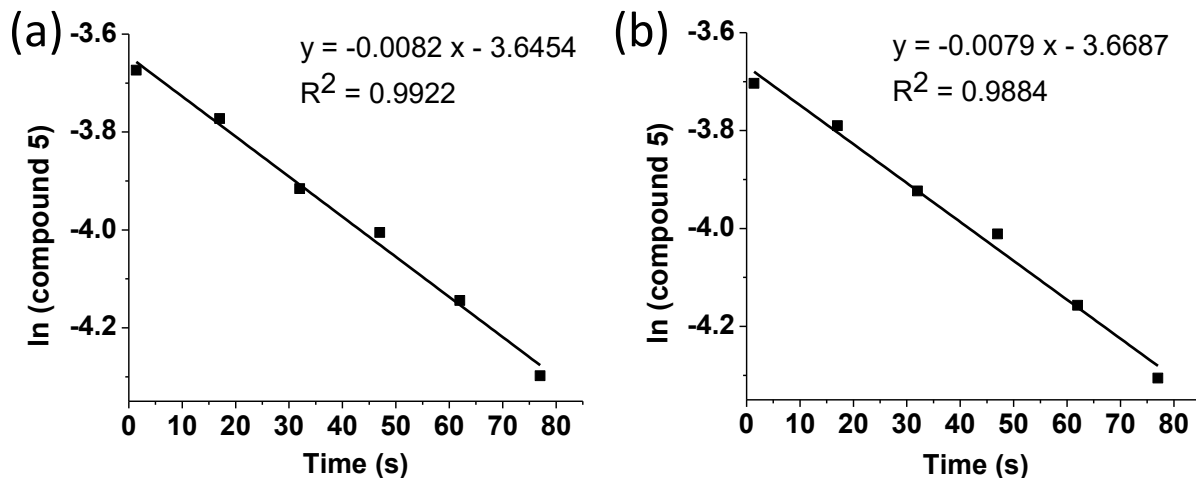


Figure 2.36. Absorbance decay of MC peak in methanol at (a) 450 nm (b) 590 nm

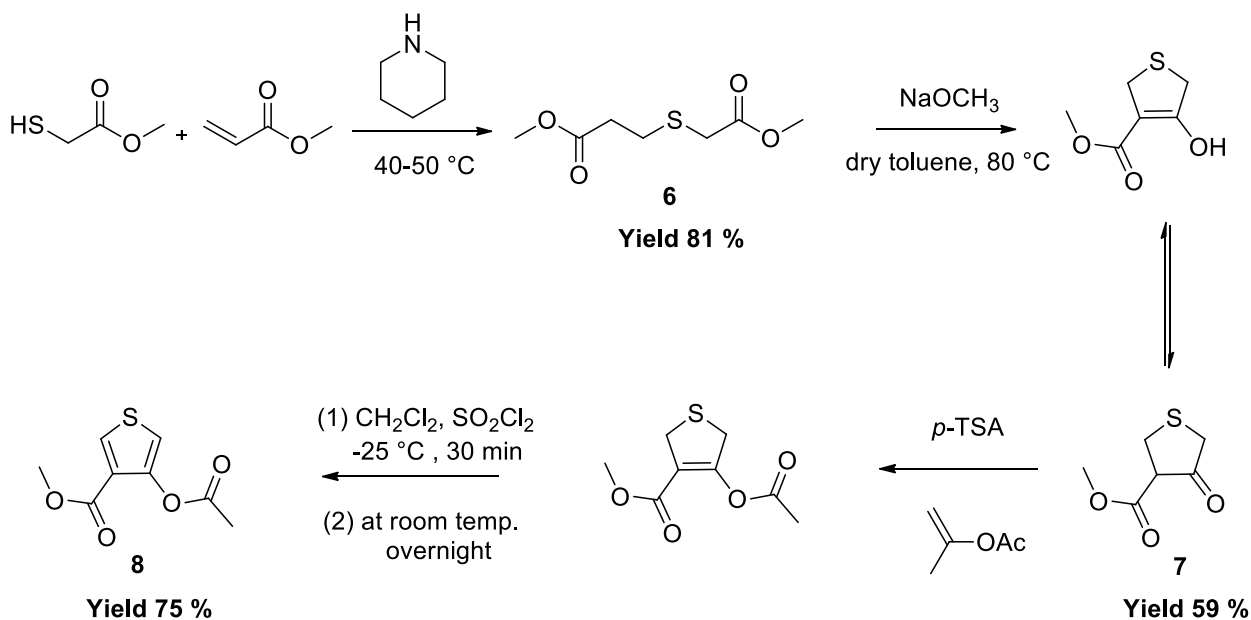
Table 2.1. Half-lives of MC decay in methanol^a

Compound	$t_{1/2}(s)$	
	Methanol ($\lambda_{max} = 450$ nm)	Methanol ($\lambda_{max} = 590$ nm)
5	72 ± 11	74 ± 12

^a Samples were run with a 2×10^{-5} M solutions and the recorded values are an average of three runs, Irradiated for the first time.

2.4.2 Synthesizing *ortho*-hydroxy aromatic aldehydes with a thiophene unit

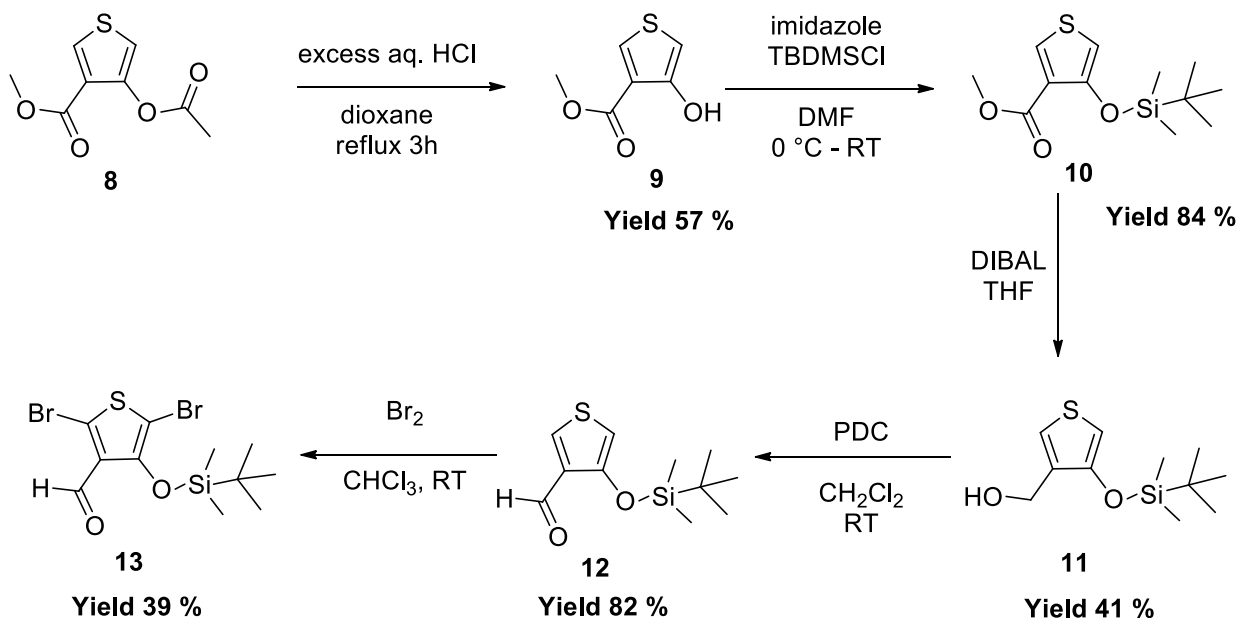
We have also studied the possibility of synthesizing *ortho*-hydroxy aromatic aldehydes with thiophene unit targeting all thiophene based photochromic polymers. As shown in scheme 2.19 compound **6** was obtained through β addition of methyl thioglycolate to methyl acrylate in the presence of piperidine. Dieckmann condensation of the compound **6** with sodium methoxide yielded the compound **7**.¹⁹ The aromatic diester (compound **8**) was obtained through a modified procedure reported by Jeffery *et al.*²¹



Scheme 2.19. Synthesis of thiophene based aromatic diester

Next compound **8** was selectively hydrolyzed to obtain compound **9** (scheme 2.20). Compound **9** was highly temperature sensitive and decomposes fast at room temperature but stable at low temperatures. Since we speculated that the instability of compound **9** arises with the hydroxyl group, a silyl ether protection was carried out to obtain compound **10**. Then the silyl ether protected compound was reduced to the alcohol with diisobutylaluminum hydride. LAH at 0 °C can also use for the reduction to obtain comparable yield. However, the reaction needs to be carried out at low temperatures to yield compound **11**. Pyridinium dichromate oxidation of the alcohol yielded the aldehyde **12**. Dibrominated compound of **12** can be obtained with bromine at room temperature.

N-bromosuccinimide bromination yielded only the 5-monobrominated product even under reflux conditions.



Scheme 2.20. Synthesis of the dibrominated silyl ether protected *ortho*-hydroxy aromatic aldehyde of thiophene

Ability to form SP with the silyl ether protected compound **12** and **13** was carried out using 1,3,3-trimethyl-2-methyleneindoline in methanol followed by dropwise addition of TBAF. None of the compounds yielded a photochromic compound. We believe that this is due to the highly unstable nature of hydroxyl group at 4-position. Gronowitz and co-workers had also reported that this *ortho*-hydroxy aromatic aldehyde of thiophene decomposes rapidly to a resin.²² From the above observations, we have concluded that all thiophene based photochromic polymer synthesis is not achievable through a thiophene based *ortho*-hydroxy aromatic aldehyde.

2.4.3 Benzene based photochromic SPs

A suitable and a possible route to incorporate SP into thiophene based polymers would be to use dibrominated benzene based SP compound and co-polymerize it with thiophene based moiety. The dibrominated salicylaldehyde (compound **14**) was obtained using the similar reaction condition used in obtaining compound **4** (scheme 2.21). Reacting compound **14** with 1,2,3,3-tetramethyl-

3H-indoleium iodide in the presence of triethyl amine yielded compound **15** (rough crystal structure is given in figure 2.37).

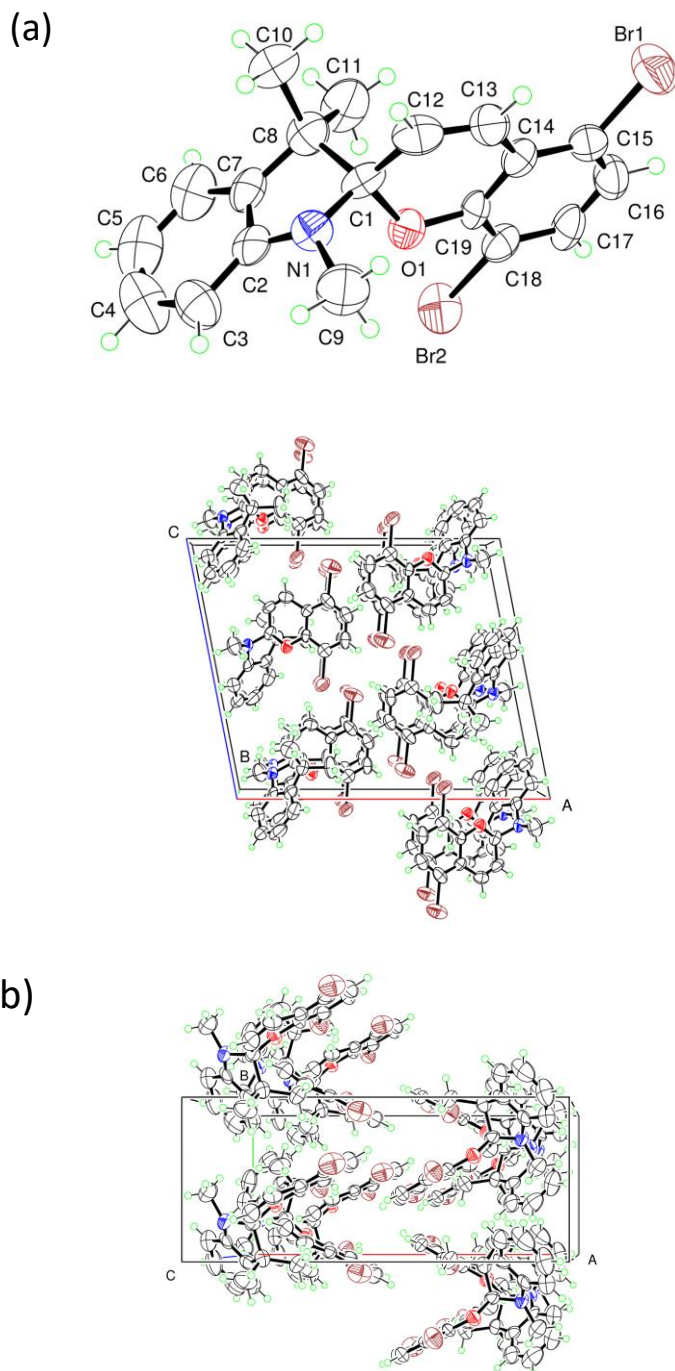
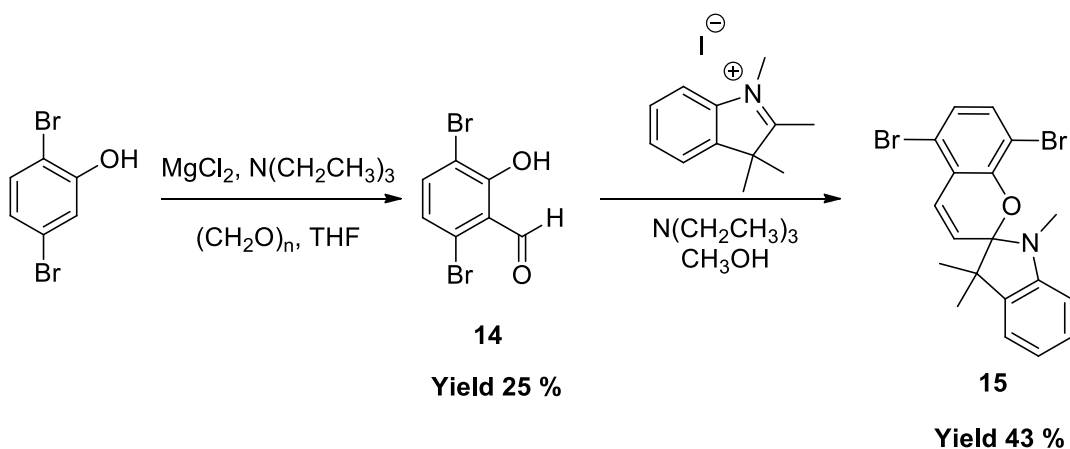
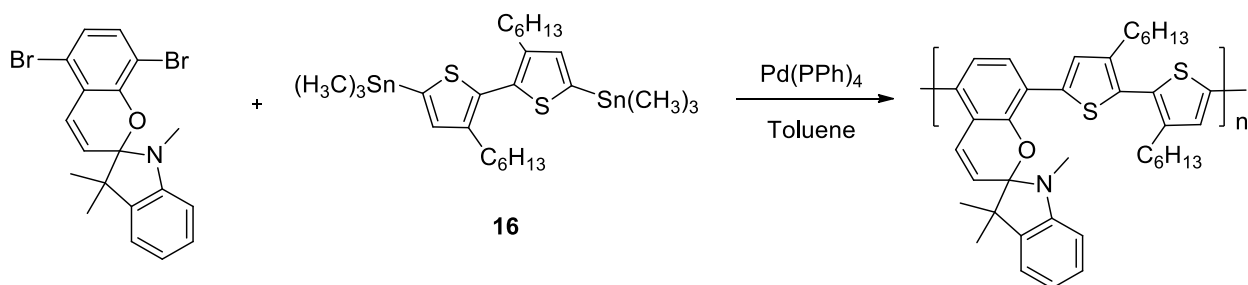


Figure 2.37. Rough crystal structure of compound **15** ($R_1 = 0.10$), the bond distances and angles are comparable to compound **1** of previously reported literature²³ (a) Side view (b) Top view

Copolymerization of compound **15** with compound **16** via Stille cross coupling reaction in the presence of tetrakis(triphenylphosphine)-palladium(0) catalyst (scheme 2.22) yielded a low molecular weight polymer ($M_n = 2730 \text{ g mol}^{-1}$). This could be due to the close proximity of *ortho*-bromine substituent to nitrogen and oxygen which provide a steric barrier to the catalyst.¹² Further investigation of different catalytic systems are needed to improve the molecular weight. A better approach would be to start the synthesis with 2,5-dibromo-4-fluorophenol or 2,5-dibromo-3,4-difluorophenol and carry out the synthesis to obtain the dibrominated compound prior to the synthesis of SP as shown in scheme 2.23. This places the bromine further away from the nitrogen and oxygen, thus eliminating the steric barrier to the catalyst and can improve the molecular weight of the polymer.



Scheme 2.21. Synthesis of benzene based photochromic SP



Scheme 2.22. SP Polymer synthesis

2.4.4 Photochromism of the SP polymer

The photochromism of the low molecular weight polymer that we have obtained in scheme 2.22 was tested upon irradiating polymer solutions (toluene) and thin films using a mercury arc lamp with a 334 nm line filter. Neither polymer solutions in toluene nor the thin films show photochromism upon irradiation with UV light. UV-Vis spectrum of polymer in toluene solution (black) and in thin film (red) is given in figure 2.38. As the polymer is not soluble in methanol, investigation of photochromism in methanol is not attainable. However, we have further investigated the photochromism of the polymer in chloroform solution and in thin films. Even though the thin films did not show photochromism, appearance of a weak peak around 575 nm upon irradiating polymer solution in chloroform suggested that incorporation of SP into thiophene based polymer via chromene moiety did not prevented the photochromism of SP. But, attaching more electron withdrawing substituents such as fluorine to benzene moiety (scheme 2.23) or copolymerize the dibrominated SP unit with more electron withdrawing acceptor units would result in better photochromism in thiophene based spiropyran conjugated polymers.

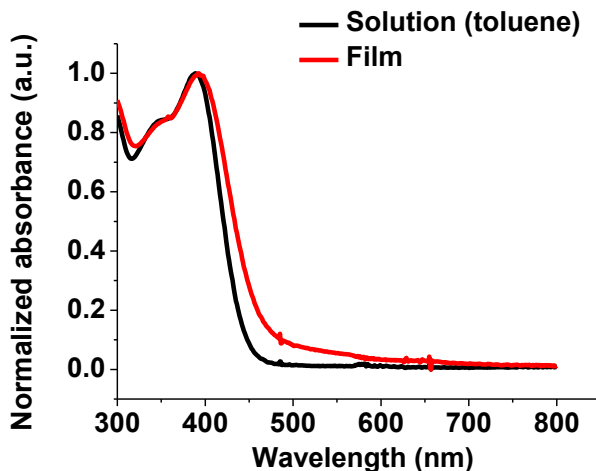


Figure 2.38. UV-Vis spectra of polymer in toluene solution (black) and in thin film (red)

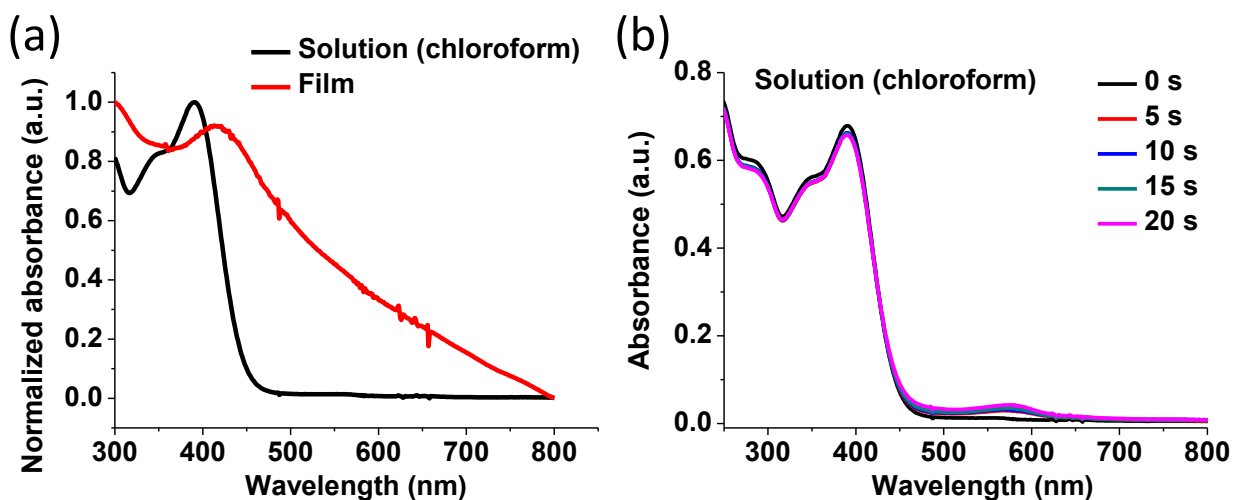
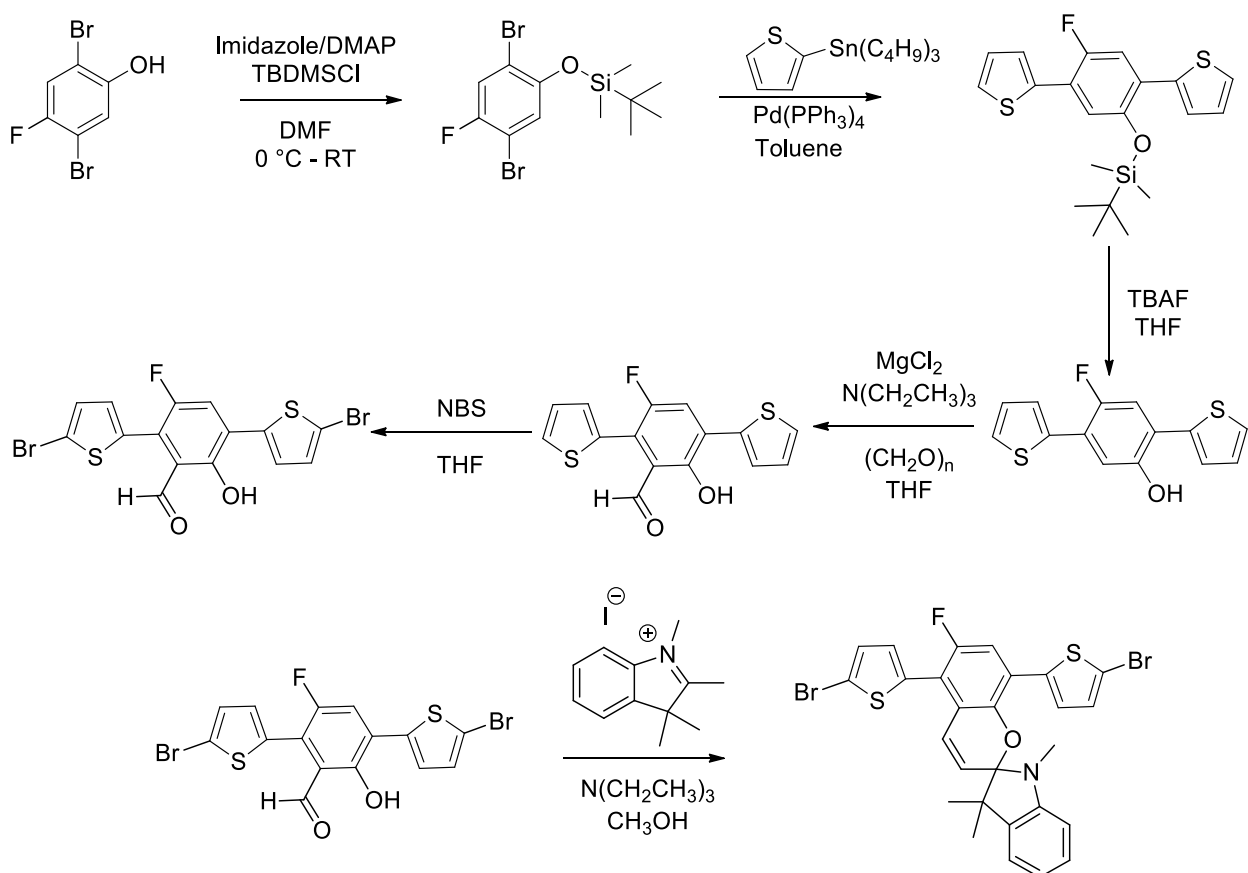


Figure 2.39. (a) UV-Vis spectra of polymer in chloroform solution (black) and in thin film (red) (b) Optical absorbance of photomerocyanine the polymer in chloroform solution upon irradiating with mercury arc lamp with a 334 nm line filter.

2.5 Conclusions and Future work

A new synthetic method was demonstrated to incorporate thiophene substituents into chromene moiety of SPs. This compound showed photochromism in methanol and in toluene (only upon continuous irradiation). This new strategy illustrates the possibility of preserving photochromism in SP when incorporated into thiophene based polymer through the chromene moiety. Due to the instability of *ortho*-hydroxy group of thiophene, synthesis of all thiophene based photochromic polymers is unachievable through a thiophene based *ortho*-hydroxy aromatic aldehyde. Synthesis of a new benzene based SP was demonstrated as a possible route to incorporate SP into thiophene based polymers. This polymer showed the photochromism in chloroform solution, but not in thin films. This attempt is expected to establish a new strategy to obtain SP based main conjugated polymers targeting molecular electronic applications.



Scheme 2.23. A possible route to obtain dibrominated derivative of SP

2.6 Acknowledgments

The authors would like to thank the NSF (DMR-1505950) and Welch Foundation (AT-1740) for the financial support provided for this research.

2.7 References

1. Orgiu, E.; Samorì, P. 25th Anniversary Article: Organic Electronics Marries Photochromism: Generation of Multifunctional Interfaces, Materials, and Devices. *Advanced Materials* **2014**, *26*, 1827-1845.
2. Berkovic, G.; Krongauz, V.; Weiss, V. Spiropyran and Spiroxazines for Memories and Switches. *Chemical Reviews* **2000**, *100*, 1741-1754.
3. Wakayama, Y.; Hayakawa, R.; Seo, H.-S. Recent progress in photoactive organic field-effect transistors. *Science and Technology of Advanced Materials* **2014**, *15*, 024202.

4. Fu, L.-N.; Leng, B.; Li, Y.-S.; Gao, X.-K. Photoresponsive organic field-effect transistors involving photochromic molecules. *Chinese Chemical Letters* **2016**, *27*, 1319-1329.
5. Sergei, M. A. Spiroprans: structural features and photochemical properties. *Russian Chemical Reviews* **1990**, *59*, 663.
6. Shen, Q.; Cao, Y.; Liu, S.; Steigerwald, M. L.; Guo, X. Conformation-Induced Electrostatic Gating of the Conduction of Spiropyran-Coated Organic Thin-Film Transistors. *The Journal of Physical Chemistry C* **2009**, *113*, 10807-10812.
7. Bunker, B. C.; Kim, B. I.; Houston, J. E.; Rosario, R.; Garcia, A. A.; Hayes, M.; Gust, D.; Picraux, S. T. Direct Observation of Photo Switching in Tethered Spiroprans Using the Interfacial Force Microscope. *Nano Letters* **2003**, *3*, 1723-1727.
8. Klajn, R. Spiropyran-based dynamic materials. *Chemical Society Reviews* **2014**, *43*, 148-184.
9. Florea, L.; Diamond, D.; Benito-Lopez, F. Photo-Responsive Polymeric Structures Based on Spiropyran. *Macromolecular Materials & Engineering* **2012**, *297*, 1148-1159.
10. Harvey, C. P.; Tovar, J. D. Main-chain photochromic conducting polymers. *Polymer Chemistry* **2011**, *2*, 2699-2706.
11. Yang, J.; Ng, M.-K. Synthesis of a Photochromic Conjugated Polymer Incorporating Spirobenzopyran- in the Backbone. *Synthesis* **2006**, *2006*, 3075-3079.
12. Sommer, M.; Komber, H. Spiropyran Main-Chain Conjugated Polymers. *Macromolecular Rapid Communications* **2013**, *34*, 57-62.
13. Davis, D. A.; Hamilton, A.; Yang, J.; Cremer, L. D.; Van Gough, D.; Potisek, S. L.; Ong, M. T.; Braun, P. V.; Martínez, T. J.; White, S. R.; Moore, J. S.; Sottos, N. R. Force-induced activation of covalent bonds in mechanoresponsive polymeric materials. *Nature* **2009**, *459*, 68-72.
14. Lee, C. K.; Davis, D. A.; White, S. R.; Moore, J. S.; Sottos, N. R.; Braun, P. V. Force-Induced Redistribution of a Chemical Equilibrium. *Journal of the American Chemical Society* **2010**, *132*, 16107-16111.
15. Wagner, K.; Zanoni, M.; Elliott, A. B. S.; Wagner, P.; Byrne, R.; Florea, L. E.; Diamond, D.; Gordon, K. C.; Wallace, G. G.; Officer, D. L. A merocyanine-based conductive polymer. *Journal of Materials Chemistry C* **2013**, *1*, 3913-3916.
16. Wagner, K.; Byrne, R.; Zanoni, M.; Gambhir, S.; Dennany, L.; Breukers, R.; Higgins, M.; Wagner, P.; Diamond, D.; Wallace, G. G.; Officer, D. L. A Multiswitchable Poly(terthiophene) Bearing a Spiropyran Functionality: Understanding Photo- and Electrochemical Control. *Journal of the American Chemical Society* **2011**, *133*, 5453-5462.

17. Dissanayake, D. S.; McCandless, G. T.; Stefan, M. C.; Biewer, M. C. Systematic variation of thiophene substituents in photochromic spiropyrans. *Photochemical & Photobiological Sciences* **2017**.
18. Lukyanov, B.; Lukyanova, M. Spiropyrans: Synthesis, Properties, and Application. (Review). *Chemistry of Heterocyclic Compounds* **2005**, *41*, 281-311.
19. Woodward, R. B.; Eastman, R. H. Tetrahydrothiophene (“Thiophane”) Derivatives. *Journal of the American Chemical Society* **1946**, *68*, 2229-2235.
20. Hansen, T. V.; Skattebøl, L.: *ortho*-Formylation of Phenols; Preparation of 3-Bromosalicylaldehyde. In *Organic Syntheses*; John Wiley & Sons, Inc., 2003.
21. Press, J. B.; Hofmann, C. M.; Safir, S. R. Thiophene systems. 2. Synthesis and chemistry of some 4-alkoxy-3-substituted thiophene derivatives. *The Journal of Organic Chemistry* **1979**, *44*, 3292-3296.
22. Gronowitz, S. B., A. On the Tautomerism of Some 3-Hydroxythiophene Aldehydes and Acids. *Acta Chem. Scand* **1966**, *20*, 261-262.
23. Beckett, J. O. S.; Olmstead, M. M.; Fettinger, J. C.; Gray, D. A.; Manabe, S.; Mascali, M. Crystal structure determination as part of an undergraduate laboratory experiment: 1',3',3'-trimethylspiro[chromene-2,2'-indoline] and 1',3',3'-trimethyl-4-[(E)-(1,3,3-trimethylindolin-2-ylidene)methyl]spiro[chroman-2,2'-indoline]. *Acta Crystallographica Section E* **2016**, *72*, 1659-1662.

CHAPTER 3
ATTACHMENT OF SPIROPYRAN AS A PENDENT GROUP TO THIOPHENE BASED
MATERIALS

Authors - Dushanthi S. Dissanayake, Gregory T. McCandless, Mihaela C. Stefan and
Michael C. Biewer

Department of Chemistry and Biochemistry, BE26

The University of Texas at Dallas

800 West Campbell Road

Richardson, Texas 75080-3021

Dushanthi S. Dissanayake carried out the synthesis and characterization of the compounds. Gregory T. McCandless performed the single crystal X-ray diffraction analysis. Professors Mihaela C. Stefan and Michael C. Biewer developed the initial idea for the project, aided in troubleshooting during the project, and edited chapter for publication.

Reproduced (adapted) by permission of the European Society for Photobiology, the European Photochemistry Association, and the Royal Society of Chemistry.

Dissanayake, D. S.; McCandless, G. T.; Stefan, M. C.; Biewer, M. C. Systematic variation of thiophene substituents in photochromic spiropyrans, *Photochem. Photobiol. Sci.*, **2017**, *16*, 1057-1062.

3.1 Abstract

A new synthetic method was developed to incorporate photochromic spiropyran (SP) substituents that are conjugated to thiophene repeat units. A series of compounds with a systematic variation of substituents were synthesized (SP-T, SP-T-Br, SP-T-T, SP-T-T-T and SP-T-T-T-T-SP) and their photochromism in both polar (methanol) and non-polar (toluene) solvents were studied. The decay rate of the open merocyanine form decreased with an increasing thiophene chain length. Further attempts are being made to synthesize the dibrominated derivative. Findings suggested that a suitable substituent at 7-position of spiropyran would lead to a successful dibrominated derivative.

3.2 Introduction

Well known thiophene based semiconducting polymers such as poly(3-hexylthiophene) have been studied in blends with SPs in organic field effect transistors.^{1,2} However, the major challenge lies with phase separation of SPs within these blends. Therefore, it is very important to design and synthesize new SPs with improved properties such as excellent reversibility, stability of both isomers, fast response, low fatigue and excellent blending ability. We believe that this could be successfully achieved by covalently attaching the SP to thiophene based materials. Despite the few reports on attaching thiophene based moieties to SP via indoline nitrogen,³⁻⁵ a detailed study on photochromic properties of thiophene based SP via other positions of SP is lacking. Furthermore, it is very important to systematically vary substituents and study them under identical experimental conditions to allow a direct comparison of substituent effect on photochromic properties. A very recent study by Louie and co-workers emphasized the importance of this concept and demonstrated the effect of electron withdrawing and donating substituents on C-O bond lability and therefore the photochromic properties.⁶ In this study we systematically varied the thiophene substituents in photochromic SP at the 5-position and studied their kinetics parameters. This study is expected to give a fundamental understanding of photochromic properties of SP when attached to a thiophene based chain.

3.3 Experimental

3.3.1 Materials

All commercial chemicals were purchased either from Sigma Aldrich Chemical Co. LLC. or from Fisher Scientific Co. LLC. and were used without further purification unless otherwise noted. All glassware and syringes were dried at 120 °C for at least 24 h before use and cooled in a desiccator. Tetrahydrofuran (THF) and toluene were dried over sodium/benzophenone ketyl and freshly distilled under nitrogen prior to use. Acetonitrile was distilled in the presence of calcium hydride under nitrogen and dried over molecular sieves before use.

3.3.2 Analysis

NMR analysis: ^1H and ^{13}C NMR spectra and all 2D-NMR analysis were recorded at 25 °C using a Bruker AVANCE III 500 MHz NMR spectrometer, and were referenced to residual protio solvent (CHCl_3 : δ 7.26 ppm, DMSO: δ 2.5 ppm, Acetone: δ 2.05 ppm). The data are reported as follows: chemical shifts are reported in ppm on δ scale, multiplicity (s = singlet, d = doublet, t = triplet, q = quartet, m = multiplet).

GC-MS analysis: GC-MS analysis was performed on Hewlett-Packard Agilent 6890-5973 GC-MS workstation equipped with a Hewlett-Packard fused silica capillary GC column cross-linked with 5 % phenylmethylsiloxane. Helium was used as the carrier gas (1 mL min^{-1}). Sample analysis conditions: injector and detector temperature = 250 °C, initial temperature = 70 °C, temperature ramp = $10 \text{ }^\circ\text{C min}^{-1}$, final temperature = 280 °C.

Single crystal X-ray diffraction analysis: Single crystal X-ray diffraction analysis was performed using single crystals grown by slow evaporation method in ethyl acetate/hexanes solvent mixture or diethyl ether, low temperature ($T = 90 \text{ K}$) single crystal X-ray diffraction datasets were collected for compounds **SP-T** (scd0687), **SP-T-Br** (scd0686) and tribrominated derivative (scd0591) with a Bruker Kappa D8 Quest diffractometer. This diffractometer has a microfocus Mo $K\alpha$ radiation source, liquid nitrogen cryostream, and CMOS Photon 100 detector.

After data collection, the datasets were integrated (Bruker SAINT) and scaled (Bruker SADABS, multi-scan absorption correction method). Afterwards, starting structural models were generated with SHELXT (intrinsic phasing method)⁷ for compounds **SP-T** and **SP-T-Br**. These structural models were subsequently refined in SHELXL2014 with anisotropic non-hydrogen atomic sites and “riding” hydrogen atomic sites.⁸ Due to positional disorder, the brominated thiophene substituent of compound **SP-T-Br** was modelled with two different orientations in the “average” structure. The refined ratio of the two orientations is approximately 70:30 (where the major conformation is indicated with solid bonds and the minor conformation is indicated with dashed bonds in figure 3.42).

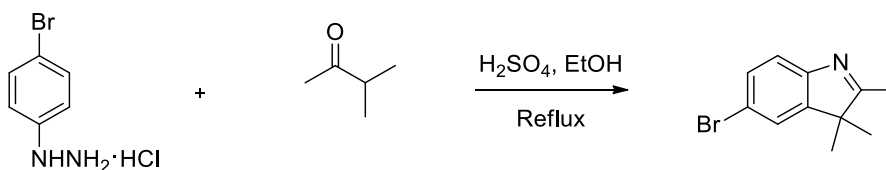
CCDC 1520537 and 1520538 contain the supplementary crystallographic data for compounds **SP-T** and **SP-T-Br**, respectively, and can be obtained free of charge from The Cambridge Crystallographic Data Centre via www.ccdc.cam.ac.uk/structures.

HR-MS analysis: HR-MS analysis was performed with Shimadzu LCMS IT-TOF instrument. Samples were re-suspended in CHCl₃, vortexed and injected (15 μL).

UV-Vis spectroscopic analysis: UV-Vis kinetics experiments were carried using an Agilent 8453 UV-Vis spectrometer coupled with a 500 W Oriel Hg arc lamp containing a 334 nm line filter. 1 cm cuvettes were used for the experiments. All the experiments were performed in identical experimental conditions of 1×10⁻⁵ M solutions. The solutions were freshly prepared prior to each experiment by stirring each compound overnight in the respective solvent.

3.3.3 Synthetic procedures

*Synthesis of 5-bromo-2,3,3-trimethyl-3H-indole*⁹



Scheme 3.1. Synthesis of 5-bromo-2,3,3-trimethyl-3H-indole

A solution of 4-bromophenyl hydrazine (1.0 g, 4.5 mmol), isopropylmethylketone (0.81 g, 9.3 mmol), ethanol (100 mL), and concentrated H₂SO₄ (0.44 g, 4.5 mmol) in a 250 mL round bottomed flask was heated under reflux for 12 h. After cooling down to room temperature, the mixture was quenched in 10 % NaHCO₃, extracted with ether, washed with deionized water, dried over anhydrous MgSO₄ and evaporated under reduced pressure to obtain the crude product as a reddish oil (1.0 g, 96 %) which was used in the next step without further purifications. ¹H-NMR (CDCl₃, 500 MHz; 7.42(m, 3H), 2.27(s, 3H), 1.30(s, 6H). ¹³C-NMR (CDCl₃, 500 MHz; 188.57, 152.47, 147.76, 130.70, 124.88, 121.24, 118.94, 54.14, 30.33, 22.94, 15.41). ¹H-NMR and ¹³C-NMR spectra are given in figure 3.1 and figure 3.2.

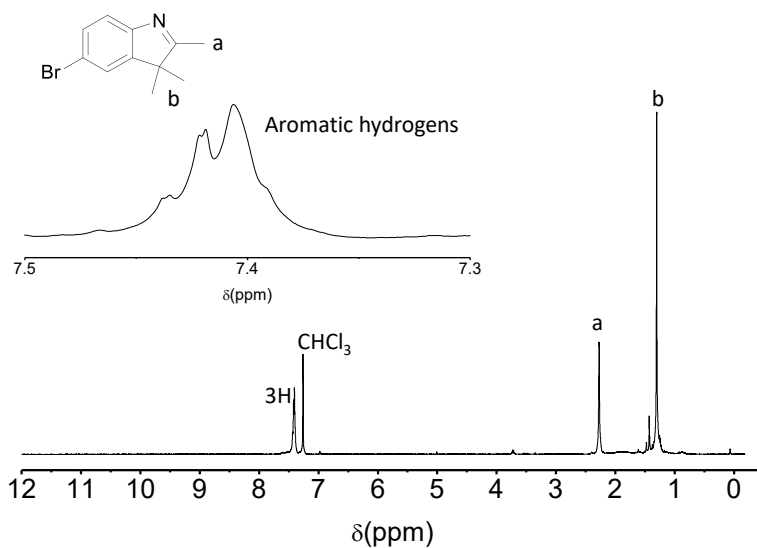


Figure 3.1. ¹H-NMR spectrum of 5-bromo-2,3,3-trimethyl-3H-indole

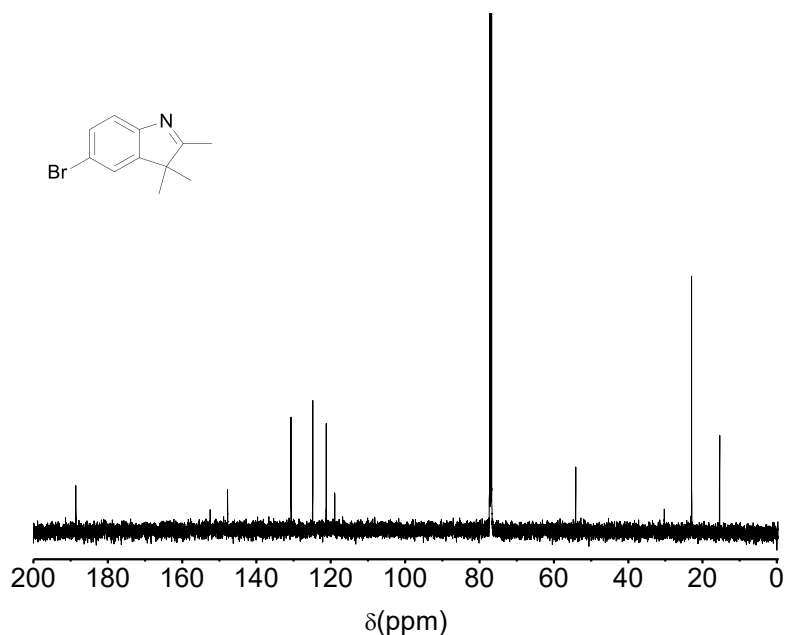
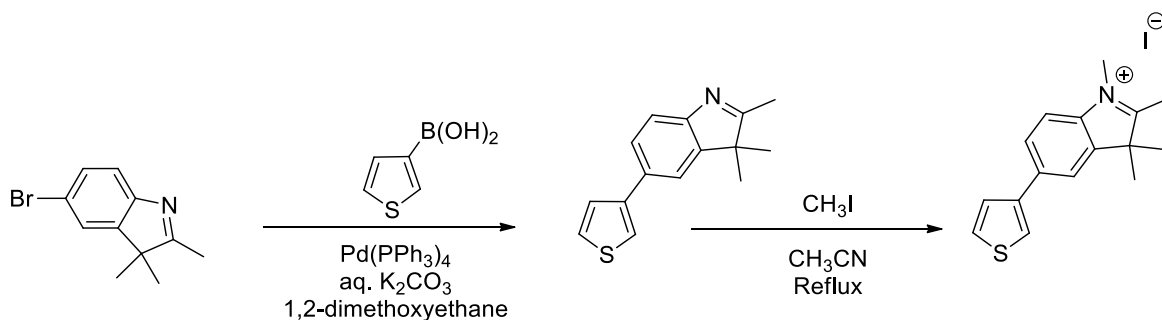


Figure 3.2. ^{13}C -NMR spectrum of 5-bromo-2,3,3-trimethyl-3H-indole

Synthesis of 1,2,3,3-tetramethyl-5-(thiophene-3-yl)-3H-indol-1-ium iodide (modified procedure)¹⁰



Scheme 3.2. Synthesis of 1,2,3,3-tetramethyl-5-(thiophene-3-yl)-3H-indol-1-ium iodide

Step 1

Synthesis of 2,3,3-trimethyl-5-(thiophene-3-yl)-3H-indole

Thiophene-3-boronic acid (0.76 g, 5.7 mmol) and 5-bromo-2,3,3-trimethyl-3H-indole (1.0 g, 4.2 mmol) were dissolved in 1,2-dimethoxy ethane (20 mL). Nitrogen was bubbled through this solution for 15 min prior to the addition of potassium carbonate in water (1.6 g, 12 mmol in 6.0

mL of water). Nitrogen was bubbled through this solution for further 5 min prior to the addition of tetrakis(triphenylphosphine)-palladium(0) (0.13 g, 0.11 mmol). The reaction mixture was allowed to reflux under nitrogen for 12 h and then was cooled down to room temperature, quenched with deionized water, extracted with ether dried over anhydrous MgSO₄ and evaporated under reduced pressure. The crude product was used in step 2 directly without further purification. (M⁺ = 241.1)

Step 2

Synthesis of 1,2,3,3-tetramethyl-5-(thiophene-3-yl)-3H-indole-1-ium-iodide

2,3,3-trimethyl-5-(thiophene-3-yl)-3H-indole (1.0 g, 4.1 mmol) was dissolved in anhydrous acetonitrile (20 mL) and kept under nitrogen prior to the addition of methyl iodide (1.2 g, 8.7 mmol). The reaction mixture was allowed to reflux overnight under nitrogen. The solvent was then evaporated under reduced pressure and the residue was treated with ethyl acetate (100 mL). The final reddish color solid was collected by filtration and washed with ethyl acetate to obtain the product (0.96 g, 2.5 mmol, 57 %). ¹H-NMR (DMSO-d₆, 500 MHz; 8.22(d, 1H, J=1.4), 8.08-8.07 (dd, 1H, J=2.8, J=1.4), 8.00-7.98(dd, 1H, J=8.4, J=1.6), 7.92 (d, 1H, J=8.4), 7.73-7.72(dd, 1H, J=5.1, J=2.9), 7.70-7.69(dd, 1H, J=5.0, J=1.2), 3.98 (s, 3H), 2.75(s, 3H), 1.56(s, 6H)). ¹³C-NMR (CDCl₃, 500 MHz; 195.98, 142.94, 141.42, 140.60, 136.77, 128.11, 126.89, 123.15, 121.45, 115.98, 54.43, 35.13, 22.28, 14.46). ¹H-NMR and ¹³C-NMR spectra are given in figure 3.3 and figure 3.4. 2D-NMR analysis is given in figure 3.5 and figure 3.6.

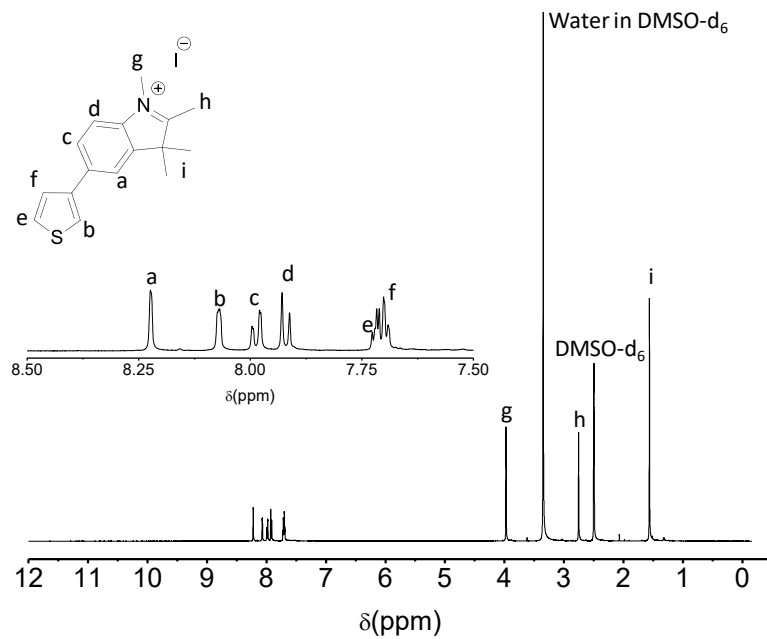


Figure 3.3. $^1\text{H-NMR}$ spectrum of 1,2,3,3-tetramethyl-5-(thiophene-3-yl)-3*H*-indol-1-ium iodide

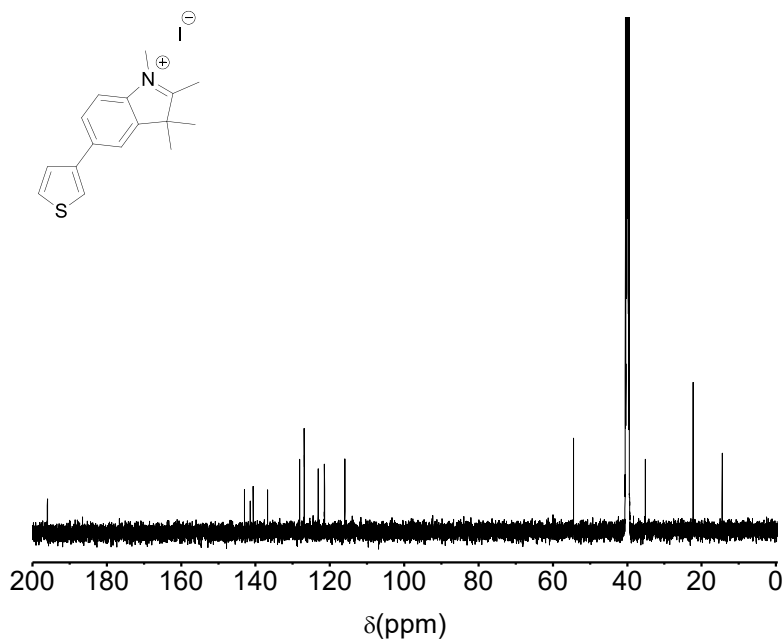


Figure 3.4. $^{13}\text{C-NMR}$ spectrum of 1,2,3,3-tetramethyl-5-(thiophene-3-yl)-3*H*-indol-1-ium iodide

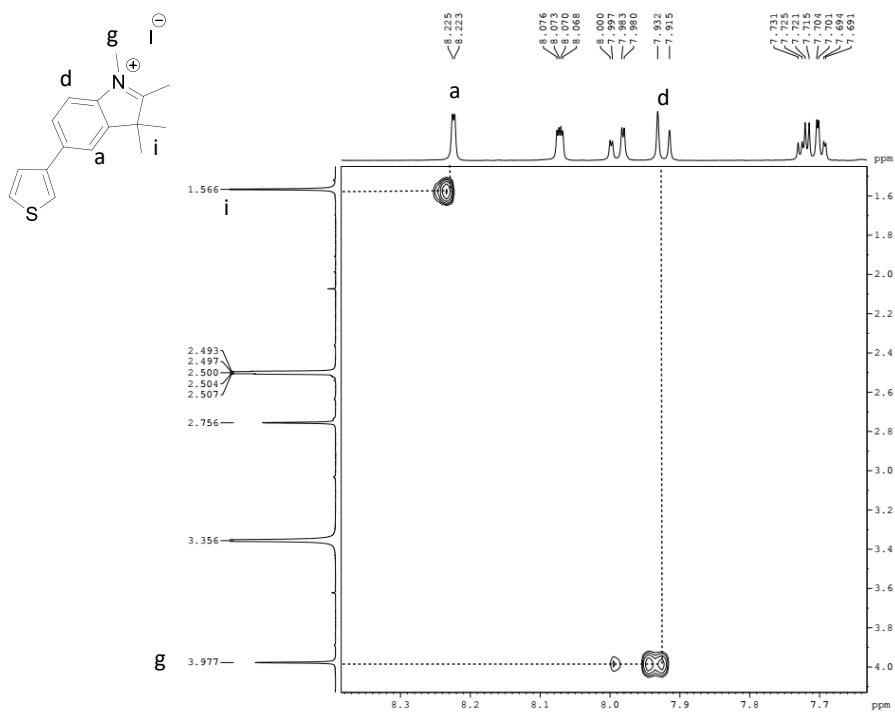


Figure 3.5. Expanded ^1H - ^1H NOESY spectrum of 1,2,3,3-tetramethyl-5-(thiophene-3-yl)-3*H*-indol-1-ium iodide

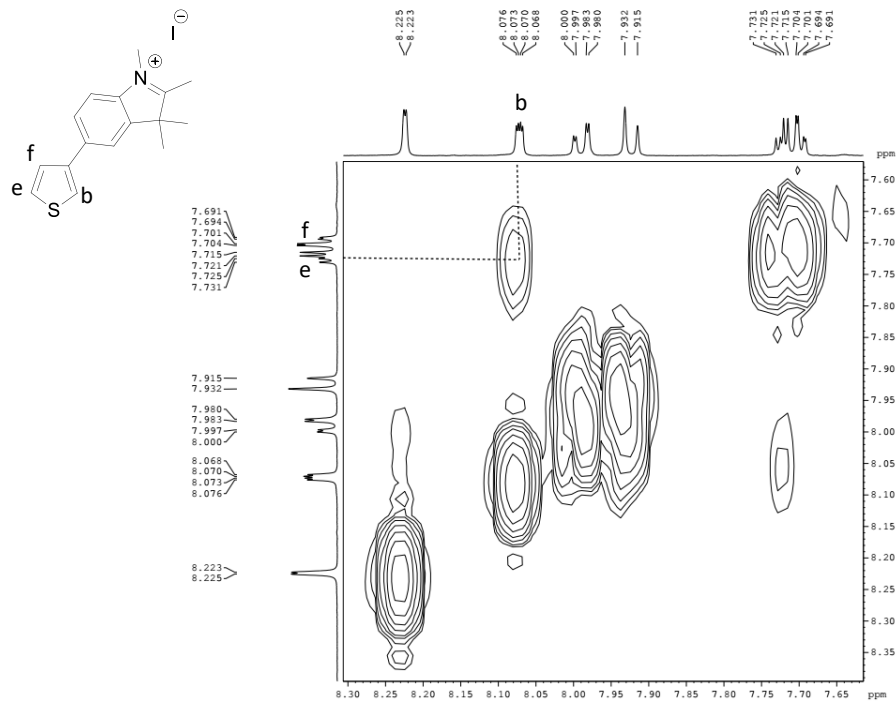
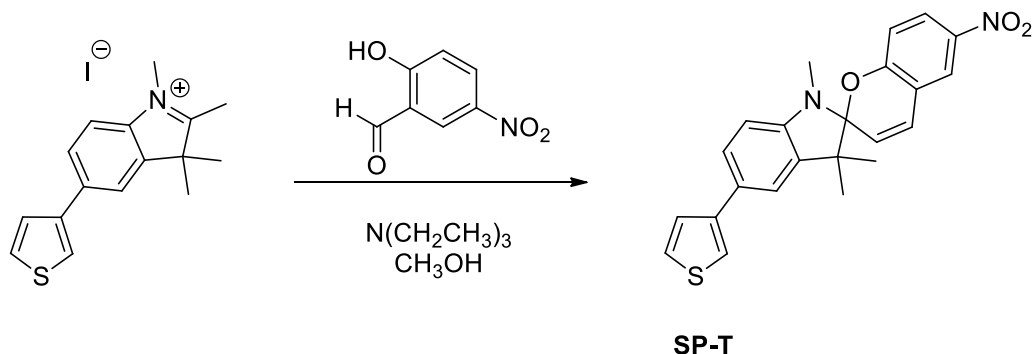


Figure 3.6. Expanded ^1H - ^1H COSY spectrum of 1,2,3,3-tetramethyl-5-(thiophene-3-yl)-3*H*-indol-1-ium iodide

Synthesis of 1',3'3'-trimethyl-6-nitro-5'-(thiophene-3-yl)spiro[chromene-2,2'-indoline]



Scheme 3.3. Synthesis of 1',3'3'-trimethyl-6-nitro-5'-(thiophene-3-yl)spiro[chromene-2,2'-indoline]

1,2,3,3-Tetramethyl-5-(thiophene-3-yl)-3H-indole-1-ium iodide (0.84 g, 2.2 mmol) and 2-hydroxy-5-nitrobenzaldehyde (0.38 g, 2.2 mmol) were kept under nitrogen for 10 min prior to the addition of methanol (100 mL). Four drops of triethylamine were added at room temperature and the reaction mixture was allowed to reflux gently for 3 h under nitrogen, allowed to cool to room temperature, quenched in deionized water and extracted with ethyl acetate (100 mL \times 3). The combined organic layer was washed with deionized water (100 mL \times 3), dried over magnesium sulfate and the solvent was evaporated under reduced pressure. The crude was purified by column chromatography using ethyl acetate:hexane (1:4) as the eluting solvent. The pure compound was obtained as a yellow crystalline solid (0.18 mg, 0.46 mmol, 21 %, MP = 222-225 °C). $^1\text{H-NMR}$ (CDCl_3 , 500 MHz; 8.03 (m, 2H), 7.45(dd, 1H, $J=8.0$, $J=1.1$), 7.37(m, 2H), 7.34(m, 1H), 7.31(m, 1H), 6.93(d, 1H, $J=10.3$), 6.78(d, 1H, $J=8.6$), 6.58(d, 1H, $J=8.0$), 5.87(d, 1H, $J=10.3$), 2.77(s, 3H), 1.34(s, 3H), 1.23(s, 3H)). $^{13}\text{C-NMR}$ (CDCl_3 , 500 MHz; 159.74, 147.07, 142.83, 141.02, 136.79, 128.38, 128.22, 126.36, 126.24, 125.94, 125.93, 122.73, 121.45, 120.08, 118.65, 118.34, 115.51, 107.22, 106.47, 52.34, 28.97, 25.97, 19.99). $^1\text{H-NMR}$ and $^{13}\text{C-NMR}$ spectra are given in figure 3.7 and figure 3.8. 2D-NMR analysis is given in figure 3.9, figure 3.10, figure 3.11, figure 3.12 and figure 3.13.

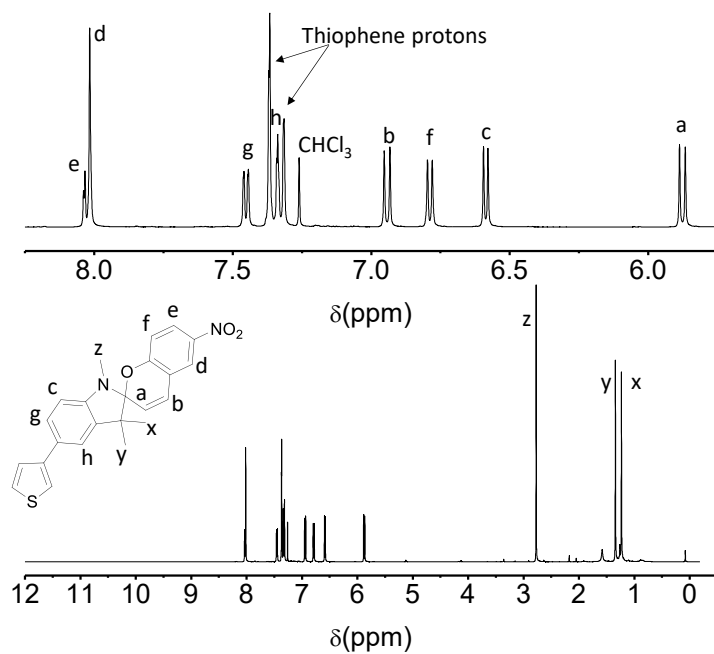


Figure 3.7. $^1\text{H-NMR}$ spectrum of 1',3'3'-trimethyl-6-nitro-5'-(thiophene-3-yl)spiro[chromene-2,2'-indoline]; peak assignment is based on 2D-NMR analysis.

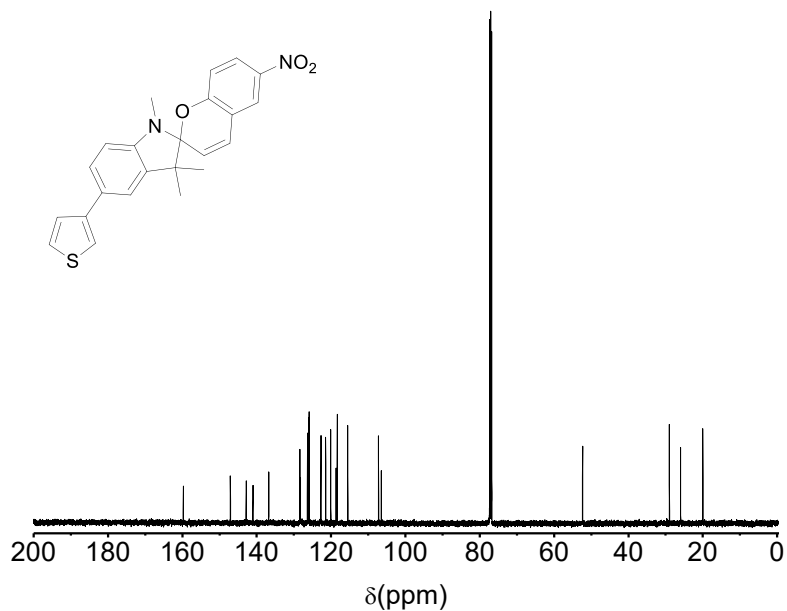


Figure 3.8. $^{13}\text{C-NMR}$ spectrum of 1',3'3'-trimethyl-6-nitro-5'-(thiophene-3-yl)spiro[chromene-2,2'-indoline]

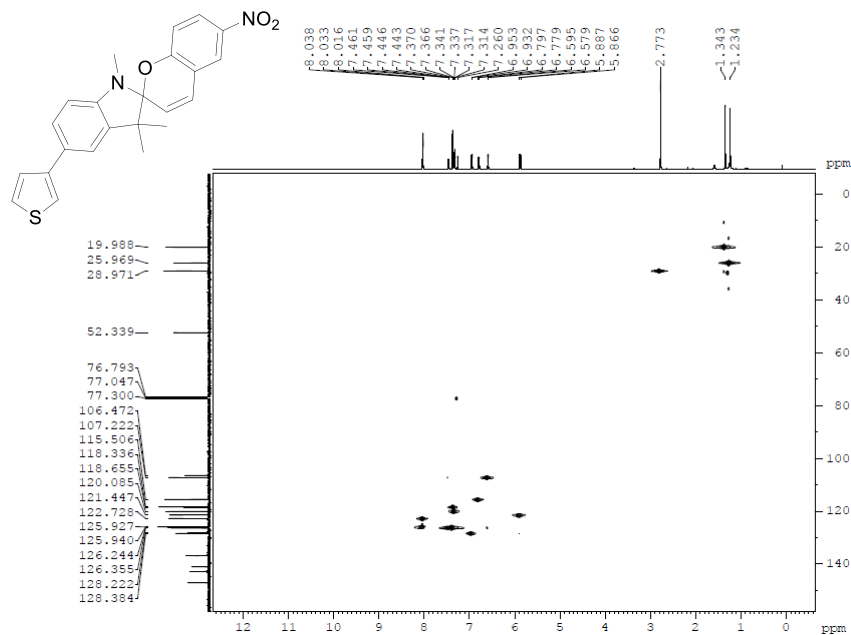


Figure 3.9. 2D-HSQC spectrum of 1',3,3'-trimethyl-6-nitro-5'-(thiophene-3-yl)spiro[chromene-2,2'-indoline]

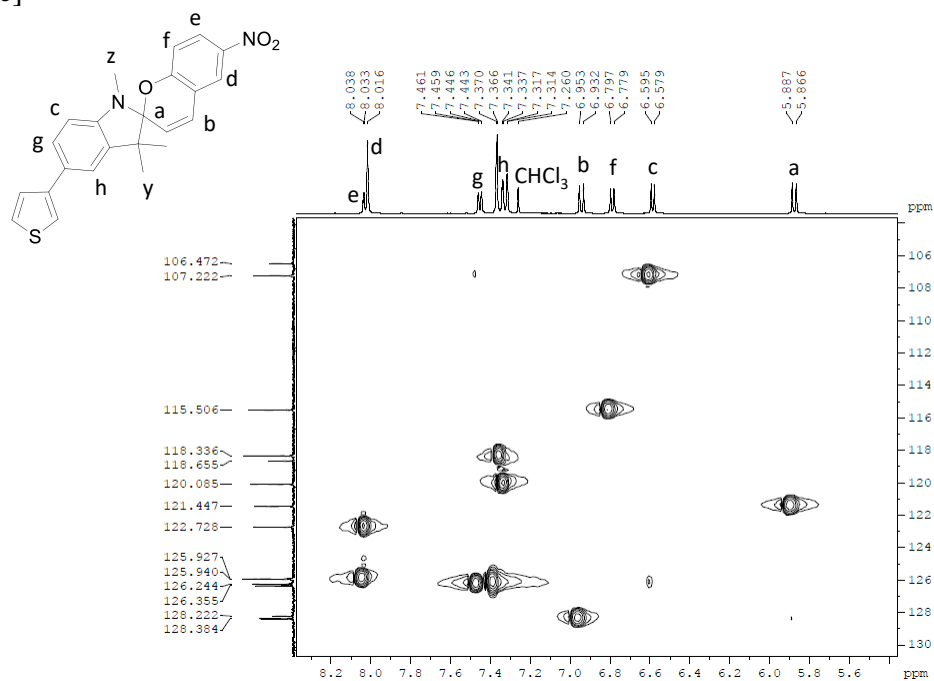


Figure 3.10. Expanded 2D-HSQC spectrum of 1',3,3'-trimethyl-6-nitro-5'-(thiophene-3-yl)spiro[chromene-2,2'-indoline]

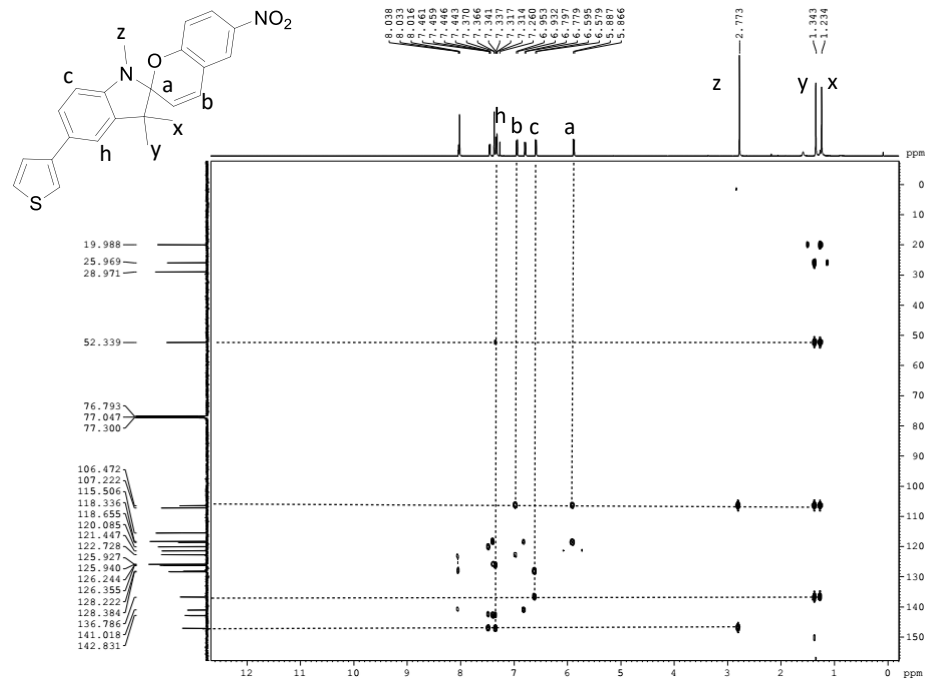


Figure 3.11. 2D-HMBC spectrum of 1',3,3'-trimethyl-6-nitro-5'-(thiophene-3-yl)spiro[chromene-2,2'-indoline]

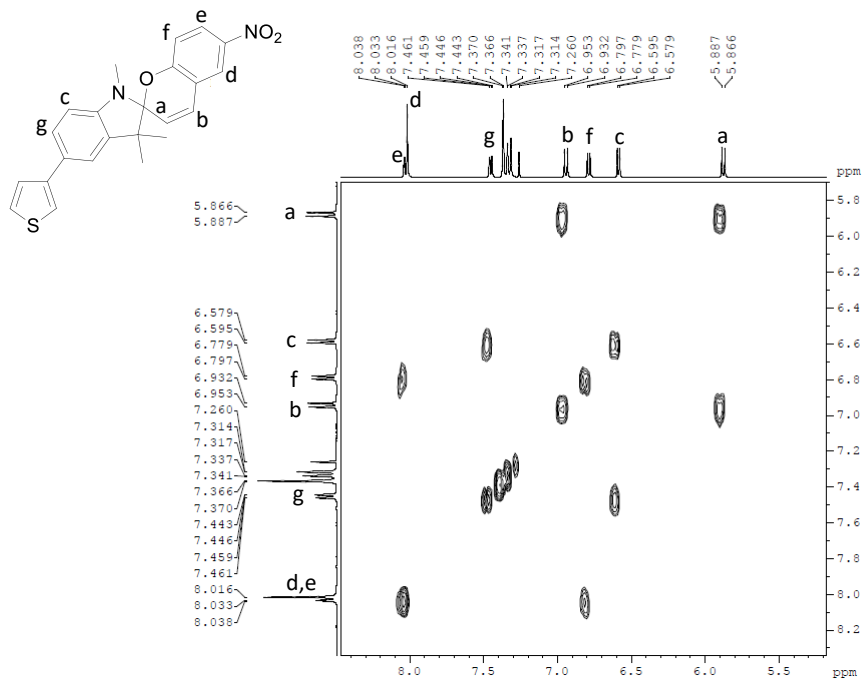


Figure 3.12. Expanded ^1H - ^1H COSY spectrum of 1',3,3'-trimethyl-6-nitro-5'-(thiophene-3-yl)spiro[chromene-2,2'-indoline]

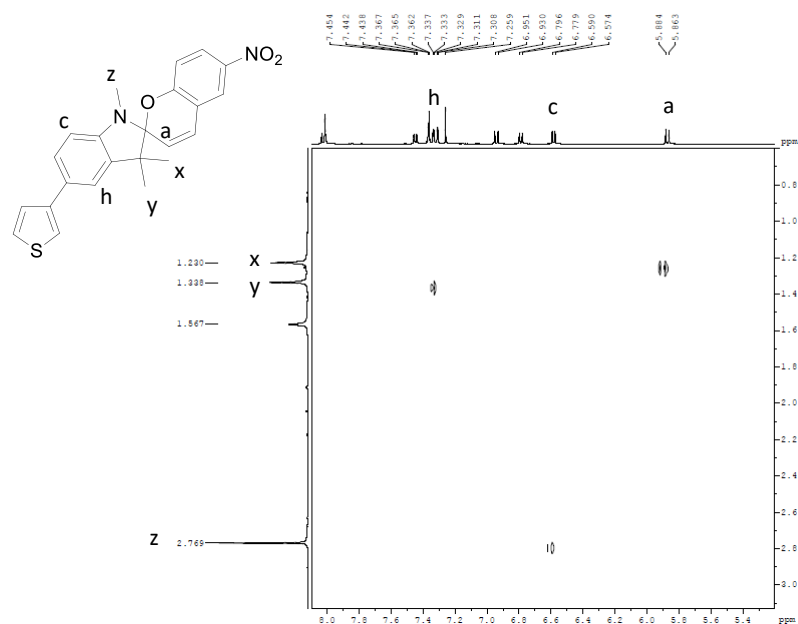
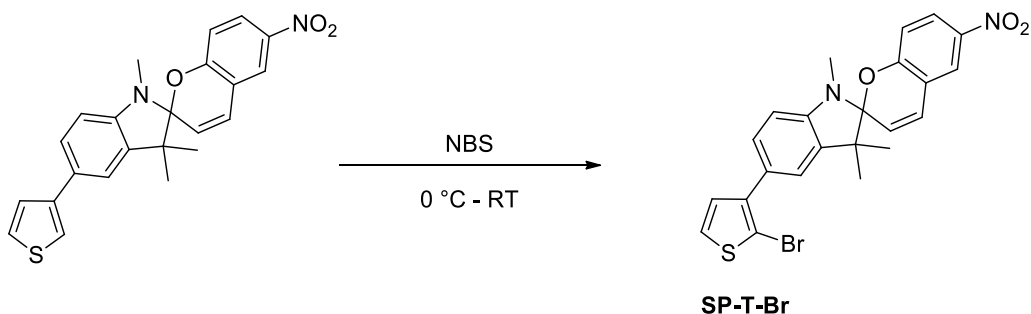


Figure 3.13. Expanded ¹H-¹H NOESY spectrum of 1',3',3'-trimethyl-6-nitro-5'-(thiophene-3-yl)spiro[chromene-2,2'-indoline]

Synthesis of 5'-(2-bromothiophen-3-yl)-1',3',3'-trimethyl-6-nitrospiro[chromene-2,2'-indoline]



Scheme 3.4. Synthesis of 5'-(2-bromothiophen-3-yl)-1',3',3'-trimethyl-6-nitrospiro[chromene-2,2'-indoline]

1',3',3'-Trimethyl-6-nitro-5'-(thiophene-3-yl)spiro[chromene-2,2'-indoline] (45 mg, 0.11 mmol) was dissolved in freshly distilled tetrahydrofuran (30 mL) prior to the addition of N-bromosuccinimide (20 mg, 0.11 mmol) at 0 °C over a period of 15 min. The reaction mixture was allowed to stir for 2 h while maintaining the temperature between 0 °C and room temperature. After 2 h the reaction mixture was quenched with deionized water and extracted with diethyl ether.

Combined organic layer was washed with deionized water, dried over MgSO_4 and evaporated under reduced pressure to obtain the crude as a yellow solid. (62 mg, MP = 209-215 °C) $^1\text{H-NMR}$ (CDCl_3 , 500 MHz; 8.03(m, 2H), 7.40(dd, 1H, $J=8.0$, $J=1.4$), 7.30(m, 2H), 7.04(d, 1H, $J=5.6$), 6.93(d, 1H, $J=10.4$), 6.81(d, 1H, $J=8.8$), 6.60(d, 1H, $J=8.0$), 5.86(d, 1H, $J=10.4$), 2.78(s, 3H), 1.33(s, 3H), 1.23(s, 3H)). $^{13}\text{C-NMR}$ (CDCl_3 , 500 MHz; 159.705, 147.233, 141.473, 141.032, 136.217, 129.184, 128.388, 128.366, 126.625, 125.926, 125.606, 122.724, 122.171, 121.470, 118.632, 115.546, 107.256, 106.718, 106.373, 52.34, 28.89, 25.99, 20.01). $^1\text{H-NMR}$ and $^{13}\text{C-NMR}$ spectra are given in figure 3.14, figure 3.15 and figure 3.16. 2D-NMR analysis is given in figure 3.17 and figure 3.18.

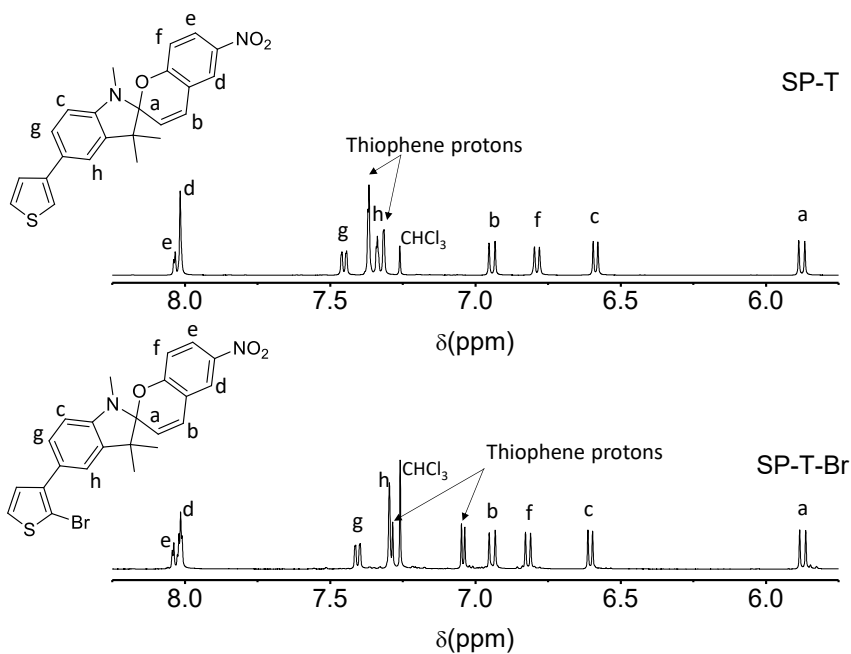


Figure 3.14. $^1\text{H-NMR}$ spectrum of 5'-(2-bromothiophen-3-yl)-1',3',3'-trimethyl-6-nitrospiro[chromene-2,2'-indoline] in comparison with 1',3',3'-trimethyl-6-nitro-5'-(thiophene-3-yl)spiro[chromene-2,2'-indoline] in downfield region

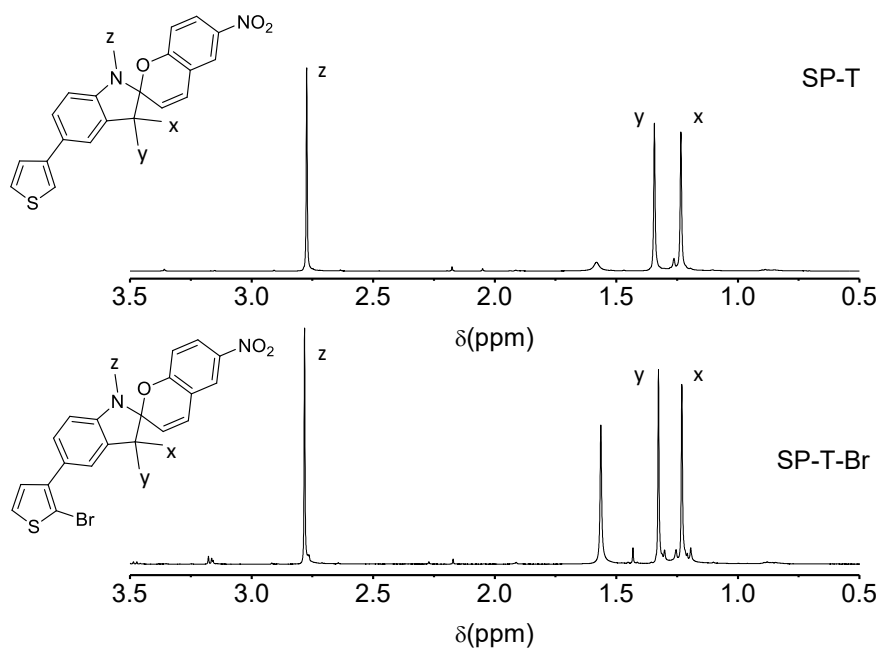


Figure 3.15. $^1\text{H-NMR}$ spectrum of 5'-(2-bromothiophen-3-yl)-1',3,3'-trimethyl-6-nitrospiro[chromene-2,2'-indoline] in comparison with 1',3,3'-trimethyl-6-nitro-5'-(thiophene-3-yl)spiro[chromene-2,2'-indoline] in upfield region

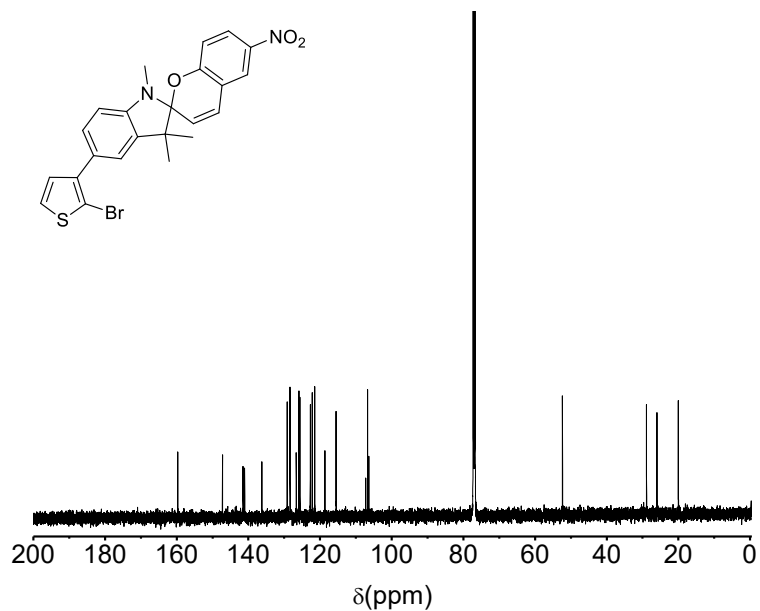


Figure 3.16. $^{13}\text{C-NMR}$ spectrum of 5'-(2-bromothiophen-3-yl)-1',3,3'-trimethyl-6-nitrospiro[chromene-2,2'-indoline]

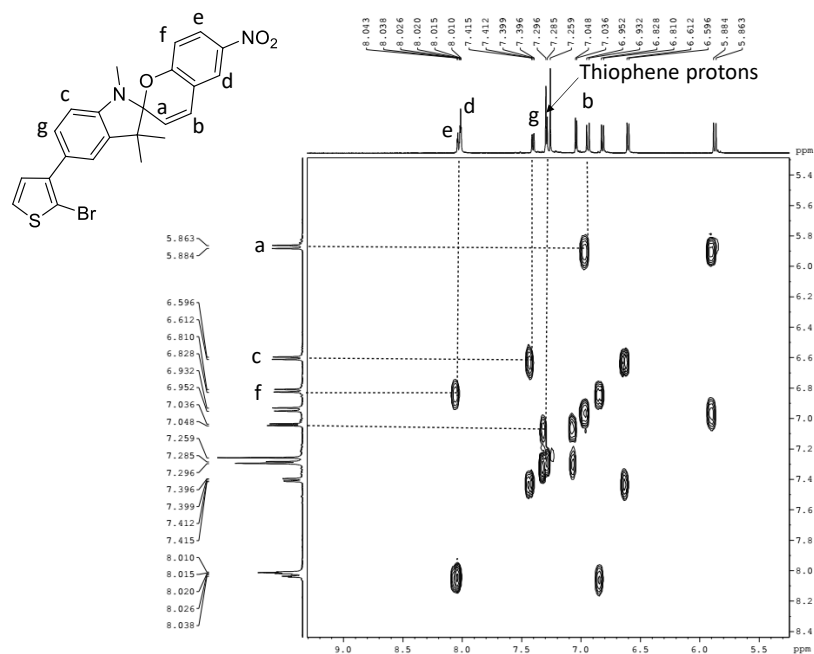


Figure 3.17. Expanded ^1H - ^1H COSY spectrum of 5'-(2-bromothiophen-3-yl)-1,3,3'-trimethyl-6-nitrospiro[chromene-2,2'-indoline]

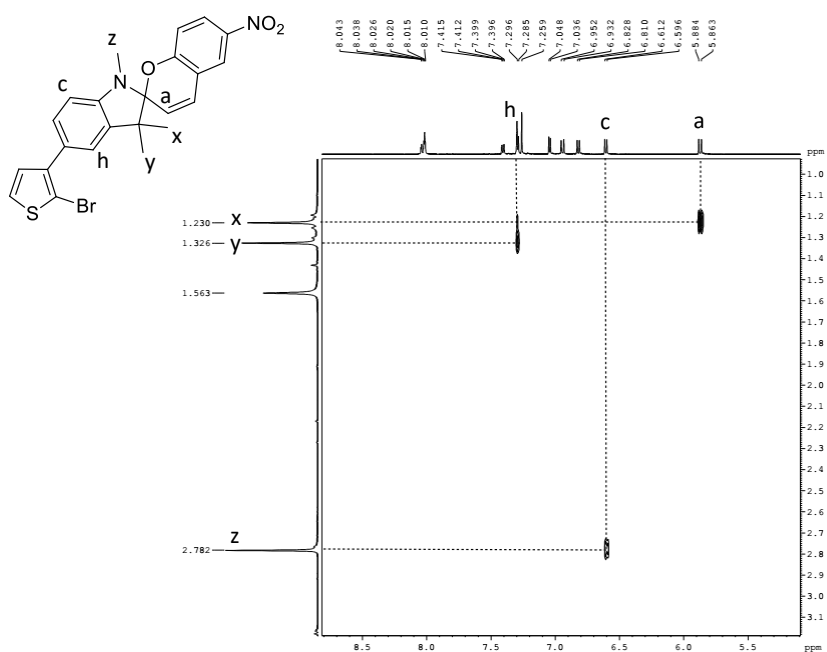
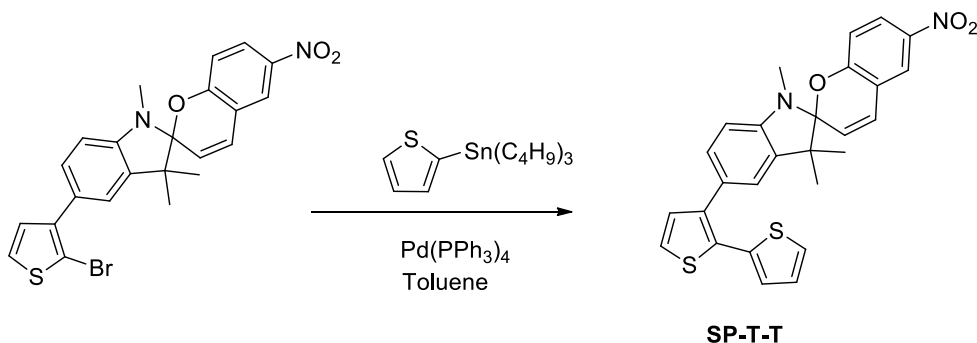


Figure 3.18. Expanded ^1H - ^1H NOESY spectrum of 5'-(2-bromothiophen-3-yl)-1,3,3'-trimethyl-6-nitrospiro[chromene-2,2'-indoline]

Synthesis of 5'-([2,2'-bithiophene]-3-yl)-1',3',3'-trimethyl-6-nitrospiro[chromene-2,2'-indoline]



Scheme 3.5. Synthesis of 5'-([2,2'-bithiophene]-3-yl)-1',3',3'-trimethyl-6-nitrospiro[chromene-2,2'-indoline]

5'-([2-Bromothiophen-3-yl]-1',3',3'-trimethyl-6-nitrospiro[chromene-2,2'-indoline] (50 mg, 0.10 mmol) was dissolved in dry toluene (10 mL) in a three neck flask and 2-(tributylstannyl) thiophene (0.03 mL, 0.10 mmol) was added under nitrogen and nitrogen was bubbled through this solution for 15 min prior to the addition of tetrakis(triphenylphosphine)-palladium(0) (12 mg, 0.01 mmol). The reaction mixture was allowed to reflux under nitrogen for 24 h, cooled to room temperature, quenched with acidified deionized water (50 mL) and extracted with diethyl ether (50 mL \times 3). Combined organic layers were washed with deionized water (50 mL \times 3), dried over anhydrous MgSO_4 and evaporated under reduced pressure. The crude was purified by column chromatography using ethyl acetate:hexane (1:4) as the eluting solvent to obtain the product as a brownish solid (47 mg, 0.097 mmol, 97 %). $^1\text{H-NMR}$ (CDCl_3 , 500 MHz; 8.02(m, 2H), 7.25(s, 1H), 7.22(dd, 1H, $J=7.9$, $J=1.5$), 7.18(d, 1H, $J=5.1$), 7.10(d, 1H, $J=5.2$), 7.04(m, 2H), 6.94(m, 2H), 6.80(d, 1H, $J=8.8$), 6.54(d, 1H, $J=8.0$), 5.84(d, 1H, $J=10.4$), 2.77(s, 3H), 1.21(s, 3H), 1.15(s, 3H)). $^{13}\text{C-NMR}$ (CDCl_3 , 500 MHz; 159.75, 147.03, 140.99, 139.51, 136.43, 136.18, 130.54, 130.49, 128.75, 128.27, 127.61, 126.96, 126.50, 125.89, 125.51, 123.81, 123.01, 122.72, 121.57, 118.66, 115.51, 106.79, 106.37, 52.24, 28.87, 25.80, 19.90). HRMS (ESI) m/z calcd for $\text{C}_{27}\text{H}_{22}\text{N}_2\text{O}_3\text{S}_2^+$ ($\text{M} + \text{H}$) $^+$ 487.1145, found 487.1148. $^1\text{H-NMR}$ and $^{13}\text{C-NMR}$ spectra are given in figure 3.19, figure 3.20 and figure 3.21. 2D-NMR analysis is given in figure 3.22 and figure 3.23.

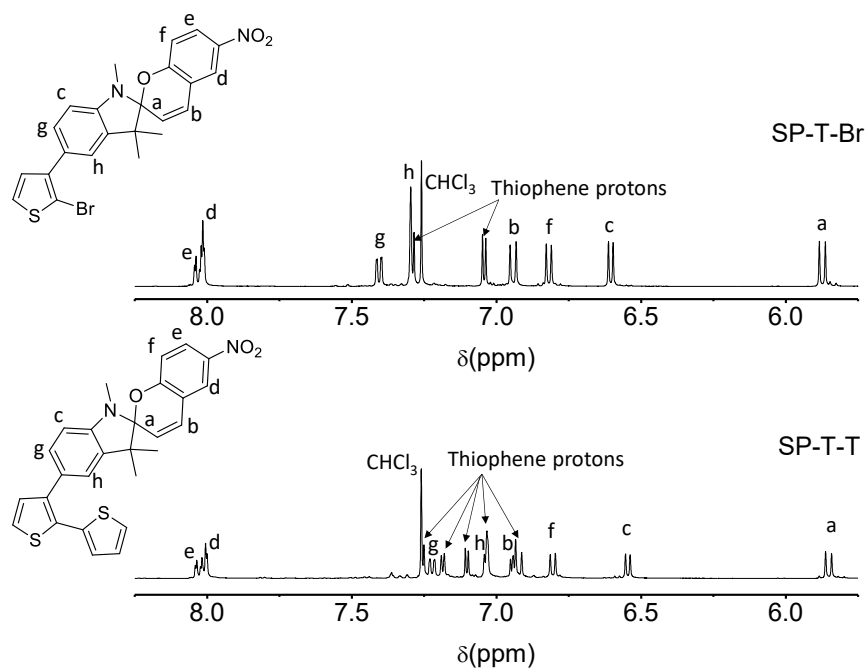


Figure 3.19. $^1\text{H-NMR}$ spectrum of 5'-([2,2'-bithiophene]-3-yl)-1',3',3'-trimethyl-6-nitrospiro[chromene-2,2'-indoline] in comparison with 5'-(2-bromothiophen-3-yl)-1',3',3'-trimethyl-6-nitrospiro[chromene-2,2'-indoline] in the downfield region

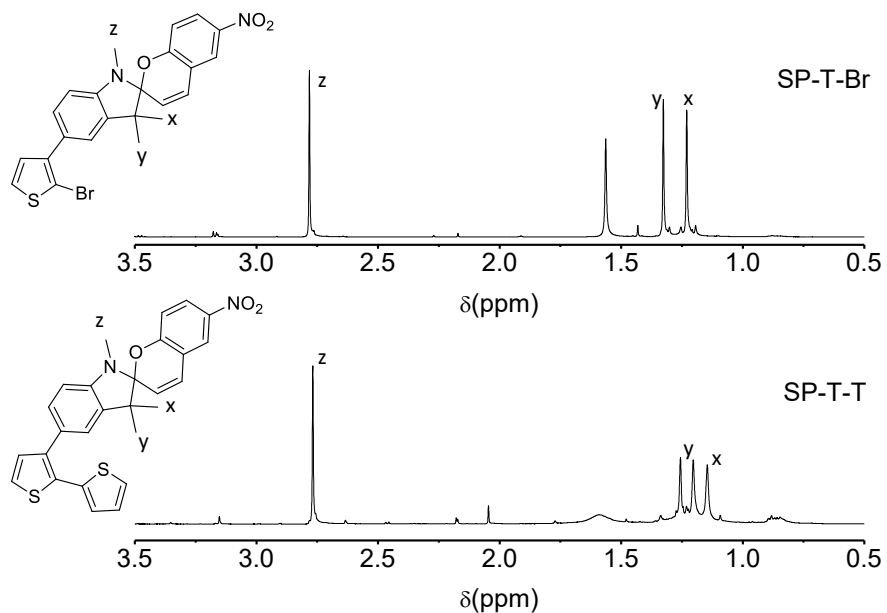


Figure 3.20. $^1\text{H-NMR}$ spectrum of 5'-([2,2'-bithiophene]-3-yl)-1',3',3'-trimethyl-6-nitrospiro[chromene-2,2'-indoline] in comparison with 5'-(2-bromothiophen-3-yl)-1',3',3'-trimethyl-6-nitrospiro[chromene-2,2'-indoline] in the upfield region

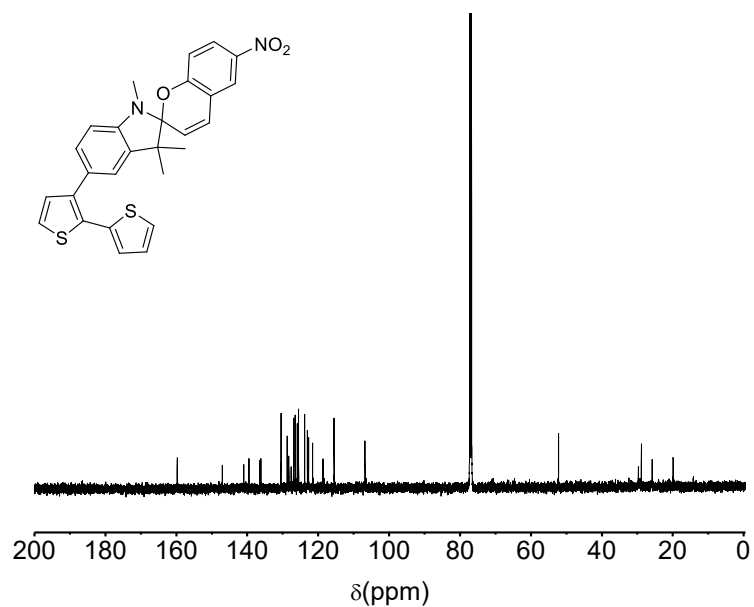


Figure 3.21. ^{13}C -NMR spectrum of 5'-([2,2'-bithiophene]-3-yl)-1',3',3'-trimethyl-6-nitrospiro[chromene-2,2'-indoline]

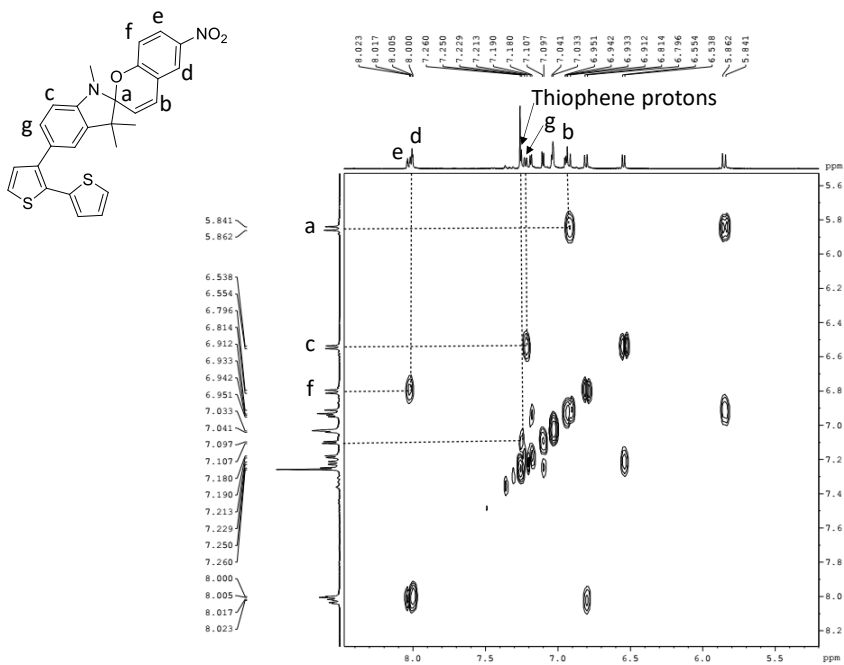


Figure 3.22. Expanded ^1H - ^1H COSY spectrum of 5'-([2,2'-bithiophene]-3-yl)-1',3',3'-trimethyl-6-nitrospiro[chromene-2,2'-indoline]

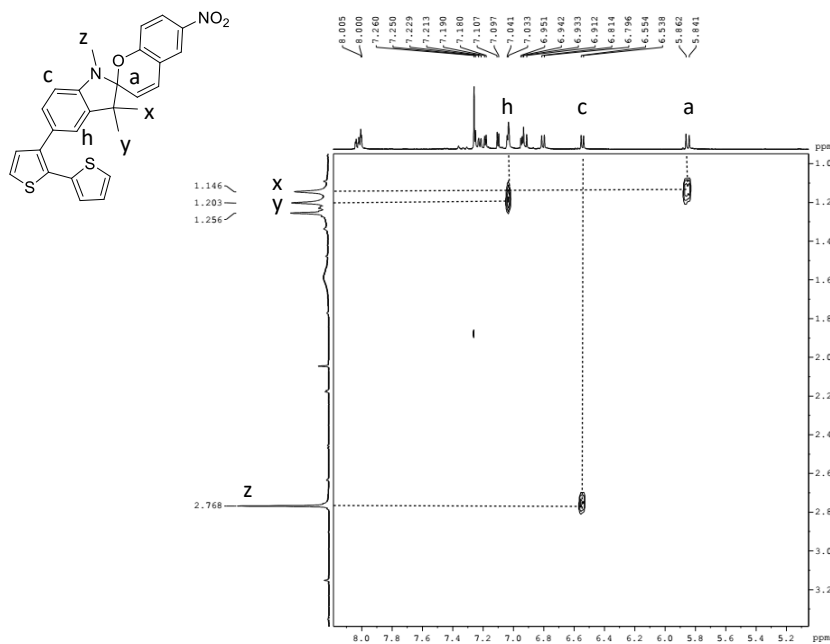
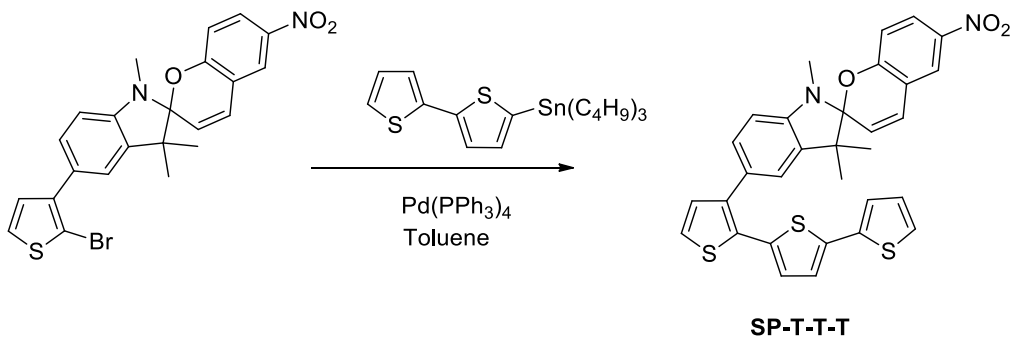


Figure 3.23. Expanded ^1H - ^1H NOESY spectrum of 5'-([2,2'-bithiophene]-3-yl)-1',3',3'-trimethyl-6-nitrospiro[chromene-2,2'-indoline]

Synthesis of 5'-([2,2':5',2''-terthiophene]-3-yl)-1',3',3'-trimethyl-6-nitrospiro[chromene-2,2'-indoline]



Scheme 3.6. Synthesis of 5'-([2,2':5',2''-terthiophene]-3-yl)-1',3',3'-trimethyl-6-nitrospiro[chromene-2,2'-indoline]

5'-([2-bromothiophen-3-yl]-1',3',3'-trimethyl-6-nitrospiro[chromene-2,2'-indoline] (50 mg, 0.10 mmol) was dissolved in toluene (10 mL) in a three neck flask and [2,2'-bithiophene]-5-yltributylstannane (45.5 mg, 0.10 mmol) was added under nitrogen and nitrogen was bubbled through this solution for 15 min prior to the addition of tetrakis(triphenylphosphine)-palladium(0)

(12 mg, 0.01 mmol). The reaction mixture was allowed to reflux under nitrogen for 24 h, cooled to room temperature, quenched with acidified deionized water (50 mL) and extracted with diethyl ether (50 mL \times 3). Combined organic layers were washed with deionized water (50 mL \times 3), dried over anhydrous MgSO₄ and evaporated under reduced pressure. The crude was purified through column chromatography using ethyl acetate:hexane (1:4) as the eluting solvent to obtain the product as a brownish solid (33 mg, 0.058 mmol, 58 %). ¹H-NMR (CDCl₃, 500 MHz; 8.02(m, 2H), 7.24(m, 2H), 7.18(d, 1H, J=4.4), 7.07(m, 3H), 6.98(m, 3H), 6.91(d, 1H, J=10.2), 6.76(d, 1H, J=8.4), 6.57(d, 1H, J=7.8), 5.85(d, 1H, J=10.3)). ¹³C-NMR (CDCl₃, 500 MHz; 159.76, 147.28, 140.99, 139.60, 137.31, 137.07, 136.24, 135.53, 130.69, 130.58, 128.76, 128.31, 127.77, 127.36, 126.87, 125.87, 124.36, 123.79, 123.54, 123.47, 123.25, 122.72, 121.55, 118.67, 115.50, 107.02, 106.42, 52.34, 28.91, 25.80, 19.87). HRMS (ESI) m/z calcd for C₃₁H₂₄N₂O₃S₃⁺ (M + H)⁺ 569.1022, found 569.1033. ¹H-NMR and ¹³C-NMR spectra are given in figure 3.24, figure 3.25 and figure 3.26. 2D-NMR analysis is given in figure 3.27 and figure 3.28.

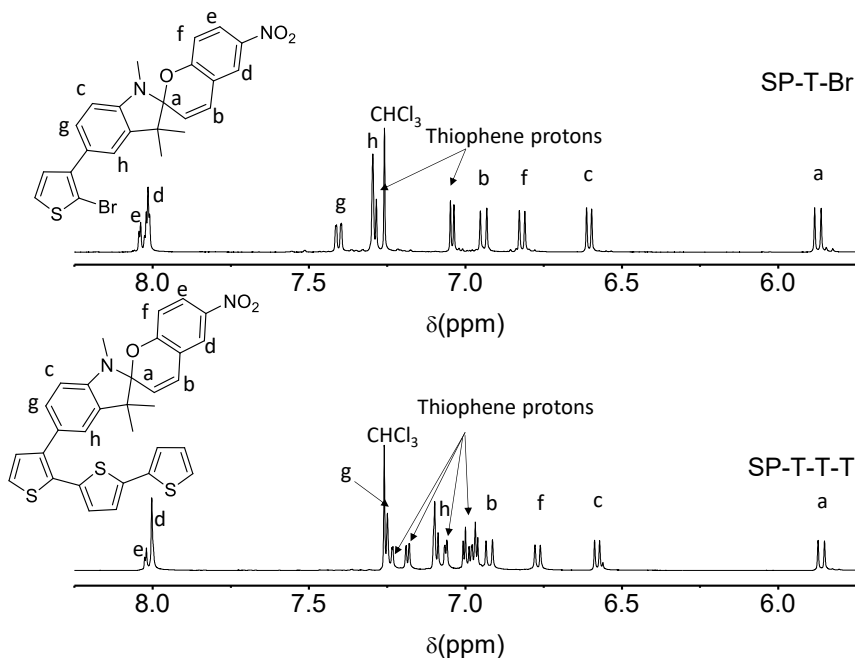


Figure 3.24. ¹H-NMR spectrum of 5'-([2,2':5',2''-terthiophene]-3-yl)-1',3',3'-trimethyl-6-nitrospiro[chromene-2,2'-indoline] in comparison with 5'-(2-bromothiophen-3-yl)-1',3',3'-trimethyl-6-nitrospiro[chromene-2,2'-indoline] in the downfield region

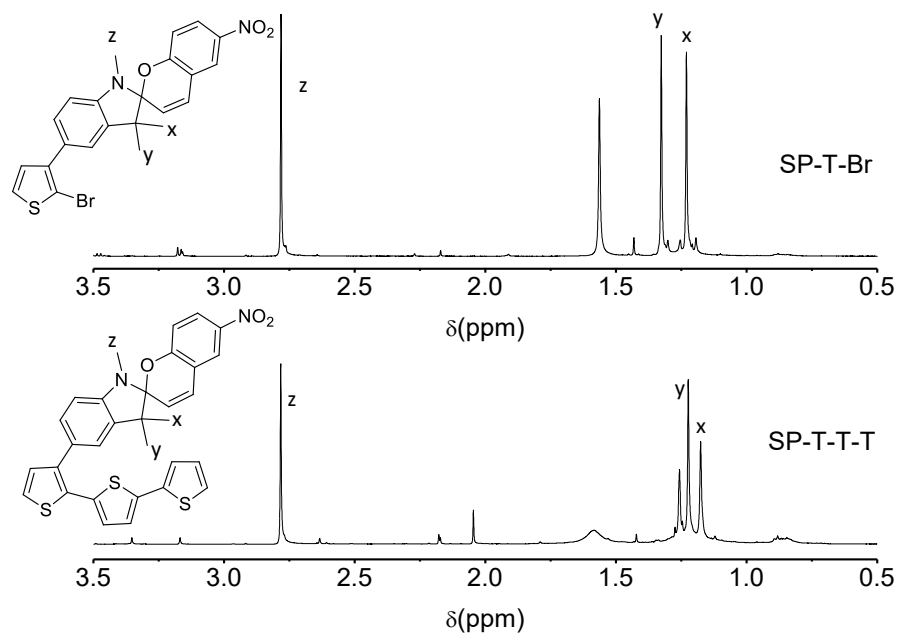


Figure 3.25. $^1\text{H-NMR}$ spectrum of 5'-([2,2':5',2''-terthiophene]-3-yl)-1',3',3'-trimethyl-6-nitrospiro[chromene-2,2'-indoline] in comparison with 5'-(2-bromothiophen-3-yl)-1',3',3'-trimethyl-6-nitrospiro[chromene-2,2'-indoline] in the upfield region

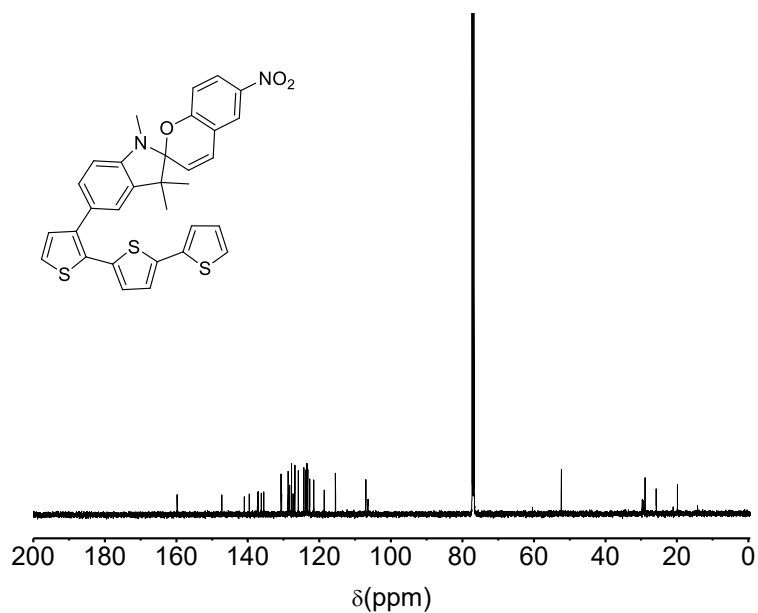


Figure 3.26. $^{13}\text{C-NMR}$ spectrum of 5'-([2,2':5',2''-terthiophene]-3-yl)-1',3',3'-trimethyl-6-nitrospiro[chromene-2,2'-indoline]

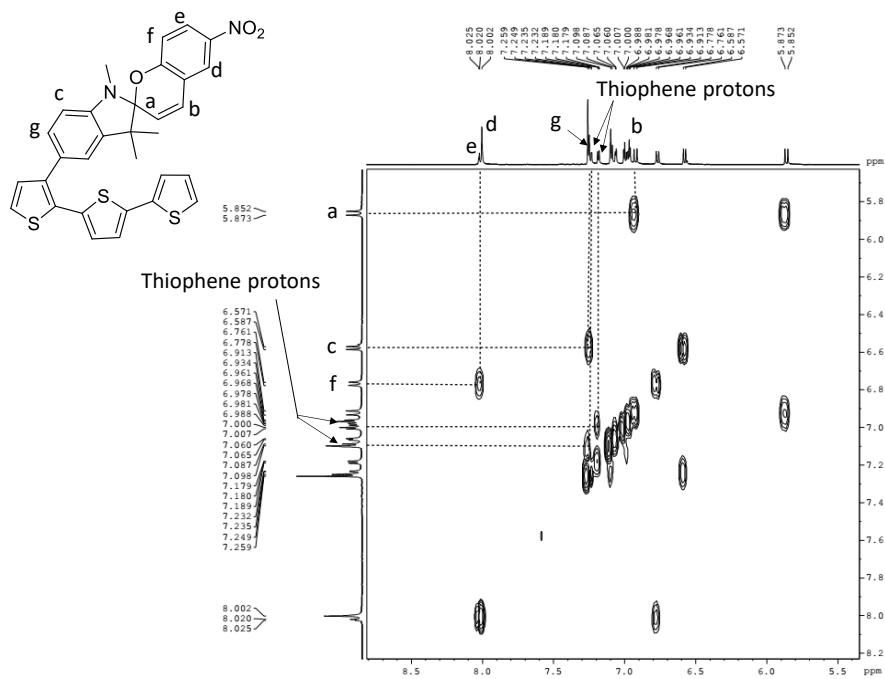


Figure 3.27. Expanded ^1H - ^1H COSY spectrum of 5'-([2,2':5',2''-terthiophene]-3-yl)-1',3',3'-trimethyl-6-nitrospiro[chromene-2,2'-indoline]

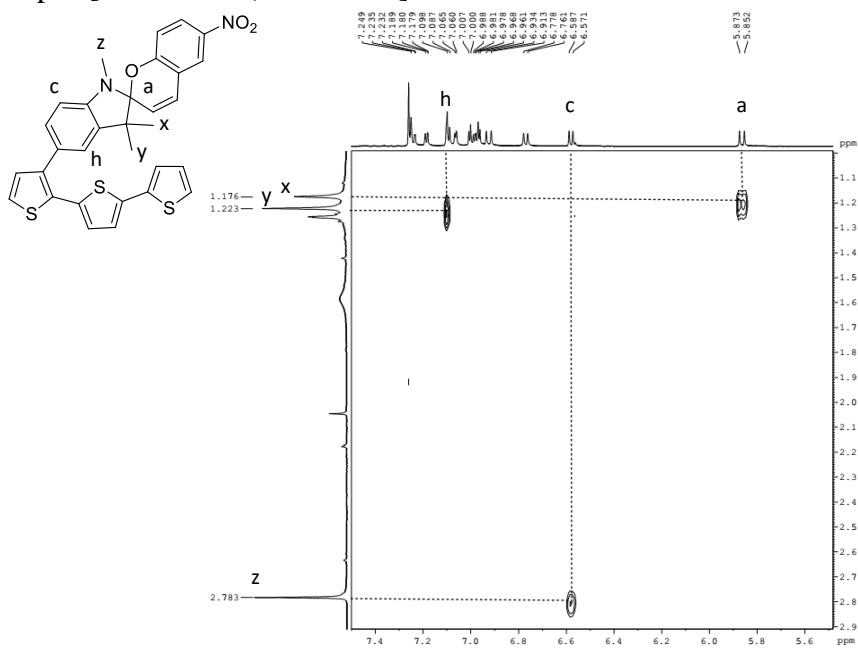
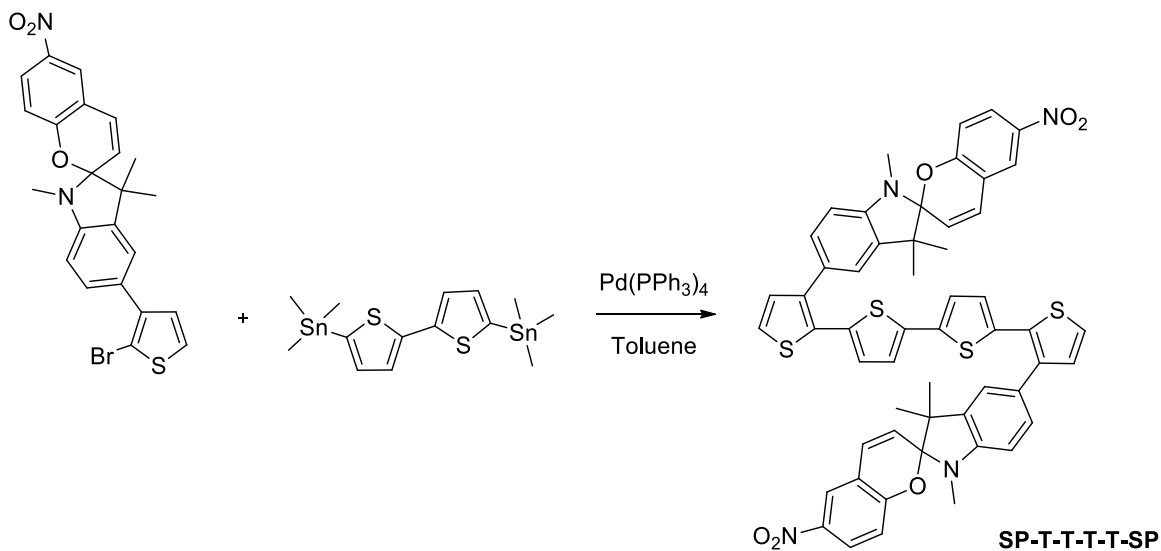


Figure 3.28. Expanded ^1H - ^1H NOESY spectrum of 5'-([2,2':5',2''-terthiophene]-3-yl)-1',3',3'-trimethyl-6-nitrospiro[chromene-2,2'-indoline]

Synthesis of 3,3'''-bis(1',3',3'-trimethyl-6-nitrospiro[chromene-2,2'-indolin]-5'-yl)-2,2':5',2'':5'',2'''-quaterthiophene



Scheme 3.7. Synthesis of 3,3'''-bis(1',3',3'-trimethyl-6-nitrospiro[chromene-2,2'-indolin]-5'-yl)-2,2':5',2'':5'',2'''-quaterthiophene

5'-(2-bromothiophen-3-yl)-1',3',3'-trimethyl-6-nitrospiro [chromene-2,2'-indoline] (62mg, 0.13 mmol) and 5,5'-bis(trimethylstannyl)-2,2'-bithiophene (32 mg, 0.065 mmol) were kept under nitrogen in a three neck flask prior to the addition of dry toluene (10 mL). Nitrogen was bubbled through this solution for 15 min prior to the addition of tetrakis(triphenylphosphine)-palladium(0) (15 mg, 0.013 mmol). The reaction mixture was allowed to reflux under nitrogen for 24 h, cooled to room temperature, quenched with acidified deionized water (50 mL) and extracted with diethyl ether (50 mL \times 3). Combined organic layers were washed with deionized water (50 mL \times 3), dried over anhydrous MgSO₄ and evaporated under reduced pressure. The crude was purified through column chromatography using ethyl acetate:hexane (1:4) as the eluting solvent to obtain the product as a brownish solid (24 mg, 0.025 mmol, 19 %). ¹H-NMR (CDCl₃, 500 MHz; 7.99 (d, 1H, J=2.4), 7.93 (dd, 1H, J=9.0, 2.6), 7.20 (d, 1H, J=8.0), 7.08(m, 2H), 6.90(m, 3H), 6.74(d, 1H, J=9.0), 6.55(d, 1H, J=7.9), 5.83(d, 1H, J=10.6), 2.77(s, 3H), 1.19(s, 3H), 1.14(s, 3H)), Acetone-d₆, 500 MHz; 12 aromatic protons). HRMS (ESI) m/z calcd for C₅₄H₄₂N₄O₆S₄⁺ (M + H)⁺ 971.2060, found 971.2031. ¹H-NMR spectrum is given in figure 3.29. 2D-NMR analysis is given in figure 3.30 and figure 3.31.

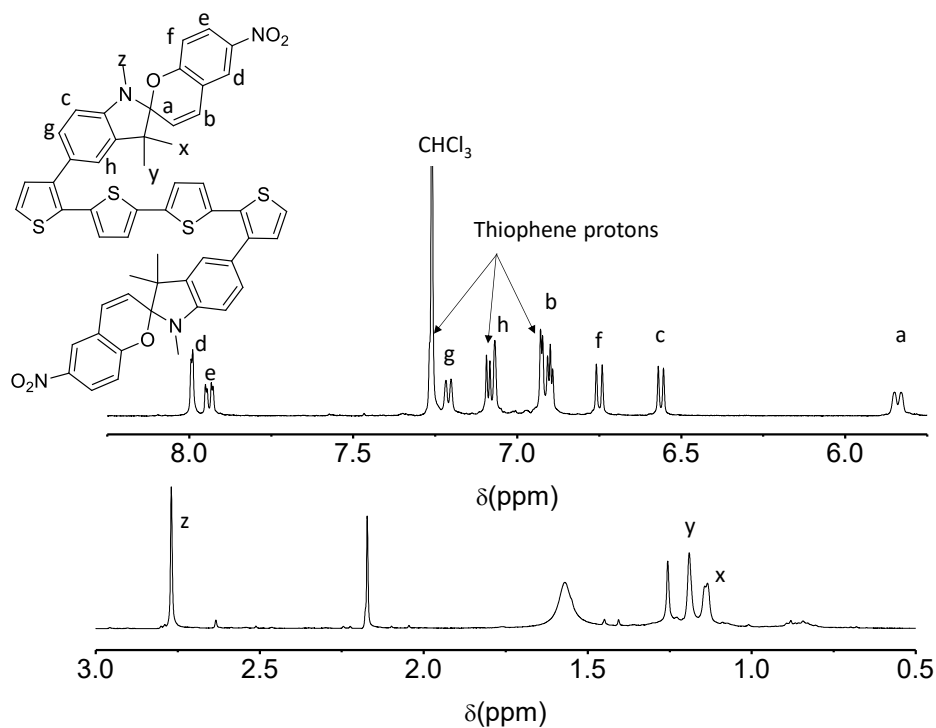


Figure 3.29. $^1\text{H-NMR}$ spectrum of 3,3'''-bis(1',3',3'-trimethyl-6-nitrospiro[chromene-2,2'-indolin]-5'-yl)-2,2':5',2'':5'',2'''-quaterthiophene

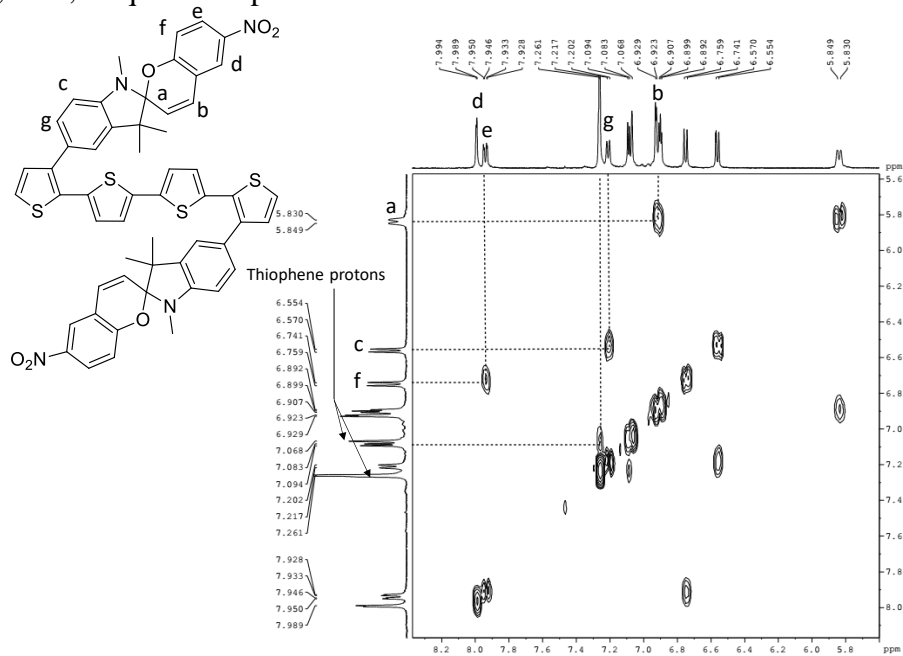


Figure 3.30. Expanded $^1\text{H-}^1\text{H}$ COSY spectrum of 3,3'''-bis(1',3',3'-trimethyl-6-nitrospiro[chromene-2,2'-indolin]-5'-yl)-2,2':5',2'':5'',2'''-quaterthiophene

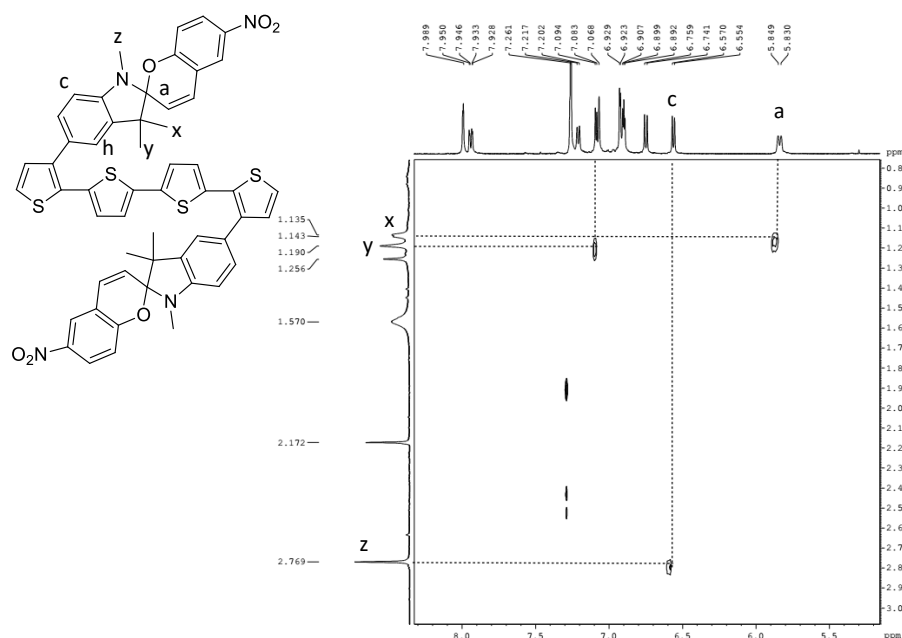
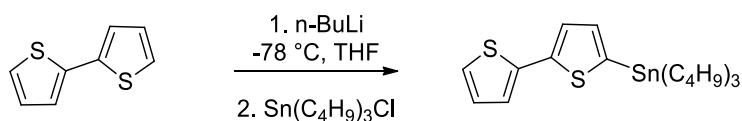


Figure 3.31. Expanded ^1H - ^1H NOESY spectrum of 3,3'''-bis(1',3',3'-trimethyl-6-nitrospiro[chromene-2,2'-indolin]-5'-yl)-2,2':5',2'':5'',2'''-quaterthiophene

Synthesis of [2,2'-bithiophene]-5-yltributylstannane



Scheme 3.8. Synthesis of [2,2'-bithiophene]-5-yltributylstannane

A solution of 2,2'-bithiophene (0.50 g, 3.0 mmol) in freshly distilled THF was cooled down to -78 °C under nitrogen prior to the addition of *n*-butyllithium (1.2 mL, 3.0 mmol) at -78 °C. The reaction mixture was stirred at -78 °C for 1 h under nitrogen. The solution was warmed to ~ -40 °C, upon which tributyltin chloride (1.0 mL, 6.3 mmol) was added and then the mixture was stirred at room temperature overnight. The reaction mixture was quenched with deionized water and extracted with ethyl acetate (100 mL \times 3). Combined organic layer was washed with deionized water and brine (100 mL \times 3), dried over MgSO_4 and evaporated under reduced pressure. The crude compound was dissolved in hexane and filtered. The filtrate was evaporated under reduced

pressure to obtain [2,2'-bithiophene]-5-yltributylstannane as a yellow oil (868 mg, 1.9 mmol, 64 %). $^1\text{H-NMR}$ (CDCl_3 , 500 MHz; 7.29 (d, 1H, $J=3.2$), 7.18 (m, 2H), 7.06 (d, 1H, $J=3.3$), 7.00 (t, 1H), 1.58 (m, 6H), 1.36 (m, 6H), 1.12 (m, 6H), 0.91 (m, 9H)). $^{13}\text{C-NMR}$ (CDCl_3 , 500 MHz; 142.77, 137.72, 136.65, 136.08, 127.74, 124.99, 123.97, 123.46, 28.97, 27.28, 13.69, 10.90). $^1\text{H-NMR}$ and $^{13}\text{C-NMR}$ spectra are given in figure 3.32 and figure 3.33.

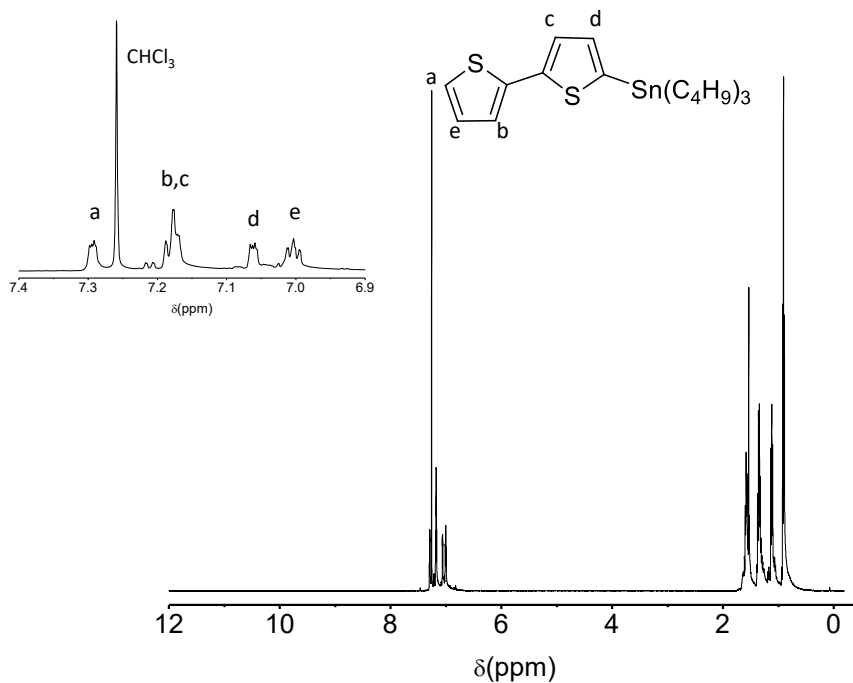


Figure 3.32. $^1\text{H-NMR}$ spectrum of [2,2'-bithiophene]-5-yltributylstannane

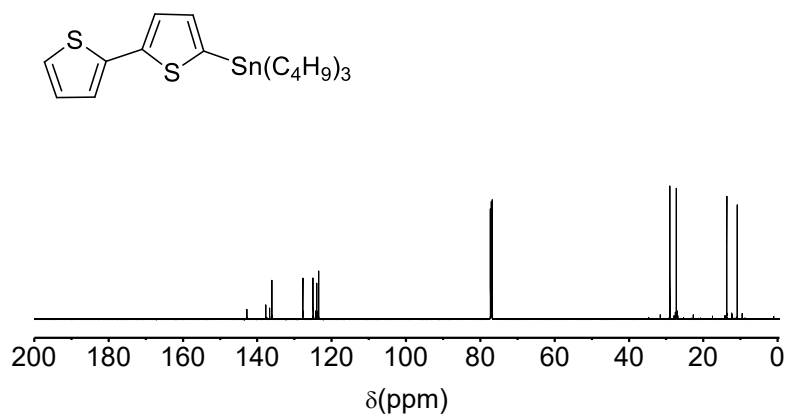
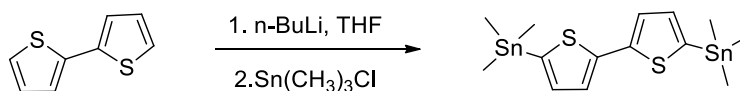


Figure 3.33. ^{13}C -NMR spectrum of [2,2'-bithiophene]-5-yltributylstannane

Synthesis of 5,5'-bis(trimethylstannyl)-2,2'-bithiophene¹¹



Scheme 3.9. Synthesis of 5,5'-bis(trimethylstannyl)-2,2'-bithiophene

A solution of 2,2'-bithiophene (0.50 g, 3.0 mmol) in freshly distilled THF was cooled down to -78°C under nitrogen prior to the addition of n-butyllithium (2.5 mL, 6.3 mmol) at -78°C . The reaction mixture was stirred at -78°C for 1 h under nitrogen. The solution was warmed to 0°C , upon which trimethyltin chloride (6.3 mL, 6.3 mmol) was added and then the mixture was stirred at room temperature overnight. The reaction mixture was quenched with deionized water and extracted with ethyl acetate. Combined organic layer was washed with deionized water and brine, dried over MgSO_4 and evaporated under reduced pressure. The crude compound was purified by recrystallization using ethanol to obtain the pure compound as light blue color crystals. (478 mg, 0.97 mmol, 32 %, MP = $95\text{--}97^\circ\text{C}$). ^1H -NMR (CDCl_3 , 500 MHz; 7.28 (d, 2H, $J=3.4$), 7.09(d, 2H,

$J=3.4$), 0.38 (s, 18 H). ^{13}C -NMR (CDCl_3 , 500 MHz; 143.04, 137.07, 135.86, - 8.22). ^1H -NMR and ^{13}C -NMR spectra are given in figure 3.34 and figure 3.35.

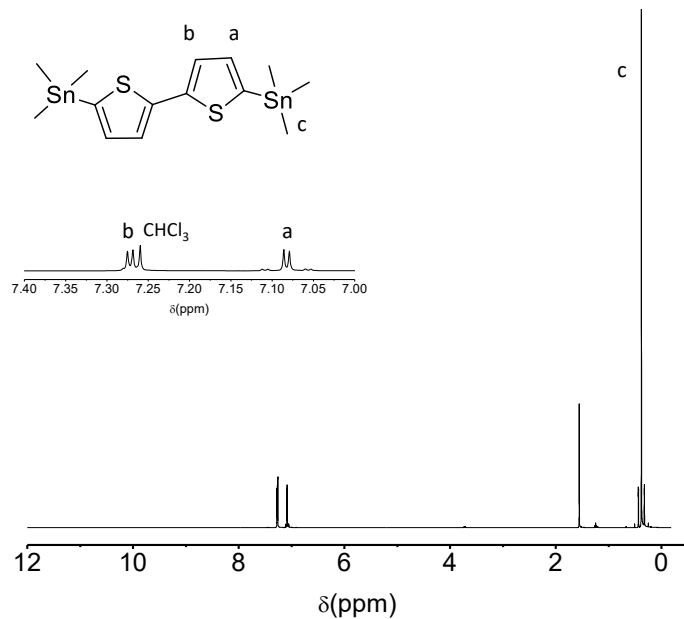


Figure 3.34. ^1H -NMR spectrum of 5,5'-bis(trimethylstannyl)-2,2'-bithiophene

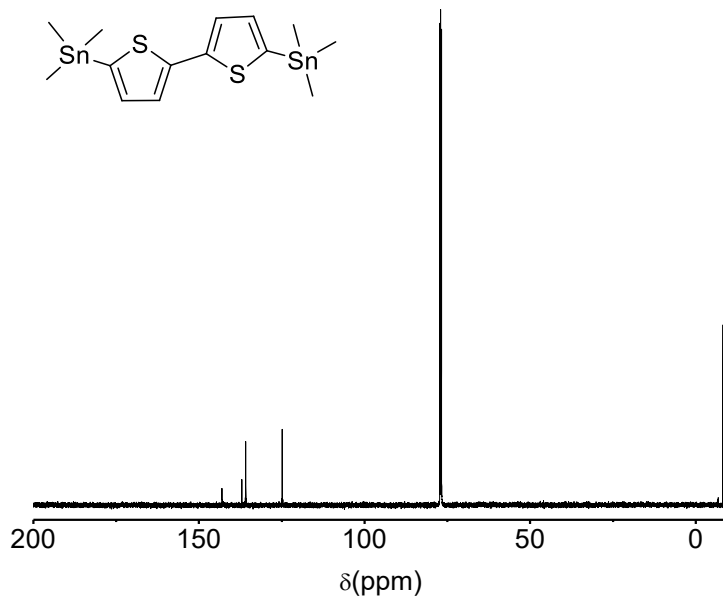
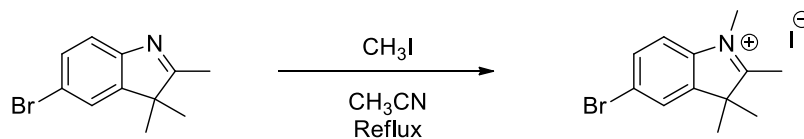


Figure 3.35. ^{13}C -NMR spectrum of 5,5'-bis(trimethylstannyl)-2,2'-bithiophene

Synthesis of 5-bromo-1,2,3,3-tetramethyl-3*H*-indol-1-ium iodide



Scheme 3.10. Synthesis of 5-bromo-1,2,3,3-tetramethyl-3*H*-indol-1-ium iodide

5-bromo-2,3,3-trimethyl-3*H*-indole (200 mg, 0.84 mmol) in anhydrous acetonitrile was kept under N_2 prior to the addition of methyl iodide (251 mg, 1.68 mmol) at room temperature and the reaction mixture was heated under reflux. An aliquot was taken out in 6 h and 12 h intervals, quenched with deionized water, extracted with ether and GC-MS analysis were carried out to monitor the consumption of starting materials. With no starting materials remaining after 12 h, the reaction mixture was allowed to cool to room temperature, the product was filtered off and washed with acetonitrile (108 mg, 0.43 mmol, 51 %). $^1\text{H-NMR}$ (DMSO-d_6 , 500 MHz; 8.16(s, 6H), 7.88-7.84(m, 2H), 3.94(s, 3H), 2.74(s, 3H), 1.52(s, 6H)). $^{13}\text{C-NMR}$ (DMSO-d_6 , 500 MHz; 197.02, 144.34, 141.92, 132.22, 127.18, 123.13, 117.56, 54.66, 35.29, 21.93, 14.63). $^1\text{H-NMR}$ and $^{13}\text{C-NMR}$ spectra are given in figure 3.36 and figure 3.37.

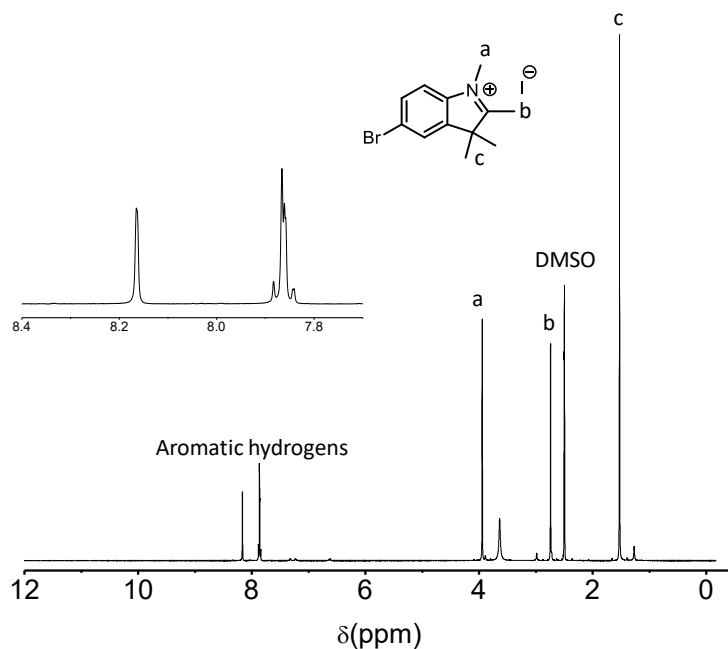


Figure 3.36. $^1\text{H-NMR}$ spectrum of 5-bromo-1,2,3,3-tetramethyl-3*H*-indol-1-ium iodide

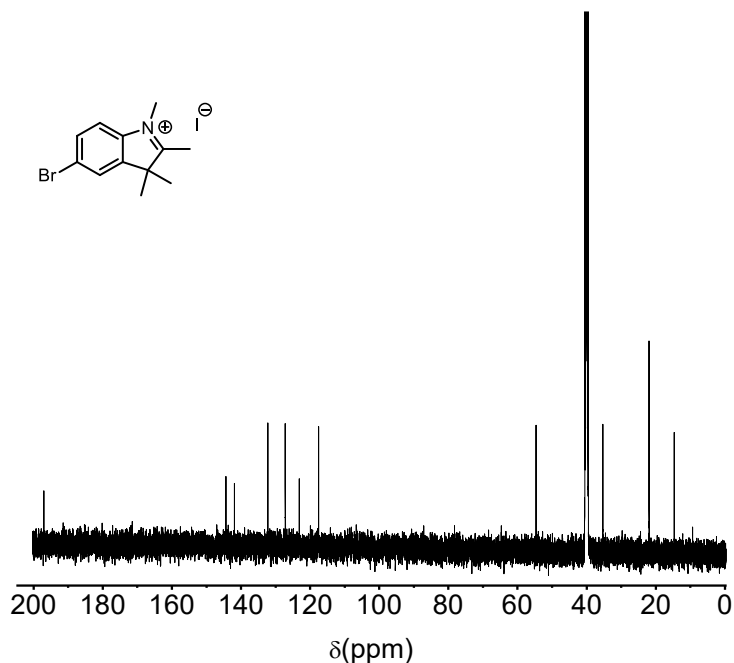
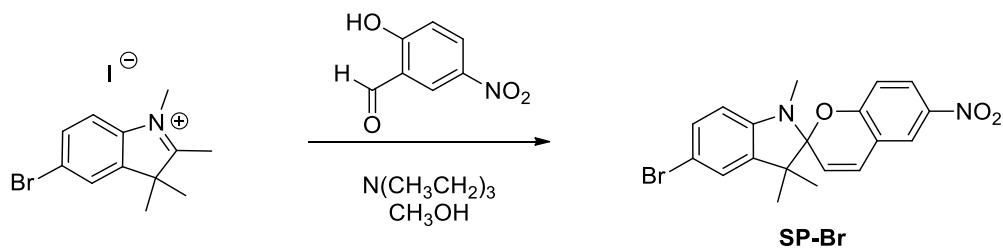


Figure 3.37. ^{13}C -NMR spectrum of 5-bromo-1,2,3,3-tetramethyl-3*H*-indol-1-ium iodide

Synthesis of 5'-bromo-1',3',3'-trimethyl-6-nitrospiro[chromene-2,2'-indoline]



Scheme 3.11. Synthesis of 5'-bromo-1',3',3'-trimethyl-6-nitrospiro[chromene-2,2'-indoline]

5-Bromo-1,2,3,3-tetramethyl-3*H*-indol-1-ium iodide (0.50 g, 1.98 mmol) and 2-hydroxy-5-nitrobenzaldehyde (0.33 g, 1.98 mmol) were kept under N_2 for 15 min prior to the addition of methanol (50 mL). To the above stirred solution four drops of triethylamine was added at room temperature and the reaction mixture was allowed to reflux gently for 3 h under N_2 , allowed to cool to room temperature, quenched in deionized water and extracted with ethyl acetate (100 mL \times 3). The combined organic layer was washed with deionized water (100 mL \times 3), dried over

magnesium sulfate and the solvent was evaporated under reduced pressure. The crude in chloroform was purified by column chromatography using ethyl acetate:hexane (1:4) as the eluting solvent. The pure compound was obtained as a yellow solid (178 mg, 0.44 mmol, 22 %). $^1\text{H-NMR}$ (CDCl_3 , 500 MHz; 8.02 (m, 2H), 7.28(dd, 2H, $J=8.2$, $J=1.2$), 7.16(d, 1H, $J=1.2$), 6.93(d, 1H, $J=10.3$), 6.77(d, 1H, $J=8.9$), 6.42(d, 1H, $J=8.2$), 5.83(d, 1H, $J=10.3$), 2.71(s, 3H), 1.27(s, 3H), 1.18(s, 3H)). $^{13}\text{C-NMR}$ (CDCl_3 , 500 MHz; 159.50, 146.83, 141.12, 138.50, 130.48, 128.58, 125.98, 124.90, 122.76, 121.05, 118.54, 115.47, 111.53, 108.60, 106.24, 52.32, 28.93, 25.73, 19.78). $^1\text{H-NMR}$ and $^{13}\text{C-NMR}$ spectra are given in figure 3.38, figure 3.39 and figure 3.40.

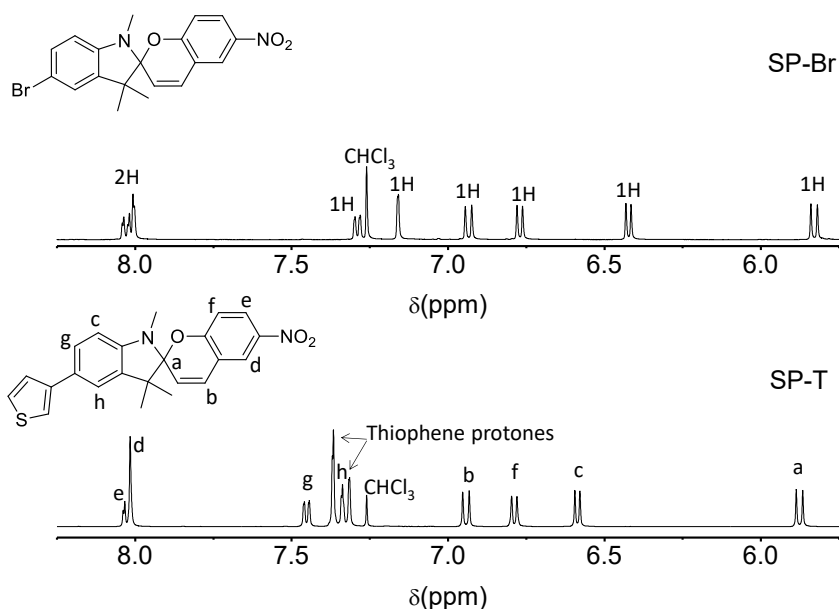


Figure 3.38. $^1\text{H-NMR}$ spectrum of 5'-bromo-1',3',3'-trimethyl-6-nitrospiro[chromene-2,2'-indoline] in comparison with 1',3',3'-trimethyl-6-nitro-5'-(thiophene-3-yl)spiro[chromene-2,2'-indoline] in downfield region

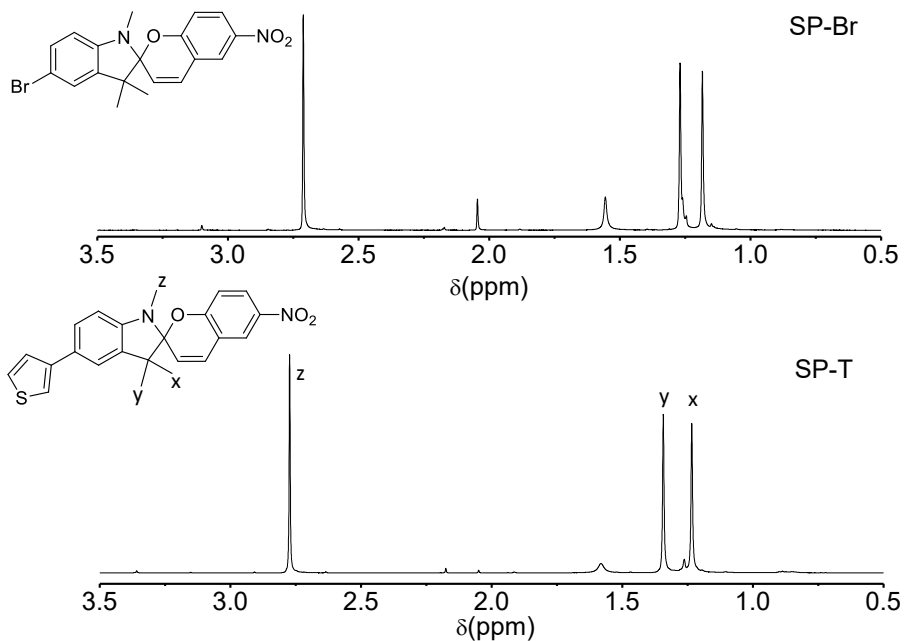


Figure 3.39. $^1\text{H-NMR}$ spectrum of 5'-bromo-1',3',3'-trimethyl-6-nitrospiro[chromene-2,2'-indoline] in comparison with 1',3',3'-trimethyl-6-nitro-5'-(thiophene-3-yl)spiro[chromene-2,2'-indoline] in upfield region

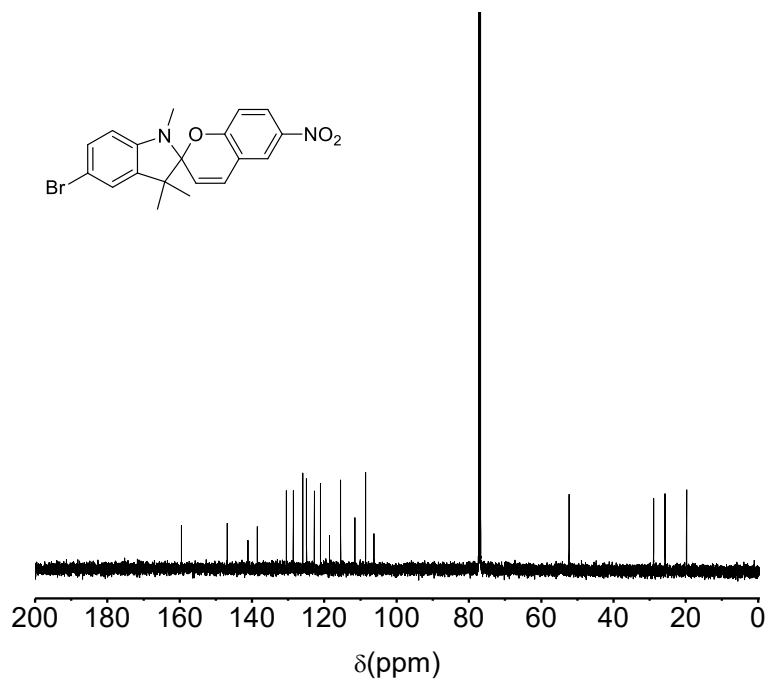
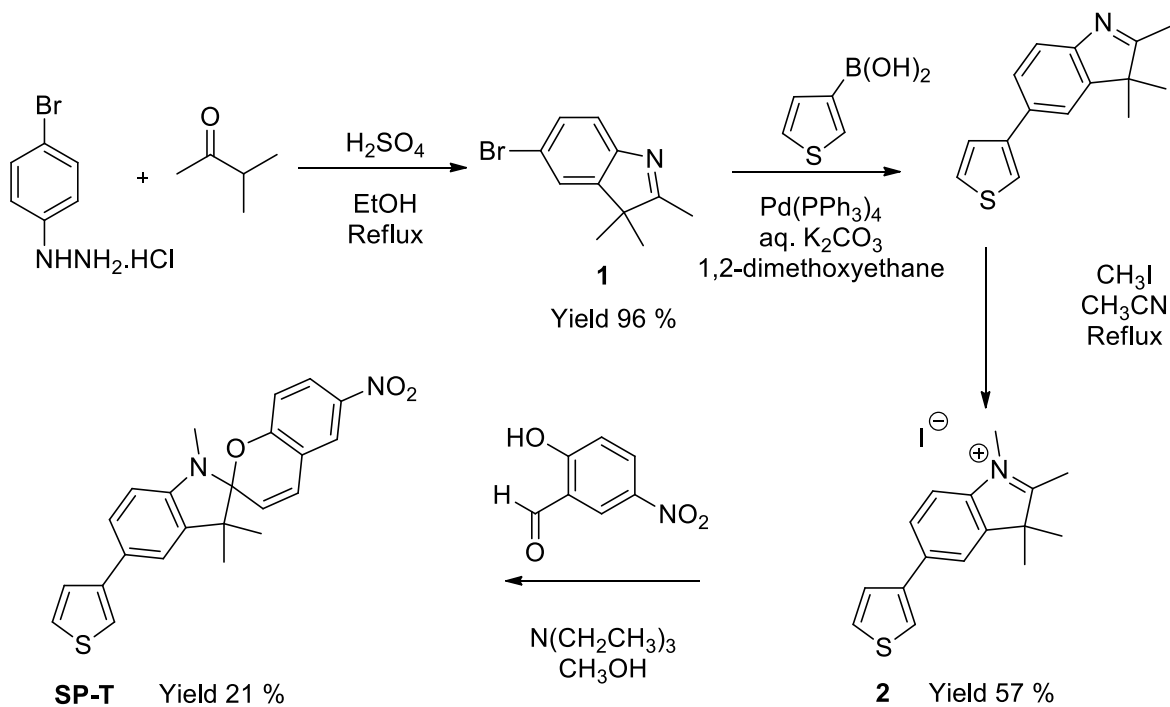


Figure 3.40. $^{13}\text{C-NMR}$ spectrum of 5'-bromo-1',3',3'-trimethyl-6-nitrospiro[chromene-2,2'-indoline]

3.4 Results and Discussion

3.4.1 Thiophene substituted spiropyran (SP-T)

Indoline SP can be synthesised by condensation of indolium salts with *ortho*-hydroxy aromatic aldehydes in the presence of a base (or methylene bases with *ortho*-hydroxy aromatic aldehydes).¹² To incorporating SP as a pendent group into thiophene based material via a conjugated pathway we modified the indolium iodide moiety with thiophene substituent and reacted with nitro salicylaldehyde which is a well-known *o*-hydroxy aromatic aldehyde used in SP synthesis. As shown in scheme 3.12 compound **1** was obtained through a Fischer indole synthesis of 4-bromophenyl hydrazine with isopropylmethylketone in the presence of sulfuric acid.⁹ A Suzuki coupling between compound **1** and thiophene-3-boronic acid in the presence of tetrakis(triphenylphosphine)-palladium(0) catalyst followed by a methylation yielded compound **2**. This procedure is a modification to Guido et al. work to obtain higher yields.¹⁰ The photochromic compound **SP-T** was then synthesized by reacting compound **2** with 2-hydroxy-5-nitrobenzaldehyde in the presence of triethylamine. Crystal structures of **SP-T** is given in figure 3.41.



Scheme 3.12. Synthesis of **SP-T**

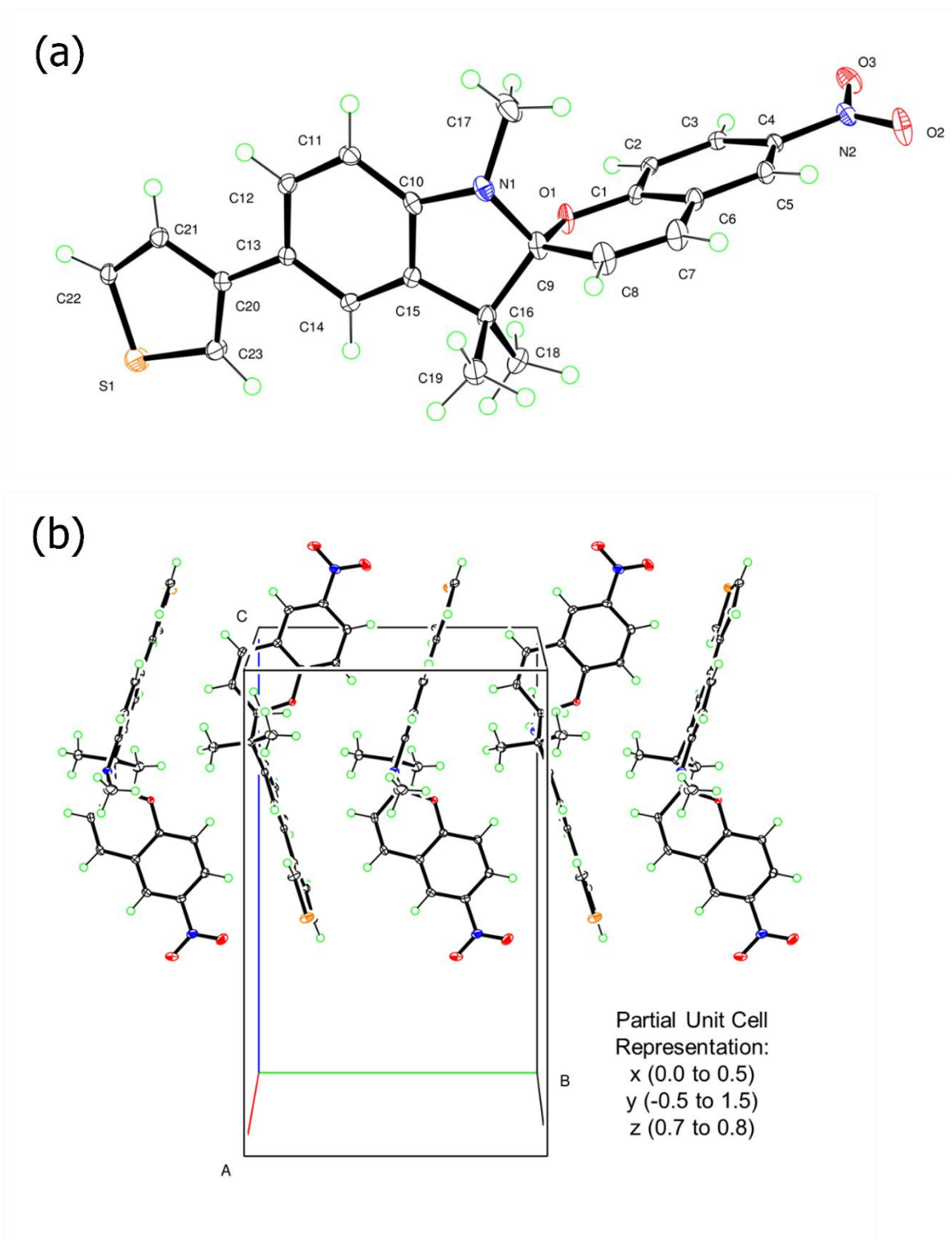
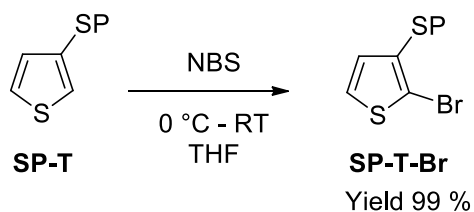


Figure 3.41. (a) Crystal structure and (b) partial unit cell representation of **SP-T** ($R[F^2 > 2\sigma(F^2)] = 0.050$).

3.4.2 Monomrominated derivative (SP-T-Br)

SP-T-Br was obtained through bromination of **SP-T** with N-bromosuccinimide (scheme 3.13). When a thiophene moiety is incorporated in SP via the 5-position, monobromination selectively occurred at the 2-position of thiophene. Crystal structures of **SP-T-Br** is given in figure 3.42.



Scheme 3.13. Synthesis of **SP-T-Br**

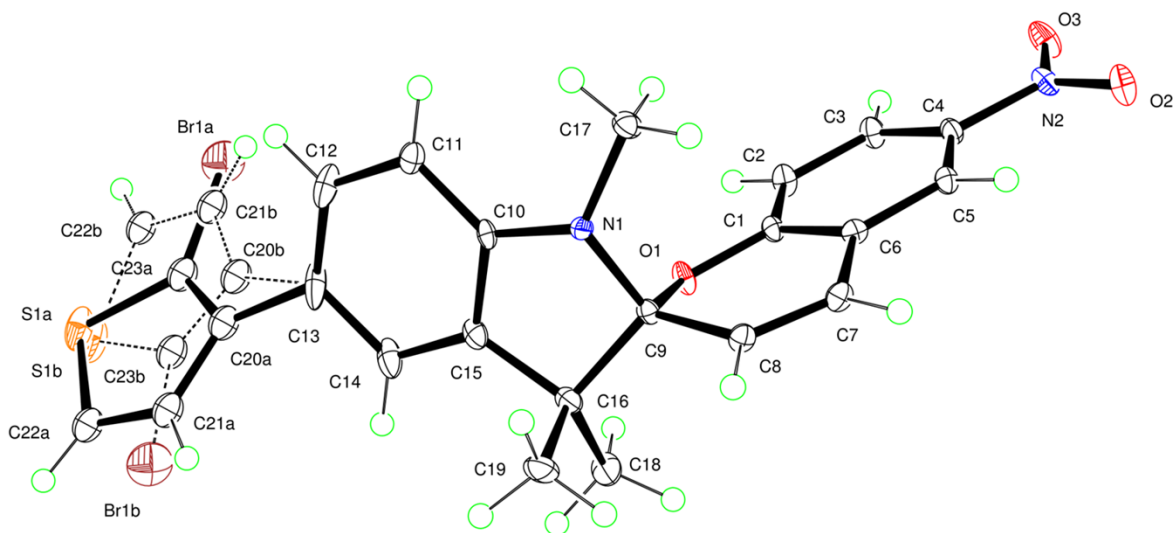
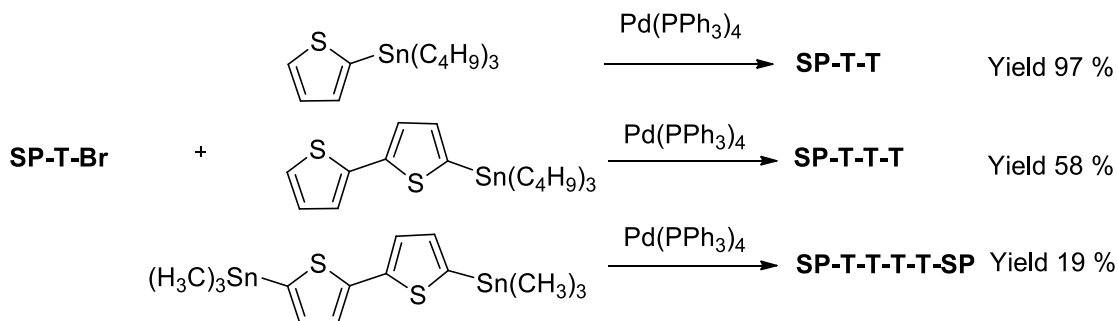


Figure 3.42. Crystal structure of **SP-T-Br** indicating ratio between the two thiophene conformations in approximately 70:30 (the major conformation is indicated with solid bonds and the minor conformation is indicated with dashed bonds) ($R[F^2 > 2\sigma(F^2)] = 0.080$).

3.4.3 Systematic variation of thiophene substituents

A series of compounds, **SP-T-T**, **SP-T-T-T** and **SP-T-T-T-T-SP** were synthesized by Stille coupling reactions of **SP-T-Br** using tetrakis(triphenylphosphine)-palladium (0) as the catalyst

(scheme 3.14) and their photochromic properties were studied. A model SP compound that has a bromine substituent at the 5-position of the indoline instead of thiophene (**SP-Br**) was also prepared for comparison.



Scheme 3.14. Synthesis of **SP-T-T**, **SP-T-T-T** and **SP-T-T-T-T-SP**

3.4.4 UV-Vis kinetics

Photochromism of SP strongly depends on the structure of the compound and the medium, therefore a common polar solvent methanol ($\epsilon \sim 33$) and non-polar solvent Toluene ($\epsilon \sim 2$) have been used in this study.

The structure of **SP-T** and its isomerization is shown in figure 3.43 (a). The molecule is composed of an indoline with an attached thiophene and a chromene moiety (nitro-substituted SP were studied because they are the most common SP used, and therefore, the results in this study may be compared to other systems). These two heterocyclic parts are linked together through a common spiro junction and are in two orthogonal planes (see partial unit cell representation in figure 3.41b). In solution, SP shows an absorption spectrum below 400 nm. Absorption in this range cleaves the C-O bond to yield the colored merocyanine (MC) isomer.¹³ When a **SP-T** solution was photolyzed with a 500 W Oriel Hg arc lamp containing a 334 nm line filter, a maximum absorbance was noted at 540 nm (in methanol) and 616 nm (in toluene). Typically, all the studied compounds showed similar behavior upon irradiating with UV light except **SP-T-T-T-T-SP** which showed a λ_{max} of the MC isomer in methanol at 545 nm (figure 3.44a, denoted by an arrow).

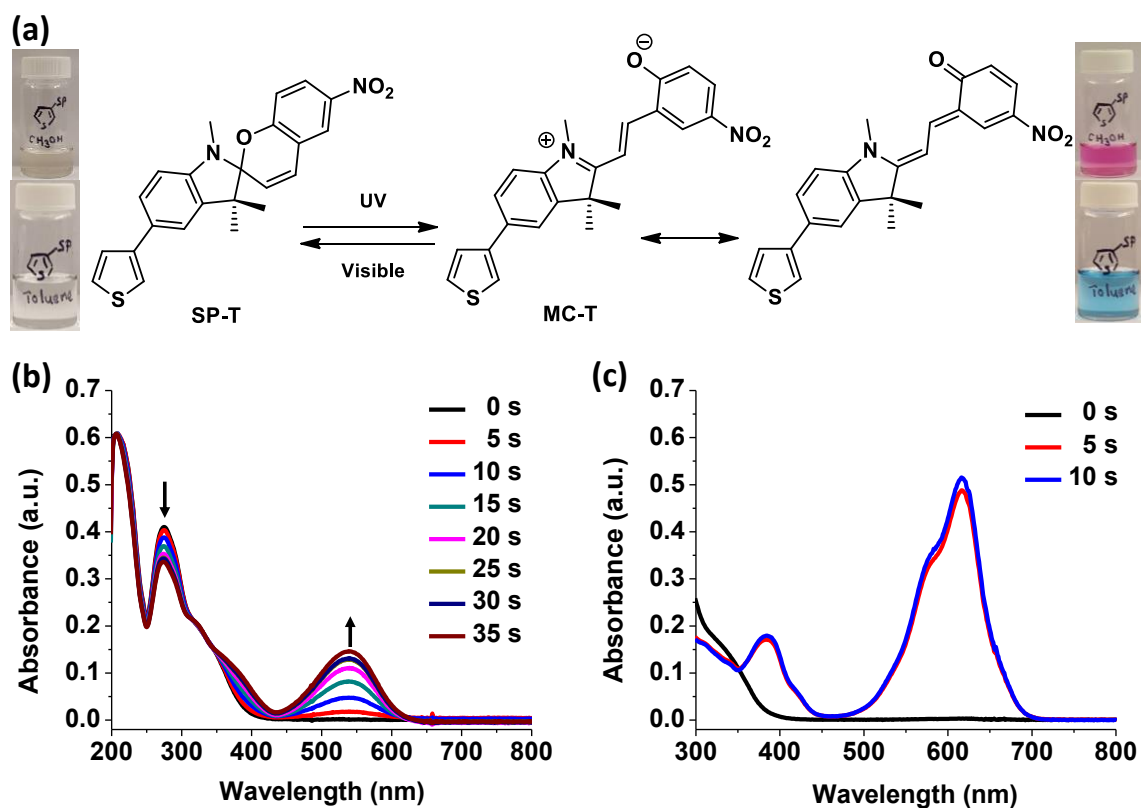


Figure 3.43. Isomerization of **SP-T** (a) Optical absorbance of photomerocyanine (MC) of **SP-T** (b) in methanol (c) in toluene. All spectra are obtained upon irradiating 1×10^{-5} M solutions using a mercury arc lamp with a 334 nm line filter.

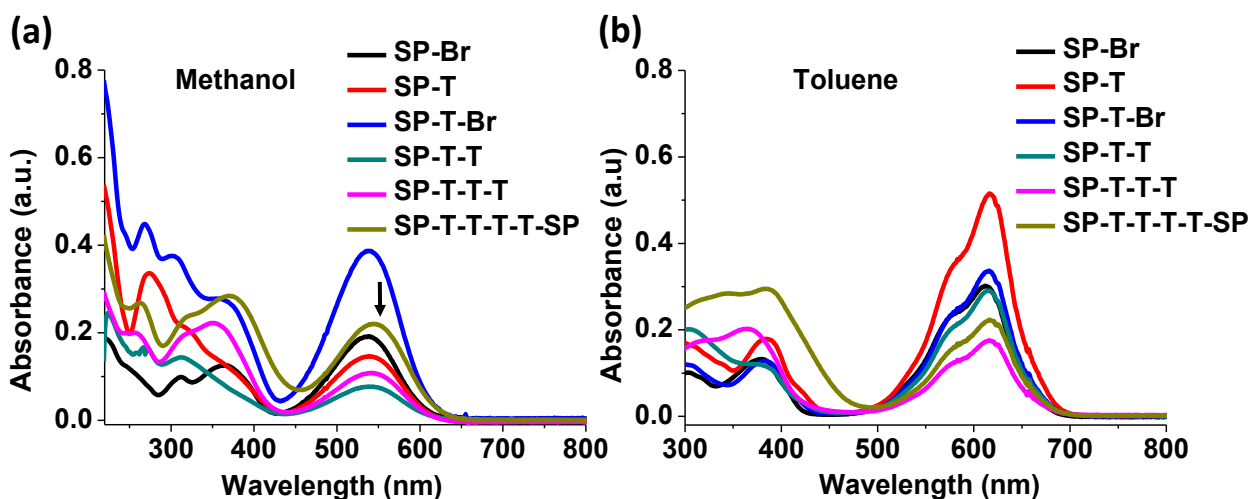


Figure 3.44. Maximum optical absorbance of photomerocyanine (a) in methanol (b) in toluene. All spectra are obtained upon irradiating 1×10^{-5} M solutions using a mercury arc lamp with a 334 nm line filter.

Even though the mechanism of the ring opening reaction of SP has been broadly studied, only a few mechanisms have been suggested. A proposed theory is that this reaction undergoes a heterolytic C-O bond cleavage affording two mesomeric forms that are a zwitterionic form or quinoidal form and the final MC form is a hybrid of these resonance forms.^{13,14} When a polar solvent is used as the medium, zwitterionic state is preferentially stabilized through hydrogen bonding with the solvent, while the quinoidal form could be favored in non-polar solvents. The higher absorbance that we have observed in toluene (figure 3.45b) could be due to this favorable quinoidal form.

The MC isomer tends to aggregate in non-polar solvents and this behavior was observed predominantly with nitro substituted SPs.^{15,16} However, a SP molecule which has the exactly the same substituents except a H at 5-position showed an absorbance band at 605 nm and a shoulder at 580 nm for a solution of MC in toluene. The 605 nm band was assigned to monomer MC and shoulder at 580 nm was assigned to dimer MC.¹⁶ A similar peak pattern was observed with 5-position substituted SPs used in this study (figure 3.44 and 3.45). The position of the shoulder did not change with increase in thiophene units (figure 3.44).

Strong H-bonding and solute-solvent interactions in polar solvents allow less tendency for aggregation. Therefore, in methanol we have not seen any additional peak or shoulder peak appearance in any of the compounds that we have studied. Position of the λ_{max} in methanol did not change with increase in thiophene units whereas, red shift of λ_{max} in SP-T-T-T-T-SP could be attributed to charge distribution along the π -electron system which influences the polarity and H-bonding ability of the molecule.¹⁷

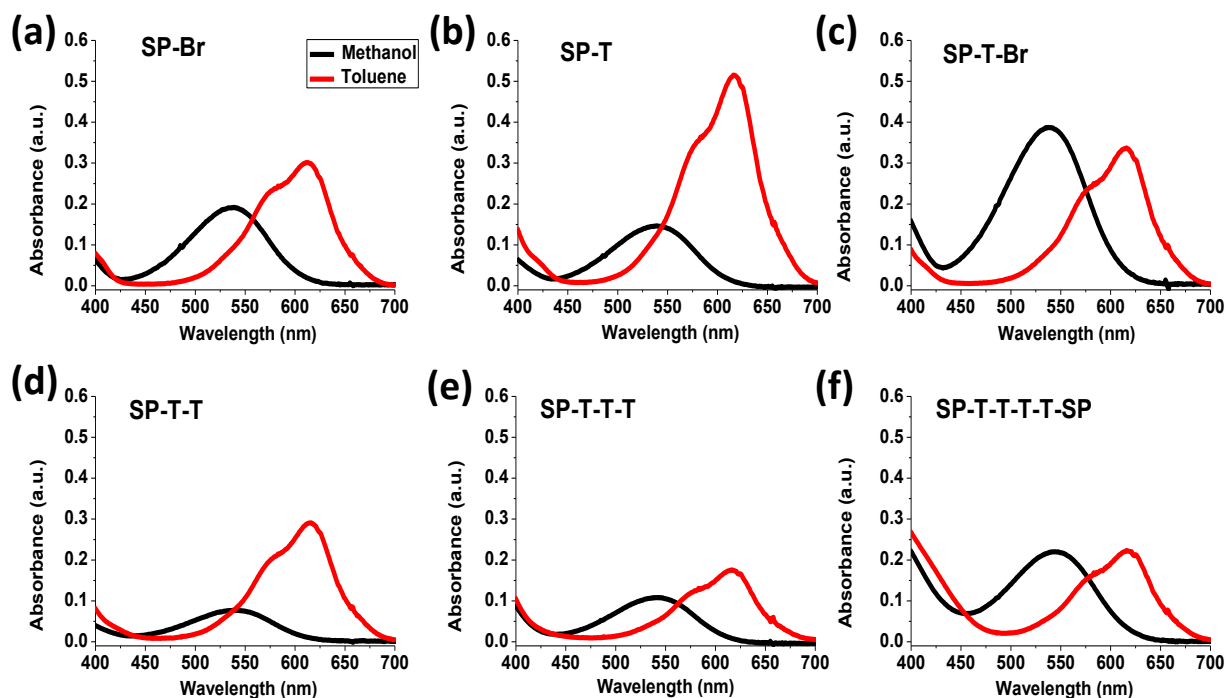


Figure 3.45. Comparison of maximum optical absorbance of photomerocyanines in methanol and in toluene, all spectra are obtained upon irradiating 1×10^{-5} M solutions using a mercury arc lamp with a 334 nm line filter.

The MC state is thermally unstable and the rate of conversion to the SP state can be controlled by stabilizing the MC in a fluid media through electrostatic interactions or in a rigid media via hindering the conformational mobility. Our group has studied various aspect in this regard.¹⁸⁻²³ In the current study, thermal decay was measured in polar and non-polar solvents. Typically, the measurements were performed during the photoexcitation of the colorless SP to MC and taking an absorbance reading of the λ_{max} of the MC as it decays every 15–30 s over 90–180 s (figure 3.46 and 3.47). In both polar (methanol) and non-polar(toluene) solvents MC showed a first order decay. Table 3.1 summarizes the decay rates in each solvent. The decay rates in methanol are relatively slow due to the stabilization of the polar MC through hydrogen bonding with the solvent.²⁰ Upon increasing the number of thiophene units gradually (SP-T to SP-T-T to SP-T-T-T) the decay rates significantly lowered in methanol. At least with the short thiophene chains in

this study, the decay rate decreased with an increasing thiophene chain length. This might reflect the more conjugated thiophene chain stabilizing either the changed zwitterionic or quinoidal MC form. When a bromine atom was connected at 5-position of indoline moiety (**SP-Br**) the thermal decay rate was slower than with one thiophene substituent (**SP-T**) because bromine can act as an electron donating group stabilizing positive charge on indoline nitrogen on MC. **SP-T-T-T-T-SP** also showed slow decay rate in methanol.

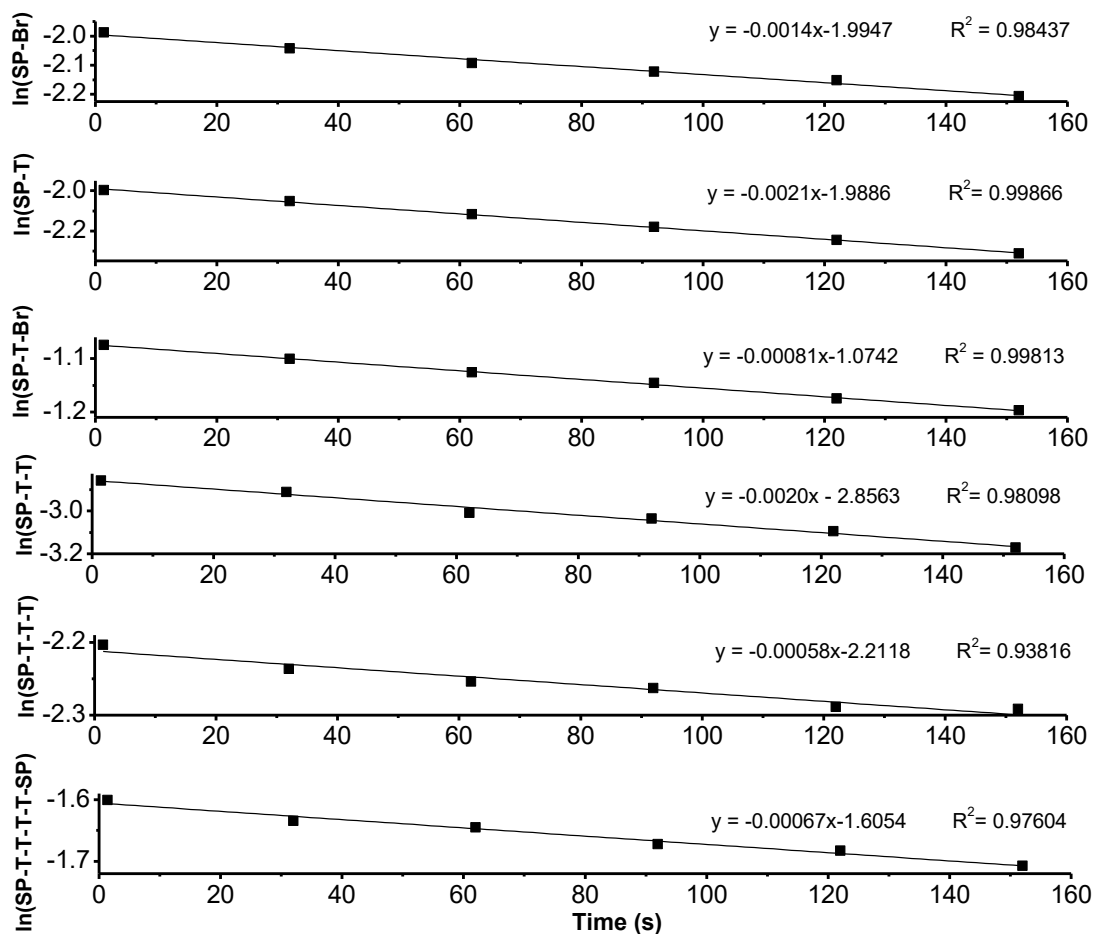


Figure 3.46. Absorbance decay of photochromic peak in methanol

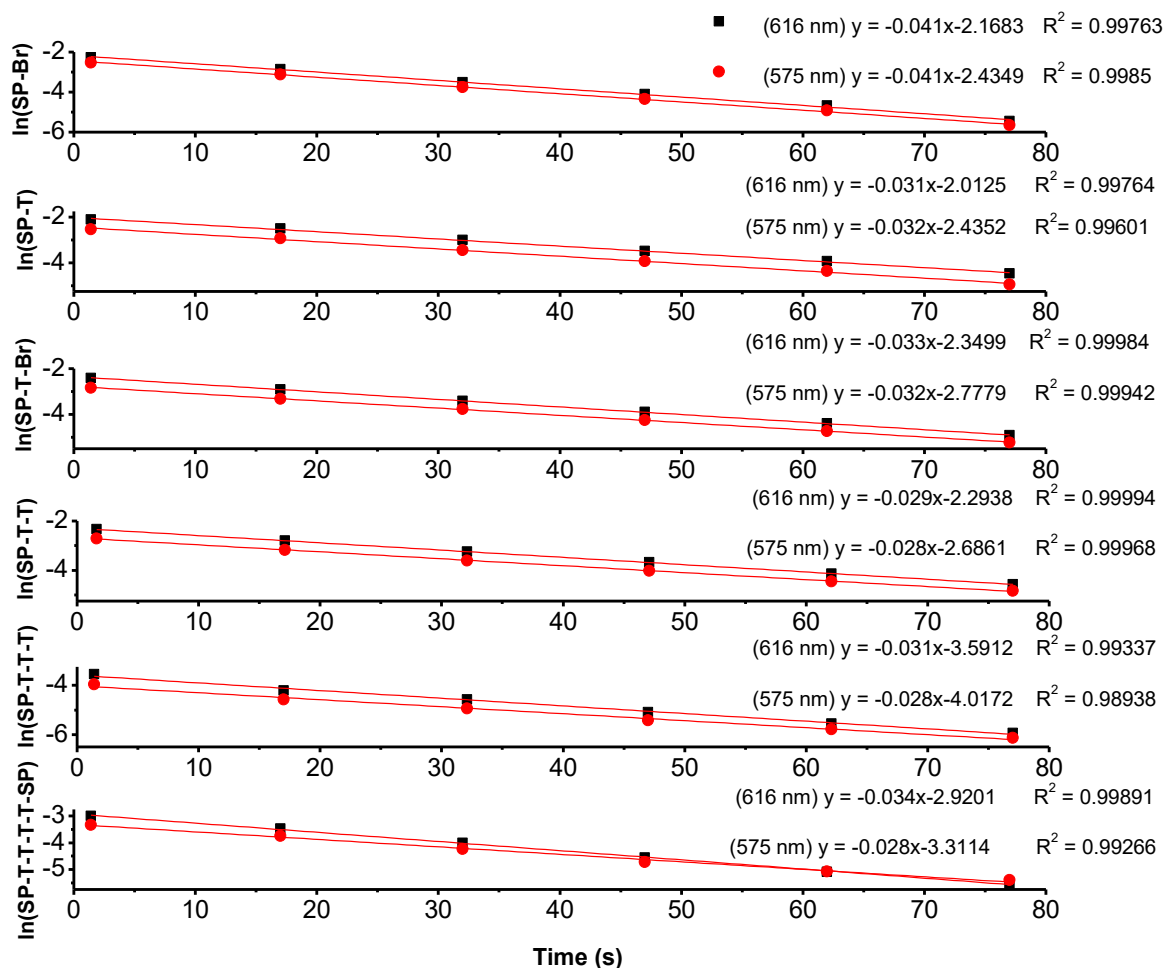


Figure 3.47. Absorbance decay of photochromic peak in toluene

The decay rates in non-polar toluene solvent were several orders of magnitude higher than in methanol and showed relatively similar values irrespective of the compound. All compounds except **SP-T-T-T-T-SP** displayed similar decay rates for the λ_{max} peak at 616 nm and the shoulder peak at 575 nm (figure 3.47). In **SP-T-T-T-T-SP** the shoulder peak at 575 nm showed a relatively slower decay rate compared with that of 616 nm peak.

Photodegradation of the compounds were tested with multiple irradiation in the same solution. After three consecutive irradiations in methanol, **SP-Br**, **SP-T**, **SP-T-Br**, **SP-T-T**, **SP-T-T-T**, **SP-T-T-T-T-SP** showed average of 6 %, 7 %, 10 %, 10 %, 6 %, 9 % photodegradation relative to the first irradiation respectively (table 3.2). It was encouraging to observe photochromism in the bulky **SP-T-T-T-T-SP** even after multiple cycles of irradiation.

Table 3.1. Half-lives and rate of SP decay in various solvents^a

Compound	t _{1/2} (s)		Rate (s ⁻¹)		
	Methanol (λ _{max} = 540 nm)	Toluene (λ _{max} = 616 nm)	Methanol (λ _{max} = 540 nm)	Toluene (λ _{max} = 616 nm)	Toluene (λ _{max} = 575 nm)
SP-Br	520±22	14±3	0.0013±0.000058	0.052±0.0092	0.052±0.0089
SP-T	293±42	20±3	0.0024±0.00036	0.035±0.0047	0.033±0.0042
SP-T-Br	755±119	21±2	0.00093±0.00015	0.034±0.0031	0.034±0.0025
SP-T-T	404±50	21±3	0.0017±0.00023	0.034±0.0043	0.033±0.0046
SP-T-T-T	1100±95	19±4	0.00063±0.000058	0.038±0.0076	0.037±0.0086
SP-T-T-T-T-SP	1045±95 ^b	18±6	0.00067 ^b ±0.000058	0.043±0.018	0.038±0.017

^aSamples were run with a 1×10^{-5} M solutions and the recorded values are an average of three runs, Irradiated for the first time.

^bMeasured at 545 nm

Table 3.2. Photodegradation of SP in methanol^a

Compound	Absorbance upon first irradiation	Absorbance upon second irradiation	Absorbance upon third irradiation
SP-Br	0.183±0.00765	0.169±0.00760	0.172±0.00508
SP-T	0.142±0.0132	0.148±0.00762	0.145±0.00248
SP-T-Br	0.359±0.0232	0.369±0.0545	0.355±0.0283
SP-T-T	0.0795±0.00522	0.0692±0.00131	0.0712±0.00198
SP-T-T-T	0.110±0.00411	0.100±0.00536	0.106±0.00866
SP-T-T-T-T-SP	0.214±0.00104 ^b	0.181±0.0134 ^b	0.196±0.0110 ^b

^a Recorded value is an average of three independent runs, absorbance = Abs(t)- Abs(t=0), Abs(t) indicates the maximum absorbance at 540 nm, Abs(t=0) indicates the absorbance at 540 nm before any irradiation begins.

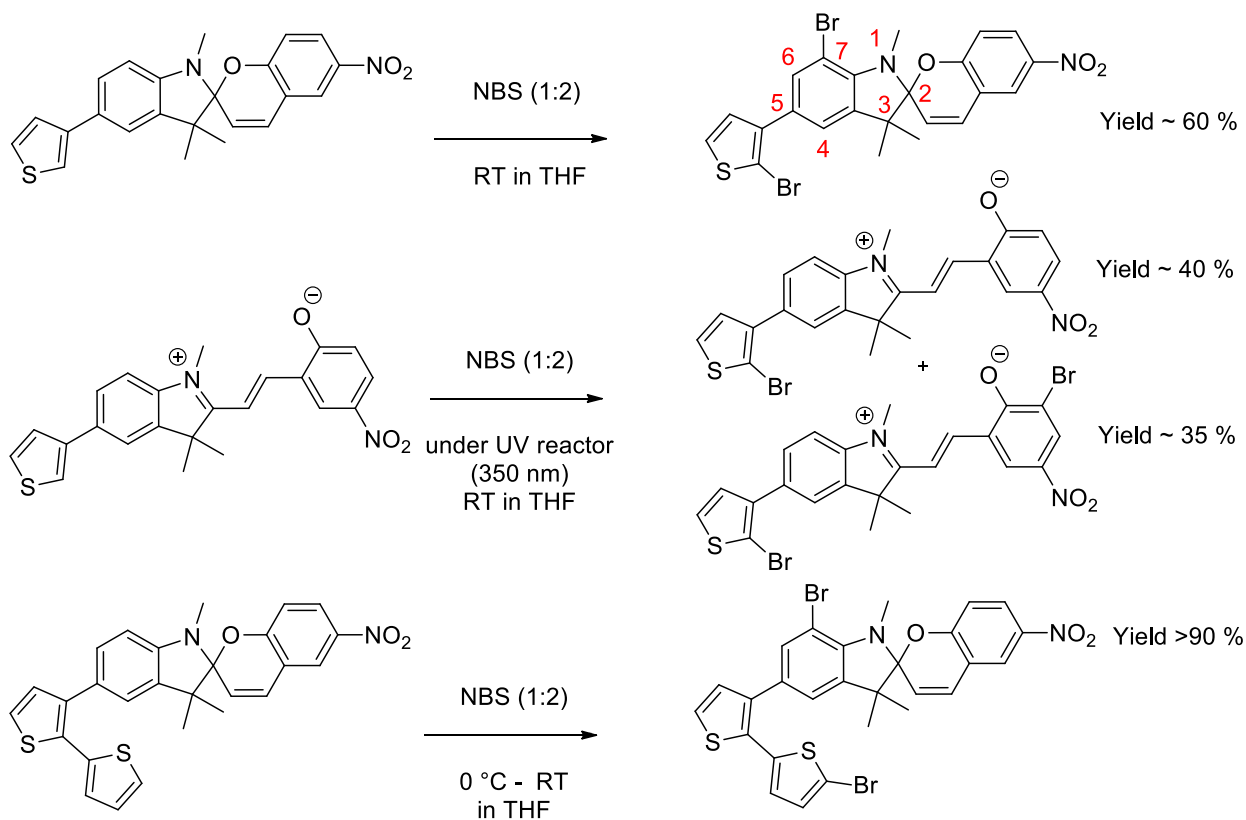
^bMeasured at 545 nm

3.4.5 Dibrominated derivative of SP-T

SP-T-Br is not amenable to polymerization methods involving nickel mediated catalytic systems due to the nitro functional group incompatibility.²⁴ Other methods involving reactive butyl lithium reagents or C-H activation type polymerizations are difficult to perform due to the highly electron

deficient protons *ortho* to nitro group in SP.²⁵ Hence, palladium catalyzed cross coupling polymerizations are the most likely to be performed on our **SP-T** compound, which require dibrominated compound of **SP-T**.²⁶

Bromination occurred at 2-position of thiophene and 7-position of SP when the bromination of **SP-T** was carried with N-bromosuccinimide in 1:2 ratio at room temperature (scheme 3.15). Bromination of 7-position (position c in figure 3.48(i)) of SP was indicated by the disappearance of proton a 7-position in ¹H-NMR spectrum (figure 3.48(ii) - indicated by an arrow) and at the same time, shifting the δ value of the N-methyl protons to weak field up to 0.4 ppm.²⁷ In order to prevent the bromination on electron rich 7-position of SP, the bromination was carried with the same reaction conditions under a UV reactor in open MC form of **SP-T**. While the 2-position of thiophene was still amenable to bromination, the second bromination occurred *ortho* to the phenolate ion in the chromene moiety (figure 3.48(iii) and 3.48(iv)). Increasing the number of thiophene units at 5-position of SP also directed the second bromine to 7-position of SP (figure 3.48(v)).



Scheme 3.15. Dibrominated derivatives of **SP-T**

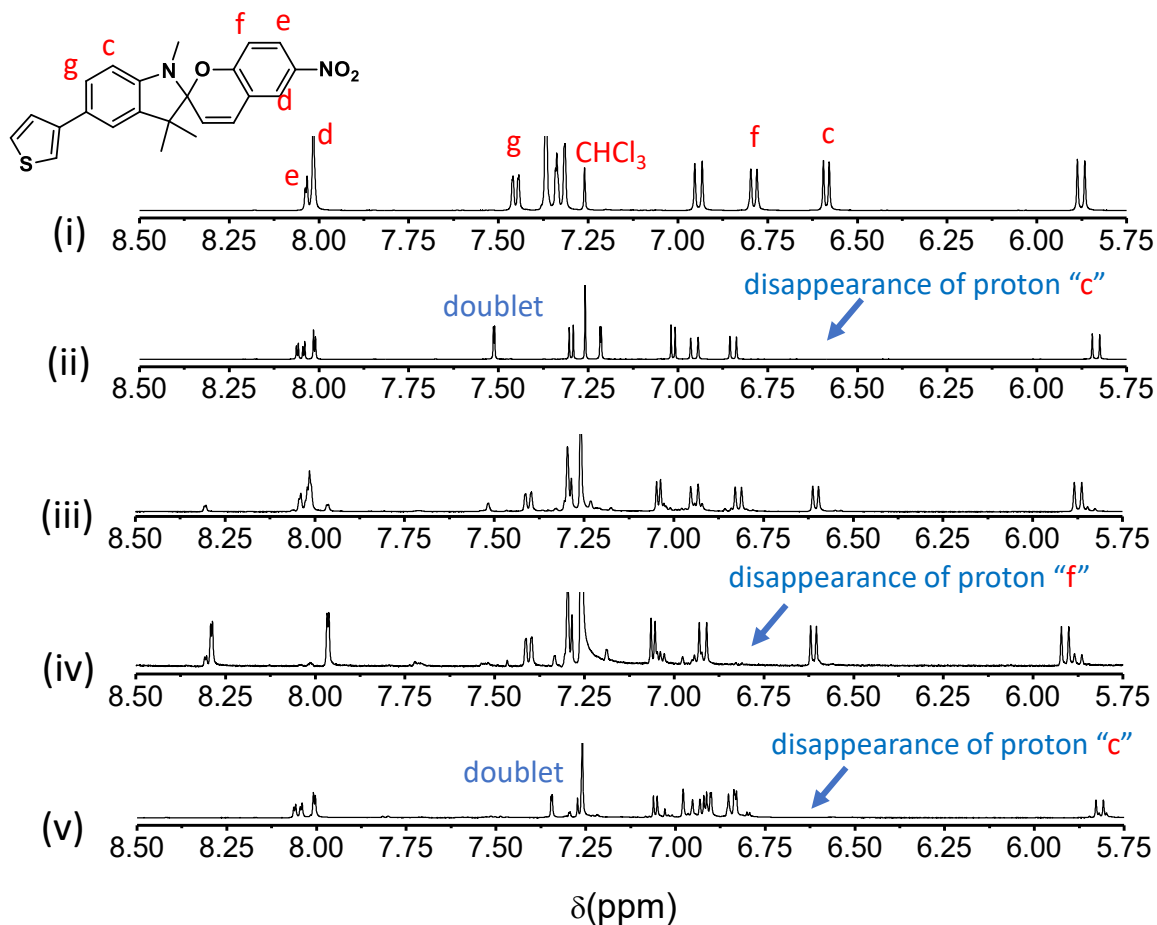
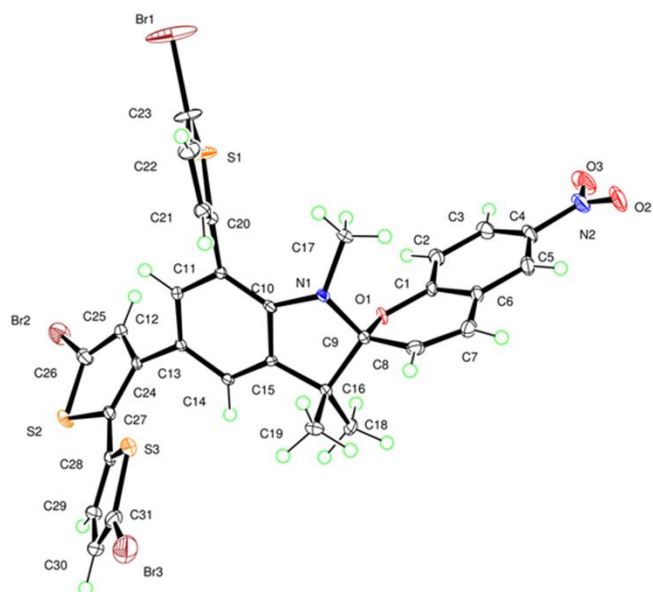


Figure 3.48. $^1\text{H-NMR}$ analysis of the dibrominated compounds of **SP-T** in downfield region

3.4.6 Tribrominated derivative of SP-T

Upon attaching two thiophene units to 2-position of thiophene and 7-position of SP, bromination occurred in all 5-positions of thiophene. Crystal structures of this compound is given in figures 3.49. This observation suggested that a suitable substituent at 7-position of SP could lead to dibromination to occur on 2, 5- positions of thiophene on SP. Our group is currently studying new aspects in this regard.

(a)



(b)

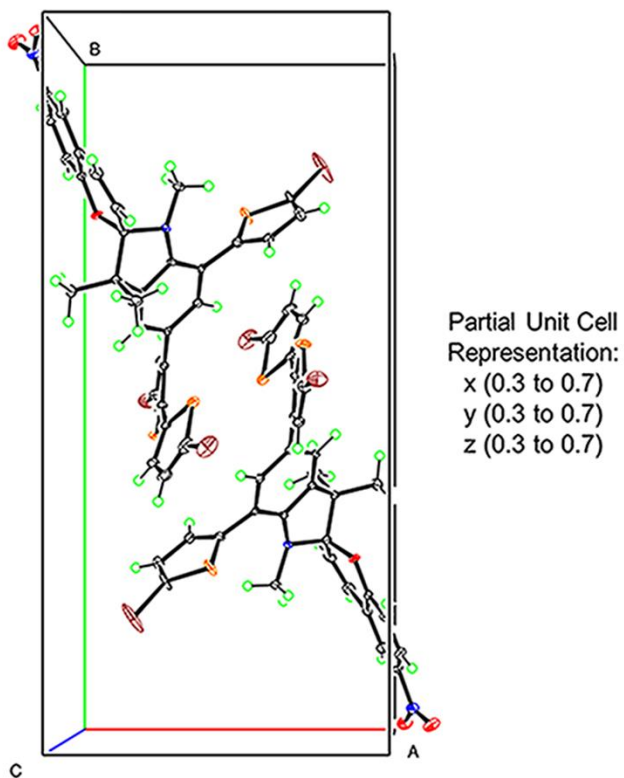


Figure 3.49. (a) Crystal structure and (b) partial unit cell representation of tribrominated compound ($(R[F^2 > 2\sigma(F^2)]) = 0.065$).

3.5 Conclusions

A novel synthetic method to incorporate SP in thiophene based materials was successfully demonstrated and their optical absorbance in polar (methanol) and nonpolar (toluene) solvents was measured under identical experimental conditions. When a thiophene moiety is incorporated in SP via the 5-position, monobromination selectively occurred at the 2-position of thiophene. Incorporating two to three thiophene units at this position caused a decrease in the thermal decay rate of the reverse reaction, thus increasing the half-life of MC in methanol. When two SP units were connected at the two ends of a quarterthiophene unit, thermal decay rate of the reverse reaction was relatively low in methanol. These compounds show 5-10 % photodegradation in methanol upon three consecutive irradiations. All the compounds of interest showed relatively similar thermal decay rate of the reverse reaction in toluene. Overall, this study is expected to give a new insight to different synthetic route to develop thiophene based SP materials with improved photochromic properties. The photochromic thiophene molecules are designed as materials that are capable of actuated changes of their optical and electronic properties. Furthermore, findings suggested that a suitable substituent at 7-position of spiropyran would lead to a successful dibrominated derivative of **SP-T**.

3.6 Acknowledgments

The authors would like to thank the NSF (DMR-1505950) and Welch Foundation (AT-1740) for the financial support provided for this research.

3.7 References

1. Li, Y.; Zhang, H.; Qi, C.; Guo, X. Light-driven photochromism-induced reversible switching in P3HT-spiropyran hybrid transistors. *Journal of Materials Chemistry* **2012**, *22*, 4261-4265.
2. Ishiguro, Y.; Hayakawa, R.; Chikyow, T.; Wakayama, Y. Optically Controllable Dual-Gate Organic Transistor Produced via Phase Separation between Polymer Semiconductor and Photochromic Spiropyran Molecules. *ACS Applied Materials & Interfaces* **2014**, *6*, 10415-10420.

3. Moustrou, C.; Samat, A.; Guglielmetti, R.; Dubest, R.; Garnier, F. Synthesis of Thiophene-Substituted Spiropyrans and Spirooxazines, Precursors of Photochromic Polymers. *Helvetica Chimica Acta* **1995**, *78*, 1887-1893.
4. Moustrou, C.; Campredon, M.; Samat, A.; Guglielmetti, R.; Garnier, F.; Robillard, J. New Spiropyrans and Spirooxazines Compounds With one or two Thiophene Nuclei. Applications to Anticopying Protection Materials. *Molecular Crystals and Liquid Crystals Science and Technology. Section A. Molecular Crystals and Liquid Crystals* **1994**, *246*, 29-32.
5. Wagner, K.; Byrne, R.; Zanoni, M.; Gambhir, S.; Dennany, L.; Breukers, R.; Higgins, M.; Wagner, P.; Diamond, D.; Wallace, G. G.; Officer, D. L. A Multiswitchable Poly(terthiophene) Bearing a Spiropyran Functionality: Understanding Photo- and Electrochemical Control. *Journal of the American Chemical Society* **2011**, *133*, 5453-5462.
6. Balmond, E. I.; Tautges, B. K.; Faulkner, A. L.; Or, V. W.; Hodur, B. M.; Shaw, J. T.; Louie, A. Y. Comparative Evaluation of Substituent Effect on the Photochromic Properties of Spiropyrans and Spirooxazines. *The Journal of Organic Chemistry* **2016**, *81*, 8744-8758.
7. Sheldrick, G. SHELXT - Integrated space-group and crystal-structure determination. *Acta Crystallographica Section A* **2015**, *71*, 3-8.
8. Sheldrick, G. Crystal structure refinement with SHELXL. *Acta Crystallographica Section C* **2015**, *71*, 3-8.
9. Jin, L.-M.; Li, Y.; Ma, J.; Li, Q. Synthesis of Novel Thermally Reversible Photochromic Axially Chiral Spirooxazines. *Organic Letters* **2010**, *12*, 3552-3555.
10. Sauter, G. H.-J., B.; Reichlin, N. Preparation of 5-aryl-1,3,3-trimethyl-2-methylene-indoles and their iminium salts for the temporary dyeing of hair fibers.
11. Choi, J.; Kim, K.-H.; Yu, H.; Lee, C.; Kang, H.; Song, I.; Kim, Y.; Oh, J. H.; Kim, B. J. Importance of Electron Transport Ability in Naphthalene Diimide-Based Polymer Acceptors for High-Performance, Additive-Free, All-Polymer Solar Cells. *Chemistry of Materials* **2015**, *27*, 5230-5237.
12. Lukyanov, B.; Lukyanova, M. Spiropyrans: Synthesis, Properties, and Application. (Review). *Chemistry of Heterocyclic Compounds* **2005**, *41*, 281-311.
13. Guglielmetti, R.: 4n+2 Systems: Spiropyran. In *Photochromism : Molecules and Systems*; Durr, H. B.-L., H., Ed.; Elsevier, 2003; pp 314-466.
14. Swansburg, S.; Buncel, E.; Lemieux, R. P. Thermal Racemization of Substituted Indolinobenzospiropyrans: Evidence of Competing Polar and Nonpolar Mechanisms. *Journal of the American Chemical Society* **2000**, *122*, 6594-6600.

15. Klajn, R. Spiropyran-based dynamic materials. *Chemical Society Reviews* **2014**, *43*, 148-184.
16. Barachevskii, V.; Karpov, R. Photonics of nanostructured systems based on photochromic spiro compounds. *High Energy Chemistry* **2007**, *41*, 188-199.
17. Tian, W.; Tian, J. An insight into the solvent effect on photo-, solvato-chromism of spiropyran through the perspective of intermolecular interactions. *Dyes and Pigments* **2014**, *105*, 66-74.
18. de Leon, L.; Biewer, M. C. Preparation of self-assembled monolayers with specific intermolecular interactions. *Tetrahedron Letters* **2000**, *41*, 3527-3530.
19. Iyengar, S.; Biewer, M. C. Observation of photochromic [gamma]-cyclodextrin host-guest inclusion complexes. *Chemical Communications* **2002**, 1398-1399.
20. Shumburo, A.; Biewer, M. C. Stabilization of an Organic Photochromic Material by Incorporation in an Organogel. *Chemistry of Materials* **2002**, *14*, 3745-3750.
21. Patel, K.; Castillo-Muzquiz, A.; Biewer, M. C. Studying monolayer/solvent interactions with a photochromic compound in a self-assembled monolayer. *Tetrahedron Letters* **2002**, *43*, 5933-5935.
22. Iyengar, S.; Biewer, M. C. Solid-State Interactions in Photochromic Host-Guest Inclusion Complexes. *Crystal Growth & Design* **2005**, *5*, 2043-2045.
23. Yang, M.-H.; Biewer, M. C. Monitoring surface reactions optically in a self-assembled monolayer with a photochromic core. *Tetrahedron Letters* **2005**, *46*, 349-351.
24. Slagt, V. F.; de Vries, A. H. M.; de Vries, J. G.; Kellogg, R. M. Practical Aspects of Carbon-Carbon Cross-Coupling Reactions Using Heteroarenes. *Organic Process Research & Development* **2010**, *14*, 30-47.
25. Pouliot, J.-R.; Grenier, F.; Blaskovits, J. T.; Beaupré, S.; Leclerc, M. Direct (Hetero)arylation Polymerization: Simplicity for Conjugated Polymer Synthesis. *Chemical Reviews* **2016**, *116*, 14225-14274.
26. Nicolaou, K. C.; Bulger, P. G.; Sarlah, D. Palladium-Catalyzed Cross-Coupling Reactions in Total Synthesis. *Angewandte Chemie International Edition* **2005**, *44*, 4442-4489.
27. Zakhs, É. R.; Zvenigorodskaya, L. A.; Leshenyuk, N. G.; Martynova, V. P. Bromination of spiropyranes and reduction of their nitro derivatives. *Chemistry of Heterocyclic Compounds* **1977**, *13*, 1055-1061.

CHAPTER 4
TRIETHYLENE GLYCOL MONOMETHYL ETHER SUBSTITUTED
POLYTHIOPHENE FOR ORGANIC ELECTRONIC APPLICATIONS

Authors - Dushanthi S. Dissanayake,^a Samodha S. Gunathilake, ^a Jia Du,^a Katherine E. Washington,^a Sang Ha Yoo,^b Youngmin Lee,^b Enrique D. Gomez,^{b#}, Mihaela C. Stefan ^a and Michael C. Biewer^a

^a Department of Chemistry and Biochemistry BE26, University of Texas at Dallas, 800 West Campbell Road, Richardson, Texas 75080-3021

^bDepartment of Chemical Engineering, [#]Materials Research Institute, The Pennsylvania State University, University Park, Pennsylvania 16802

Dushanthi S. Dissanayake and Samodha S. Gunathilake contributed to the synthesis and characterization of compounds. Dushanthi S. Dissanayake performed the initial organic field effect transistor measurements and showed the potential of this material as an alternative to commercially available PEDOT:PSS. Jia Du provided the guidance for space charge limited current measurements. Katherine E. Washington performed TEM analysis. Sang Ha Yoo, Youngmin Lee and Enrique D. Gomez performed GIWAXS, GISAXS and organic field effect transistor measurements. Professors Mihaela C. Stefan and Michael C. Biewer developed the initial idea for the project, aided in troubleshooting during the project, and edited chapter for publication.

4.1 Abstract

Charge carrier mobility of the triethylene glycol monomethyl ether substituted polythiophene was demonstrated with field-effect transistors and in Schottky diode. Most importantly, the polymer showed high conductivity upon doping with iodine and also had high stability in the doped state. Furthermore, the doping caused transparency to thin films of the polymer and the films were resistant to solubility with common organic solvents indicating great potential of this polymer as an alternative to commercially available PEDOT: PSS.

4.2 Introduction

Polythiophenes (PTs) are attractive due to their potential use as semiconducting materials in various applications such as organic field effect transistors (OFETs),¹ organic photovoltaic devices,² and sensors.³⁻⁵ Electrical and optical properties of PTs depend on the type of substituents on thiophene.⁶ Poly(3-hexylthiophene)(P3HT) is a widely studied polymer among poly(alkylthiophene)s which easily self-assembles to form a well-ordered two-dimensional lamellar structure,^{7,8} a crucial requirement in charge transportation. P3HT also has good solubility in organic solvents,⁹ and it has good conductivities in doped or oxidized state. However, P3HT is not stable over time in its doped state and upon removal from contact with its dopant the conductivity drops very fast.^{10,11} However, poly(alkoxythiophene)s such as poly(thiophene-3-[2-(2-methoxyethoxy)ethoxy]-2,5-diyl) (P3MEET) has been reported with increased conductivity upon doping and were stable over time.¹²⁻¹⁴ Incorporation of alkoxy substituents on a thiophene ring, can make the resulting polymer insoluble in organic solvents due to α,β' coupling between thiophene rings.¹² Many attempts have been made to overcome issues associated with both poly(alkylthiophenes)s and poly(alkoxythiophene)s and to synthesize polymers with improved properties. For example, sulfonated-P3MEET based polymers have drawn attention as an improved alternative to commercially available poly(3,4-ethylenedioxythiophene):poly(styrenesulfonate) (PEDOT:PSS).¹⁵⁻¹⁷ PEDOT:PSS is not an ideal hole transporting layer owing to its hygroscopicity and acidity which negatively impact the stability of the devices.¹⁸⁻²⁰ A recent study by McCulloch and co-workers highlighted the importance of MEEET based units on organic electrochemical transistor applications.²¹ Furthermore, diblock copolymers of P3HT and poly(3-

[2-[2(2-methoxyethoxy)ethoxy]ethoxy]thiophene) (P3MEEET) have also been reported by Hayward and co-workers showing composition dependent helical nanowire formation via complexation with K^+ ions and polymers with amphiphilic nature by Park and co-workers.^{22,23} A pyrimidine containing polymer with MEEET and 3HT units is also reported.²⁴ Organic electronic applications of the co-polymer of bithiophene units composed of 3HT and MEEET however, has not yet been reported.

4.3 Experimental

4.3.1 Materials and methods

All commercial chemicals were purchased either from Sigma Aldrich Chemical Co. LLC. or from Fisher Scientific Co. LLC. and were used without further purification unless otherwise noted. All glassware and syringes were dried at 120 °C for at least 24 h before use and cooled in a desiccator. Tetrahydrofuran (THF) and toluene were dried over sodium/benzophenone ketyl and freshly distilled under nitrogen prior to use. Synthesis of the triethylene glycol monomethyl ether substituted polythiophene and its characterization is carried out according to a previously reported procedure.²⁵

4.3.2 Analysis

NMR analysis: 1H and ^{13}C NMR spectra and all 2D-NMR analysis were recorded at 25 °C using a Bruker AVANCE III 500 MHz NMR spectrometer, and were referenced to residual protio solvent ($CHCl_3$; δ 7.26 ppm). The data are reported as follows: chemical shifts are reported in ppm on δ scale, multiplicity (s = singlet, d = doublet, t = triplet, q = quartet, m = multiplet).

GC-MS analysis: GC-MS analysis was performed on Hewlett-Packard Agilent 6890-5973 GC-MS workstation equipped with a Hewlett-Packard fused silica capillary GC column cross-linked with 5 % phenylmethylsiloxane. Helium was used as the carrier gas (1 mL min^{-1}). Sample analysis conditions: injector and detector temperature = 250 °C, initial temperature = 70 °C, temperature ramp = $10\text{ }^\circ\text{C min}^{-1}$, final temperature = 280 °C.

Size Exclusion Chromatography (SEC) analysis: SEC analysis was performed on a Viscotek VE 3580 system equipped with ViscoGEL™ columns (GMHHR-M), connected to a refractive index detector/UV detector. GPC solvent/sample module (GPCmax) was used with HPLC grade THF eluent. The calibration was based on polystyrene standards. Sample analysis conditions: flow rate = 1.0 mL min⁻¹, injector volume = 100 μL, detector temperature = 30 °C and column temperature = 35 °C. Sample dissolved in THF was filtered through PTFE syringe (0.2 μm) filter prior to injection.

UV-Vis spectroscopic analysis: UV-visible absorption spectra of polymer solution in chloroform solvent was carried out in 1 cm cuvettes using an Agilent 8453 UV-vis spectrometer. Thin films of polymer was obtained by evaporation of chloroform solvent from polymer solution on glass microscope slides.

Cyclic voltammetric analysis: Cyclic voltammogram was obtained with a BAS CV-50W voltammetric analyzer (Bioanalytical Systems, Inc.). The electrochemical cell was comprised with three electrode system: platinum inert working electrode, a platinum wire auxiliary electrode, and a Ag/Ag⁺ reference electrode. The electrolyte solution: 0.1 M electrochemical grade tetrabutylammoniumhexafluorophosphate in freshly distilled acetonitrile (acetonitrile was distilled under nitrogen over calcium hydride and collected over molecular sieves). The electrolyte solution was placed in a cell and purged with argon. A drop of polymer solution in chloroform was evaporated in ambient air. The film was immersed into electrochemical cell containing the electrolyte, and the oxidation and reduction potentials were recorded. Ferrocene/ferrocenium (Fc/Fc⁺) was used as internal reference for UV calibration and the E_{1/2} of the redox couple measured under same condition was located at 0.09 V vs. Ag/Ag⁺ reference electrode. HOMO and LUMO energy levels were calculated by using the following equations (4.1) and (4.2):

$$\text{HOMO (eV)} = (E_{\text{ox}} + 4.71) \text{ eV} \quad (4.1)$$

$$\text{LUMO (eV)} = (E_{\text{red}} + 4.71) \text{ eV} \quad (4.2)$$

where E_{ox} and E_{red} are the measured potentials relative to Ag/Ag⁺

Transmission electron microscopy (TEM) analysis: TEM imaging of the polymer was performed on a Tecnai G2 Spirit Biotwin microscope by FEI and images were analyzed using Image J software. Samples were prepared by treating copper mesh grid with 0.3 mg mL⁻¹ solutions.

Dynamic Light Scattering (DLS) Analysis: DLS analysis of the polymer in chloroform was carried out using 0.3 mg mL⁻¹ solutions and the solution was filtered through PTFE syringe (0.45 μm) filter prior to measurements. Size measurements were recorded at 25 °C in triplicate.

Grazing-incidence wide angle X-ray scattering (GIWAXS) analysis: GIWAXS measurements were carried out at beamline 7.3.3 of Advanced Light Source in Lawrence Berkeley National Laboratory. Beamline 7.3.3 operates at an energy of 10.0 keV with $\lambda = 1.2398 \text{ \AA}$. Scattering data were acquired at an incident angle of 0.15°. In-plane data was extracted as line cuts from the 2D images and is presented as a function of the scattering vector, q ($q = 4\pi \sin(\theta/2)/\lambda$). GIWAXS intensities were also azimuthally averaged and presented versus q .

Thermogravimetric analysis (TGA): TGA of the polymer was carried out on SDT Q600 instrument.

Differential Scanning Calorimetry (DSC) analysis: DSC analysis was carried out using Mettler Toledo DSC 1 Star System. Aluminum standard pans were filled with polymer sample (2.55 mg). The polymer sample was subjected to heat–cool–heat cycle and data were recorded by heating and cooling the sample from 25 °C to 200 °C and vice versa at the rate of 10 °C min⁻¹.

Conductivity measurements: The conductivity of the polymer was measured using Pro-4 Four point resistivity systems. The polymer solution in chloroform was drop-casted on a cleaned glass substrate in chloroform chamber. After complete solvent evaporation, polymers were chemically oxidized by exposure to iodine vapor for various amounts of time. The conductivities were calculated by the equation (4.3). At least three consecutive measurements were performed per one measurement.

$$\sigma = \frac{1}{4.53 \times Rl} \quad (4.3)$$

Where σ = conductivity

R = resistance (S); $R = V/I$

l = film thickness (cm)

The film thickness was measured by using a Veeco Dektak VIII profilometer.

Mobility measurements: Vertical charge carrier mobility was measured using Shottky diodes which was made with the device structure of ITO/PEDOT:PSS/Polymer/Al. The measurements of space charge limited current (SCLC) of pure polymers were carried out in Keithley 2400 source meter interfaced with Labview software under nitrogen atmosphere under dark conditions. The voltage was increased from 0 V to 2.5 V. Each pixel had area of 10 mm^2 with film thickness around 33 nm. The mobility was calculated by the following equation (4.4):

$$J = \frac{9\varepsilon_0\varepsilon_r\mu V^2}{8L^3} \quad (4.4)$$

where

μ is the charge mobility

J is the current density

ε_0 is vacuum permittivity and equals to $8.854 \times 10^{-12} \text{ F/m}$

ε_r is relative permittivity of semiconducting materials. (3.5 was used)

V is the applied bias on the diode.

L is the film thickness

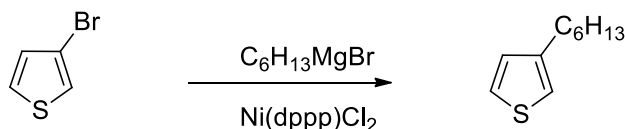
Field-effect mobilities were extracted from thin-film transistors with the polymer as the active layer and a bottom-gate, bottom-contact configuration fabricated as previously described.²⁶ Boron-doped p-type silicon wafers with a 300 nm thick thermally grown SiO_2 layer serve as the gate electrode and gate dielectric ($C = 10.6 \text{ nF/cm}^2$, Process Specialties). Gold source and drain electrodes were approximately 100 nm thick and were deposited using conventional double-layer photolithography. Self-assembled monolayers were not applied (UV-Ozone treatment only).

Polymer was spun cast at 1000 rpm for 4 minutes from 10 mg/mL in 1,2,4-trichlorobenzene solutions and annealed at 150 °C for 3 h prior to electrical measurements. The device channel width was 220 μm and the length was 320 μm .

Transmittance analysis: %T was measured using Cary 7000 UV-Vis-NIR spectrophotometer.

4.3.3 Synthetic procedures

Synthesis of 3-hexylthiophene



Scheme 4.1. Synthesis of 3-hexylthiophene

3-Bromothiophene (70.2 g, 431 mmol) was placed in a three-neck round bottomed flask and nitrogen was purged for 15 min. Diethyl ether (300 mL) was added to the mixture and it was kept under nitrogen for another 10 min prior to the addition of $\text{Ni}(\text{dppp})\text{Cl}_2$ (0.255 g, 255 mg). Hexylmagnesium bromide (230 mL, 460 mmol) was added to a dropping funnel and it was allowed to mix with the solution in the flask in small quantities. The resultant black colored solution was stirred overnight under nitrogen at 40 °C. The mixture was poured in to a beaker with ice and allowed to stand for 30 min prior to wash with deionized water and then with brine. Ether fractions were collected, dried over anhydrous MgSO_4 , evaporated under reduced pressure and allowed to stand under vacuum to remove the remaining solvent prior to the vacuum distillation. Product was obtained as a clear oil (58.0 g, 80 %). $^1\text{H-NMR}$ (CDCl_3 , 500 MHz; 7.24(dd, 1H, $J=4.7$, $J=3.0$), 6.94(d, 1H, $J=4.8$), 6.93(s, 1H), 2.64(t, 2H), 1.64(m, 2H), 1.33(m, 6H), 0.90(t, 3H)). $^{13}\text{C-NMR}$ (CDCl_3 , 500 MHz; 143.29, 128.30, 125.03, 119.76, 31.71, 30.55, 30.31, 29.04, 22.64, 14.11). $^1\text{H-NMR}$ and $^{13}\text{C-NMR}$ spectra are given in figure 4.1 and figure 4.2.

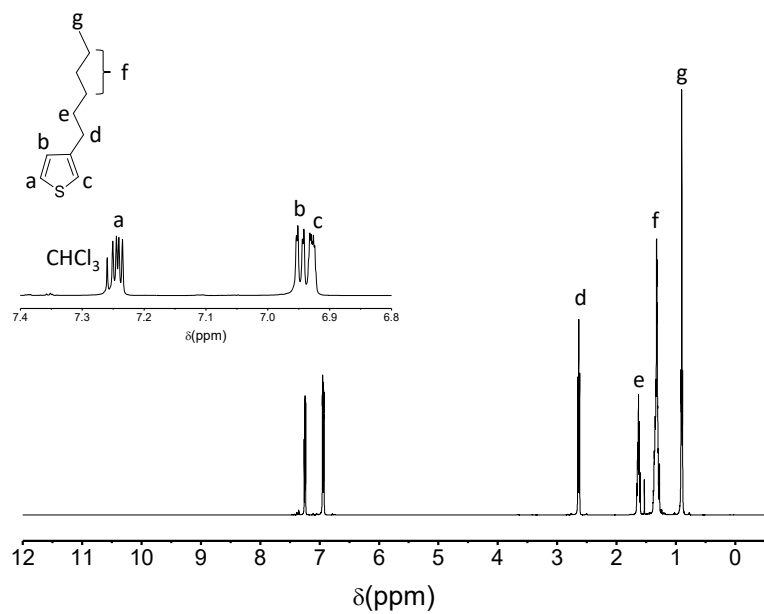


Figure 4.1. ^1H NMR spectrum of 3-hexylthiophene

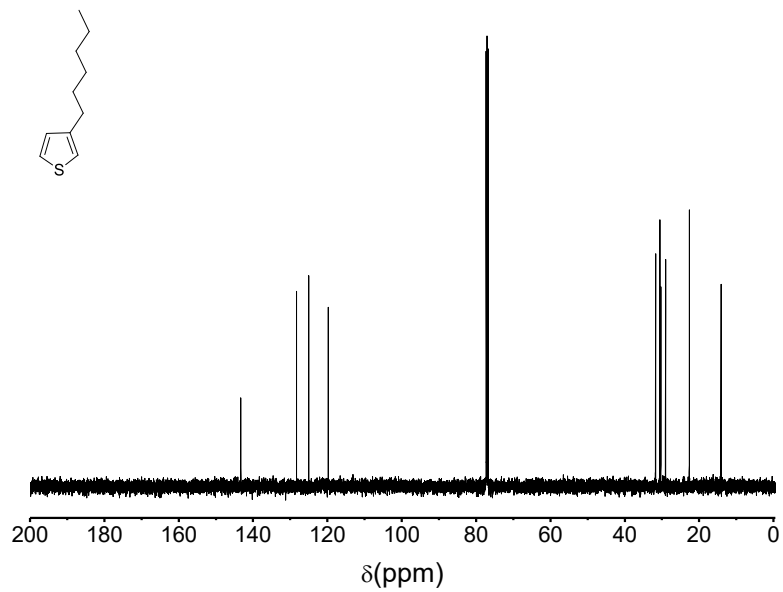
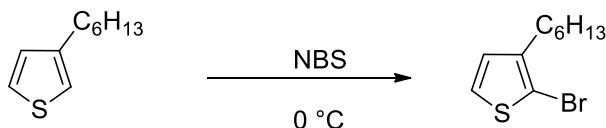


Figure 4.2. ^{13}C NMR spectrum of 3-hexylthiophene

Synthesis of 2-bromo-3-hexylthiophene



Scheme 4.2. Synthesis of 2-bromo-3-hexylthiophene

3-Hexylthiophene (5.00 g, 0.0297 mol) was dissolved in THF:hexane (9:1) solvent mixture (60 mL) in a round bottomed flask and N-bromosuccinimide (5.36 g, 0.0302 mol) was added slowly while stirring at 0 °C over a period of 1 h. The reaction mixture was stirred at room temperature for two hours, quenched in water, extracted with diethyl ether (3×100 mL), washed with deionized water (3×100 mL), dried over anhydrous MgSO₄ and evaporated under reduced pressure to obtain yellow colored oil which was purified by column chromatography using hexane as the eluting solvent to obtain a clear oil (6.11 g, 76 %). ¹H-NMR (CDCl₃, 500 MHz; 7.18 (d, 1H, J=5.6), 6.79 (d, 1H, J=5.6), 2.56 (t, 2H), 1.57 (m, 2H), 1.31 (m, 6H), 0.89 (t, 3H). ¹³C-NMR (CDCl₃, 500 MHz; 141.99, 128.24, 125.12, 108.79, 31.62, 29.71, 29.40, 28.90, 22.60, 14.09). ¹H-NMR and ¹³C-NMR spectra are given in figure 4.3 and figure 4.4.

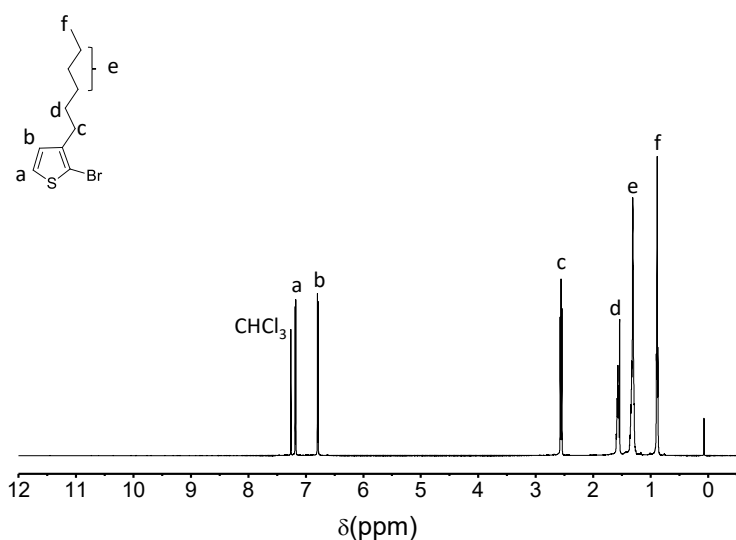


Figure 4.3. ¹H NMR spectrum of 2-bromo-3-hexylthiophene

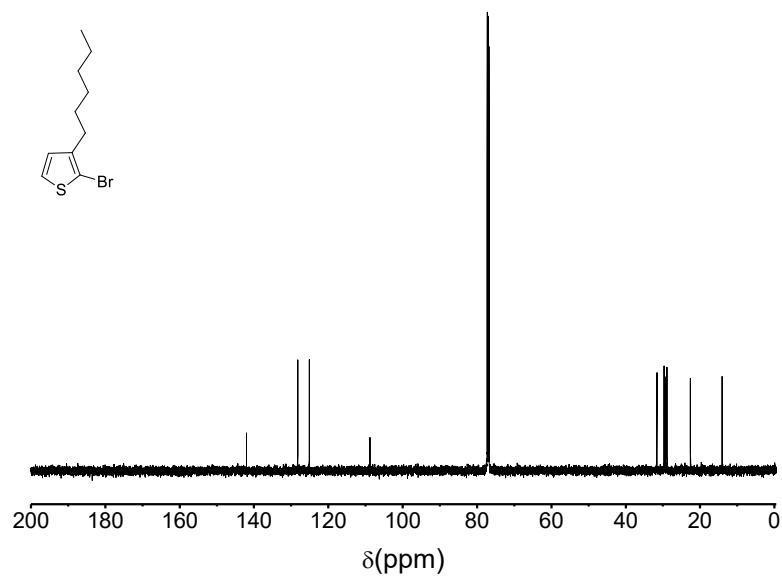
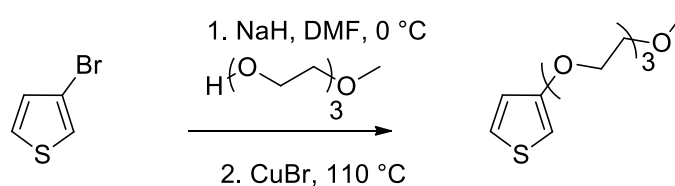


Figure 4.4. ^{13}C NMR spectrum of 2-bromo-3-hexylthiophene

Synthesis of 3-(2-(2-(2-methoxyethoxy)ethoxy)ethoxy)thiophene



Scheme 4.3. Synthesis of 3-(2-(2-(2-methoxyethoxy)ethoxy)ethoxy)thiophene

NaH (3.68 g, 153 mmol) was introduced to a three-neck round bottomed flask equipped with a condenser and mixed with dry DMF (20 mL) under nitrogen. Triethylene glycol monomethyl ether (20.5 g, 116 mmol) was added dropwise from a syringe over a period of 30 min while maintaining the temperature at 0 °C. The mixture was stirred for an hour at 0 °C to assure complete consumption of NaH. 3-Bromothiophene (12.9 g, 79.1 mmol) and CuBr (0.45 g, 3.14 mmol) were added to the reaction mixture at this point and it was heated to 110 °C. After 30 min at the elevated temperature, an aliquot was taken out, quenched with a 1 M aqueous solution of NH_4Cl , extracted

with diethyl ether and subjected to GC-MS analysis. As abundance of starting materials were present in the reaction mixture an additional amount of CuBr (0.57 g, 3.97 mmol) was added at this point and the reaction was allowed to proceed at the elevated temperature for 1 h. The progress of the reaction was monitored with GC-MS analysis and more CuBr (1.51 g, 10.5 mmol) was added until 3-bromothiophene was consumed. Reaction mixture was heated at 110 °C overnight after which no 3-bromothiophene was present. The mixture was poured into a 1 M aqueous solution of NH₄Cl (100 ml) and stirred for 10 min, extracted with hexane, dried over anhydrous MgSO₄ and evaporated under reduced pressure to obtain the yellow colored crude oily product (11.6 g) which was used for the next step without further purification. ¹H-NMR (CDCl₃, 500 MHz; 7.16(dd, 1H, J=5.2, J=3.2), 6.77(d, 1H, J=5.2), 6.26(s, 1H), 4.12(t, 2H), 3.84-3.54(m, 10H), 3.38(s, 3H). ¹³C-NMR (CDCl₃, 500 MHz; 157.62, 124.64, 119.61, 97.51, 71.94, 70.79, 70.67, 70.58, 69.70, 69.58, 59.04). ¹H-NMR and ¹³C-NMR spectra are given in figure 4.5 and figure 4.6.

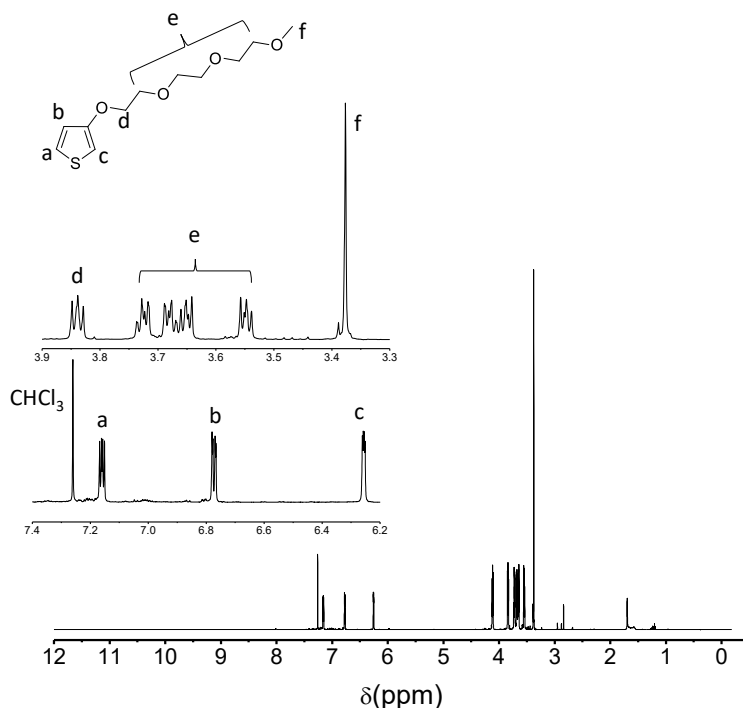


Figure 4.5. ¹H NMR spectrum of 3-(2-(2-(2-methoxyethoxy)ethoxy)ethoxy)thiophene

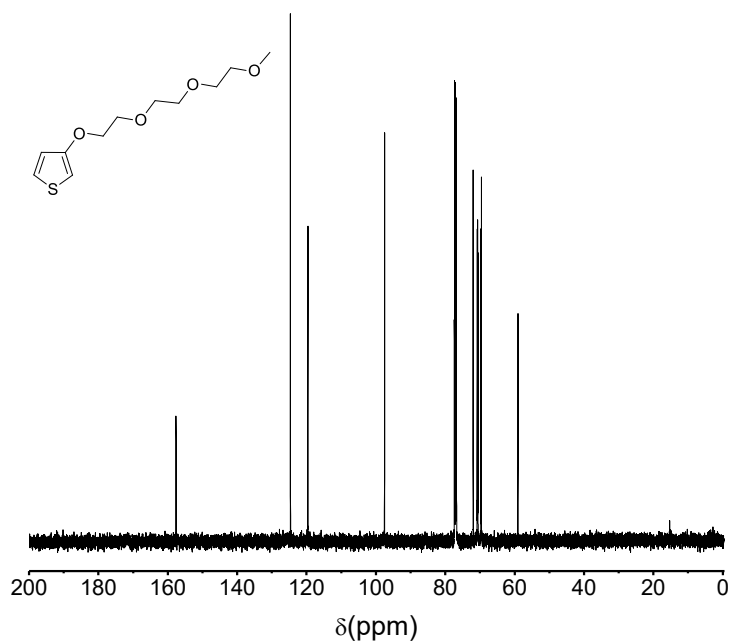
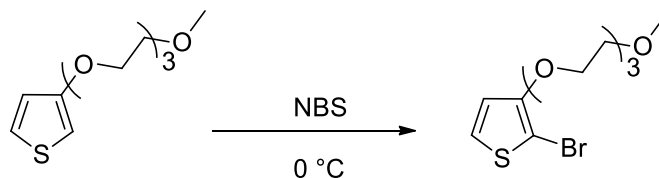


Figure 4.6. ^{13}C NMR spectrum of 3-(2-(2-(2-methoxyethoxy)ethoxy)ethoxy)thiophene

Synthesis of 2-bromo-3-(2-(2-(2-methoxyethoxy)ethoxy)ethoxy)thiophene



Scheme 4.4. Synthesis of 2-bromo-3-(2-(2-(2-methoxyethoxy)ethoxy)ethoxy)thiophene

The crude 3-(2-(2-methoxyethoxy)ethoxy)ethoxy)thiophene (4.93 g, 20.0 mmol) was dissolved in THF: Hexane mixture (9:1, 150 mL) in a round bottomed flask and cooled down to $-5\text{ }^{\circ}\text{C}$. N-bromosuccinimide (3.58 g, 20.0 mmol) was added in to the mixture in small portions over a period of 1 h. After all the NBS have been added the reaction mixture was stirred for 2 h at $0\text{ }^{\circ}\text{C}$. The mixture was poured into a beaker with deionized water and extracted with hexane ($3\times 100\text{ mL}$). Combined organic layers were washed with deionized water, dried over anhydrous MgSO_4 and evaporated under reduced pressure. The crude compound was purified by column chromatography using ethyl acetate: hexane (2:3) as the eluting solvents (4.04g, 62 %). $^1\text{H-NMR}$ (CDCl_3 , 500

MHz; 7.18(d, 1H, J=6.0), 6.77(d, 1H, J=6.0), 4.20(t, 2H), 3.83-3.54(m, 10H), 3.38(s, 3H). ¹³C-NMR (CDCl₃, 500 MHz; 154.44, 124.31, 118.04, 92.30, 72.00, 71.73, 71.01, 70.72, 70.62, 69.90, 59.10). ¹H-NMR and ¹³C-NMR spectra are given in figure 4.7 and figure 4.8.

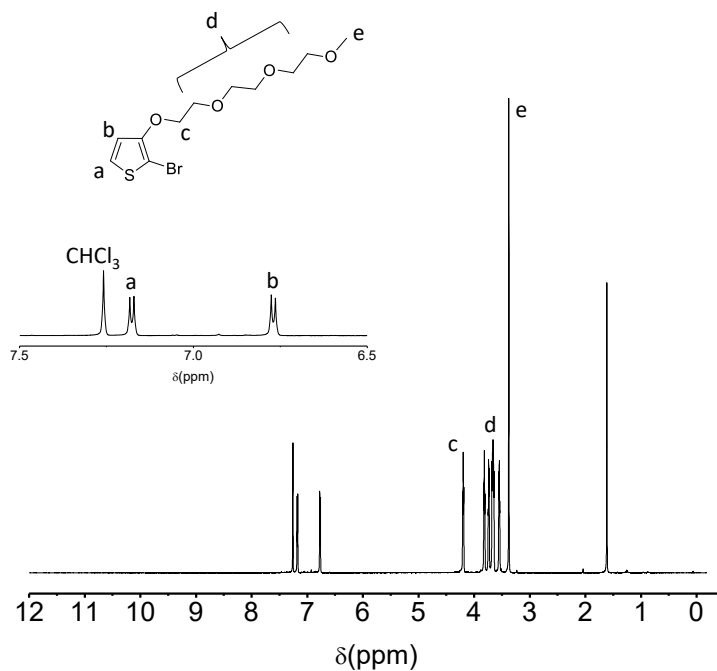


Figure 4.7. ¹H NMR spectrum of 2-bromo-3-(2-(2-(2-methoxyethoxy)ethoxy)ethoxy)thiophene

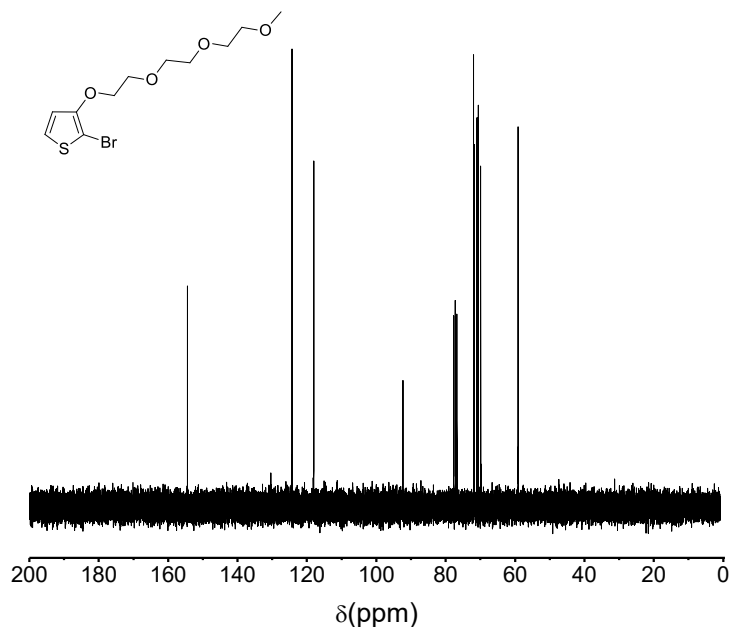
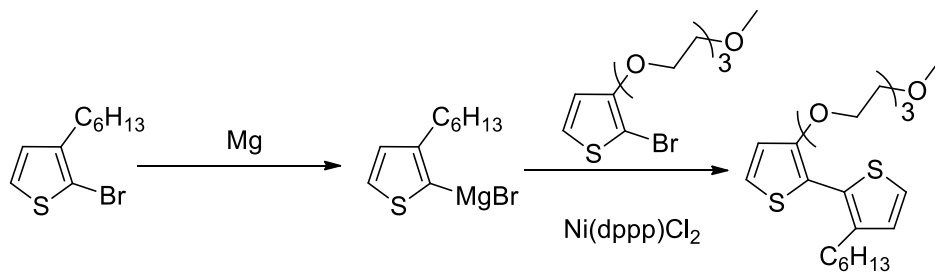


Figure 4.8. ^{13}C NMR spectrum of 2-bromo-3-(2-(2-(2-methoxyethoxy)ethoxy)ethoxy)thiophene

Synthesis of 3-hexyl-3'-(2-(2-(2-methoxyethoxy)ethoxy)ethoxy)bithiophene



Scheme 4.5. Synthesis of 3-hexyl-3'-(2-(2-(2-methoxyethoxy)ethoxy)ethoxy)bithiophene

Mg (0.401g, 16.5 mmol) was kept under vacuum in a 100 mL three-necked round bottomed flask equipped with a reflux condenser prior to the addition of THF (10 mL) and 2-bromo-3-hexylthiophene (2.73 g, 11.0 mmol) under nitrogen. The Grignard reaction was allowed to proceed for 2 h at 60 °C. Ni(dppp)Cl₂ (0.357 g, 0.659 mmol) was kept under vacuum in another 100 mL three-neck round bottomed flask equipped with a reflux condenser prior to the addition of THF (50 mL) and 2-bromo-3-(2-(2-(2-methoxyethoxy)ethoxy)ethoxy)thiophene (0.390 g, 11.0 mmol)

under nitrogen. The Grignard mixture was cannulated to the other flask containing 2-bromo-3-(2-(2-(2-methoxyethoxy)ethoxy)ethoxy)thiophene and the catalyst Ni(dppp)Cl₂. The resultant mixture was stirred under reflux for 5 days, quenched in water, extracted with hexane (3×100 mL). Combined organic layers were washed with deionized water, dried over anhydrous MgSO₄ and evaporated under reduced pressure to obtain the crude product. Purification was carried out by column chromatography using ethyl acetate:hexane (2:3) as eluting solvents (1.82 g, 37 %). ¹H-NMR (CDCl₃, 500 MHz; 7.22(d, 1H, J=5.2), 7.18(d, 1H, J=5.6), 6.90(d, 1H, J=5.2), 6.88(d, 1H, J=5.6) 4.16(t, 2H), 3.78-3.46 (m, 10H), 3.37(s, 3H), 2.67(t, 2H), 1.32(m, 8H), 0.88(t, 3H). ¹³C-NMR (CDCl₃, 500 Mz; 153.24, 140.85,128.85, 127.50, 124.56, 123.27,118.16, 114.31, 71.95, 71.35, 70.85, 70.67, 70.56, 69.91, 59.05, 31.70, 30.55, 29.35, 29.26, 22.63, 14.11). ¹H-NMR and ¹³C-NMR spectra are given in figure 4.9 and figure 4.10.

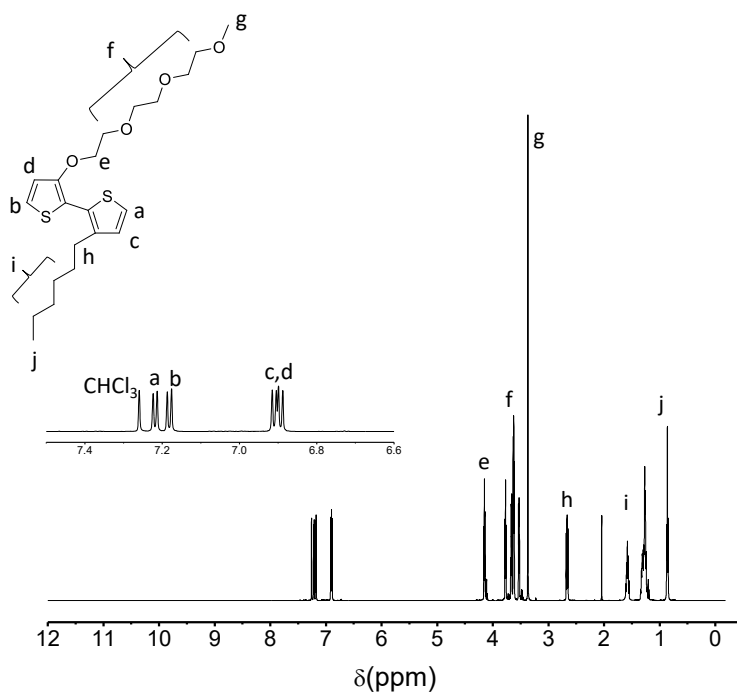


Figure 4.9. ¹H NMR spectrum of 3-hexyl-3'-(2-(2-(2-methoxyethoxy)ethoxy)ethoxy)bithiophene

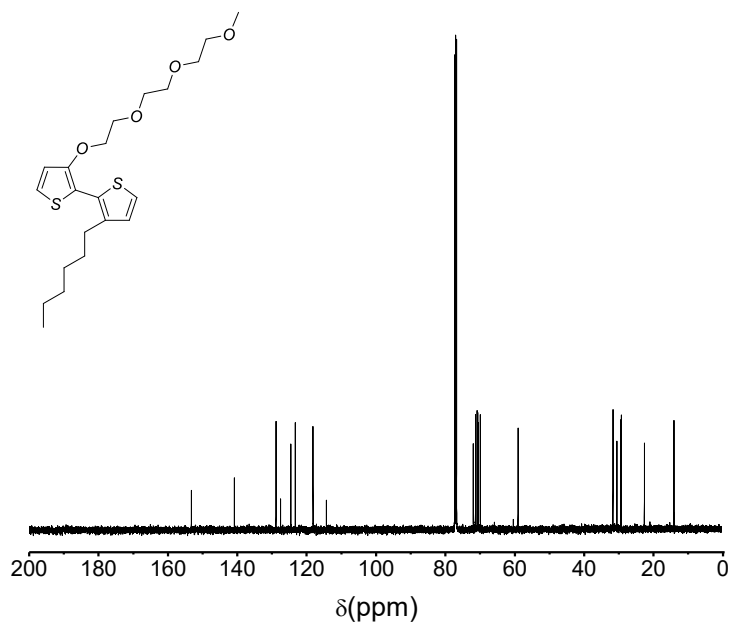
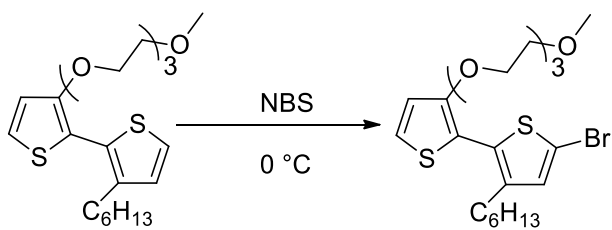


Figure 4.10. ^{13}C NMR spectrum of 3-hexyl-3'-(2-(2-(2-methoxyethoxy)ethoxy)ethoxy)bithiophene

Synthesis of 2-bromo-3-hexyl-3'-(2-(2-(2-methoxyethoxy)ethoxy)ethoxy)bithiophene



Scheme 4.6. Synthesis of 2-bromo-3-hexyl-3'-(2-(2-(2-methoxyethoxy)ethoxy)ethoxy)bithiophene

3-hexyl-3'-(2-(2-(2-methoxyethoxy)ethoxy)ethoxy)-2,2'-bithiophene (1.82 g, 4.42 mmol) was dissolved in THF: Hexane mixture (9:1, 300 mL) in a round bottomed flask and cooled down to 0 °C. N-bromosuccinimide (0.788 g, 4.42 mmol) was added in to the mixture in small portions over a period of 30 min. After all the N-bromosuccinimide have been added the reaction mixture was stirred for 2 h at 0 °C. The mixture was poured into a beaker with deionized water and

extracted with ether (3×100 mL). Combined organic layers were washed with deionized water (3×100 mL), dried over anhydrous MgSO₄ and evaporated under reduced pressure. The crude compound was purified by column chromatography using ethyl acetate: hexane (1:4) as the eluting solvents to obtain the orange colored oil (1.32 g, 61 %). ¹H-NMR (CDCl₃, 500 MHz; 7.19(d, 1H, J=5.6), 6.89(d, 1H, J=5.6), 6.86(s, 1H), 4.18(t, 2H), 3.81-3.53(m, 10H), 3.37(s, 3H), 2.62(t, 2H), 1.27(m, 8 H), 0.88(t, 2H). ¹³C-NMR (CDCl₃, 500 MHz; 153.53, 140.95, 131.52, 129.33, 123.58, 117.75, 113.26, 111.08, 71.95, 71.38, 70.87, 70.68, 70.58, 69.86, 59.06, 31.64, 30.37, 29.44, 29.16, 22.60, 14.10). ¹H-NMR and ¹³C-NMR spectra are given in figure 4.11 and figure 4.12. 2D-NMR analysis is given in figure 4.13 and figure 4.14.

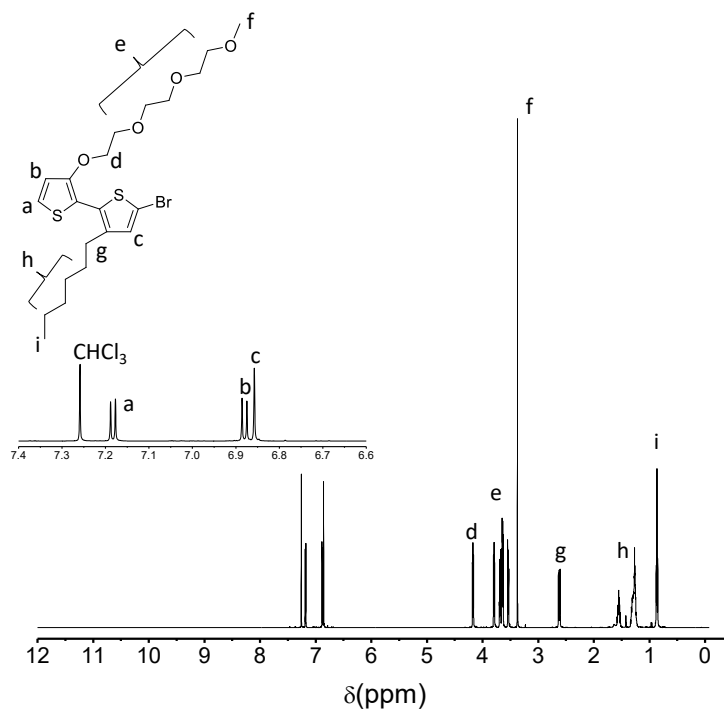


Figure 4.11. ¹H NMR spectrum of 2-bromo-3-hexyl-3'-(2-(2-(2-methoxyethoxy)ethoxy)ethoxy)bithiophene

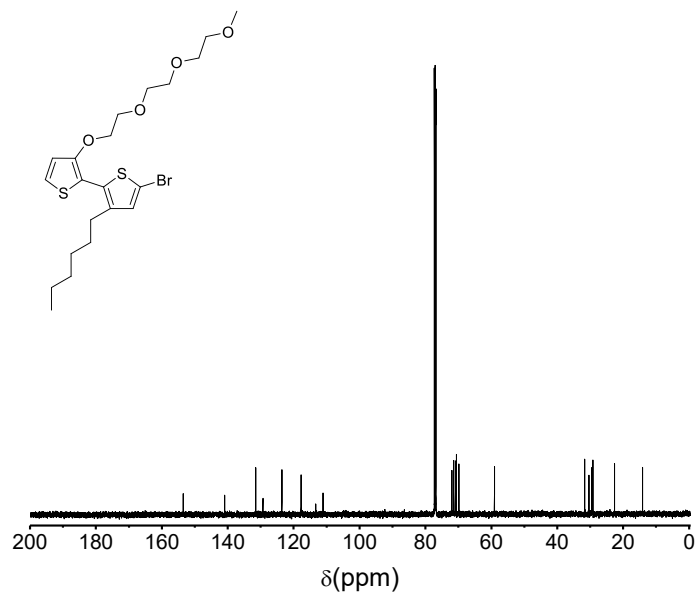


Figure 4.12. ^{13}C NMR spectrum of 2-bromo-3-hexyl-3'-(2-(2-(2-methoxyethoxy)ethoxy)ethoxy)bithiophene

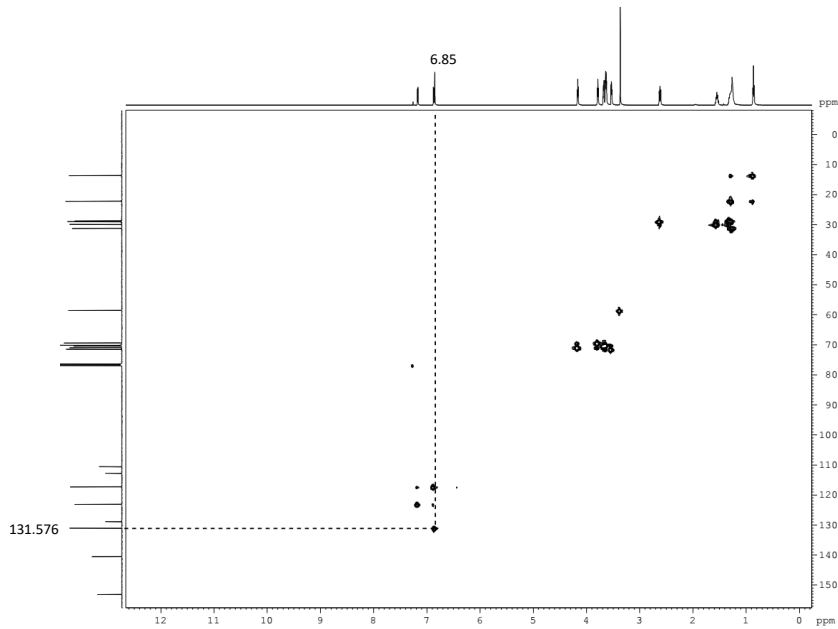


Figure 4.13. HSQC spectrum of 2-bromo-3-hexyl-3'-(2-(2-(2-methoxyethoxy)ethoxy)ethoxy)bithiophene

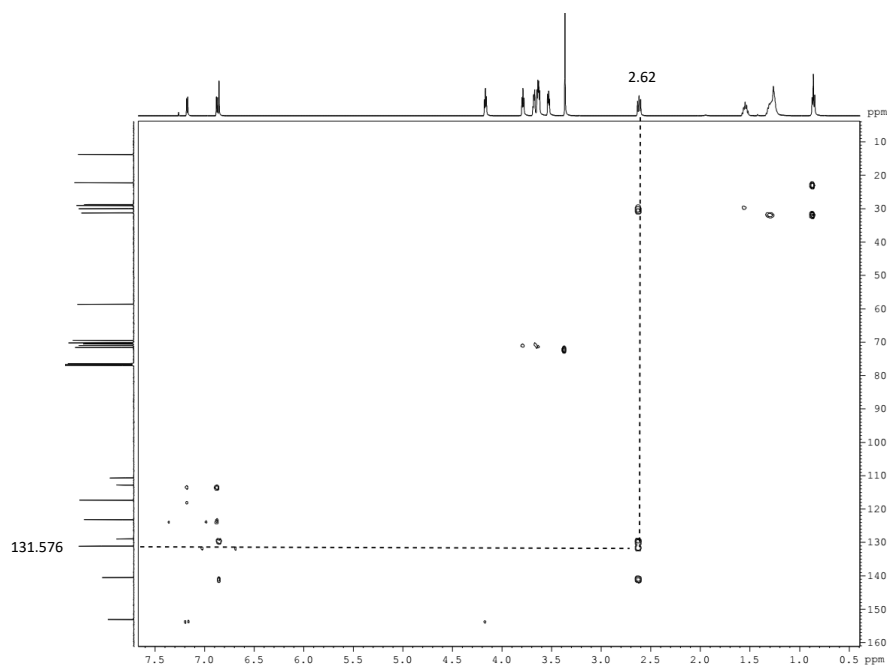
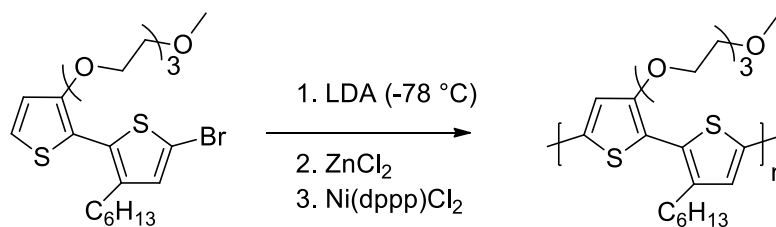


Figure 4.14. HMBC spectrum of 2-bromo-3-hexyl-3'-(2-(2-(2-methoxyethoxy)ethoxy)ethoxy)bithiophene

Synthesis of poly[3-hexyl-3'-(2-(2-(2-methoxyethoxy)ethoxy)ethoxy)bithiophene]



Scheme 4.7. Synthesis of poly[3-hexyl-3'-(2-(2-(2-methoxyethoxy)ethoxy)ethoxy)bithiophene]

Freshly distilled isopropylamine (0.55 mL, 3.87 mmol) was added to a three neck round bottom flask containing dry THF (10 mL) under nitrogen. The solution was then cooled to $-78\text{ }^{\circ}\text{C}$ and *n*-BuLi (1.30 mL, 3.22 mmol) was added while stirring. The reaction mixture was allowed to stir at the same temperature for 1 h. To this mixture, 2-Bromo-3-hexyl-3'-(2-(2-(2-methoxyethoxy)ethoxy)ethoxy)bithiophene (1.32 g, 2.69 mmol) in dry THF (10 mL) was added at $-78\text{ }^{\circ}\text{C}$ and the reaction mixture was stirred at the same temperature for 1 h. After 1 h of stirring the round

bottomed flask was lifted up from the cold bath in a such a way that it barely touches the surface of the cold bath ($\sim -40\text{ }^{\circ}\text{C}$) and ZnCl_2 (0.586g, 4.30 mmol) was added and stirred for 1 h at $-78\text{ }^{\circ}\text{C}$. The reaction mixture was allowed to warm to room temperature and $\text{Ni}(\text{dppp})\text{Cl}_2$ (7.26 mg, 0.0134 mmol) (monomer: catalyst 200:1) was added at room temperature while stirring. The reaction mixture was stirred at $40\text{ }^{\circ}\text{C}$ for 4 h before cooling to room temperature and precipitated in methanol. The solid was filtered and the polymer was purified via Soxhlet extractions with methanol, hexane and chloroform. Polymer was obtained as a dark blue solid by evaporating chloroform (200 mg, 18 %). $^1\text{H-NMR}$ (CDCl_3 , 500 MHz; 7.01 (s, 1H), 6.98 (s, 1H), 4.26 (t, 2H), 2.73 (t, 2H), 3.35 (s, 3H), 0.90 (t, 3H)) SEC: $M_n = 9332$, PDI = 2.25. $^1\text{H-NMR}$ spectrum is given in figure 4.15.

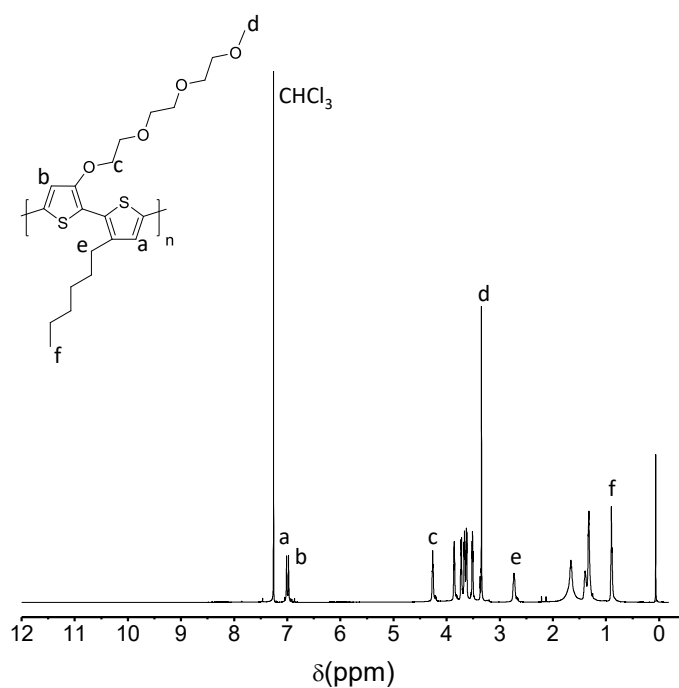


Figure 4.15. $^1\text{H-NMR}$ spectrum of poly[3-hexyl-3'-(2-(2-(2-methoxyethoxy)ethoxy)ethoxy)bithiophene]

4.4 Results and Discussion

The synthesis of poly[3-hexyl-3'-(2-(2-(2-methoxyethoxy)ethoxy)ethoxy)bithiophene] was carried out as follows; Starting material 2-bromo-3-hexylthiophene was synthesized by a nickel catalyzed Kumada coupling reaction between 3-bromothiophene and hexylmagnesium bromide followed by bromination with N-bromosuccinimide (NBS). Starting material 2-bromo-3-(2-(2-(2-methoxyethoxy)ethoxy)ethoxy)thiophene was synthesized by copper mediated substitution of 3-bromothiophene,²⁷ followed by bromination with NBS. The dimer 2-bromo-3-hexyl-3'-(2-(2-(2-methoxyethoxy)ethoxy)ethoxy)bithiophene was synthesized by nickel catalyzed Kumada coupling reaction between 2-bromo-3-hexylthiophene and 2-bromo-3-(2-(2-(2-methoxyethoxy)ethoxy)ethoxy)thiophene, followed by a bromination with NBS. The position of the monobromination of 2-bromo-3-hexyl-3'-(2-(2-(2-methoxyethoxy)ethoxy)ethoxy)bithiophene was confirmed via 2D NMR analysis and the spectra are given in (figure 4.13 and 4.14). HMBC correlation of hexyl α carbon with thiophene singlet proton revealed that the monobromination occurred on the hexyl thiophene ring.

McCullough method was used for polymerization of 2-bromo-3-hexyl-3'-(2-(2-(2-methoxyethoxy)ethoxy)ethoxy)bithiophene, in which LDA was used to abstract the bithiophene proton at the 5'-position followed by metal exchange via the addition of $ZnCl_2$. The polymerization was then catalyzed with $Ni(dppp)Cl_2$.²⁸

The polymer formation was confirmed by SEC analysis (table 4.1) and 1H -NMR analysis. The 1H -NMR spectrum of the polymer is shown in figure 4.15. The two singlet protons around 7 ppm are due to the thiophene protons. The triplet around 4.3 ppm is due to the αCH_2 in the alkoxy chains and singlet around 3.3 ppm is due to the methoxy groups. The two triplets around 2.7 ppm and 0.9 ppm are due to the αCH_2 protons in hexyl chains and terminal CH_3 groups, respectively.

Table 4.1. Molecular weights and optoelectronic properties of the polymer

Molecular weight ^a (g mol ⁻¹)	9332
PDI	2.25
λ_{max} (CHCl ₃) ^b (nm)	476
λ_{max} (film) ^c (nm)	549, 579, 640
Optical Band gap (eV)	1.48
HOMO (eV) ^d	-4.74
LUMO (eV) ^e	-2.96
E _g (eV)	1.78

Determined by ^aSEC (THF eluent),^bUV-Vis absorption maxima of polymer solution in chloroform, ^cUV-Vis absorption maxima of polymer film drop-casted from chloroform solution, ^dEstimated from the onset of oxidation peak of the cyclic voltammogram, ^eEstimated from the onset of reduction peak of the cyclic voltammogram.

The HOMO and LUMO energy levels of the polymer was estimated by cyclic voltammetry from the onset of oxidation and reduction peaks, respectively (figure 4.16). Due to the strong electron donating properties of MEEE side chains, the resultant polymer showed significantly high HOMO levels and hence lower band gap. The values are given in table 4.1.

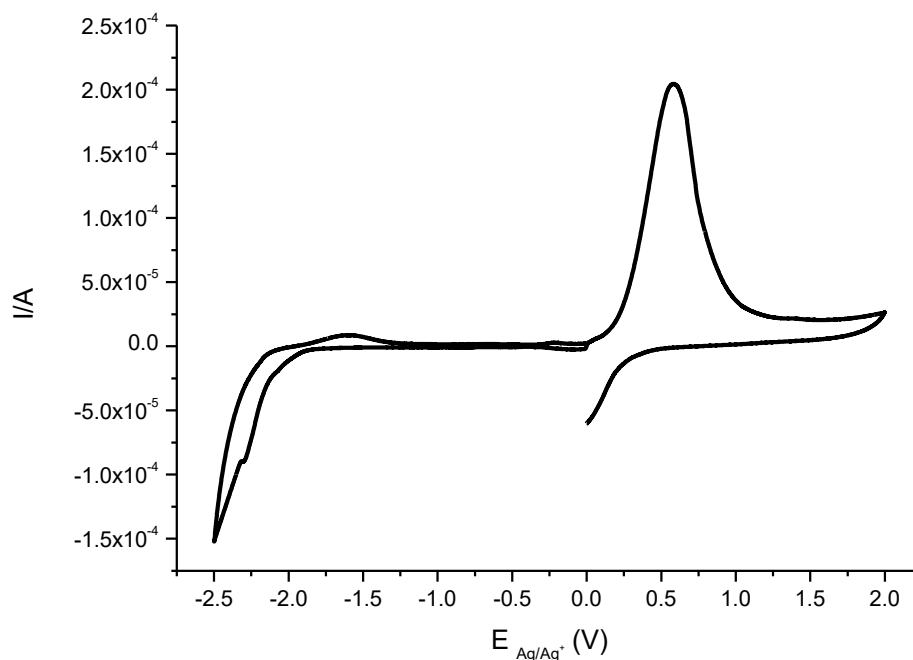


Figure 4.16. Cyclic voltammogram of the polymer

The optical properties of the polymer was characterized by UV-visible spectroscopy (figure 4.17a). The UV-Vis spectra in chloroform solution showed one absorption maximum around 476 nm (table 4.1), attributed to the absorption of π - π^* transition of the conjugated polymer main chain. In thin film the absorption maximum is red shifted by ~100 nm with shoulder peaks indicating increased intermolecular ordering of the polymer in solid state compared to the solution.

Furthermore, the polymers showed solvatochromism in THF/Water solvent mixtures (figure 4.17b). Incremental addition of water (non-solvent for PTs) to a solution of polymers in THF, a good solvent for the polymer resulted in a red-shifted absorption and concentration independent vibronic structures. We observed the same phenomenon in our previous work of regioregular P3HT based block copolymers and speculate that it is due to the formation of micellar or vesicular aggregates formed by self-assembly to generate core-shell type structure.²⁹⁻³¹ In this case we believe that the observed red-shift may be due to the aggregates that we have observed in TEM images of the polymer drop-casted from THF/water (3:2) solvent mixture (figure 4.17d).

Interestingly the polymer displayed different morphologies in different solvents. The morphology of the polymers drop-casted from chloroform, and THF/water was studied using TEM and the images are shown in figure 4.17. In chloroform, the hydrophilic MEEE segments might tend to self-assemble so that the hydrophilic chains stay away from the solvent resulting in micellar like aggregates (figure 4.17c). In THF/water mixture the MEEE segments shows more favorable interactions with the solvent showing more linear aggregates (figure 4.17d). We further investigated the size distribution of the micellar aggregates using DLS analysis (figure 4.18). DLS analysis showed a uniform micellar distribution of ~100 nm whereas TEM image shows a larger micellar size. We speculate that this could be due to the aggregation of micelles upon thin film deposition as seen in TEM image.

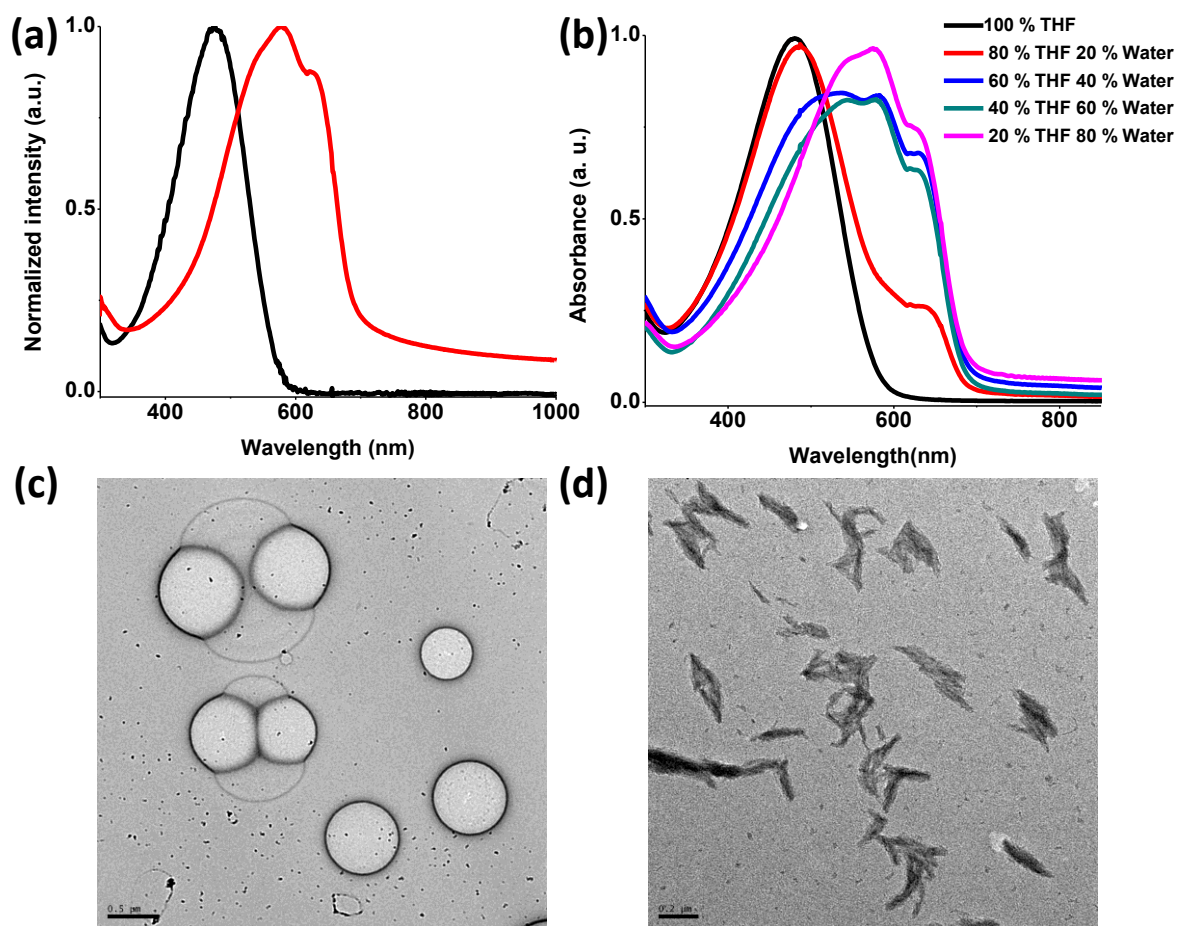


Figure 4.17. UV-vis spectra of polymer in chloroform solution (black) and in thin film (red) (b) solution UV-Vis spectra of the polymer in THF and THF/water mixtures. (c) TEM images of the polymer drop-casted from (c) chloroform (d) THF/water (3:2) solvent mixture with 0.30 mg mL^{-1} .

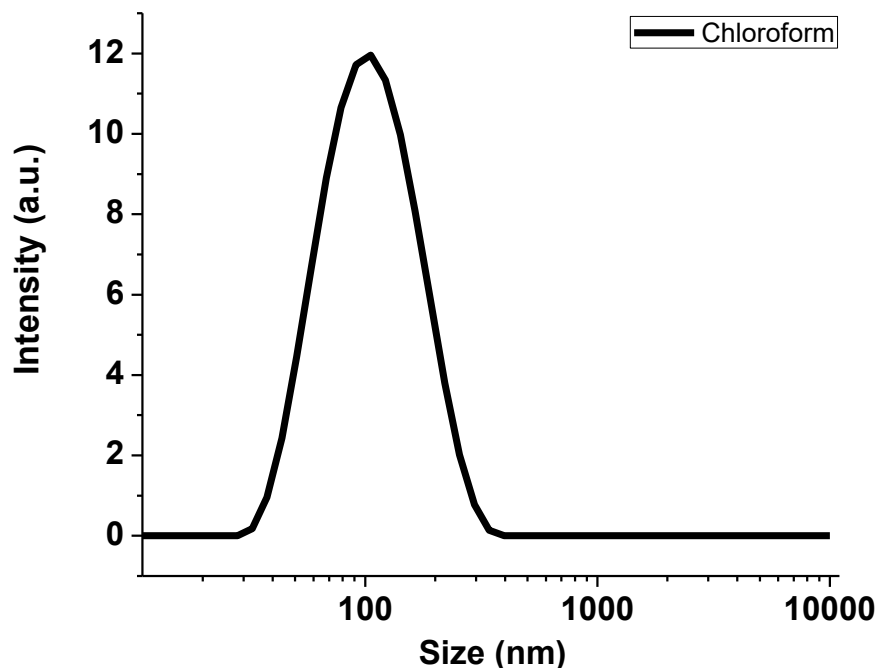


Figure 4.18. DLS analysis of the polymer in chloroform

Furthermore, GIWAXS data was also obtained from a film of the polymer and the data is shown in figure 4.19. We assigned the peak at $q \sim 0.4 \text{ \AA}^{-1}$ to the distance between polymer backbones through the alkyl side-chains. The broad peak at q of 1.53 \AA^{-1} corresponds to a π - π stacking distance of 4.1 \AA , which is larger than that of P3HT.³² Another peak was visible at 0.83 \AA^{-1} in the in-plane data shown in figure 4.19b. This peak suggested the crystal structure of MEEE substituted polythiophene may differ from that of P3HT.^{32,33}

Comparing the π -stacking peak of MEEE substituted polythiophene to regio-random P3HT, which is amorphous, the breadth and position are similar.³⁴ The broad π stacking peak suggests weak coupling between chains. As a consequence, the GIWAXS data suggests that MEEE substituted polythiophene will exhibit lower charge mobilities when compared to regioregular P3HT. Figure 4.20 shows the in-plane and out of plane intensities of GIWAXS data with GISAXS data.

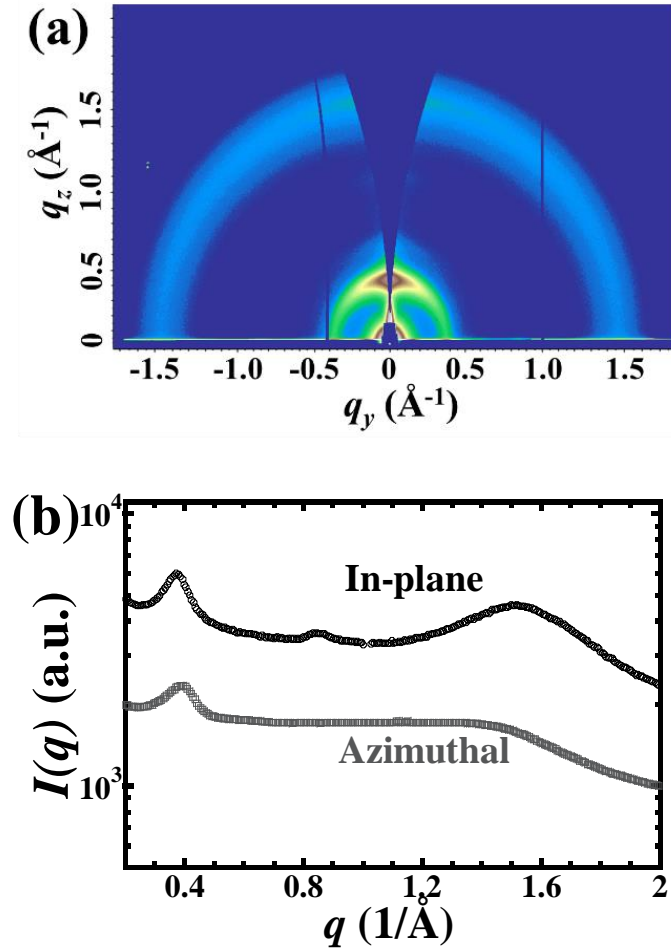


Figure 4.19. (a) GIWAXS data from a film of the polymer. (b) GIWAXS intensity vs scattering vector q . Both azimuthally-averaged data and in-plane line cuts are shown.

Thermogravimetric analysis of the polymer showed thermal stability up to ~ 300 $^{\circ}\text{C}$ and showed 5% weight loss at 340 $^{\circ}\text{C}$ (figure 4.21). According to the DSC analysis (figure 4.22), the glass transition temperature is observed around 90 $^{\circ}\text{C}$, melting of the polymer around 160 - 170 $^{\circ}\text{C}$ and the crystallization temperature around 125 $^{\circ}\text{C}$.

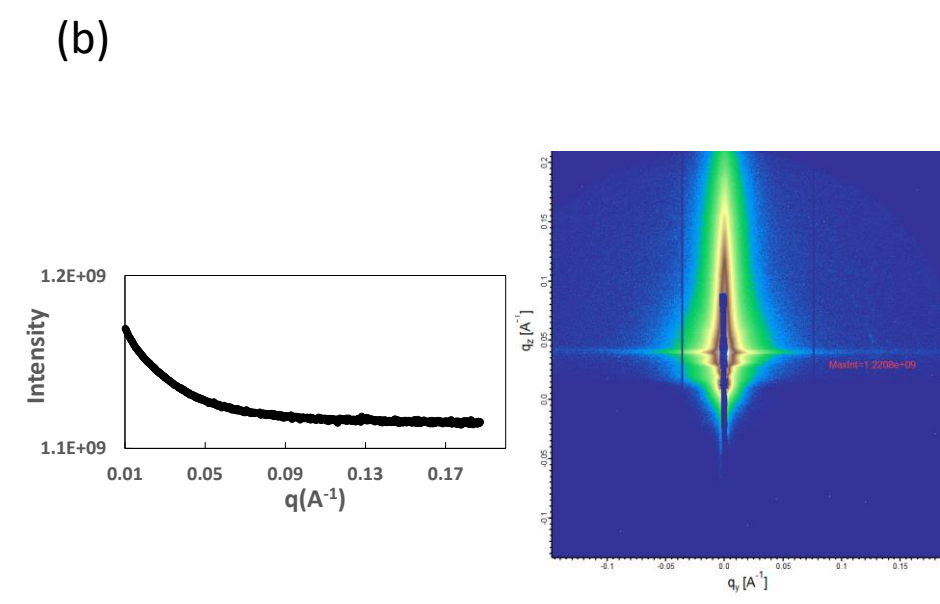
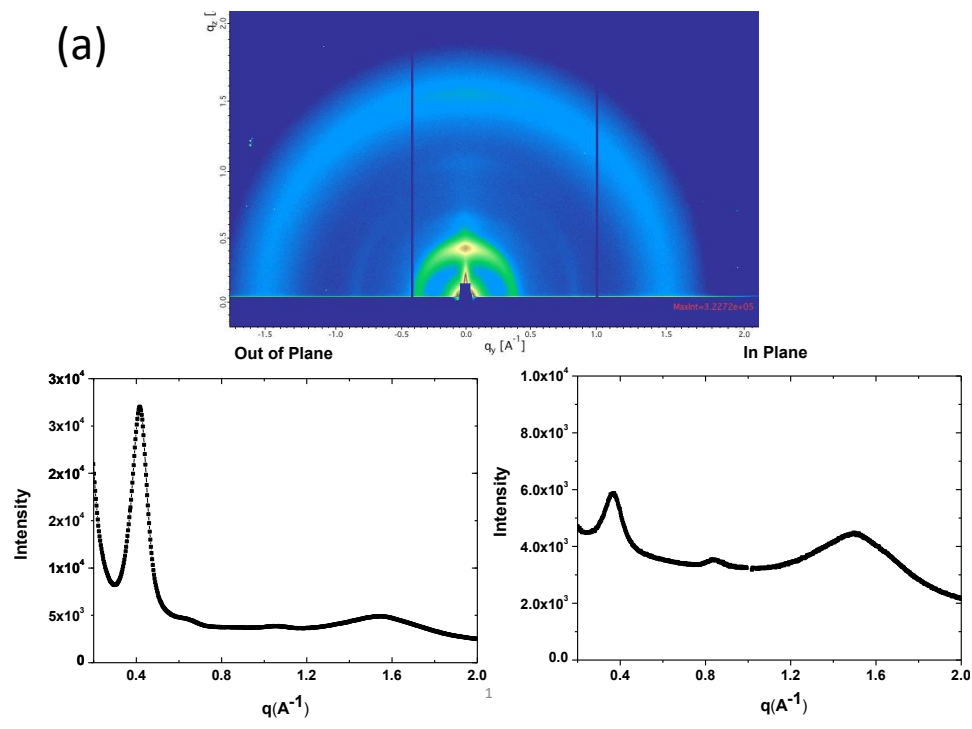


Figure 4.20. (a) GIWAXS data in-plane and out of plane intensities (b) GISAXS data for the polymer

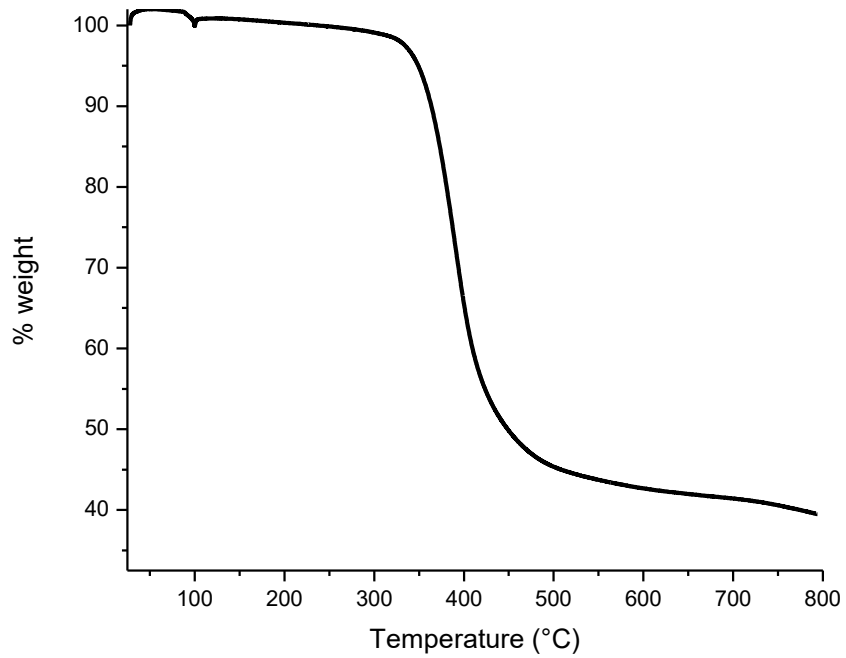


Figure 4.21. TGA thermogram of the polymer

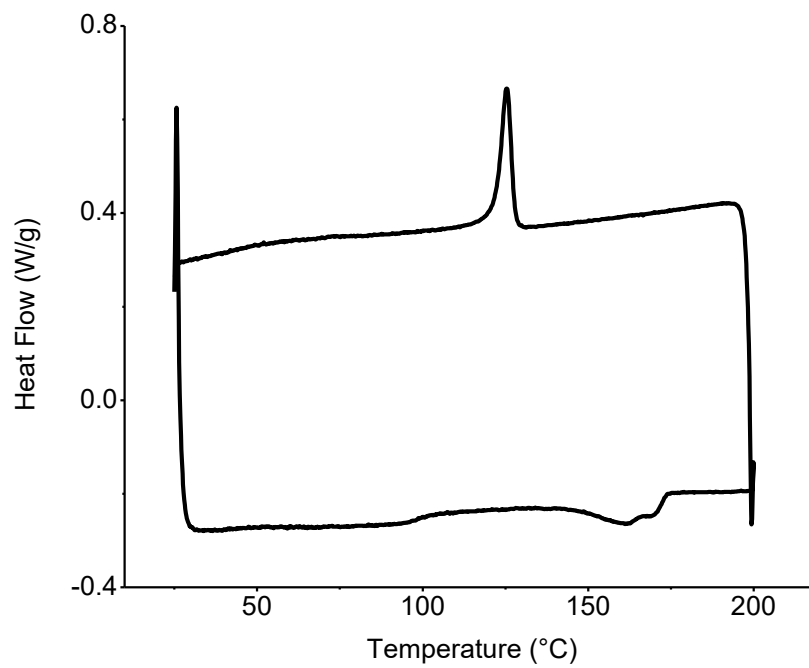


Figure 4.22. DSC analysis of the polymer at $10\text{ }^{\circ}\text{C min}^{-1}$

In order to study the mobility of the charge carriers, the polymer was tested in field effect transistors as well as in Schottky diode. Field-effect mobilities were extracted from the electrical characterization of thin-film transistors with the polymer as the active layer. Devices were fabricated with a bottom-gate, bottom-contact configuration. Surfaces were cleaned with UV-Ozone treatment for 10 min; no other surface treatment was applied, because self-assembled monolayers such as octadecyltrichlorosilane deposited on the dielectric surface led to dewetting of the polymer. I_D vs. V_D curves are given in figure 4.23a. The linear behavior at low source-drain voltages suggests a lack of significant contact barriers. I_D vs V_G is shown in figure 4.23b, and the average threshold voltage is -30 V (± 22.2 V) and the on/off ratio is 8.8×10^1 ($\pm 5.1 \times 10^1$). The field-effect mobility was obtained from the slope of $I_D^{1/2}$ vs. V_G (saturation regime) using:

$$\mu_{sat} = \frac{2L}{WC_i} m^2 \quad (4.5)$$

Where, μ_{sat} is the field-effect mobility obtained in the saturation regime, L is the channel length, W is the channel width, C_i is the capacitance of the dielectric and m is the slope of the plot of $I_D^{1/2}$ vs. V_G at saturation. The average mobility of devices with the polymer as the active layer is $4.2 \times 10^{-4} \text{ cm}^2 \text{ V}^{-1} \text{ s}^{-1}$ ($\pm 4.8 \times 10^{-5} \text{ cm}^2 \text{ V}^{-1} \text{ s}^{-1}$), which is lower than that of devices with regioregular P3HT as the active layer, even when devices lack self-assembled monolayers at the dielectric surface.²⁶ Space charge limited current model in Schottky diode revealed that the polymer has vertical hole mobility of $3.47 \times 10^{-7} \text{ cm}^2 \text{ V}^{-1} \text{ s}^{-1}$ ($\pm 6.67 \times 10^{-8} \text{ cm}^2 \text{ V}^{-1} \text{ s}^{-1}$) (figure 4.24)

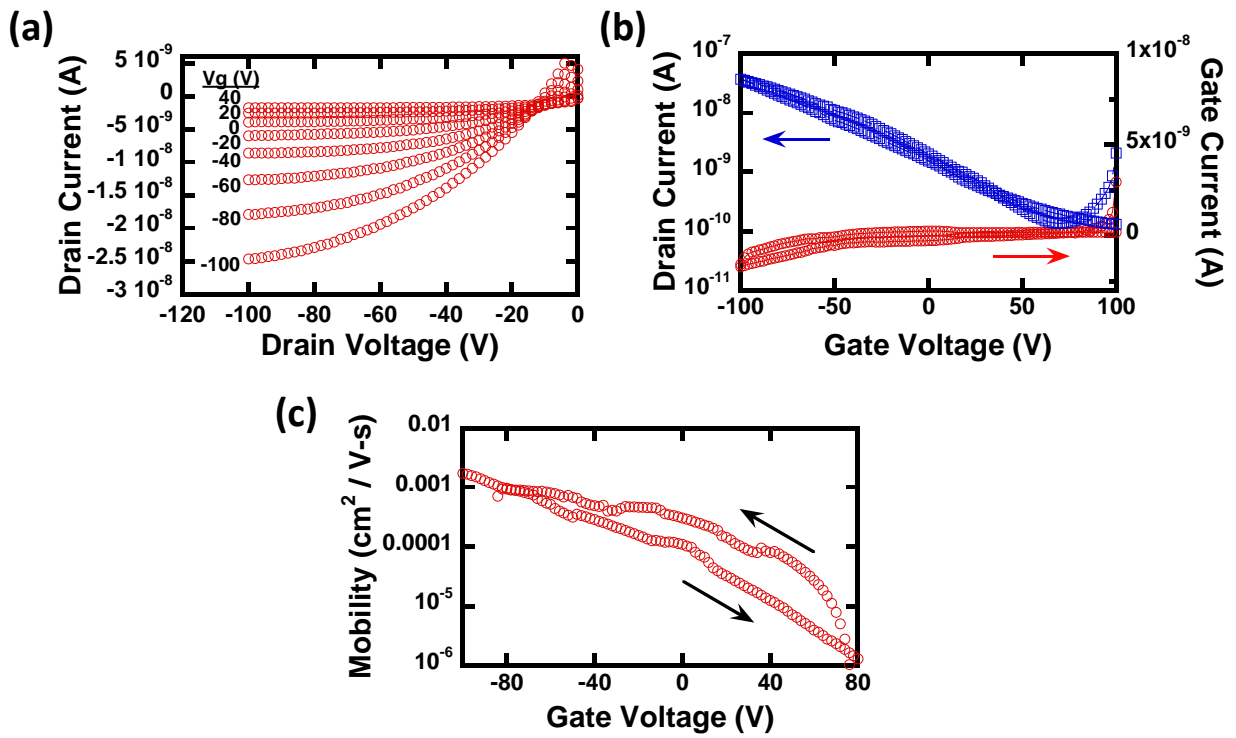


Figure 4.23. (a) Output curves of the polymer at different gate voltages (I_D Vs. V_D curves) (b) I_D Vs V_G (c) saturation mobility

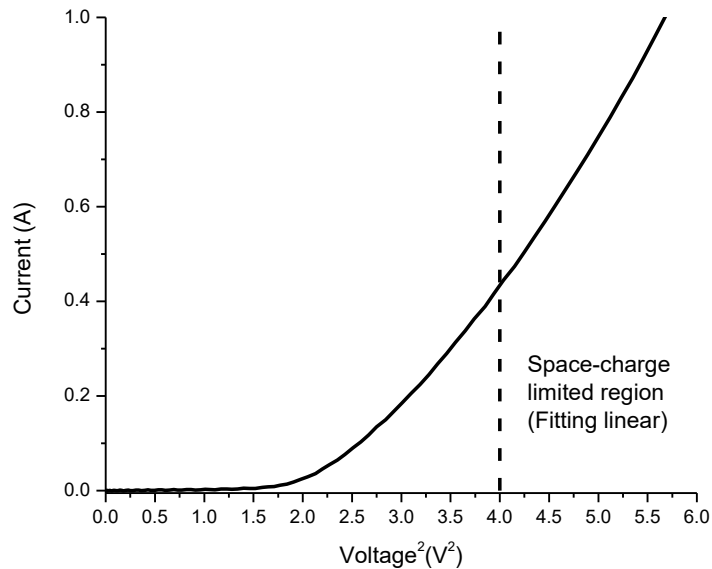


Figure 4.24. Fitting lines of $I-V^2$ curves for the calculation of charge mobility in pure polymer with the SCLC model in Schottky diodes.

The high conductivity upon doping with iodine vapor and the conductivity persisting for days under ambient conditions is a prominent feature in MEET based polymers.¹³ Our polymers shows similar behavior when the conductivity measurements were carried out using a 4-point probe. The conductivity of the polymer increases upon chemical doping with iodine, with and without thermal annealing. Thermally annealed polymer showed slightly lower conductivity than the non-annealed polymer. Conductivity did not increase with increasing time. To study the stability of the doped states of the polymers, polymer films doped by iodine vapor for 3 hours were kept in air and the conductivities were measured over time (table 4.2). Conductivities were reduced by an order of magnitude after a week and then remained stable for about a month, indicating that these polymers have stable oxidized states. This could be due to the better stabilization of charge carriers by alkoxy side chains on the polymer.

Table 4.2. Conductivity of the polymer upon doping with iodine vapor and stability of doped films on air

Doping time/ time in open air	Average conductivities (S cm ⁻¹)	
	Non-annealed	Annealed
No doping	0.0828	0.0843
30 min	36.9	31.3
1 h	28.4	18.4
3 h	32.8	26.8
After doping, day 1	44.8	17.6
1 week	2.87	2.08
1 month	2.19	1.92

Film thickness: non-annealed 1.57 μm , annealed 1.58 μm (annealing at 100 °C for 5 minutes)

Due to the interesting conductivity features upon doping we have investigated the applicability of polymer as a hole injection layer for photovoltaic applications. Different concentrations of the polymer were spin coated from chloroform solution on ITO substrates with different spin rates. The resultant polymer films were doped with iodine vapor for 30 min and their transmittance was

investigated (figure 4.25). 30 min was more reasonable time scale for doping in real applications and the conductivity does not change considerably as doping time increases (table 4.2).

Upon doping with iodine vapors, the polymer films became more transparent (inset of figure 4.25) and no longer soluble in common organic solvents such as chloroform and chlorobenzene. This is a crucial requirement in active layer deposition in photovoltaic applications as the active layer is deposited on top of the hole injection layer by using a common organic solvent. Both 5 mg/mL samples showed similar transmittance as PEDOT: PSS in IR regions and above 80 % transmittance in UV and visible regions. Since both 5 mg/mL samples showed similar behavior 5 mg/mL sample spin coated at 3000 rpm can be considered as best conditions as this speed gives a reasonable average film thickness of 16 nm. This film thickness is comparable with the PEDOT:PSS film thickness.³⁶ PEDOT:PSS needs an additional annealing step prior to active layer deposition and shows hygroscopicity and acidity. By contrast, our polymers show greater potential as a hole injection layer as none of the above drawbacks are associated with it.

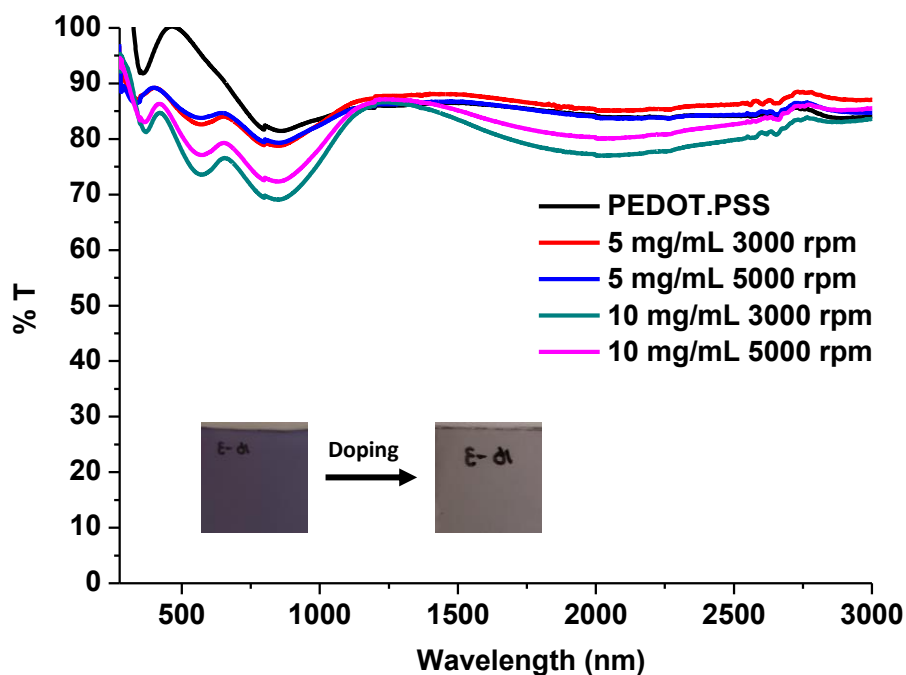


Figure 4.25. Transmittance of the polymer compared with that of PEDOT: PSS

4.5 Conclusion

β -functionalized poly(alkoxythiophene)s synthesized by McCullough method displayed a range of promising optical, electrical, and thermal properties such as better ordering in solid state, reduced band gap due to the high lying HOMO level, better thermal stability up to ~ 300 °C and in thin-film transistors polymer showed an average mobility of $4.2 \times 10^{-4} \text{ cm}^2 \text{ V}^{-1} \text{ s}^{-1}$. Furthermore, polymer showed high conductivity upon chemical doping with iodine vapors which persisted for days due to the stable oxidized states. Due to the increased transparency upon doping this polymer revealed great potential as an alternative to commercially available PEDOT: PSS.

4.6 Acknowledgments

We are gratefully acknowledging the financial support from NSF (DMR-0956116) and Welch Foundation (AT-1740).

The authors would like to thank Prof. Qing Wang, Department of Materials Science and Engineering, The Pennsylvania State University, University Park, Pennsylvania 16802, United States for GIWAXS data analysis.

4.7 References

1. Nielsen, C. B.; McCulloch, I. Recent advances in transistor performance of polythiophenes. *Progress in Polymer Science* **2013**, *38*, 2053-2069.
2. Lu, L.; Zheng, T.; Wu, Q.; Schneider, A. M.; Zhao, D.; Yu, L. Recent Advances in Bulk Heterojunction Polymer Solar Cells. *Chemical Reviews* **2015**, *115*, 12666-12731.
3. Zanardi, C.; Terzi, F.; Seeber, R. Polythiophenes and polythiophene-based composites in amperometric sensing. *Analytical & Bioanalytical Chemistry* **2013**, *405*, 509-531.
4. Béra-Abérem, M.; Ho, H.-A.; Leclerc, M. Functional polythiophenes as optical chemo- and biosensors. *Tetrahedron* **2004**, *60*, 11169-11173.
5. Huynh, T.-P.; Sharma, P. S.; Sosnowska, M.; D'Souza, F.; Kutner, W. Functionalized polythiophenes: Recognition materials for chemosensors and biosensors of superior sensitivity, selectivity, and detectability. *Progress in Polymer Science* **2015**, *47*, 1-25.

6. Leclerc, M.; Faid, K. Electrical and optical properties of Processable Polythiophene Derivatives: Structure-Property relationships. *Advanced Materials* **1997**, *9*, 1087-1094.
7. Sirringhaus, H.; Tessler, N.; Friend, R. H. Integrated optoelectronic devices based on conjugated polymers. *Science* **1998**, *280*, 1741-1744.
8. Bhatt, M. P.; Magurudeniya, H. D.; Rainbolt, E. A.; Huang, P.; Dissanayake, D. S.; Biewer, M. C.; Stefan, M. C. Poly(3-Hexylthiophene) Nanostructured Materials for Organic Electronics Applications. *Journal of Nanoscience and Nanotechnology* **2014**, *14*, 1033-1050.
9. McCullough, R. D. The Chemistry of Conducting Polythiophenes. *Advanced Materials* **1998**, *10*, 93-116.
10. Jen, K.-Y.; Miller, G. G.; Elsenbaumer, R. L. Highly conducting, soluble, and environmentally-stable poly(3-alkylthiophenes). *Journal of the Chemical Society, Chemical Communications* **1986**, 1346-1347.
11. Iovu, M. C.; Craley, C. R.; Jeffries-El, M.; Krankowski, A. B.; Zhang, R.; Kowalewski, T.; McCullough, R. D. Conducting Regioregular Polythiophene Block Copolymer Nanofibrils Synthesized by Reversible Addition Fragmentation Chain Transfer Polymerization (RAFT) and Nitroxide Mediated Polymerization (NMP). *Macromolecules* **2007**, *40*, 4733-4735.
12. Chen, S. A.; Tsai, C. C. Structure/properties of conjugated conductive polymers. 2. 3-Ether-substituted polythiophenes and poly(4-methylthiophenes). *Macromolecules* **1993**, *26*, 2234-2239.
13. Sheina, E. E.; Khersonsky, S. M.; Jones, E. G.; McCullough, R. D. Highly Conductive, Regioregular Alkoxy-Functionalized Polythiophenes: A New Class of Stable, Low Band Gap Materials. *Chemistry of Materials* **2005**, *17*, 3317-3319.
14. Bryce, M. R.; Chissel, A.; Kathirgamanathan, P.; Parker, D.; Smith, N. R. M. Soluble, conducting polymers from 3-substituted thiophenes and pyrroles. *Journal of the Chemical Society, Chemical Communications* **1987**, 466-467.
15. Belaine, D.; Png, R.-Q.; McGuinness, C. L.; Mathai, M.; Seshadri, V.; Ho, P. K. H. A High-Performance p-Doped Conducting Polymer Blend Based on Sulfonated Polyalkoxythiophene and Poly(4-hydroxystyrene). *Chemistry of Materials* **2014**, *26*, 4724-4730.
16. Mauger, S. A.; Li, J.; Ozmen, O. T.; Yang, A. Y.; Friedrich, S.; Rail, M. D.; Berben, L. A.; Moule, A. J. High work-function hole transport layers by self-assembly using a fluorinated additive. *Journal of Materials Chemistry C* **2014**, *2*, 115-123.
17. Mauger, S. A.; Moulé, A. J. Characterization of new transparent organic electrode materials. *Organic Electronics* **2011**, *12*, 1948-1956.

18. Voroshazi, E.; Verreet, B.; Buri, A.; Müller, R.; Di Nuzzo, D.; Heremans, P. Influence of cathode oxidation via the hole extraction layer in polymer:fullerene solar cells. *Organic Electronics* **2011**, *12*, 736-744.
19. Jørgensen, M.; Norrman, K.; Krebs, F. C. Stability/degradation of polymer solar cells. *Solar Energy Materials and Solar Cells* **2008**, *92*, 686-714.
20. Norrman, K.; Gevorgyan, S. A.; Krebs, F. C. Water-Induced Degradation of Polymer Solar Cells Studied by H218O Labeling. *ACS Applied Materials & Interfaces* **2009**, *1*, 102-112.
21. Nielsen, C. B.; Giovannitti, A.; Sbircea, D.-T.; Bandiello, E.; Niazi, M. R.; Hanifi, D. A.; Sessolo, M.; Amassian, A.; Malliaras, G. G.; Rivnay, J.; McCulloch, I. Molecular Design of Semiconducting Polymers for High-Performance Organic Electrochemical Transistors. *Journal of the American Chemical Society* **2016**, *138*, 10252-10259.
22. Lee, E.; Hammer, B.; Kim, J.-K.; Page, Z.; Emrick, T.; Hayward, R. C. Hierarchical Helical Assembly of Conjugated Poly(3-hexylthiophene)-block-poly(3-triethylene glycol thiophene) Diblock Copolymers. *Journal of the American Chemical Society* **2011**, *133*, 10390-10393.
23. Kim, J.; Siva, A.; Song, I. Y.; Park, T. Synthesis and characterization of all-conjugated diblock copolymers consisting of thiophenes with a hydrophobic alkyl and a hydrophilic alkoxy side chain. *Polymer* **2011**, *52*, 3704-3709.
24. Gunathilake, S. S.; Magurudeniya, H. D.; Huang, P.; Nguyen, H.; Rainbolt, E. A.; Stefan, M. C.; Biewer, M. C. Synthesis and characterization of novel semiconducting polymers containing pyrimidine. *Polymer Chemistry* **2013**, *4*, 5216-5219.
25. Gunathilake, S. S. Route towards incorporation of pyrimidine in conjugated polymers and b-alkoxy functionalized poly(thiophene) via McCullough method. Ph.D. Dissertation, University of Texas at Dallas, 2014.
26. Vakhshouri, K.; Smith, B. H.; Chan, E. P.; Wang, C.; Salleo, A.; Wang, C.; Hexemer, A.; Gomez, E. D. Signatures of Intracrystallite and Intercrystallite Limitations of Charge Transport in Polythiophenes. *Macromolecules* **2016**, *49*, 7359-7369.
27. Keegstra, M. A.; Peters, T. H. A.; Brandsma, L. Copper(I) halide catalysed synthesis of alkyl aryl and alkyl heteroaryl ethers. *Tetrahedron* **1992**, *48*, 3633-3652.
28. McCullough, R. D.; Lowe, R. D. Enhanced electrical conductivity in regioselectively synthesized poly(3-alkylthiophenes). *Journal of the Chemical Society, Chemical Communications* **1992**, 70-72.
29. Alemseghed, M. G.; Gowrisanker, S.; Servello, J.; Stefan, M. C. Synthesis of Di-block Copolymers Containing Regioregular Poly(3-hexylthiophene) and Poly(tetrahydrofuran) by a

Combination of Grignard Metathesis and Cationic Polymerizations. *Macromolecular Chemistry and Physics* **2009**, *210*, 2007-2014.

30. Alemseghed, M. G.; Servello, J.; Hundt, N.; Sista, P.; Biewer, M. C.; Stefan, M. C. Amphiphilic Block Copolymers Containing Regioregular Poly(3-hexylthiophene) and Poly(2-ethyl-2-oxazoline). *Macromolecular Chemistry and Physics* **2010**, *211*, 1291-1297.

31. Hundt, N.; Hoang, Q.; Nguyen, H.; Sista, P.; Hao, J.; Servello, J.; Palaniappan, K.; Alemseghed, M.; Biewer, M. C.; Stefan, M. C. Synthesis and Characterization of a Block Copolymer Containing Regioregular Poly(3-hexylthiophene) and Poly(γ -benzyl-L-glutamate). *Macromolecular Rapid Communications* **2011**, *32*, 302-308.

32. Prosa, T. J.; Winokur, M. J.; Moulton, J.; Smith, P.; Heeger, A. J. X-ray structural studies of poly(3-alkylthiophenes): an example of an inverse comb. *Macromolecules* **1992**, *25*, 4364-4372.

33. Smith, B. H.; Clark, M. B.; Kuang, H.; Grieco, C.; Larsen, A. V.; Zhu, C.; Wang, C.; Hexemer, A.; Asbury, J. B.; Janik, M. J.; Gomez, E. D. Controlling Polymorphism in Poly(3-Hexylthiophene) through Addition of Ferrocene for Enhanced Charge Mobilities in Thin-Film Transistors. *Advanced Functional Materials* **2015**, *25*, 542-551.

34. Wang, C.; Rivnay, J.; Himmelberger, S.; Vakhshouri, K.; Toney, M. F.; Gomez, E. D.; Salleo, A. Ultrathin Body Poly(3-hexylthiophene) Transistors with Improved Short-Channel Performance. *ACS Applied Materials & Interfaces* **2013**, *5*, 2342-2346.

35. Bartuš, J. Electrically Conducting Thiophene Polymers. *Journal of Macromolecular Science: Part A - Chemistry* **1991**, *28*, 917-924.

36. Yan, H.; Arima, S.; Mori, Y.; Kagata, T.; Sato, H.; Okuzaki, H. Poly(3,4-ethylenedioxythiophene)/poly(4-styrenesulfonate): Correlation between colloidal particles and thin films. *Thin Solid Films* **2009**, *517*, 3299-3303.

APPENDIX

structure report

Abstract

Experimental

(scd0687)

Crystal data

$C_{25}H_{29}N_2O_4S$
 $M_r = 404.47$
Monoclinic, $P2_1/n$
 $a = 10.020$ (2) Å
 $b = 11.238$ (3) Å
 $c = 17.984$ (5) Å
 $\beta = 101.851$ (11)°

$V = 1981.9$ (9) Å³
 $Z = 4$
Mo $K\alpha$ radiation, $\lambda = 0.71073$ Å
 $\mu = 0.19$ mm⁻¹
 $T = 90$ K
 $0.18 \times 0.18 \times 0.04$ mm

Data collection

Bruker Kappa D8 Quest CMOS
diffractometer (with an Oxford Cryosystems
cryostream cooler)
Absorption correction: multi-scan
SADABS (Sheldrick, 2002)

$T_{\min} = 0.696$, $T_{\max} = 0.746$
40647 measured reflections
6036 independent reflections
4727 reflections with $I > 2\sigma(I)$
 $R_{\text{int}} = 0.052$

Refinement

$R[F^2 > 2\sigma(F^2)] = 0.050$
 $wR(F^2) = 0.125$
 $S = 1.04$
6036 reflections
265 parameters

0 restraints
H-atom parameters constrained
 $\Delta\rho_{\max} = 0.58$ e Å⁻³
 $\Delta\rho_{\min} = -0.44$ e Å⁻³

Data collection: Bruker *APEX2*; cell refinement: Bruker *SAINT*; data reduction: Bruker *SAINT*; program(s) used to solve structure: *SHELXTL* Intrinsic Phasing (Sheldrick, 2014); program(s) used to refine structure: *SHELXL2014/7* (Sheldrick, 2014); molecular graphics: *ORTEP-3 for Windows* (Farrugia, 2012); software used to prepare material for publication: *publCIF* (Westrip, 2010).

References

NOT FOUND

Abstract**Experimental****(scd0686_SimplerModel)***Crystal data* $C_{25}H_{19}BrN_2O_3S$ $M_r = 483.37$ Monoclinic, $P2_1/c$ $a = 19.967 (7) \text{ \AA}$ $b = 11.759 (3) \text{ \AA}$ $c = 8.670 (2) \text{ \AA}$ $\beta = 94.660 (18)^\circ$ $V = 2028.8 (10) \text{ \AA}^3$ $Z = 4$ Mo $K\alpha$ radiation, $\lambda = 0.71073 \text{ \AA}$ $\mu = 2.16 \text{ mm}^{-1}$ $T = 90 \text{ K}$ $0.24 \times 0.20 \times 0.04 \text{ mm}$ *Data collection*Bruker Kappa D8 Quest CMOS
diffractometer (with an Oxford Cryosystems
cryostream cooler)

Absorption correction: multi-scan

SADABS (Sheldrick, 2002)

 $T_{\min} = 0.600$, $T_{\max} = 0.746$

41789 measured reflections

6241 independent reflections

4775 reflections with $I > 2\sigma(I)$ $R_{\text{int}} = 0.072$ *Refinement* $R[F^2 > 2\sigma(F^2)] = 0.080$ $wR(F^2) = 0.200$ $S = 1.05$

6241 reflections

275 parameters

13 restraints

H-atom parameters constrained

 $\Delta\rho_{\max} = 1.87 \text{ e \AA}^{-3}$ $\Delta\rho_{\min} = -2.51 \text{ e \AA}^{-3}$

Data collection: Bruker *APEX2*; cell refinement: Bruker *SAINT*; data reduction: Bruker *SAINT*; program(s) used to solve structure: *SHELXTL* Intrinsic Phasing (Sheldrick, 2014); program(s) used to refine structure: *SHELXL2014/7* (Sheldrick, 2014); molecular graphics: *ORTEP-3 for Windows* (Farrugia, 2012); software used to prepare material for publication: *publCIF* (Westrip, 2010).

References

NOT FOUND

Abstract**Experimental**

(scd0591)

Crystal data

$C_{31}H_{21}Br_3N_2O_3S_3$
 $M_r = 805.41$
Monoclinic, $P2_1/c$
 $a = 11.072$ (3) Å
 $b = 23.190$ (5) Å
 $c = 11.836$ (3) Å
 $\beta = 92.440$ (9)°

$V = 3036.3$ (12) Å³
 $Z = 4$
Mo $K\alpha$ radiation, $\lambda = 0.71073$ Å
 $\mu = 4.23$ mm⁻¹
 $T = 100$ K
0.18 × 0.14 × 0.06 mm

Data collection

Bruker Kappa D8 Quest CMOS
diffractometer (with an Oxford Cryosystems
cryostream cooler)
Absorption correction: multi-scan
SADABS (Sheldrick, 2002)

$T_{min} = 0.630$, $T_{max} = 0.746$
90916 measured reflections
9330 independent reflections
7332 reflections with $I > 2\sigma(I)$
 $R_{int} = 0.068$

Refinement

$R[F^2 > 2\sigma(F^2)] = 0.065$
 $wR(F^2) = 0.151$
 $S = 1.10$
9330 reflections
382 parameters

0 restraints
H-atom parameters constrained
 $\Delta\rho_{max} = 2.07$ e Å⁻³
 $\Delta\rho_{min} = -1.66$ e Å⁻³

Data collection: Bruker *APEX2*; cell refinement: Bruker *SAINT*; data reduction: Bruker *SAINT*; program(s) used to solve structure: *SHELXTL* Intrinsic Phasing (Sheldrick, 2014); program(s) used to refine structure: *SHELXL2014/7* (Sheldrick, 2014); molecular graphics: *ORTEP-3 for Windows* (Farrugia, 2012); software used to prepare material for publication: *pubCIF* (Westrip, 2010).

References

NOT FOUND

BIOGRAPHICAL SKETCH

Dushanthi S. Dissanayake received her B.Sc. in Chemistry from University of Peradeniya, Sri Lanka in 2009. From 2009–2012 she worked for her M.Phil. degree studying intercalation and synthetic modification of bioactive natural products with layered double hydroxides and cationic clays at Postgraduate Institute of Science at University of Peradeniya, Sri Lanka. In 2012, she entered the Ph.D. program in Chemistry at The University of Texas at Dallas.

CURRICULUM VITAE

Dushanthi S. Dissanayake
dushanthi.dissanayake@utdallas.edu

EDUCATION

Department of Chemistry and Biochemistry, University of Texas at Dallas.

- Ph.D. in Chemistry 2017

Postgraduate Institute of Science (PGIS) of the University of Peradeniya, Sri Lanka.

Board of Study in Chemical Sciences

- M.Phil. in Chemical Sciences 2009-2012

Faculty of Science, University of Peradeniya, Sri Lanka.

- B.Sc. in Special Degree in Chemistry (honors) Second Class Upper Division (GPA 3.50/4.00) 2005-2009
- Minor in Computer Science and Statistics

TEACHING EXPERIENECE

Teaching Assistant for Organic Chemistry I, II and Introductory Quantitative Methods in Chemistry Labs 2012-2015

Department of Chemistry and Biochemistry, University of Texas at Dallas.

- Conduct lectures, prepare solutions and materials for lab experiments, demonstrate lab experiments and guide students to perform lab experiments effectively and efficiently.
- Guide students to practice critical thinking for problem solving.
- Grade pre-lab reports, post-lab reports and design new exercises.
- Pre-perform new experiments and develop them into a level acceptable for the respective degree level.

Teaching Assistant – Organic Chemistry

April 2011

Department of Pharmacy, Faculty of Allied Health Sciences, University of Peradeniya, Sri Lanka.

–
June 2011

- Assisted and instructed undergraduate students in classroom and laboratory settings
- Preparing laboratory manuals and grading laboratory reports.

Teaching Assistant – General Chemistry
Department of Chemistry, Faculty of Science, University of Peradeniya.

September
2009 –
August
2010

- Assisted and instructed undergraduate students in classroom and laboratory settings
- Preparing laboratory manuals and grading laboratory reports.
- Participating Science camps organized by Science education unit at Faculty of Science, University of Peradeniya as a resource person for giving practical science experimental knowledge for mid school and high school students.

RESEARCH EXPERIENCE

Department of Chemistry and Biochemistry, University of Texas at Dallas.
Graduate Student with Dr. Michael C. Biewer

2012-2017

Tentative Thesis Title: Functionalization of polythiophenes towards organic electronics: photochromic spiropyran and alkoxy groups

- Developing synthetic methodologies to obtain new photochromic compounds.
- Synthesis of polymers and characterize them using instrumental techniques such as SEC, NMR, UV-Vis, CV, TGA, DSC, XRD.
- Working experience in a clean room environment (organic field effect transistors and solar cell fabrication).
- Condition optimization for thin film transistor device applications and solar cell applications of synthesized polymers.

Postgraduate Institute of Science (PGIS) of the University of Peradeniya, Sri Lanka. Board of Study Chemical Sciences
Research Assistant, Supervised by Prof. B. M. R. Bandara

2009-2012

Thesis Title: Intercalation of bioactive natural products into layered double hydroxides and cationic clays

- Extraction of organic compounds from natural products
- Modification of naturally occurring clay materials and synthesis of new materials
- Preparation of organic-inorganic hybrid materials and characterize them using instrumental techniques such as XRD, TGA, DSC.
- Study the releasing behavior of organic-inorganic hybrid materials

Department of Chemistry, Faculty of Science, University of Peradeniya, Sri Lanka.

Undergraduate final year research project – Supervised by Prof. B. M. R. Bandara 2008-2009

Thesis Title: Autocondensation of cyclic ketones on modified montmorillonite clay catalysts

- An independent study on modification of naturally occurring clay materials and use them as catalysts
- Characterization of prepared materials and synthesized compound with the use of instrumental techniques such as GC, GC-MS, NMR.

Industrial Technology Institute (ITI), Colombo 07, Sri Lanka

Research Intern July 2008 – August 2008

Project: Synthesis studies of coconut black beetle aggregation pheromone ethyl 4-methyloctanoate using hexanal and ethyl acrylate.

- Develop methodologies to synthesize materials with readily available commercial compounds.

SKILLS AND TECHNIQUES

- Synthesizing organic molecules targeting specific applications, purification and characterization them using instrumental techniques.
- Synthesis of semiconducting polymers using various coupling reactions such as Kumada, Stille, Suzuki and Direct Hereto Arylation.
- Thin film transistor fabrication in clean room environment and work on a Keithley 4200-SCS semiconductor characterization system to probe the devices.
- Bulk heterojunction solar cell fabrication and work on a solar stimulator and Keithley 2400 source meter interfaced with Labview software to get solar cell application data.
- Instrumental techniques such as GC-MS, UV-Vis, UV-Vis coupled with mercury arc lamp, NMR, FT-IR, SEC, CV, TGA, DSC, MALDI-TOF, AFM, four-point probe, profilometer.

OTHER ACADEMIC ACHIEVEMENTS, HONORS AND ACTIVITIES

- Co-chair of Symposium of General Topics: New Synthesis and Characterization, Division of Polymer Chemistry at 253rd National meeting of the American Chemical Society, San Francisco, CA, April 2-6, 2017.
- Selected for Sci-Mix (top 10 % of the posters in the Division of Polymer Chemistry) at 251st National meeting of the American Chemical Society, San Diego, CA, March 13-17, 2016.

- PhD Research Small Grant for Spring 2016 and Spring 2017, Program to assist PhD students at UT Dallas with dissertation-based research and travel expenses by offering supplemental financial support of up to \$1,000 on a competitive basis.
- UTD Graduate Studies Scholarship (Fall 2012-Present), Covers all costs for UTD tuition and fees, subject to satisfactory performance this scholarship renews each year.
- University Research Fellowship for the academic year 2010/2011, awarded by University of Peradeniya for few selected post-graduate students depending on their achievements.

OUTREACH ACTIVITIES

- Secretary of Sri Lankan Students Association, University of Texas at Dallas 2014-2015

AFFILIATIONS

- Member of American Chemical Society since 2013

CONFERENCE PROCEEDINGS AND ABSTRACTS

Oral Presentations

- 1) **Dissanayake, D. S.**; Gunathilake S. S.; Du, J.; Pathirana, T.; Sheina, E.; Gomez, E. D.; Stefan, M. C.; Biewer, M. C. Triethylene glycol monomethyl ether substituted polythiophenes for organic electronic applications Abstracts of papers, 253rd National meeting of the American Chemical Society, San Francisco, CA, April 2-6, 2017; American Chemical Society: 1155 Sixteenth Street, NW, Washington, DC 20036, USA.
- 2) **Dissanayake, D. S.**; Stefan, M. C.; Biewer, M. C. Developing novel synthetic routes towards incorporating photochromic spiropyran into thiophene based semiconducting polymers Abstracts of papers, Southwest Regional Meeting, Greater Houston Local Section, Galveston, TX, November 10-13, 2016.
- 3) **Dissanayake, D. M. D. S.**; Wijeratne, S.; Bandara, B.M.R. Autocondensation of cyclic ketones on clay catalysts. Proceedings of the Peradeniya University Research Sessions PURSE-2009, Vol. 14, Part 1, 3rd December 2009. pp 239-241.

Poster Presentations

- 1) **Dissanayake, D. S.**; Stefan, M. C.; Biewer, M. C. Novel synthetic route towards incorporating photochromic spiropyran into thiophene based semiconducting polymers. Abstracts of papers, 251st National meeting of the American Chemical Society, San Diego, CA, Mar 13-17, 2016; American Chemical Society: 1155 Sixteenth Street, NW, Washington, DC 20036, USA.
- 2) **Dissanayake, D. S.**; Huang, P.; Stefan, M. C.; Biewer, M. C. Synthesis of block copolymers containing regioregular poly(3-hexylthiophene) and poly(4-vinylphenol) for organic field

effect transistors. Abstracts of papers, 247th National meeting of the American Chemical Society, Dallas, TX, Mar 16-20, 2014; American Chemical Society: 1155 Sixteenth Street, NW, Washington, DC 20036, USA.

PUBLICATIONS

- 1) **Dissanayake, D. S.**; McCandless, G. T; Stefan, M. C.; Biewer, M. C. Systematic variation of thiophene substituents in photochromic spiropyrans, *Photochem. Photobiol. Sci.*, **2017**, *16*, 1057-1062.
- 2) **Dissanayake, D. S.**; Sheina, E.; Biewer, M. C.; McCullough, R. D.; Stefan, M. C. Determination of absolute molecular weight of regioregular poly(3-hexylthiophene) by ¹H-NMR analysis. *J. Polym. Sci. A Polym. Chem.* **2017**, *55*, 79-82.
- 3) Du, J.; Fortney, A.; Washington, K. E.; Bulumulla, C.; Huang, P.; **Dissanayake, D.**; Biewer, M. C.; Kowalewski, T.; Stefan, M. C. Systematic Investigation of Benzodithiophene-Benzothiadiazole Isomers for Organic Photovoltaics *ACS Appl. Mater. Interfaces*, **2016**, *8*, 33025–3303.
- 4) Bhatt, M. P.; Magurudeniya, H. D.; Rainbolt, E. A.; Huang, P.; **Dissanayake, D. S.**; Biewer, M. C.; Stefan, M. C. Poly(3-Hexylthiophene) Nanostructured Materials for Organic Electronics Applications *J. Nanosci. Nanotechnol.* **2014**, *14*, 1033–1050.

REFEREES

- 1) Michael C. Biewer, Ph.D.
Associate Professor of Chemistry
The University of Texas at Dallas
Department of Chemistry, BE26
800 West Campbell Road
Richardson, Texas 75080-3021
Phone: (972)883-2811
Fax: (972)883-2925
E-mail: biewerm@utdallas.edu
- 2) Mihaela C. Stefan, Ph.D.
Associate Professor
The University of Texas at Dallas
Department of Chemistry and Department of Bioengineering
BE 26
800 West Campbell Road
Richardson, Texas 75080-3021
Phone: (972)-883-6581
E-mail: mihaela@utdallas.edu

3) Dr. Jeremiah J Gassensmith
The University of Texas at Dallas
Dept. of Chemistry & Biochemistry, BS13
800 West Campbell Road
Richardson, Texas 75080-3021
Tel +1 (972) 883-3596
Fax +1 (972) 883-2925
Email: gassensmith@utdallas.edu

4) Paul Pantano, Ph.D.
Associate Professor
The University of Texas at Dallas
Department of Chemistry, BE26
800 West Campbell Road
Richardson, Texas 75080-3021
Office:(972) 883-6226
Labs:(972) 883-6278
Fax:(972) 883-2925
E-mail: pantano@utdallas.edu